Generalized Anxiety Disorder is Not Just in your Head: A Threat-Based fMRI Study of the Brain and Spinal Cord

by

Tiffany A. Kolesar

A Thesis submitted to the Faculty of Graduate Studies of
The University of Manitoba
In partial fulfillment of the requirements of the degree of

DOCTOR OF PHILOSOPHY

Department of Physiology and Pathophysiology
Max Rady College of Medicine
Rady Faculty of Health Sciences
The University of Manitoba
Winnipeg, Manitoba

Running head: Generalized Anxiety Disorder—Not Just in your Head

Abstract

Generalized Anxiety Disorder (GAD) is a highly prevalent anxiety disorder, characterized by chronic, excessive worry. Physical symptoms are prevalent in GAD, but physiological data are often inconsistent. The goal of the present research is to investigate the neural responses to threat in GAD versus healthy controls (HC). To achieve this goal, we collected data from the largest span of the central nervous system to-date, using functional magnetic resonance imaging (fMRI). This work was broken down into the following three aims: to identify neural activity differences between GAD and HC groups in response to threat in Aim 1) the brain, Aim 2) the cervical spinal cord, and Aim 3) the thoracic spinal cord. All three aims use data acquired from a single sample of 16 participants with GAD and 14 HC. The thesis begins with an introduction to relevant topics including GAD, physiology, and MRI technology. Aim 1) is addressed in two parts. Aim 1a is an in-depth systematic review and meta-analysis on previous neuroimaging research to identify the known neural correlates of GAD, yielding results from the dorsolateral prefrontal cortex, anterior cingulate cortex, amygdala, hippocampus, and culmen of the cerebellum, among others. Aim 1b includes a brain fMRI study in which GAD and HC participants view emotion-evoking images. First, region-of-interest analyses are conducted using regions identified in the systematic review, but results are not significant for these analyses. A follow-up whole brain analysis yields significant results for the main effect of group, corroborating many of the findings from the systematic review. Aims 2 and 3 are considered together in an identical fMRI task as Aim 1b, this time looking at the cervical and thoracic spinal cord. Spinal cord results include increased activity in ventral rostral cervical cord (innervating the neck, shoulders, and trapezius muscles) and mediolateral thoracic cord (innervating the adrenal medulla and gut) for the GAD group as compared to HC. These results provide neurological evidence for increased muscle tension and autonomic activity in the gut and adrenal glands for those with GAD. This work provides the most comprehensive fMRI study of the neurophysiological underpinnings of GAD to-date.

Acknowledgements

I would like to express my deep gratitude to those essential to my success, and to those who have guided me in earning this degree. Dr. Jennifer Kornelsen—I have learned so much under your tutelage. I owe so much of my success to you and your willingness to include me in so many of your projects. Your work piqued my interest in fMRI, and learning how to *run x, y, z* types of analyses under your direction has only furthered my dedication to the field. Dr. Chase Figley, thank you for sharing your immense knowledge with me, you always had an answer for my questions, or pointed me to great resources. Your genuine enjoyment and interest in the field has often sparked, or reignited my own. Dr. El-Gabalawy, thank you for your much appreciated clinical expertise, and for giving me insights that have improved both this, and my future research. Dr. Stroman, thank you for sharing your expansive knowledge and for your untold hours of work developing the software crucial to my success.

I would also like to acknowledge my funding sources throughout my graduate studies, including an Alexander Graham Bell Canada Graduate Scholarship (CGS), as well as a Master's CGS, in addition to institutional funding and external travel support.

Tyler, your unwavering support and incredible ability to bring joy into my life have made the last 7 years of my life the best ones yet. You make my soul happy. To my first family—thank you for all of the love, support, and wisdom you have poured into my life: it means a latte me. Grandpa, thank you for always asking me about my research and being genuinely interested in what I am investigating, it means so much to me! To my second family—I hit the jackpot when I married Tyler because I also gained all of you. Thank you for welcoming me into your family as one of your own, I could not have chosen a better family to join. I am so glad you finally gained a daughter (sorry K + D). To my Neuroimaging Girls compatriots—it is so NIfTI that I met all of you! I will be forever grateful for your friendship, encouragement, and assistance.

Contribution of Authors

For the included publication, "Systematic Review and Meta-Analyses of Neural Structural and Functional Differences in Generalized Anxiety Disorder and Healthy Controls using Magnetic Resonance Imaging," I conceived the idea for the systematic review and meta-analysis, completed the search and selected records eligible for inclusion (in tandem with E. B. and A. D. W.), and wrote the manuscript.

For Alice,

You loved the unseen,

Cared for the hurting,

And left the world completely at peace,

Unaware of the tremendous legacy left in your wake.

May I always be kind,

Welcoming, and homey (not homely),

so as to live up to my namesake.

I love you mostest roastest, Grams.

"To be great is to be the servant of all."

List of Tables

List of Figures

List of Abbreviations

AB: acceptance-based model of GAD

ACC: anterior cingulate cortex

ACTH: adrenocorticotropic hormone

AES-SDM: anisotropic effect size seed-based D mapping (software)

ALFF: amplitude of low frequency fluctuations

AMW: avoidance model of worry

ANS: autonomic nervous system

AUDIT-C: alcohol use disorders identification test-concise

BOLD: blood oxygenation level-dependent

C(followed by a number): cervical spinal cord segment x

CBT: cognitive behavioural therapy

C-COMS: comorbidity, cognition, and Multiple Sclerosis study

Cerebellar H.: cerebellar hemisphere

CNS: central nervous system

CRH: corticotropin-releasing hormone

CSF: cerebrospinal fluid

CTA: cortical thickness analysis

dlPFC: dorsolateral prefrontal cortex

DRG: dorsal root ganglion

DSM-IV: Diagnostic and Statistical Manual for Mental Disorders, 4th edition

DSM-5: Diagnostic and Statistical Manual for Mental Disorders, 5th edition

DTI: diffusion tensor imaging

ED: emotion dysregulation model of GAD

EEG: electroencephalography

EHI: Edinburgh handedness inventory

EMG: electromyography

FA: fractional anisotropy

FC: functional connectivity

FDR: false discovery rate

FID: free induction decay

fMRI: functional magnetic resonance imaging

FOV: field of view

GAD: generalized anxiety disorder

GAD-7: GAD 7 item scale

GE: gradient echo

GE-EPI: gradient-echo echo planar imaging

GLM: general linear model

GM: grey matter

GRAPPA: generalized autocalibrating partial parallel acquisition

GSP: generalized social phobia

HbO: oxygenated hemoglobin

HbR: reduced/deoxygenated hemoglobin

HC: healthy controls

HySCO: hyperelasticity susceptibility artifact correction

IAPS: international affective picture system

ICA: independent component analysis

ICP: inferior cerebellar peduncle

IML: interomediolateral zone

IU: intolerance of uncertainty model of GAD

L: left

L(followed by a number): lumbar spinal cord segment x

LMN: lower motor neuron

M1: primary motor cortex

MC: meta-cognitive model of GAD

MDD: major depressive disorder

MNI: Montreal Neurological Institute

mPFC: medial prefrontal cortex

MP-RAGE: magnetization prepared rapid gradient echo

MRI: magnetic resonance imaging

MTG: middle temporal gyrus

NST: nucleus of the solitary tract

OASIS: overall anxiety severity and impairment scale

OCD: obsessive compulsive disorder

OFC: orbitofrontal cortex

PAG: periaqueductal grey

PCC: posterior cingulate cortex

PD: panic disorder

PDD: persistent depression disorder

PFC: prefrontal cortex

PHQ-9: patient health questionnaire 9

PI-8a: pain interference short form 8a

PNS: peripheral nervous system

PPI: psychophysiological interaction

PTSD: posttraumatic stress disorder

R: right

ReHo: regional homogeneity

RF: radiofrequency

ROI: region of interest

S(followed by a number): sacral spinal cord segment x

SAD: social anxiety disorder

SCID: structured clinical interview for the DSM-IV

SCP: superior cerebellar peduncle

SCT: spinocerebellar tract

SE: spin echo

SEEP: signal enhancement by extravascular water protons

SMA: supplementary motor area

SNR: signal-to-noise ratio

SNRI: serotonin-norepinephrine reuptake inhibitor

SNS: sympathetic nervous system

SPM: statistical parametric mapping (software)

SSRI: selective serotonin-reuptake inhibitors

STG: superior temporal gyrus

T: Tesla

T(followed by a number): thoracic spinal cord segment x

TE: echo time

TR: repetition time

UMN: upper motor neuron

VAS: visual analog scale

VBM: voxel-based morphometry

Vermis L.: vermis lobule

vlPFC: ventrolateral prefrontal cortex

VPL: ventral posterolateral nucleus

VPM: ventral posteromedial nucleus

WB: whole brain

WM: white matter

WMH: white matter hyperintensity

Running head: Generalized Anxiety Disorder—Not Just in your Head

1. Chapter 1: Introduction

The present thesis deals largely with three key themes: generalized anxiety disorder (GAD), neurophysiology, and magnetic resonance imaging (MRI). Understanding of these three areas is crucial for effectively answering the basic research question: how does central nervous system (CNS) activity differ in GAD, compared to healthy controls (HC), in response to threat? In addition to the mental aspects of GAD, such as worry and difficulty concentrating, physical symptoms such as increased muscle tension and gastrointestinal distress are also common. The overall goal of the current thesis is to identify the neural correlates associated with threat in GAD, compared to HC, across the largest expanse of the central nervous system (CNS) to-date using functional magnetic resonance imaging (fMRI) technology. This goal will be accomplished via three specific aims: to investigate the neural correlates of threat in GAD compared to HC in Aim 1) the brain, Aim 2) the cervical spinal cord, and in Aim 3) the thoracic spinal cord. Aim 1a) is addressed in a systematic review and meta-analyses of the brain fMRI literature of GAD to-date while Aim 1b) is addressed by conducting *a priori* ROI-based and *post hoc* whole-brain analyses of an fMRI study of the brain, during which participants passively view threat-evoking images. Aims 2) and 3) are addressed using the same fMRI task while scanning the cervical and thoracic spinal cord, allowing us to examine motoric and autonomic responses in GAD, respectively.

To place these results in the appropriate context, the following sections review the literature to provide background of the three main topics. First, this thesis includes information regarding what GAD is (section 0), how it can be conceptualized and treated, as well as what is currently known about the physiological basis of GAD. Next, neurophysiology is reviewed (section 1.2), including brain and spinal cord physiology potentially relevant to GAD, including a look at the autonomic nervous system (ANS). Finally, MRI technology is discussed (section 1.3), including how MR images are created, the challenges associated with this technology, with a special focus on challenges unique to functional MRI (fMRI) in the spinal cord, and a brief look at previously conducted spinal cord fMRI work.

1.1 Generalized Anxiety Disorder

While sections 1.1.1 Defining GAD, 1.1.3 Modelling GAD, and 1.1.4 The Known Physiological Basis of GAD are attributed to a variety of references, as cited, section 1.1.2 Treating GAD is largely referenced from an excellent clinical review by M. B. Stein and Sareen (2015), unless otherwise cited.

1.1.1 Defining GAD

GAD is a chronic anxiety disorder characterized by excessive, uncontrollable worry, spanning a variety of domains, occurring more days than not, for a minimum of 6 months (American Psychiatric Association, 2013). For a GAD diagnosis to be made in adults, at least three out of the following six symptoms must be experienced more often than not over the past 6 months as well: being easily fatigued, sleep disturbances, restlessness or feeling keyed up or "on edge," difficulty concentrating, irritability, and muscle tension. This worry must cause clinically significant distress or impairment in important areas of functioning and cannot be due to a medical condition or the physiological effects of a substance (American Psychiatric Association, 2013; M. B. Stein & Sareen, 2015). Finally, to be classified as GAD, the symptoms cannot be better accounted for by another mental disorder (American Psychiatric Association, 2013; M. B. Stein & Sareen, 2015).

A report from 2013 indicates that the lifetime prevalence of GAD in Canada is about 8.7%, while 2.6% of Canadians sampled met criteria for past-year GAD (Pearson, Janz, & Ali, 2013), similar to rates in other developed nations (Pelletier, O'Donnell, McRae, & Grenier, 2017). GAD has a median age of onset of 31 years of age, and an interquartile range of 27 years (spanning from 20 to 47 years of age; Kessler et al., 2005). The median age of onset of GAD is more similar to that of mood disorders than to other anxiety disorders, while the large distribution of age of onset is more similar to mood disorders, panic disorder (PD), and posttraumatic stress disorder (PTSD), than it is to specific phobias, separation anxiety disorder and social anxiety disorder (SAD; Kessler et al., 2005).

Several risk factors for GAD are known, including female sex, low socio-economic status, and exposure to childhood adversity (e.g., physical or sexual abuse, neglect, parental problems with intimate-partner violence, alcoholism or drug use), and exposure to physical punishment (Culpepper, 2009; M. B. Stein & Sareen, 2015; Zhang et al., 2015); however, these factors are also associated with other anxiety or mood disorders. Although GAD has much in common with major

depressive disorder (MDD, more on this in section 1.1.2 Treating GAD) and they share many of the same risk factors, MDD is strongly associated with a family history of depression and low positive emotionality while GAD is not (Moffitt, Caspi, et al., 2007). Conversely, GAD is associated with risk factors such as high negative emotionality, and others spanning childhood including low socioeconomic status, maltreatment, and inhibited temperament, while MDD did not share these risk factors during childhood (Moffitt, Caspi, et al., 2007).

Heritability of GAD appears moderate with a 15-20% heritability rate between twins (M. B. Stein & Sareen, 2015). In a study including over 5000 twins, genetic and environmental (both shared within families, and unique to individuals) factors were modelled in order to investigate the risk factors of several anxiety disorders (Hettema, Prescott, Myers, Neale, & Kendler, 2005). Although the study had some shortcomings—criteria for many of the disorders was broadened (e.g., GAD only needed symptoms for 1 month, instead of 6)—it provides valuable insight into the factors affecting these anxiety disorders. The model that best fit the data included 2 additive genetic factors common to all anxiety disorders, a single shared environmental factor within families, and one environmental factor unique to individuals, although the specific genetic and environmental factors were not identified (Hettema et al., 2005). Although two genetic factors were associated with anxiety disorders, GAD, PD, agoraphobia, and, to a lesser extent, social phobia (albeit using SCID-III criteria) had a stronger association with one, while specific phobias had a stronger association with the other (Hettema et al., 2005). The authors posited that these results may explain the non-specific response of antidepressant medications to these disorders, and suggested that differences in the second genetic factor and environmental risk factors may explain differentiation of these disorders (Hettema et al., 2005).

Unfortunately, patients with GAD are also at a greater risk of developing other physical and mental (addressed in section 1.1.2 Treating GAD) health problems, including heart disease (Butnoriene et al., 2015) chronic pain syndromes, asthma, chronic obstructive pulmonary disease, and inflammatory bowel disease (Culpepper, 2009; El-Gabalawy, Mackenzie, Pietrzak, & Sareen, 2014; Marrie et al., 2019; M. B. Stein & Sareen, 2015). In a longitudinal study using data from the National Epidemiologic Survey on Alcohol and Related Conditions, over 10,000 older adults were assessed at two different time points to assess relationships between physical or mental health disorders at time 1, and again 3 years later (El-Gabalawy et al., 2014). While this study showed that patients with arthritis were more susceptible to developing GAD, it also showed that patients

with GAD were more likely to develop gastrointestinal disease at time 2 and any anxiety disorder resulted in increased odds of developing arthritis at time 2. However, only the finding of arthritis at time 1 predicting GAD at time 2 remained significant after controlling for the number of physical health conditions (El-Gabalawy et al., 2014). An important caveat to these results is that the physical health assessments in this study were limited to self-reported diagnoses. However an interesting review indicates a variety of mechanisms that may increase the risk of developing inflammatory bowel disease as a result of excessive anxiety, including proinflammatory properties associated with sympathetic nervous system (SNS) activity, and via increased intestinal permeability and altered gut microbiota (Bernstein, 2017). Another study looked at coronary disease risk in GAD using general measures of health (i.e., smoking status, body mass index, hypertensive/hypercholesterolemia/diabetes medication use) and found that the presence of GAD predicted an increased risk of coronary disease, in the absence of MDD (Barger & Sydeman, 2005).

The excessive worry that is a prominent characteristic of GAD is often not the primary complaint motivating patients to seek out a doctor; typically symptoms such as headaches or gastrointestinal upset are the driving factors in seeking medical help (M. B. Stein & Sareen, 2015). Unfortunately, under-recognition, and as a result, under-treatment has long been an issue plaguing anxiety disorders (Harman, Rollman, Hanusa, Lenze, & Shear, 2002), which can lead to a greater financial burden on health care systems including increased medical testing and drug costs, until a correct diagnosis and treatment are found. Mental illness is the cause of 30 percent of disability claims covered by insurance, and costs an estimated $15-33 billion annually in Canada. Unfortunately, with the mental health supports currently in place in the workforce, only 50 percent of people on long-term disability return to work, while 15 percent terminate their claims because they have surpassed their maximum benefit (Southerland & Stonebridge, 2016). If working Canadians with anxiety alone received optimal treatment and benefits, an estimated addition of $17.3 billion to the Canadian economy is expected, albeit this assumes that there is an optimal treatment that could return most anxious Canadians to work (Southerland & Stonebridge, 2016), when in reality GAD is not easy to treat. However, when treatment for mental illness is successful, it is associated with a corresponding decrease in suicide rate (Nepon, Belik, Bolton, & Sareen, 2010). This news is an important consideration in GAD as these patients are at an increased risk of suicidal ideation (Sareen et al., 2005), even in the absence of mood and personality disorders (Nepon et al., 2010).

1.1.2 Treating GAD

Before treatment can begin, a patient first needs to be assessed to inventory their symptoms, and the impact they have. At this stage, it is imperative to assess whether or not a patient is experiencing suicidal ideation, plans, or attempts. It is also important to evaluate whether or not GAD is a primary diagnosis, and if it is co-occurring with other physical—e.g., cardiac or thyroid—or mental health issues. The differential diagnosis for GAD is extensive, and diagnosis is further complicated by common comorbidities including MDD, PD, SAD, obsessive compulsive disorder (OCD), and substance use disorder (Alegria et al., 2010; Grant et al., 2005; Wittchen, Zhao, Kessler, & Eaton, 1994). MDD—the most common comorbidity, occurring in about 52.6% of Canadians with GAD (Pearson et al., 2013)—is similar in that both conditions have fatigue and insomnia as possible symptoms, and each contribute to an increased risk for deliberate self-harm and suicide attempts. Depression can be distinguished by persistent anhedonia (i.e., the inability to feel pleasure), which is not a feature of GAD. In one longitudinal study based in New Zealand spanning 32 years, when GAD and MDD were comorbid, GAD began first in one third of cases, MDD occurred first in one third, and both disorders began together in the other third of cases (Moffitt, Harrington, et al., 2007). This study also found that attempted suicide was as high as 11% for patients with comorbid GAD and MDD (Moffitt, Harrington, et al., 2007).

PD, which appears to have similar genetic loading as GAD (Hettema et al., 2005), is characterized by sudden, abrupt, and transient panic attacks, associated with intense fear or anxiety, and accompanied by physical symptoms including rapid heart rate, difficulty breathing, and feelings of constriction in the chest, among others (American Psychiatric Association, 2013). While patients with GAD can also experience anxiety attacks, a key difference is that in PD these panic attacks come on suddenly and randomly, without anxious thoughts and worries precipitating them. SAD differs from GAD as apprehension is restricted to being embarrassed or scrutinized by others. This anxiety can be performance-related (e.g., public speaking, eating, or writing in front of others) or non-performance based, such as interacting with unfamiliar people (American Psychiatric Association, 2013). While OCD and GAD share ruminating, in OCD, these are tied to irrational beliefs, such as beliefs about contamination, and are often associated with time-consuming compulsions, like hand washing (American Psychiatric Association, 2013). Finally, in PTSD—no longer classified as an anxiety disorder in the DSM-5—anxiety is confined to reminders of life-threatening trauma (American Psychiatric Association, 2013).

After a diagnosis of GAD is suspected, a measure such as the Generalized Anxiety Disorder 7-Item Questionnaire can be used to assess GAD severity, and track the effectiveness of treatments. Although there are several approaches to treating GAD (see Behar, DiMarco, Hekler, Mohlman, & Staples, 2009 for a review of how GAD can be treated by working off of the different theoretical models of GAD), in the present work, the focus will be on a step-based treatment program suggested by M. B. Stein and Sareen (2015). Step 1 of this treatment program, after the patient has been assessed, involves educating the patient and their loved ones about GAD including providing educational resources about the disorder itself, and some lifestyle modifications that can improve symptoms such as regular exercise, healthy sleep habits, and minimization/avoidance of caffeine, alcohol, nicotine and illicit drugs. If lifestyle changes alone are not enough to reduce GAD symptoms, step 2 is encouraged, which includes low-intensity psychological interventions such as self-help, educational groups, and computer-assisted cognitive behavioural therapy (CBT).

CBT is a common and an effective form of psychotherapy for treating GAD and deals with restructuring thoughts and altering behaviours (Carpenter et al., 2018; Cuijpers et al., 2014). Unsurprisingly, CBT includes both cognitive and behavioural techniques in order to treat mental disorders. Cognitive restructuring is an important component of CBT and includes identifying thoughts, emotions, and beliefs about a problem, and recognizing where thinking may be negative or inaccurate (Kaczkurkin & Foa, 2015). Next, these beliefs and thoughts are challenged and reshaped so that perceptions and views are more accurate (Kaczkurkin & Foa, 2015). In addition to the cognitive work involved in CBT, behavioural modifications are also important, and these behaviours can include exposure to a feared stimulus, applied relaxation (Kaczkurkin & Foa, 2015), and problem-solving (M. B. Stein & Sareen, 2015). Newer techniques such as metacognitive therapy and acceptance-based behaviour therapy are also being investigated for their effectiveness (Cuijpers et al., 2014). In the context of GAD, use of CBT assumes that danger in the environment is overestimated, while one's ability to cope is underestimated, and uncertainty is not well tolerated. While cognitive restructuring helps patients with GAD recognise that their worry is more harmful than helpful, behavioural methods include exposure therapy and relaxation therapy to show patients that their feelings and behaviours can be constructively changed. Perhaps not surprisingly, individuals with additional comorbid mental health disorders tend to exhibit more severe GAD symptoms, but CBT treatment for complex GAD also has a stronger, positive response to CBT than simpler cases of GAD (Newman, Przeworski, Fisher, & Borkovec, 2010).

Should step 2 of this treatment plan be unsuccessful for treating GAD, step 3 involves higher intensity psychological interventions such as individual or group-based CBT, or treatment with first-line pharmacologic treatments which include selective serotonin-reuptake inhibitors (SSRIs; e.g., sertraline, paroxetine, paroxetine CR, citalopram, and escitalopram) or serotonin-norepinephrine reuptake inhibitors (SNRIs; e.g., venlafaxine and duloxetine). All of these SSRIs and SNRIs appear to be equally effective in treating GAD and efficacy ranges from 30-50%. As the name suggests, SSRIs work by inhibiting the reuptake of serotonin, which results in increased serotonin levels throughout the brain with prolonged treatment (Yohn, Gergues, & Samuels, 2017). Similarly, SNRIs inhibit both serotonin and norepinephrine from binding with receptors (Dell'Osso, Buoli, Baldwin, & Altamura, 2010). SSRIs have common side effects such as nausea, drowsiness, insomnia, jitteriness, diarrhea, and sexual dysfunction; SNRIs share nausea, drowsiness, insomnia, and sexual dysfunction as common side effects with SSRIs, but also include dizziness and hypertension.

The final step of this treatment program, step 4, is considered treatment-refractory GAD, or complex GAD. In such cases, patients medications are changed and second-line pharmacologic treatments may be tried, in addition to more intensive CBT and other types of psychotherapy such as psychodynamic or acceptance and commitment therapy which goes above and beyond CBT by adding context to the framework in an attempt to encompass more of the whole-person (Hayes, Luoma, Bond, Masuda, & Lillis, 2006). Second-line treatments include benzodiazepines (e.g., diazepam, clonazepam, lorazepam, and alprazolam), imipramine (a tricyclic antidepressant), buspirone, pregabalin, gabapentin, and quetiapine. Second-line pharmacologic treatments should be used only if first-line treatments are ineffective due to their riskier drug profile. Benzodiazepines can be used by themselves, or in conjunction with SSRIs or SNRIs, but should be used with caution in patients at risk of falling, or in patients with past or present substance-use problems because of concerns of dependence and misuse. Additionally, benzodiazepines interact with opioids and the two drug classes should not be used together. Tricyclic antidepressants are typically less safe than SSRIs and SNRIs, but can be considered if they have been useful for the patient in the past, or if neither SSRIs nor SNRIs are effective. Similar to SNRIs, tricyclic antidepressants block serotonin and norepinephrine reuptake; however, the side effects of tricyclics can be severe.

Finally, another treatment method that has shown promise is biofeedback (Tolin, Davies, Moskow, & Hofmann, 2020). This fairly inexpensive and minimally invasive method uses real-time physiological data, along with relaxation techniques such as controlled breathing. With training, as breathing gets deeper and longer, other physiological measures follow, such as decreases in heart rate/increases in heart rate variability, reduced muscle tension, and even altered brain activity (Tolin et al., 2020). Although there have been surprisingly few randomized controlled trials comparing biofeedback to other treatment methods (Banerjee & Argaez, 2017; Tolin et al., 2020), one recent comparison of metacognitive therapy, SSRIs, and electroencephalography (EEG) biofeedback found that while all treatments led to symptom improvement, the neurobiofeedback led to greater improvement than the other two treatments (Dadashi et al., 2018).

1.1.3 Modelling GAD

Over the decades, several theoretical models have been developed in order to conceptualize GAD. Five theoretical models have been described—avoidance, intolerance of uncertainty, metacognitive, emotion dysregulation, and acceptance-based models (for review see Behar et al., 2009). While all of these models tend to emphasize avoidance of internal experiences, they each highlight different aspects, and can be categorized into three types: cognitive, emotional, or integrated models. The two cognitive models include the intolerance of uncertainty (IU) and meta-cognitive (MC) models, the emotional models include the emotion dysregulation (ED) and the acceptance-based (AB) models, and the integrated model is the avoidance model of worry (AMW; Behar et al., 2009).

The integrated AMW provided the first theoretical conceptualization of GAD and posits that worry consists of verbal-linguistic thoughts, rather than image-based imaginations, and in fact, worry is expected to inhibit vivid mental imagery (Behar et al., 2009; Borkovec, 1994; Borkovec & Inz, 1990). Borkovec (1994) reviews some of the evidence for this concept: college students reported approximately 70% of cognition was thought-based and only 30% was image-based during worrisome experiences (Borkovec, Lyonfields, Wiser, & Deihl, 1993). More convincingly, patients with GAD were compared to non-anxious controls in active worrying or passive relaxation trials—both groups reported greater thought and less imagery during worry conditions; however during the relaxation trials, patients with GAD reported relatively equal mixes of thoughts and imagery while controls reported mostly imagery during this trial (Borkovec & Inz, 1990). More

recently, Leigh and Hirsch (2011) observed that verbal worry interfered with working memory capacity to a much greater extent than imagery-based worry and indicated that imagery-based solutions may provide an avenue of CBT treatment.

Another important aspect of the AMW is that this worry is an ineffective problem-solving technique that prevents the emotional processing of threat, thus resulting in cognitive avoidance (Behar et al., 2009; Borkovec, 1994). According to this model, patients with GAD view worry as a helpful, positive coping technique that can serve a variety of functions. These functions include 1) superstitious avoidance of negative events (e.g., worrying itself prevents a negative event from happening) or 2) actual avoidance of negative events (e.g., worrying allows for brainstorming ways to prevent negative events), 3) avoiding other emotional topics (e.g., worrying about more mundane things prevents the need to worry about more distressing things), 4) emotionally preparing them for a negative outcome, or 5) for motivation (e.g., worrying motivates the individual to do the work they need to do to avoid negative consequences; Borkovec, 1994). Unfortunately, these five functions tend to negatively reinforce the worry—when negative outcomes are avoided, perhaps because they are unlikely to occur initially, it can serve to provide "evidence" of the effectiveness of worrying, thus fear confrontation can be further avoided. Finally, the AMW suggests that worry also works to inhibit somatic and emotional activation (Borkovec, 1994). Interestingly, there is minimal change from baseline in the cardiovascular system in response to written emotion-evoking statements, compared to imagery of the same scenario (Vrana, Cuthbert, & Lang, 1986)—thus, one of the key components of this model is that worry, which appears to be more verbal-linguistic than imagery-based, may be used to prevent the somatic consequences of emotion-evoking situations, in a way reducing the emotion processing occurring (more on this in section 1.3; Borkovec, 1994). Supporting this view is a study in which participants were told to relax, worry verbally, or visualize images after viewing a highly aversive video—while the imagery group remained anxious following the task, worriers and relaxers had greatly reduced anxiety (Butler, Wells, & Dewick, 1995).

While the AMW equally considers cognitive and emotional aspects of GAD, the two cognitive models—the IU and MC models—rely more heavily on cognitive factors for GAD. Importantly, all three of these models (AMW, IU, and MC models) include positive beliefs about worry, i.e., that worry is a helpful or effective coping skill (Behar et al., 2009). The primary feature of the IU model is, unsurprisingly, intolerance of uncertainty: anxiety arises from situations in

which little information is available (Behar et al., 2009; Dugas, Gagnon, Ladouceur, & Freeston, 1998). Chronic worry is then experienced as a result of negative possible outcomes associated with this ambiguity, which leads to cognitive avoidance and negative problem orientation, which includes seeing problems as threats and becoming easily frustrated with them as they feel they lack control in the problem-solving process, and lacking confidence in their own skills (Behar et al., 2009; Dugas et al., 1998). Although the MC model initially begins with positive beliefs about worry, this does not remain constant throughout the duration of this disorder. According to this model, as patients with GAD hold positive beliefs about worry, and are faced with an initial anxiety-provoking situation, these thoughts result in type 1 (external) worry (Behar et al., 2009; Wells, 1995). However, as time goes on, these thoughts begin to change and beliefs about worry become more negative, for example as the worry seems uncontrollable, or inherently dangerous, which eventually results in type 2 worry, i.e., worrying about the worry or meta-worry (Wells, 1995). This results in even less effective coping as these individuals attempt to suppress this meta-worry via distraction, thought suppression, reassurance-seeking, or avoidance behaviours (Behar et al., 2009).

The emotional models of GAD, on the other hand, focus more on the emotional and behavioural aspects of GAD as contributing and maintaining factors. For example, the AB model highlights strategies and behaviours to avoid unpleasant internal experiences (i.e., thoughts, beliefs, and emotions) which ultimately lead to a reduction in valued activities (Behar et al., 2009). This model suggests that patients with GAD have problematic relationships with negative internal experiences, leading to either actively or automatically avoiding these experiences (Behar et al., 2009; Roemer & Orsillo, 2002). According to this AB model, this avoidance of internal experiences then contributes to behavioural restriction of valued activities as this internal avoidance is generalized to other scenarios; this restriction can be either due to not participating in experiences, or simply being less engaged and aware as these experiences are happening (Behar et al., 2009; Roemer & Orsillo, 2002). Unfortunately, this behavioural restriction can then cause a positive feedback loop as, once again, negative internal experiences occur (Behar et al., 2009). The AB model builds off of the AMW and suggests that treatment of GAD may be improved if mindfulness-based approaches were incorporated into CBT treatment (Roemer & Orsillo, 2002). Mindfulness is a practice involving increased attention and awareness of both externally and internally driven stimuli, and in the case of GAD, this technique is meant to raise awareness that

worry is being used as a way to avoid internal distress, and to fully experience and engage in the present moment (Behar et al., 2009).

The ED model suggests that patients with GAD have difficulty understanding and describing, and thus difficulty regulating emotions (Behar et al., 2009; Mennin, Heimberg, Turk, & Fresco, 2005). These challenges are thought to lead to patients with GAD experiencing emotional hyperarousal meaning that emotions are more intense, quicker to come about, and can be elicited by situations viewed neutrally by those without GAD (Behar et al., 2009; Mennin et al., 2005). As patients with GAD may have a lower threshold for experiencing negative emotion, they may also be more expressive of these emotions, which can lead to criticism from peers with higher emotional thresholds (Mennin et al., 2005). In turn, patients with GAD may begin to view emotions, particularly negative emotions, as threatening, especially when combined with problems identifying and describing emotions (Behar et al., 2009; Mennin et al., 2005). According to this ED model, patients with GAD are proposed to have both hyperreactivity to emotions (difficulty modulating intense emotional experiences) and hyporeactivity to emotions (frequent/automatic attempts to control or suppress emotional expression) which have considerable interplay (Mennin et al., 2005).

The two models that will be focused on in the remainder of the thesis are the AMW and ED models. Recall that the AMW model describes worry as a verbal process to avoid experiencing negative emotional experiences, and that, according to this model patients with GAD have positive beliefs about worry (recall this is the concept that worry is helpful rather than harmful). Finally, this model suggests that patients with GAD have reduced somatic and emotional activation. Interestingly, a couple systematic reviews identify the ED model of GAD as the model best supported by the neuroimaging literature to-date, citing deficient top-down control during emotion regulation. Specifically, these reviews highlight PFC and ACC hypofunction, as well as amygdala hyperactivation during emotional processing and attention and vigilance tasks and reduced hippocampus volume, perhaps accounting for prevention of fear extinction associated with this model (Hilbert, Lueken, & Beesdo-Baum, 2014; Mochcovitch, da Rocha Freire, Garcia, & Nardi, 2014). Additionally, reduced PFC-amygdala functional connectivity was discussed as a possible mechanism for ineffective emotion regulation (Hilbert et al., 2014). While the known neural correlates of GAD have a chapter devoted to them, the rest of the known physiological basis of GAD is discussed in the following section.

1.1.4 The Known Physiological Basis of GAD

While the known brain physiological basis of GAD has its own chapter devoted to it, this current section will survey the known physiological basis of GAD, apart from the brain. There are many ways to measure physiological changes in GAD, and these include muscle tension measured by electromyography (EMG) data, various heart rate data, blood pressure, skin conductance, and hormone concentrations. This physiological data is surveyed below, and has been researched for decades in GAD. In general, there seems to be a consensus that patients with GAD have a reduced physiological response to fearful stimuli compared to HC (P. J. Lang & McTeague, 2009). Researchers in one study, distinguished between fearful (specific phobia and SAD) and anxious (GAD and PD with agoraphobia) disorders—while fearful disorders evoked a larger startle (i.e., blink) response to an acoustic trigger while imagining threating situations than controls, anxious disorders had a smaller response than controls (Cuthbert et al., 2003). Interestingly, although the GAD group rated the unpleasantness of the threatening stimuli similarly to controls, they rated the emotional arousal as more intense, which runs counter-intuitive to the physiological data (Cuthbert et al., 2003).

Stress hormone levels often provide inconsistent results (Hilbert et al., 2014). Catecholamine levels (i.e., epinephrine and norepinephrine) have received little attention in the GAD literature despite their heavy involvement in stress responses (Berridge, 2008; E. R. Kandel, 2013). In the few studies measuring circulating catecholamines at rest, the results have been inconsistent showing no significant differences in norepinephrine and epinephrine between patients with GAD and HC (Mathew, Ho, Francis, Taylor, & Weinman, 1982; Munjack et al., 1990), as well as higher concentrations of these catecholamines (Mathew, Ho, Kralik, Taylor, & Claghorn, 1981). However, after undergoing several stress tests (mental mathematics, a Stroop task, and the Trier social stress test) one study indicates that norepinephrine concentrations, which did not differ in the pre-test phase, were significantly higher in the GAD group post-test (Gerra et al., 2000). Epinephrine concentrations did not differ between GAD and HC groups at pre- or post-stress test, but the authors indicated that this null finding could be due to delayed blood sampling, and at the very least that further testing should be done (Gerra et al., 2000). Adding to these results, in a study comparing the effects of alprazolam and imipramine after six weeks, alprazolam led to decreased circulating epinephrine at baseline and decreased plasma norepinephrine during a stress test, while imipramine led to increased norepinephrine levels in response to a stress test (McLeod,

Hoehn-Saric, Zimmerli, De Souza, & Oliver, 1990). Interestingly, a study investigating irritable bowel syndrome—which has high comorbidity with anxiety and depression—observed higher circulating norepinephrine, compared to HC (Pellissier et al., 2014). Additionally, an inverse relationship between circulating norepinephrine and vagal tone with no relationship between cortisol and vagal tone was observed in this irritable bowel syndrome sample. Of particular interest to the current subject matter was the authors' conclusions that this pattern of activity points to a hyperactive amygdala and hypoactive prefrontal cortex (Pellissier et al., 2014), results that will become much more meaningful for GAD in the context of Chapter 2: Systematic Review and Meta-Analyses of Neural Structural and Functional Differences in Generalized Anxiety Disorder and Healthy Controls using Magnetic Resonance Imaging, and may help to explain the common comorbidity between these gut and mental health disorders.

Another stress hormone previously thought to be altered in GAD is cortisol; however, results regarding cortisol in GAD patients are also fairly inconsistent. In some studies, no significant differences were found between GAD and control groups (Alfano, Reynolds, Scott, Dahl, & Mellman, 2013; Gerra et al., 2000; Hoehn-Saric, McLeod, Lee, & Zimmerli, 1991), others indicated patients with treated GAD had increased cortisol compared to controls (Hood et al., 2011), one study showing differences only in the afternoon (Tafet et al., 2001) and another in an elderly sample, with GAD severity positively correlating with cortisol (Mantella et al., 2008). In a few studies, decreased cortisol levels were even observed: in the elderly, after awakening (Hek et al., 2013), and in hair samples, although no differences were found in salivary concentrations (Steudte et al., 2011). In one machine learning study, questionnaires (including the Penn State worry questionnaire, Beck Depression Inventory-II, the Intolerance of Uncertainty Scale-12, and the trait version of the State-Trait-Anxiety-Index) were useful for determining the presence or absence of GAD or MDD (Hilbert, Lueken, Muehlhan, & Beesdo-Baum, 2017). However, these questionnaires did a poor job of distinguishing between GAD and MDD, while cortisol levels and grey matter differences were more accurate at distinguishing between the two (Hilbert et al., 2017). While cortisol release inhibits the release of factors that cause inflammation (Chrousos, 1998), hypocortisolism can result in increased inflammation, and can be associated with some autoimmune disorders (Heim, Ehlert, & Hellhammer, 2000). Interestingly, hypocortisolism has been reported in many stress-related disorders including inflammatory bowel disease (Minderhoud, Oldenburg, van Dam, & van Berge Henegouwen, 2003) arthritis, fibromyalgia, and

asthma, (Heim et al., 2000), some of which are often seen with GAD. Many factors that could be obscuring cortisol research in GAD may be widely varying sample sizes, measuring cortisol at different times of the day—it has a diurnal cycle (Chrousos, 1998)—comorbidities, current treatments, and testing method, whether by blood serum, saliva, urine or hair.

Finally, serotonin would be an excellent candidate for having a role in GAD, largely derived from an empirical, rather than theoretical perspective (D. J. Stein & Stahl, 2000). Firstly, treatment data shows moderately successful treatment of GAD using SSRIs or SNRIs (M. B. Stein & Sareen, 2015), although why this treatment is successful is thus far unclear (D. J. Stein & Stahl, 2000). Specifically, serotonin receptors 5-HT_{1A} are implicated in GAD treatment while receptors 5-HT_{1C}, 5-HT_2, and 5-HT_3 receptors are possibly also involved (Baldwin & Rudge, 1995). Additionally, genetic studies indicate that different serotonin transporter (Lenze et al., 2010) and receptor (Lohoff et al., 2013) polymorphisms in GAD are associated with different anxiolytic success rates. In one particularly interesting in vitro study, adding cortisol to blood samples resulted in increased serotonin uptake in peripheral blood lymphocytes in HC samples, but not in GAD or depression samples. The researchers concluded that serotonin uptake in these mental disorders was maxed out due to chronically increased blood cortisol levels (Hilbert et al., 2014; Tafet et al., 2001).

An early study of chronic worriers (typically worrying 50+% of each day) and non-worriers (0-10% each day) indicated no difference between heart rate prior to or during a period in which participants were instructed to worry about a topic currently concerning them (Borkovec, Robinson, Pruzinsky, & DePree, 1983). Conversely, an ambulatory study in which physiological data was collected throughout the day as the participant engages in their normal routine indicated that the anxiety group comprised of PD and GAD patients had elevated heart rate compared to non-anxious controls (Hoehn-Saric, McLeod, Funderburk, & Kowalski, 2004). Another study showed increased heart rate in patients with GAD compared to HC following a stress test including mental math, a Stroop task, and a Trier social stress test (Gerra et al., 2000). Compared to heart rate, heart interbeat interval (i.e., the amount of time between one beat and the next)—is a better metric for assessing parasympathetic tone and cardiovascular variability (Borkovec, 1994). Parasympathetic inflexibility, shown by less variance within interbeat intervals, has been shown in several studies (Aldao & Mennin, 2012; Hoehn-Saric et al., 2004; Hoehn-Saric, McLeod, & Zimmerli, 1989; Llera & Newman, 2010; Lyonfields, Borkovec, & Thayer, 1995). Interestingly,

patients with GAD tend to perform poorly when asked to perceive physiological changes such as heart rate, muscle tension, and perspiration while under stress (McLeod, Hoehn-Saric, & Stefan, 1986). While patients with GAD were able to accurately predict the direction of change of heart rate or perspiration, they were unable to predict the magnitude of these changes (McLeod et al., 1986)—patients with PD were better at predicting this (Hoehn-Saric et al., 2004). Finally, in a study investigating emotion dysregulation, patients with GAD and controls were randomly assigned to accept emotions that occur during film viewing (accept condition), try to think about what they are seeing differently/more objectively (reappraise condition), or no instruction conditions in response to emotion-evoking video clips. While controls showed increased cardiac flexibility in accept and reappraise conditions compared to the no instruction condition, patients with GAD showed reduced cardiac flexibility (Aldao & Mennin, 2012). Another example of parasympathetic inflexibility can be seen in reduced mean skin conductance and reduced variability in these changes in response to stress in patients with GAD compared to controls (Hoehn-Saric et al., 1989), and in an anxiety group (GAD and PD) compared to controls (Hoehn-Saric et al., 2004).

Additionally, investigations show that patients with GAD have greater muscle tension—recall this is one of six additional criteria for a diagnosis—in stressful versus baseline conditions (McLeod et al., 1986), and in relaxing and stressful conditions, compared to controls (Hazlett, McLeod, & Hoehn-Saric, 1994; Hoehn-Saric et al., 1989). Borkovec (1994) describes that because the worry experienced in GAD is a future-based threat that is internally-generated, rather than an exogenous, current physical threat, the "fight-or-flight" response is not really needed; a freezing response may be more appropriate, and can even help to explain this muscle tension. Although little attention has been given to freezing in GAD, several physiological events characteristic of freezing are observed, including increased muscle tension and reduced autonomic variability (Borkovec, 1994; Roelofs, 2017). Trait anxiety and pathological worry scores positively correlate with feelings of immobility in response to biological stress (Schmidt, Richey, Zvolensky, & Maner, 2008), and individuals with higher trait anxiety and lower hair cortisol concentrations showed reductions in body sway (i.e., increased freezing), in response to threat (Hashemi et al., 2019). Interestingly, a rat model of GAD—the Carioca model—has been developed with one of its main features being higher freezing responses to conditioned fear (de Castro Gomes, Eduardo Barroso Silva, & Landeira-Fernandez, 2011; León et al., 2020).

Although patients with GAD appear to experience greater distress and emotional arousal, this is typically not reflected well in physiological measures (Hoehn-Saric et al., 2004). Although increased concentrations of stress hormones such as epinephrine, norepinephrine, and cortisol were expected in GAD patients in early studies, the data from these studies do not consistently support these expectations. The consensus tends to be that the ANS in GAD is inflexible (Borkovec, 1994; Hoehn-Saric, 1998; Hoehn-Saric et al., 2004; Lyonfields et al., 1995). While understanding the physiological differences associated with a mental illness is important to develop an overall picture of the disorder, it is also crucial to understand the underlying physiology of the healthy brain and spinal cord, before we can fully appreciate what is occurring in the disordered brain. To this end, the following section provides a review of the relevant components of the CNS and ANS physiology.

1.2 Central Nervous System Physiology

The highly complex CNS affords humans the ability to interact intelligently with their environments and is crucial for establishing our place as apex predators in the animal kingdom. The CNS is important for locomotion, identifying and responding to threats in the environment, and experiencing and interpreting emotions, but it is also involved when these functions become dysregulated. Our tour of the CNS begins with the brain, and its general anatomy and organization, followed by its cognitive and emotional functions and then its functions in motor control. Next, the spinal cord anatomy and function will be discussed, with the final stop of the CNS tour being the ANS.

Information from the following sections can be found in these sources, unless otherwise indicated: section 1.2.1.1 General Anatomy in (Purves, 2008), 1.2.1.2 Cognition and Emotion in the Brain in (E. R. Kandel, 2013), and 1.2.1.3 Motor Function in (E. Kandel et al., 2000), 1.2.2 Spinal Cord in (Chandar & Freeman, 2014), and 1.2.3 Autonomic Nervous System in (E. R. Kandel, 2013). The figures in this chapter were produced in Microsoft PowerPoint 2010 by TAK.

1.2.1 Brain

The brain, the body's most complex organ, is highly structured and, in addition to being vital for life, is also crucial for enhancing it, allowing for vibrant colour to be seen, rich music to be heard, and aromas, tastes, and physical touch to be perceived and appreciated. In order to understand how the brain controls some of these functions, first the basic anatomy of this structure must be understood.

1.2.1.1 General Anatomy

The brain is bathed in cerebrospinal fluid (CSF), which provides the brain tissues with nutrients, and acts as a hydraulic cushion, to protect the brain from injury. Additionally, there are several protective connective tissue layers, in addition to the skull, that serve to protect the brain. Collectively, the meninges—made of the thick outer dura mater, the middle arachnoid mater (which houses the CSF), and the thin inner pia mater—help to anchor the brain and spinal cord within the skull and vertebrae, and protect the delicate local vasculature.

Continuing deeper into the brain, the next tissue is grey matter (GM) which contains the cell bodies of neurons, responsible for producing action potentials. These action potentials traverse the brain along the axon of the excited neuron; axons make up the majority of the deeper white matter (WM) of the brain. The white colour of WM arises from myelinated axons, axons that are insulated with fatty cells called oligodendrocytes in the CNS. Oligodendrocytes are classified as glial cells, a class of non-neural cells that provide support, among other functions, to the neural cells in the CNS.

The cortex, or thin outermost layer of the brain, can be organized into four lobes that broadly have general functions ascribed to them: the frontal lobe (cognitive, executive, and motor functions), the parietal lobe (somatosensation), the occipital lobe (vision), and the temporal lobes (hearing, language). However, this simplification undercuts the complex way the brain works as there are many connections between these regions, in addition to the subcortical structures of the brain that are crucial for normal functioning. As will be discussed in sections 1.2.1.2 and 1.2.1.3, for the purposes of this thesis, functions often attributed to the frontal lobe (as well as the ANS in section 1.2.3) of the brain are among the most useful for cognitive and emotional processing and will be the focus of the remainder of the brain anatomy section.

1.2.1.2 Cognition and Emotion in the Brain

While talking about GAD—an anxiety disorder—it is prudent to briefly discuss some of the known neuroanatomy underlying cognition and emotion, as these functions can be disrupted in this disorder. While emotion and feelings are often used interchangeably, it is important to distinguish between the two from a scientific perspective. Emotions are comprised of behavioural and physiological responses (e.g., changes in heart rate, blood pressure, facial expression) to personally significant stimuli (*APA Dictionary of Psychology*, 2007). Feelings are the conscious experiences accompanying these physiological responses. Although the emphasis of the present

thesis will be on the physiological response component of emotions, as feelings and emotions are highly interconnected, emotion processing typically incorporates both of these aspects. While this current section focuses on the brain circuitry for experiencing emotions—which requires input from cognition, memory, and attention—section 1.2.3 Autonomic Nervous System discusses how these emotions are experienced in the body.

Perhaps the first brain region that springs to mind when the topic of emotion crops up is the amygdala. This almond-shaped structure, located deep in the temporal lobe has long been considered "the fear centre" of the brain (Davis & Whalen, 2001). However, this view turned out to be a gross simplification of a complex group of nuclei. As time passed, this view evolved to a general unpleasantness centre, before recognizing that these nuclei also respond to positive emotion (Bonnet et al., 2015). The current view of the amygdala is that it responds more to arousal or intensity of stimuli, than type of emotion (i.e., valence; Bonnet et al., 2015). Importantly for this thesis, one of the key symptoms often experienced in GAD is a feeling of high arousal or feeling "on edge" (American Psychiatric Association, 2013). Historically, the arousal-detecting hypothesis may have largely been overlooked as stimulus sets used in emotion research tend to contain more arousing negative than neutral stimuli. Consistent with the view that the amygdala identifies salient emotional cues from stimuli, it receives widespread input from the sensory cortices (all but gustatory), as well as from thalamic regions associated with these sensory cortices. Additionally, the amygdala projects to the hypothalamus and brainstem regions regulating autonomic control (more about this in section 1.2.3), in addition to nuclei associated with reward and dopamine release.

Neuroanatomically, the neocortex is what most separates humans from other mammals, allowing our species to think critically, problem solve, and experience and recognize a wide range of emotions. Specifically, the insula, anterior cingulate cortex (ACC), and prefrontal cortex (PFC) play an important role in emotion processing, especially as emotional states—like social feelings such as empathy or embarrassment—become more complex. The ventromedial PFC (vmPFC) is particularly important in social functioning, which relies heavily on emotions and feelings. This region receives much input directly from the dorsolateral PFC (dlPFC), which plays a major role in strenuous mental activity such as complex problem solving or working memory. Important lesion studies have shown that patients with PFC damage fail to have galvanic skin responses (i.e., sympathetic autonomic responses) to emotional images or prior to making risky decisions. Patients

with frontal lobe damage also have difficulty making decisions under conditions of uncertainty—an interesting finding in light of the intolerance of uncertainty often experienced in GAD.

The insula is another structure important in emotion processing. As with most brain structures, the insula is involved in a variety of processes, and likely has a role in integrating systems we typically view as being distinct. The insula receives homeostatic information such as blood chemistry, temperature, and pain, yet it is also active in situations involving recall of feelings. Interestingly, in patients with damage to their visceral autonomic systems (with spared brains), a blunting of emotions is often observed. Similarly, the anterior cingulate cortex (ACC) is a hub of many functions. This region is generally implicated in cognitive control (Shenhav, Botvinick, & Cohen, 2013), as well as during recollection of emotional states, and the affective aspect or unpleasantness of pain (Fuchs, Peng, Boyette-Davis, & Uhelski, 2014). An important consideration in the study of the brain is that regions rarely have a single purpose, and regions rely on a variety of input from a variety of sources to adequately perform their functions.

1.2.1.3 Motor Function

One of the human brain's most important functions is locomotion. In its most simplistic definition, locomotion allows organisms to move towards resources required for survival, and away from threats to survival. The frontal lobe is largely responsible for movement; however, other structures like the cerebellum and ventral posterolateral nucleus (VPL) of the thalamus also have important contributions.

The primary motor cortex (M1)—located at the superior posterior edge of the frontal lobe—is the most basic brain region that produces motor activity, and of the brain's motor regions, it requires the least amount of electricity to produce movement when stimulated exogenously. M1 receives input from the primary somatosensory cortex (which receives sensory and proprioceptive input from the tissues), posterior parietal areas (which integrate sensory modalities), basal nuclei, and the cerebellum (via the thalamus). M1 is concentrically, somatotopically arranged (i.e., highly structured and ordered such that specific brain regions correspond to specific body regions) and individual muscles are represented in multiple places across M1. This concentric organization allows for a variety of proximal and distal muscles to interact in different ways to accomplish different motor tasks, as individual muscles are rarely active in isolation. Interestingly, activity in individual neurons in M1 is related to muscle force, while the direction that force is applied to results from the net action of groups of neurons. Movement is also strongly modulated by external

loads: as a load increases on a muscle, the neurons responsible for that muscle tone increase their firing rate to counteract the load.

The premotor cortex, located anterior to M1, is more complex than M1: while electrical stimulation of M1 results in simple muscle contraction, stimulation of the premotor cortex results in more complex movements that incorporate multiple joints and resemble natural coordinated movements. The organization of this region is such that bilateral movements can be produced by stimulating the medial brain tissue. Furthermore, the premotor cortex synapses in some of the same regions as M1, meaning that it is possible to observe movements, independently of stimulating M1. The premotor cortex receives input from many of the same regions as M1, including somatosensory and prefrontal regions, as well as the basal nuclei and cerebellum. The premotor cortex outputs information to the primary motor cortex and the spinal cord.

In addition to premotor cortex, additional structures such as the supplementary motor area (SMA), pre-SMA, and lateral premotor areas are all important for various aspects of motor control. The SMA is active during complex muscle activity and is important for practicing learned sequences—EEG studies indicate that the SMA activates about one second prior to voluntary movement. As complex motor skills change from learned sequences to automatic processes, the location of activity shifts from the SMA to the motor cortex. The pre-SMA, unsurprisingly, provides input for the SMA and is active during the planning of complex muscle activity, as well as learning motor sequences. Unlike some of the higher motor areas, there is no clear somatotopic organization of the pre-SMA. Finally, the lateral premotor areas are important for determining how sensory stimuli will be used to direct movement—i.e., associative learning, tying sensory events to specific motor outputs.

While the frontal lobe is necessary for locomotion, it also receives input from the cerebellum via the VPL nucleus in the thalamus. Although emerging evidence suggests that the cerebellum likely plays a role in emotion (Adamaszek et al., 2017), one of its primary roles is assessing and maintaining balance and coordination. Indeed, one of the main functions of the cerebellum is to assess motor programs, check for, and correct errors. The cerebellum receives input arising directly from spinal cord tracts; however, the cerebellum does not directly project to the spinal cord. Instead, the cerebellum acts through relays to modulate upper motor neuron activity via the cortex.

1.2.2 Spinal Cord

Now that the main brain structures responsible for locomotion have been identified, this motor pathway to the muscles that conduct movement can be further discussed. Additional functions of the spinal cord, such as its involvement in sensation and the ANS are described below and in section 1.2.3. However, before we continue discussing spinal cord function, it is imperative to have a basic understanding of spinal cord anatomy.

1.2.2.1 General Anatomy

The spinal cord is a thin (roughly 13 mm in diameter at its widest point in the cervical and lumbosacral enlargements; Frostell, Hakim, Thelin, Mattsson, & Svensson, 2016), long (42-45 cm) structure of neural tissue, extending from the medulla oblongata. The spinal cord floats in CSF within the spinal canal, and is protected by the same three meningeal layers as the brain—dura, arachnoid, and pia mater. The meninges of the spinal cord are continuous with those of the brain, and the potential space of the arachnoid mater, which contains CSF, is also continuous with the brain. Lateral, finger-like projections of pia mater called denticulate ligaments extend to the arachnoid to help stabilize the spinal cord within the dural sac (Tubbs, Salter, Grabb, & Oakes, 2001). The spinal cord is also protected by bone; these vertebrae consist of 7 cervical (C), 12 thoracic (T), 5 lumbar (L), 5 sacral (S), and 3-5 coccygeal bones, although the lower vertebrae are often fused (Watson, Paxinos, & Kayalioglu, 2009). Interestingly, there are 8 cervical, 12 thoracic, 5 lumbar, 5 sacral, and 1 coccygeal spinal cord segments, and 31 paired spinal nerves, each corresponding to a single spinal segment. These spinal segments are named after the location that the corresponding nerves exit the vertebral column. Interestingly, while the vertebral column continues from the base of the skull, past the pelvis, the spinal cord ends at the conus medullaris which occurs around vertebra L1. While spinal cord segments line up poorly with their vertebrae of the same name (Cadotte et al., 2015), the total length of the spinal cord itself is more consistent across people (J. Lang & Bartram, 1982), thus measuring distance from the pontomedullary junction has recently been incorporated into imaging software (Stroman, Figley, & Cahill, 2008). The filum terminale, again, an extension of pia mater, anchors the spinal cord to the inferior end of the dural sac. Although the spinal cord ends about 2/3rds of the way down the vertebral column, the spinal nerve roots continue further down the dural sac—referred to as the cauda equina—so that they can exit the vertebrae through the intervertebral foramen, at the level that they are named after. Although C1-C7 nerves exit above their corresponding vertebrae, segment C8 leaves

between the C7 and T1 vertebrae, and the rest of the nerve roots exit the cord below their corresponding vertebrae (Watson et al., 2009).

From the spinal cord, the dorsal (sensory) and ventral (motor) roots exit and join to form spinal nerves. An important feature unique to dorsal roots is a ganglion (i.e., dorsal root ganglion [DRG]), which is a small cluster of cell bodies that belong to primary sensory neurons that have dendrites and sensory receptors in the tissues. Each of the 31 pairs of spinal nerves receive sensory input from, and innervate the musculature and (via sympathetic input) blood vessels, sweat glands, and arrector pili muscles of different regions of the body. Upon exiting the vertebrae, the nerve splits into anterior and posterior rami, which then innervate different regions of the body (see Figure 1.1). Intuitively, the anterior ramus, which supplies the lateral/ventral body and sympathetic innervation of the skin, tends to be larger than the posterior ramus that supplies the dorsal side of the body (Watson et al., 2009). It is important to note that both anterior and posterior rami each contain fibres going to dorsal and from ventral regions of the spinal cord to allow sensory and motor pathways to reach the dorsal and ventral regions of the body (Watson et al., 2009).

Each of the spinal nerves corresponds to distinct tissue and musculature called dermatomes and myotomes (Katirji & Devereaux, 2014). Each dermatome is a distinct group of tissue that sends its somatosensory information to a specific level of the spinal cord, although there is some overlap between neighbouring dermatomes. For example, dermatome C6 corresponds to the thenar eminence of the thumb and the lateral aspect of the forearm (Katirji & Devereaux, 2014)—this sensory information is then transmitted to cervical spinal cord segment C6, where the primary sensory neuron synapses in the dorsal horn. Myotomes are the muscle (i.e., motor) equivalent of dermatomes—i.e., muscle innervated by a single spinal nerve (Katirji & Devereaux, 2014). Importantly, although dermatomes and myotomes are in similar regions, they do not completely overlap, and have different functions, for example, myotome C6 includes biceps and deltoid muscles (Katirji & Devereaux, 2014). Myotomes and dermatomes become critical in localizing CNS injury and dysfunction. Injury to the dorsal C6 segment would result in altered or absent sensation in the thumb and lateral forearm, whereas injury to ventral C6 would result in altered voluntary muscle control of the elbow.

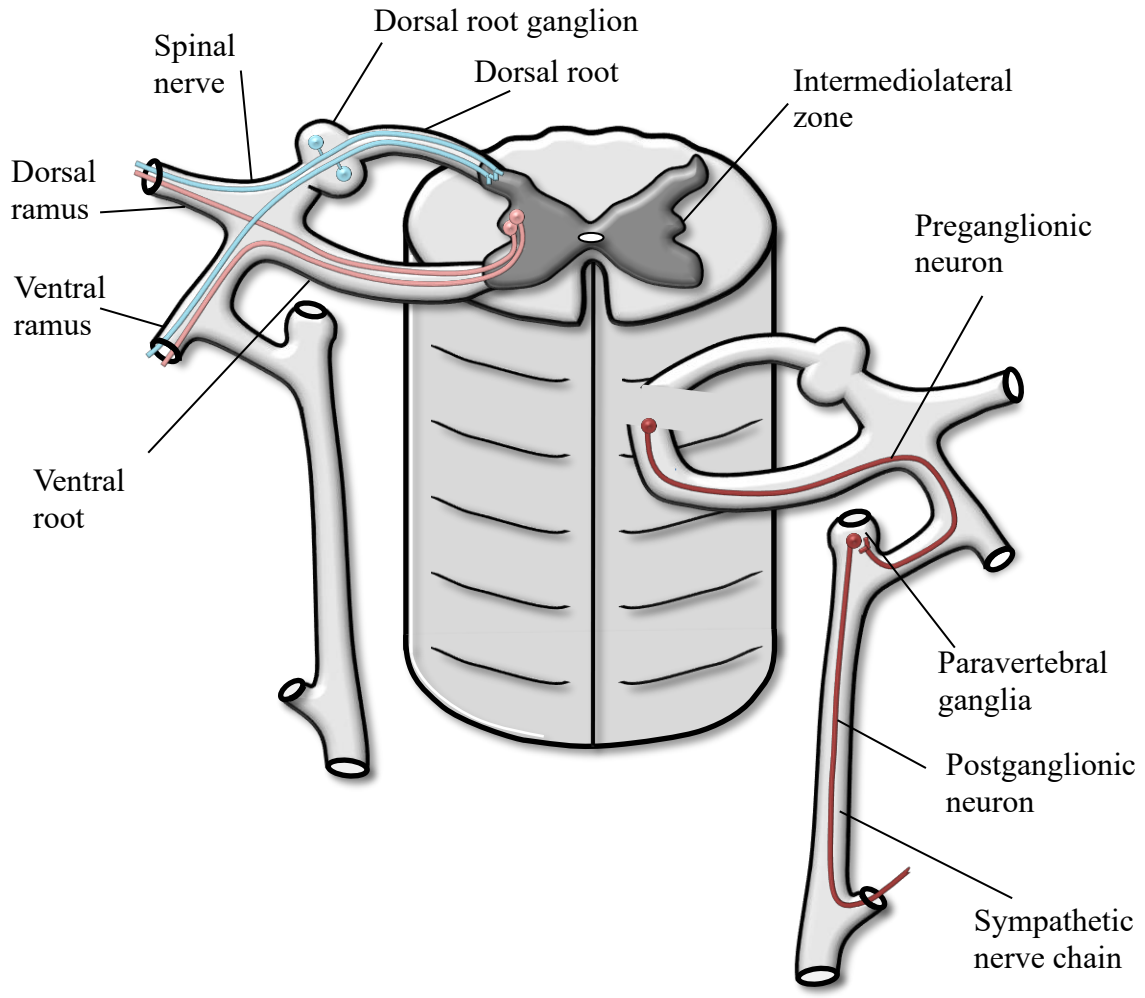

Figure 1.1: Schematic of spinal nerves, and the paravertebral sympathetic chain of the autonomic nervous system.

Like the brain, the spinal cord is a highly ordered organ. In addition to left-right, and rostral-caudal organization, the dorsal-ventral aspects of the spinal cord are crucial for understanding spinal cord function. The dorsal region of the spinal cord carries pathways involved in ascending proprioception and somatosensation from the skin and muscles, while the ventral region carries pathways involved in descending motor control. The cell bodies of the neurons in these pathways can be found in the GM, while the axons that propagate the action potential travel in WM. Unlike the brain, the spinal cord has its GM in the innermost region of the spinal cord, arranged in a butterfly-shaped manner, while the WM surrounds this GM core. Importantly, GM and WM volumes are not consistent along the length of the spinal cord: regions that innervate greater muscle mass also have greater volume of GM. Thus, the cervical and lumbar spinal cord

are thicker—i.e., cervical and lumbosacral enlargements—than the rest of the spinal cord as these regions innervate the arms (via the brachial plexus) and legs (via the lumbar plexus). Additionally, WM decreases with length as motor fibres exit the spinal cord; conversely, WM increases as the spinal cord ascends as sensory fibres enter the spinal cord.

The GM is organized in a laminar fashion, referred to as Rexed Laminae. Laminae I-VI comprise the dorsal horn, VII is the intermediate zone (or lateral horn in the thoracic and sacral regions), VIII and IX comprise the ventral horn, and X is the central GM surrounding the central canal (see Figure 1.2). Laminae I and V/VI are comprised of projection neurons whereas laminae II-IV, VII, and VIII are largely comprised of interneurons (Purves, 2008). Lamina VII specifically consists of motor interneurons and is responsible for coordinating activities of lower motor neurons, while lamina IX consists of lower motor neuron columns that govern limb musculature (Purves, 2008). Laminae I, II (also referred to as the substantia gelatinosa) and V/VI are sources of projection from the anterolateral system. Lamina II is involved in both the feedforward and feedback of pain, allowing for transmission and descending modulation of pain (Purves, 2008). Lamina VII contains projection neurons from the dorsal nucleus of Clarke (a spinocerebellar relay), as well as sympathetic preganglionic neurons of the interomediolateral cell column in the thoracic cord (T1-L2)—in the sacral cord (S2-S4), this region contains parasympathetic preganglionic neurons.

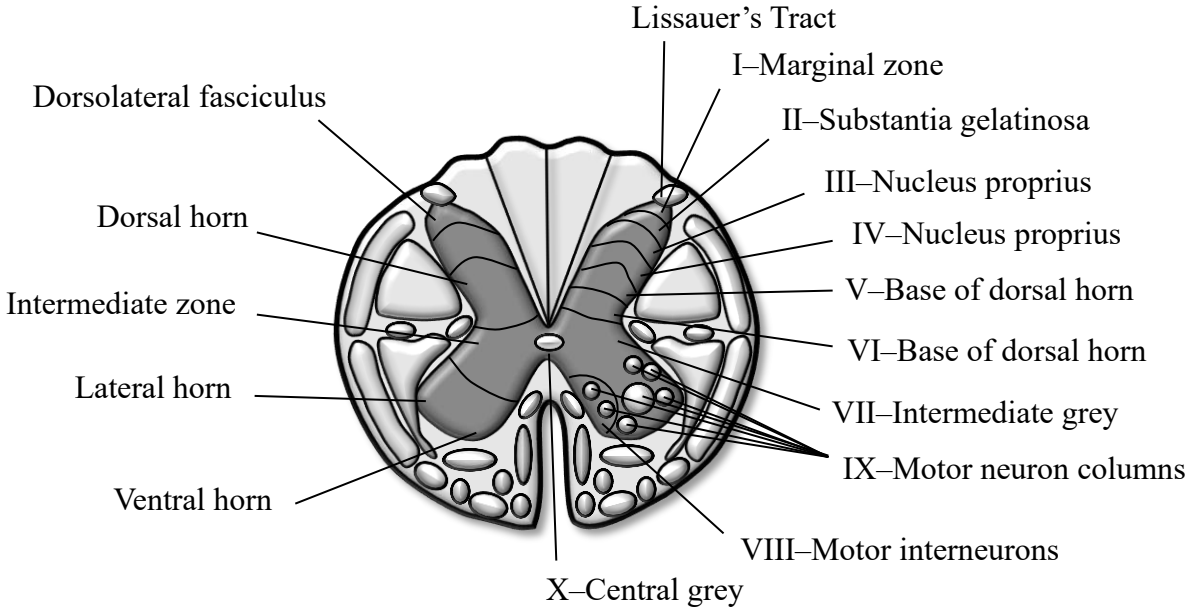

Figure 1.2: Spinal cord cross-section showing the ten Rexed Laminae.

In addition to GM organization, the WM also has laminar organization, allowing descending (ventral, motor) and ascending (dorsal, sensory) tracts to be arranged in a predictable manner, as discussed in the following sections (1.2.2.2 Descending Pathways and 0 Ascending Pathways). Dorsal (sensory) pathways can be conceptualized as a 3-neuron chain (Cramer & Darby, 2014): the cell body of the primary sensory neuron lies in the DRG outside of the spinal cord (recall Figure 1.1), with the dendrites arising from the tissues as sensory receptors and the axon synapsing with the secondary sensory neuron in the dorsal horn of the spinal cord. The cell body of the secondary sensory neuron lies in the dorsal horn of the spinal cord or the brainstem and projects upwards through the spinal cord. The tertiary sensory neuron lies within the brainstem, thalamus, or cerebellum—these ascending pathways are explained in more detail in section 0. The ventral (motor) pathways consist of 2 neurons: an upper motor neuron (UMN) with the cell body located in the motor cortex, and a lower motor neuron (LMN) located in the spinal cord, and extending to the target muscle group.

1.2.2.2 Descending Pathways

Descending pathways are responsible for movement and balance, as well as autonomic function, pain regulation, and autonomic-sensory integration. In fact, there is mounting evidence of continuous descending modulation of pain occurring in the spinal cord, even prior to noxious stimulation (Stroman, 2016; Stroman et al., 2016; Stroman, Ioachim, Powers, Staud, & Pukall, 2018). Although preganglionic neurons of the ANS also descend the spinal cord, discussion of these nerves is largely reserved for section 1.2.3 Autonomic Nervous System. These descending tracts include corticospinal, reticulospinal, vestibulospinal, rubrospinal, and tectospinal tracts (see Figure 1.3). Many of the descending pathways have collateral axons, allowing for multiple synapses from a neuron to facilitate multi-muscle functions, such as balance (Cramer & Darby, 2014).

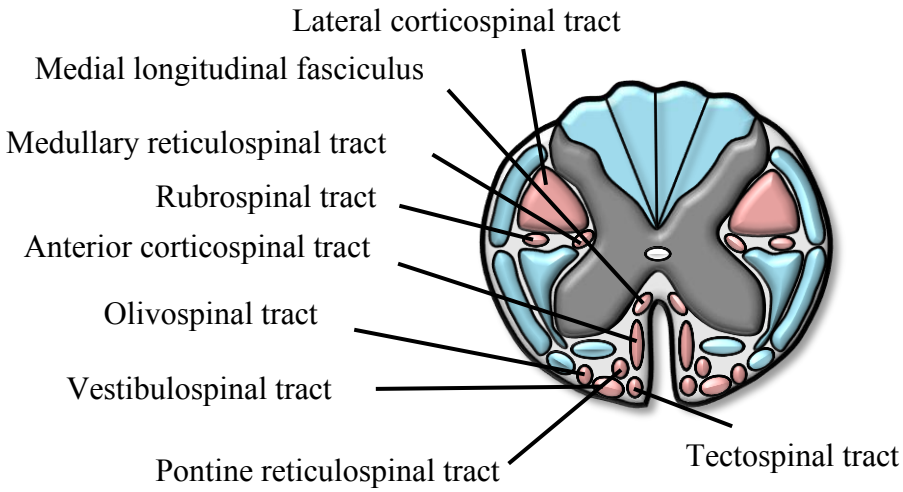

Figure 1.3: Cross-section of the descending pathways (in red) in the spinal cord.

The corticospinal tract (Figure 1.4) is a crucial tract for voluntary movement and is divided into ipsilateral (anterior) and contralateral (lateral) pathways. This tract arises from the primary sensory, motor, and premotor cortices, travels through the internal capsule, before travelling through the midbrain and pons (Purves, 2008). In the medulla, the tract diverges: approximately 85% of the fibres cross the midline at the pyramids (i.e., the decussation of the pyramids) to become the lateral corticospinal tract (Purves, 2008). This lateral tract innervates the limb musculature while the remaining fibres of the anterior corticospinal tract remain ipsilateral until they reach the target spinal cord level. Here, this tract innervates ipsilateral tissues, or collaterals cross the midline of the cord in the anterior white commissure to allow for bilateral innervation of axial and proximal limb musculature.

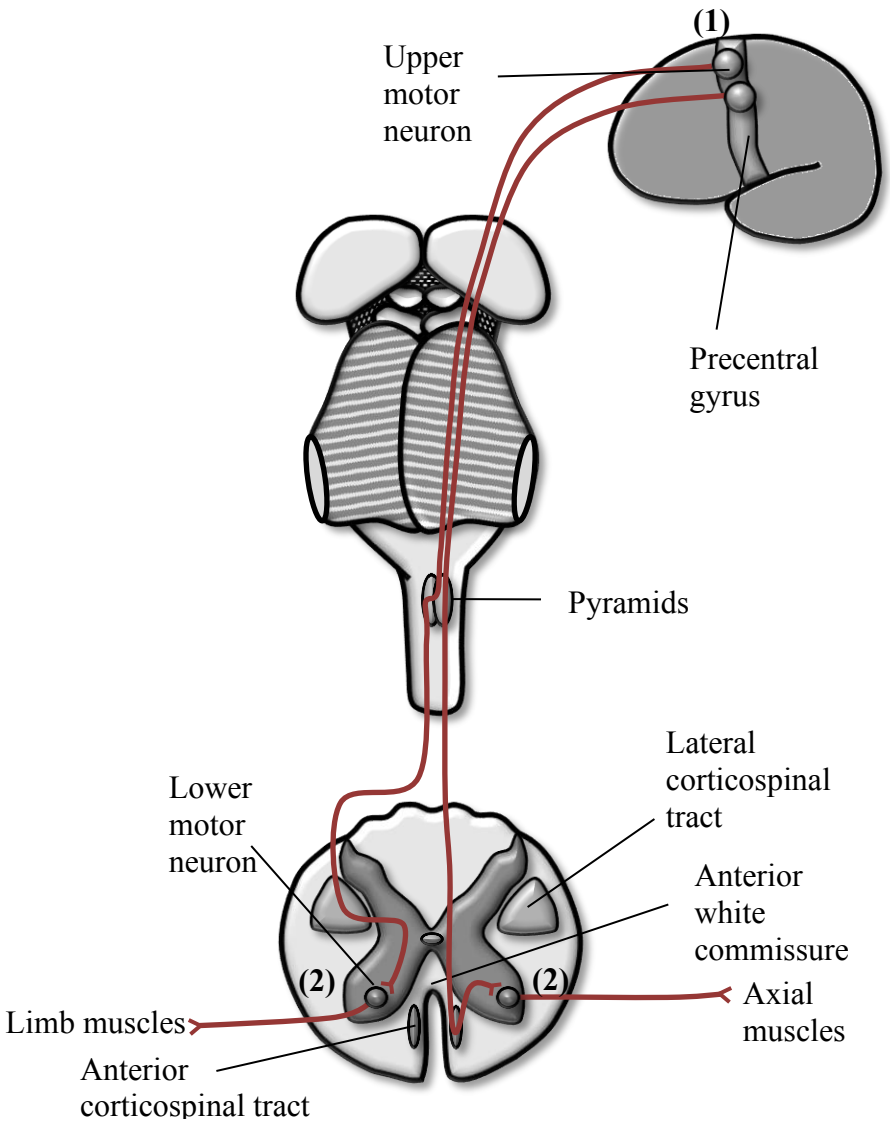

Figure 1.4: Corticospinal tract.

The reticulospinal tract is an ipsilateral tract, diverse in its function. This tract is important for motor control, as well as modulation of some autonomic and sensory functions (Mangold & Das, 2020). This tract incorporates sensory information such as visual, auditory, vestibular, and proprioceptive information to modulate balance, posture, and muscle tone (Mangold & Das, 2020). The reticulospinal tract can be divided into two divisions with distinct functions: the medullary and pontine reticulospinal tracts. The medullary reticulospinal tract is important for controlling and coordinating automatic motor patterns (such as walking), as well as the autonomic control of respiration (Mangold & Das, 2020), and receives cortical input via corticoreticular fibres (Cramer & Darby, 2014). From the medulla, this pathway continues in the ventral lateral WM before

innervating the tissues (Figure 1.5). The pontine reticulospinal tract helps stabilise the body's posture and balance, in anticipation of motor action and arises from the pons. From the pons, this tract travels through the medial ventral WM, before innervating axial and proximal muscle required for posture, and maintaining balance (Figure 1.5).

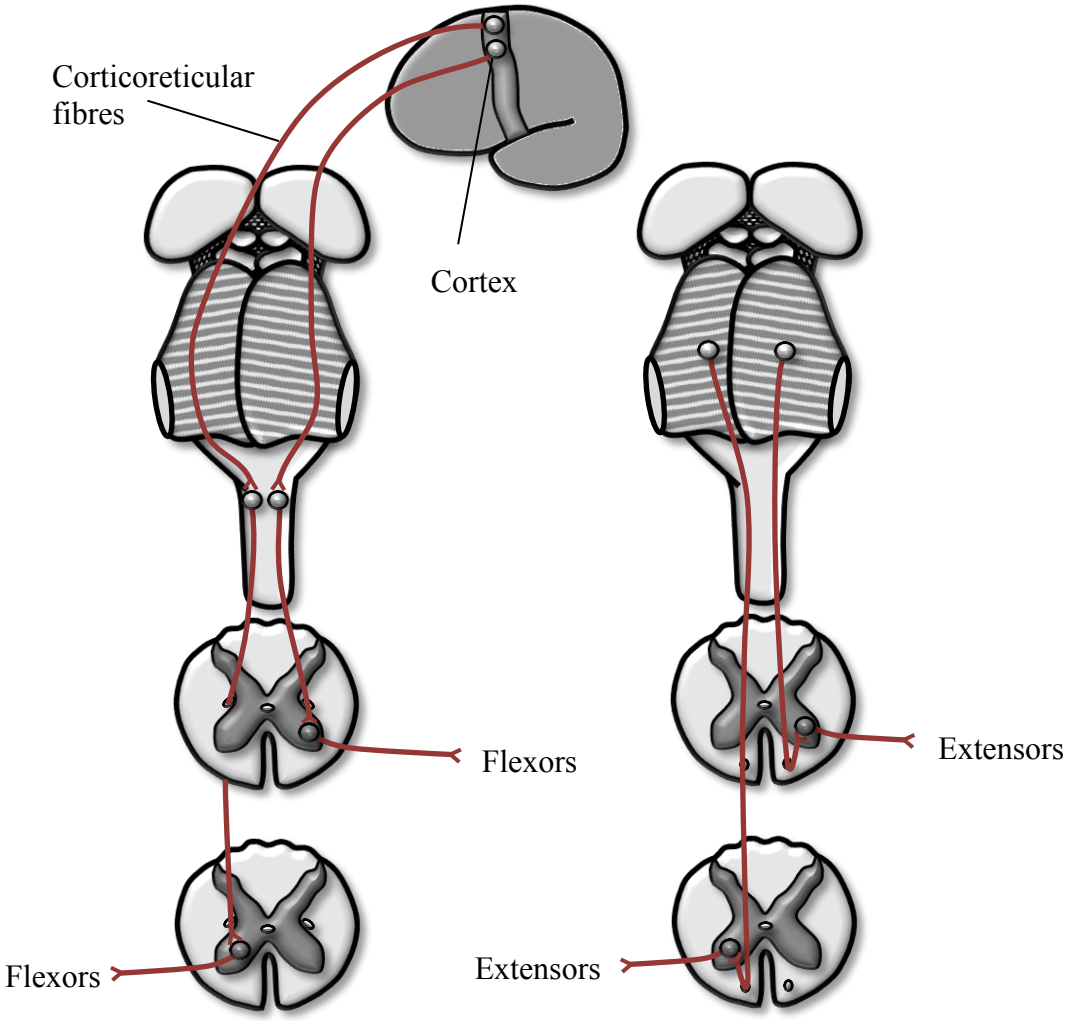

Figure 1.5: Medullary reticulospinal tract (left) and pontine reticulospinal tract (right).

The rubrospinal tract (Figure 1.6) originates in the red nucleus, and receives input from the motor cortex and the cerebellum (Cramer & Darby, 2014). The rubrospinal tract decussates immediately after leaving the red nucleus in the ventral tegmental decussation (Cramer & Darby, 2014), passing through the medial lateral white matter, ventral to the corticospinal tract (Cramer & Darby, 2014). The rubrospinal tract is only found in cervical and thoracic segments, and thus activates flexor muscles of only the upper limbs. Although this tract is highly important for other mammals, in humans the corticospinal tract is more developed; however, this tract "helps" the

lateral corticospinal tract and works to inhibit extensor motoneurons (Cramer & Darby, 2014; Purves, 2008).

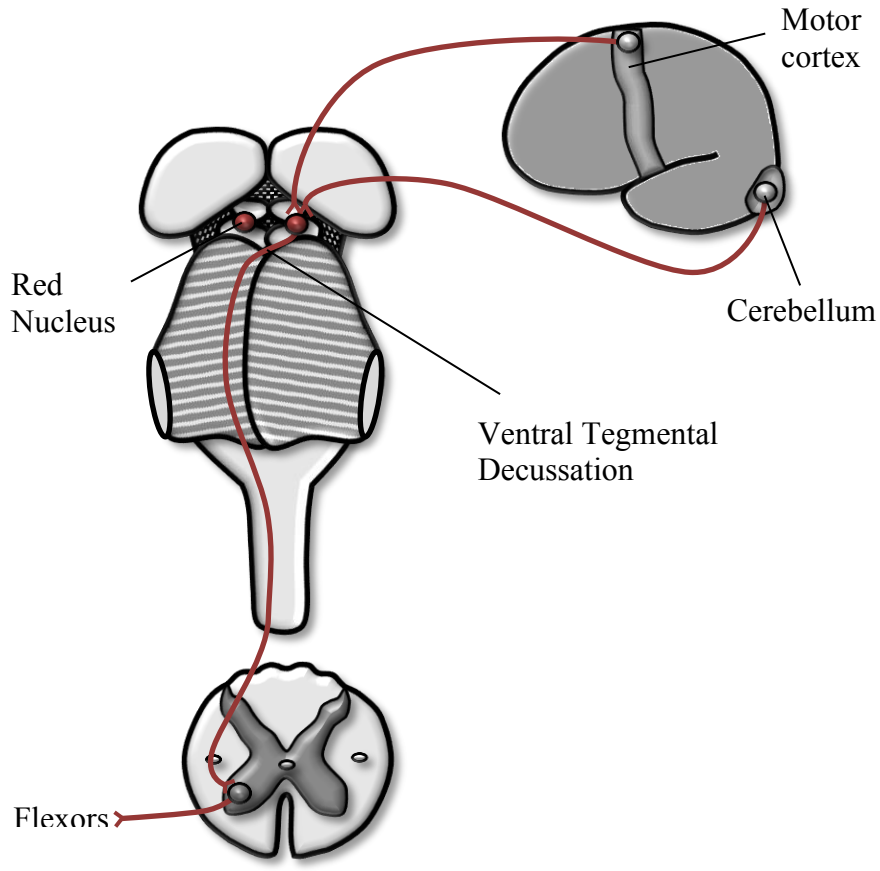

Figure 1.6: Rubrospinal tract.

The vestibulospinal tracts—both medial and lateral (Figure 1.7)—are ipsilateral tracts that help maintain balance and integration of some sensory-motor functions. These pathways are responsible for activating anti-gravity (i.e., extensor) muscles using input from the cerebellum and inner ear, which provides information regarding head tilt and acceleration, in addition to altering head position in relation to eye movements (Cramer & Darby, 2014). Interestingly, while the reticulospinal tracts act in an anticipatory fashion, the vestibulospinal tracts are reactive. For example, the action of these tracts helps a person to maintain their balance while slipping on an icy sidewalk. The medial aspect of this tract arises from the medial vestibular nucleus in the vestibular nuclear complex in the pontomedullary junction. This medial tract helps to maintain a stable image on the retina as the head moves and rotates by reflexively moving the head and neck. The lateral vestibulospinal tract, arising from the lateral vestibular nucleus, maintains balance and posture by activating axial and appendicular extensor musculature.

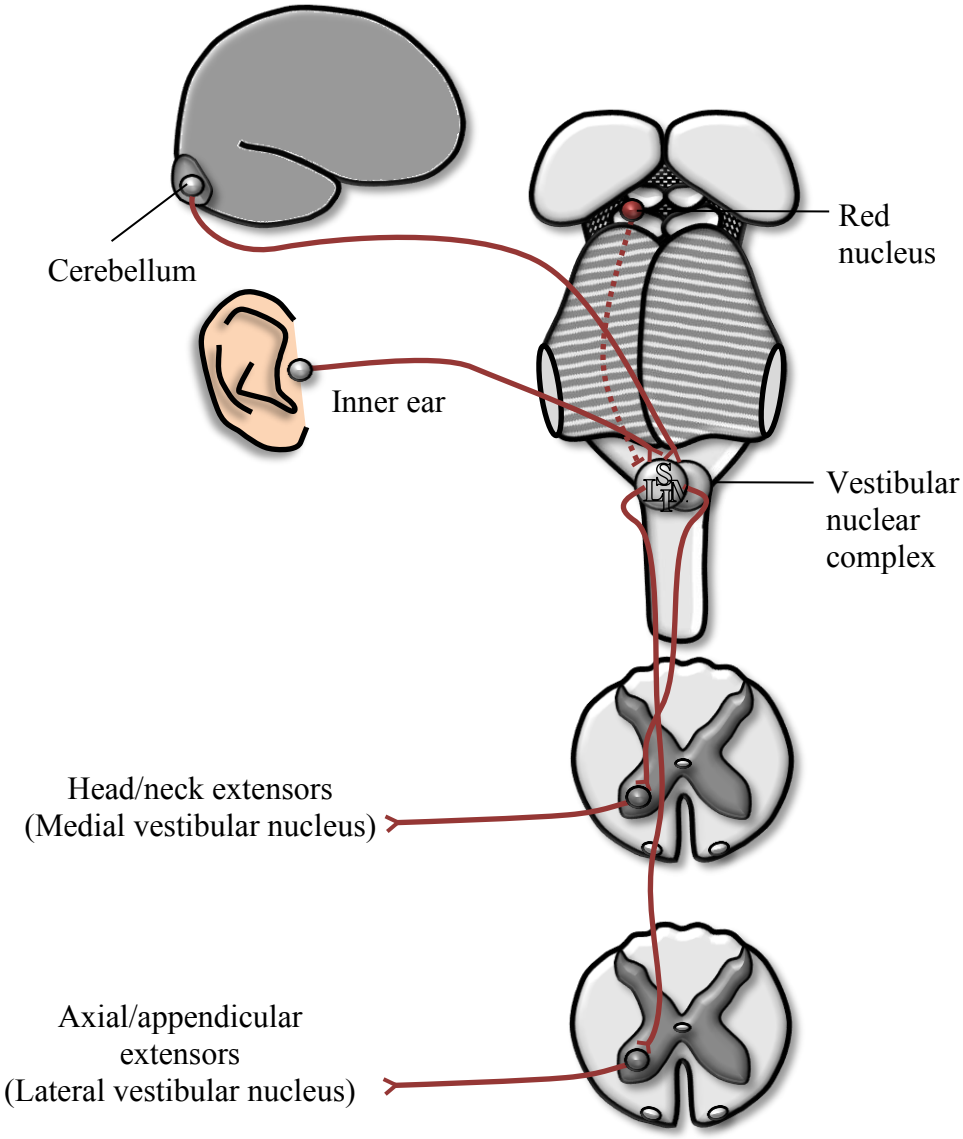

Figure 1.7: Vestibulospinal tract.

The tectospinal tract originates from the superior colliculus, after which it immediately decussates and travels in the medial ventral WM. This tract coordinates head and eye movements with sensory stimuli, and as such is relegated to the cervical and upper thoracic cord (Figure 1.8).

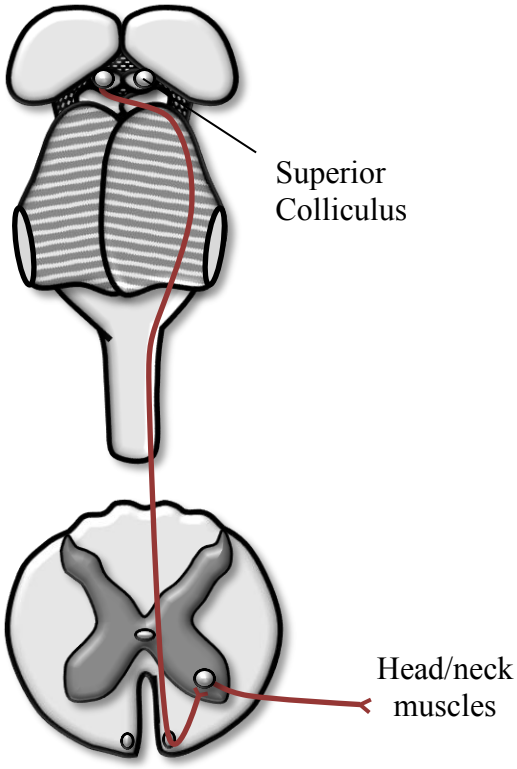

Figure 1.8: Tectospinal tract.

Finally, autonomic fibres descend the spinal cord from the hypothalamus and brainstem nuclei ipsilaterally in the intermediate gray (Cramer & Darby, 2014). These fibres synapse with preganglionic neurons in the thoracic and upper lumbar spinal cord, as well as the sacral spinal cord (Cramer & Darby, 2014); however, this is discussed in more detail in section 1.2.3.

1.2.2.3 Ascending Pathways

The ascending pathways of the spinal cord are those carrying somatosensation, proprioception, and nociception towards the brain from the periphery (Figure 1.9). The major sensory pathways from the body include the dorsal column/medial lemniscal pathway and the lateral and anterior anterolateral/spinothalamic pathways. Two additional complementary pathways include the dorsal and ventral spinocerebellar tracts.

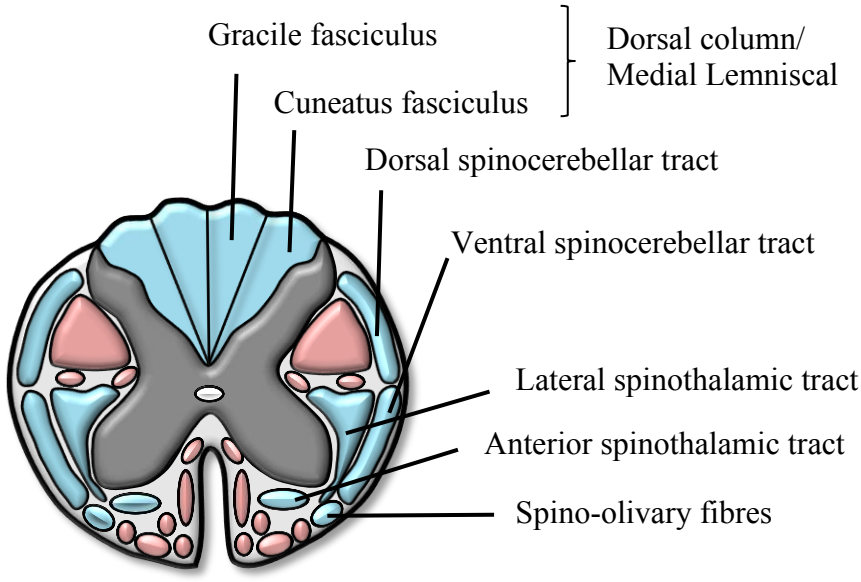

Figure 1.9: Cross-section of the ascending pathways (in blue) in the spinal cord.

The dorsal column/medial lemniscal pathway carries sensory information including conscious proprioception (i.e., knowledge of limb position), tactile, pressure, vibration sensations, and two-point discrimination. As the tract ascends in the body, additional regions are added from medial to lateral so that lower limb sensory information ascends medially (fasciculus gracilus) and upper limb sensory information ascends more laterally (fasciculus cuneatus). The axons of these primary sensory neurons travel ipsilaterally from its origin in the DRG until they reach the cuneate or gracile nuclei in the medulla. From these nuclei, the secondary sensory neurons decussate at the lemniscal decussation before synapsing in the VPL nucleus of the thalamus. From here, the tertiary sensory neuron continues to the postcentral gyrus (Figure 1.10).

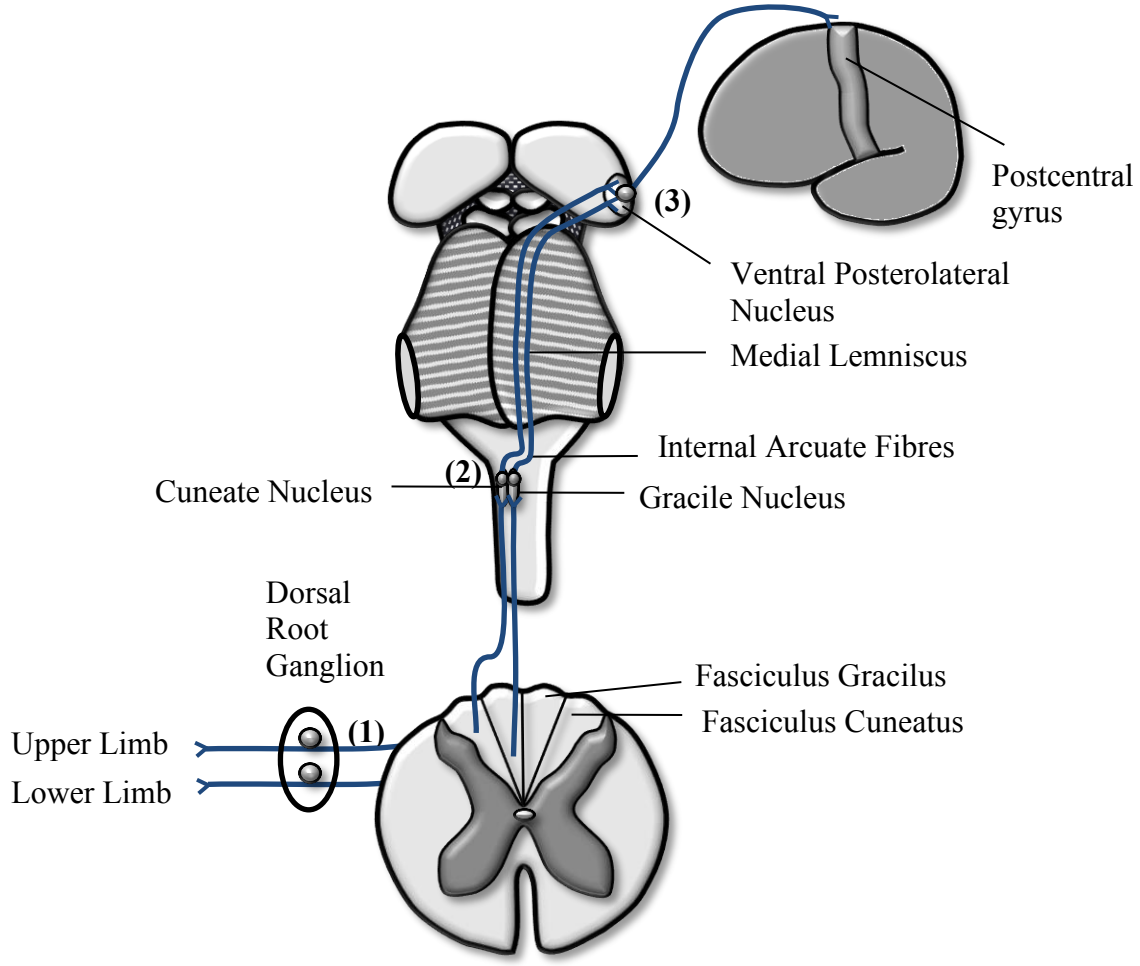

Figure 1.10: Medial lemniscal/dorsal column pathway. The numbers indicate the location of primary, secondary, and tertiary sensory neurons.

The spinothalamic tract carries information regarding pain, temperature, and deep touch. The primary sensory neurons project through the dorsal root and often ascend or descend in Lissauer's tract for a few segments before synapsing in Rexed laminae I or II (Figure 1.11). The secondary sensory neurons decussate in the ventral white commissure and continue ascending in the anterior or lateral spinothalamic tract, until it synapses in the VPL. Like the medial lemniscal tract, the tertiary sensory neurons project to the postcentral gyrus. Interestingly, the spinothalamic tract is organized opposite of the medial lemniscal pathway: inferior regions are represented laterally, with rostral regions joining the tract medially.

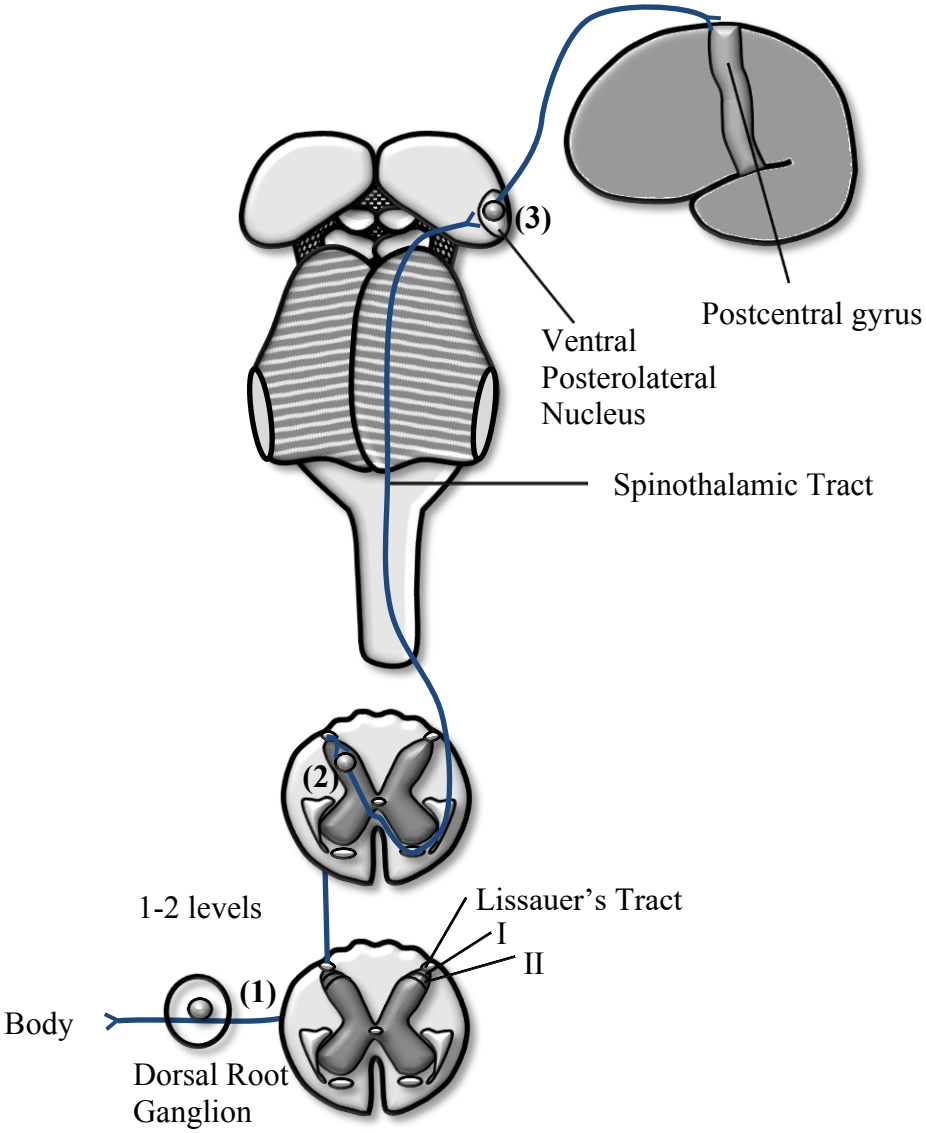

Figure 1.11: Spinothalamic Tract. The numbers indicate the location of primary, secondary, and tertiary sensory neurons.

The dorsal and ventral spinocerebellar tracts (Figure 1.12) and the spino-olivary tract (Figure 1.13) provide proprioceptive information from muscles, Golgi tendon organs, and joints, of primarily lower limbs (spinal cord levels T1-L2 via dorsal and L2/3 to coccygeal via ventral spinocerebellar tracts), directly to the cerebellum. Although all of these tracts end up sending information to the ipsilateral cerebellum, both the ventral spinocerebellar and the spino-olivary tracts cross the midline twice: once at the level of entry into the spinal cord, and again at either the medulla via the inferior cerebellar peduncle (ICP; spino-olivary tract; Cramer & Darby, 2014), or at the level of the midbrain via the superior cerebellar peduncle (SCP; ventral spinocerebellar

tract). The dorsal spinocerebellar tract is a true ipsilateral pathway that enters the cerebellum via the ICP. The spino-olivary fibres compose a minor tract involved with proprioception and synapse in the inferior olivary nucleus, before reaching the cerebellum (Cramer & Darby, 2014).

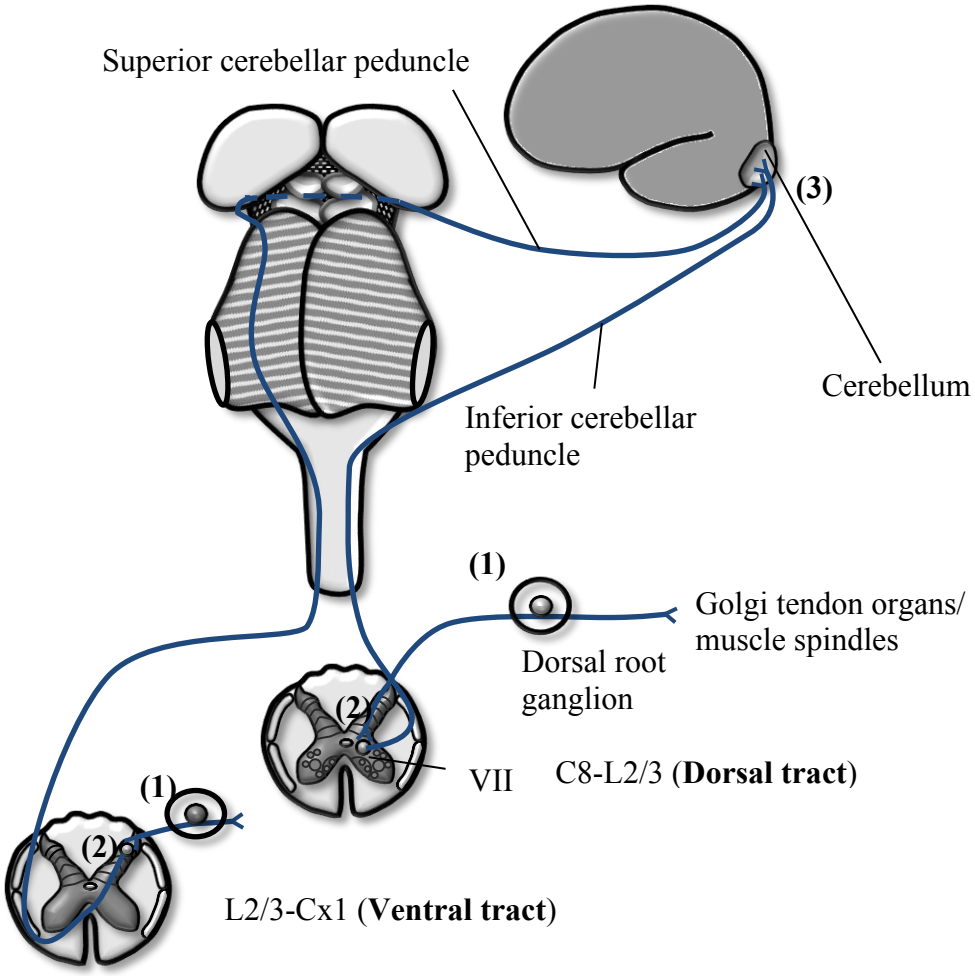

Figure 1.12: Dorsal and ventral spinocerebellar tracts (SCT). L2/3-Cx1 = lumbar spinal cord segments 2/3 to coccygeal segment 1; C8-L2/3 = cervical spinal cord segment 8 to lumbar segments 2/3; VII = Rexed laminae VII.

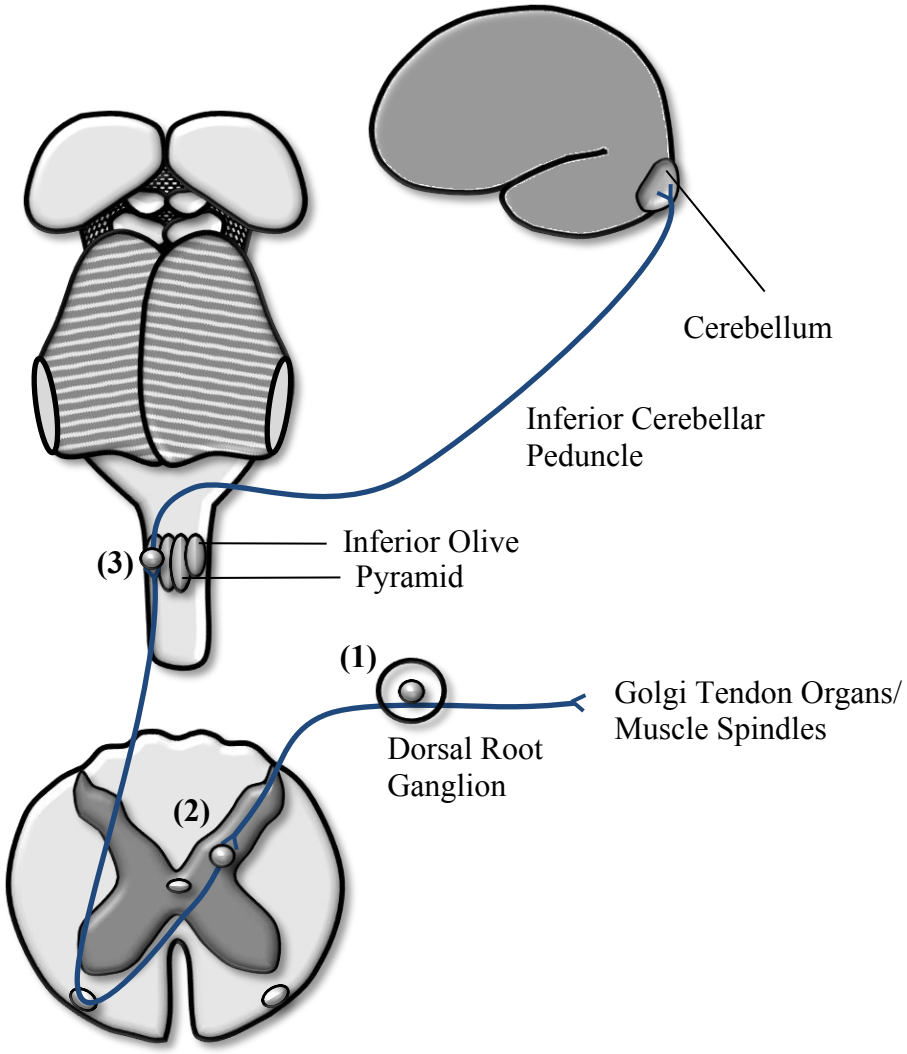

Figure 1.13: Spino-olivary tract.

Although fMRI of the spinal cord will not be able to definitively identify which ascending or descending pathways are implicated in GAD, it is important to understand which ones are more or less likely to be involved, based on the quadrant of the spinal cord implicated. For example, because increased muscle tension is a common and consistent finding in GAD, descending tracts such as the corticospinal (i.e., voluntary movement) and reticulospinal tracts (i.e., voluntary movement and integration of visual stimuli and muscle tone) are likely to be involved. However, the vestibulospinal tracts, because they tend to be more reactionary (e.g., correcting balance on an icy sidewalk) than anticipatory, they will not likely be observed in our study, as participants will be lying supine in the MRI scanner. Additionally, in response to the motor act of increasing muscle tone that may occur, sensory feedback of this tension is also likely to occur, which is carried via

the dorsal column/medial lemniscal pathways in the dorsal horn. Input from the spinothalamic tract is also possible if muscle tension increases to the point of pain; however, unless participants experience increased pain in response negative emotion-evoking stimuli, these effects are likely to cancel-out. Finally, as the ANS may play a role in GAD, autonomic fibres may also contribute to increased neural activity in the thoracic spinal cord.

1.2.3 Autonomic Nervous System

The ANS is a system crucial for animal survival—without it, animals would be unable to defend themselves, do physically demanding tasks, regulate body temperature, and regulate glucose availability: all functions that mammals depend on for maintaining homeostasis. The ANS is largely controlled by the hypothalamus, which is crucial for regulating physiological responses in reaction to emotional and behavioural responses. For example, feelings such as fear or happiness are associated with recognizable physiological responses, and are often accompanied by recognizable behaviours. The ANS controls cardiac and smooth muscle, as well as exocrine glands, and although the ANS is considered a motor system, it is important to recognize that it is separate from, and has many more neurons than the voluntary, somatic motor system discussed in section 1.2.1.3, although it is important that these systems work in tandem.

The ANS can be divided into three divisions: sympathetic, parasympathetic, and enteric. While the enteric division is the largest and most complex division of the ANS, it is beyond the scope of the current thesis. Suffice it to say that this system controls the entire gastrointestinal system, and many parts of it function largely without input from other nervous system components. The SNS is responsible for the “fight-or-flight” response which, for example, increases heart rate and blood pressure, alters sweat and arrector pili muscle levels to control body temperature, dilates pupils, and mobilises blood sugar and reduces glandular output. The parasympathetic nervous system is responsible for “rest-and-digest” functions. These functions include reducing heart rate, constricting pupils, and increased secretion of digestive enzymes. Although the ANS may often mistakenly be highlighted for its role in extreme cases, such as avoiding danger, it is crucially important to daily homeostatic demands. Clearly, the sympathetic and parasympathetic divisions play opposing roles, which help to maintain homeostasis. Another thing to keep in mind about these systems is that the sympathetic division has a much more global role in the body as it innervates sweat glands, arrector pili muscles (allowing for goosebumps), and local vasculature in

the tissues. The parasympathetic division has a more centralized role and has a much more limited reach in terms of its target tissues.

The autonomic motor system consists of a specialized two neuron chain, containing preganglionic and postganglionic neurons. Preganglionic cell bodies are located in the CNS—in the brainstem or sacral spinal cord (S2-S4) for the parasympathetic division, and in the interomediolateral cell column of the thoracic and upper lumbar spinal cord (T1-L3) for the sympathetic division. Postganglionic neurons are located in the peripheral nervous system (PNS), in autonomic ganglia. Postganglionic neurons are typically unmyelinated and are considered motor neurons—unlike somatic motor neurons, there are no specialized postsynaptic endings in postganglionic neurons (Hamill, Shapiro, & Vizzard, 2011). Instead, nerve endings have swellings called varicosities, which have transmitter-filled vesicles (Hamill et al., 2011). Additionally, synaptic transmission occurs in multiple sites along the branched axon terminals, and can rely on diffusion up to several hundred nanometers to allow more diffuse control than somatic motor neurons which rely on a motor end plate for successful transmission (Hamill et al., 2011). Importantly, some sensory fibres project to the CNS, and to autonomic ganglia to allow autonomic reflexes to occur.

Preganglionic neurons leave the spinal cord at the same level as the cell body via ventral roots—alongside somatic lower motor neurons—briefly running together with the spinal nerve, before projecting via white (myelinated) communicating rami (Purves, 2008), and synapsing in one of several locations: paravertebral and prevertebral ganglia (sympathetic), and cranial and terminal ganglia (parasympathetic). The parasympathetic preganglionic neurons synapse in the cranial ganglia, associated with the head and its digestion and glandular functions, or terminal ganglia, located near their target organs. The paravertebral ganglia are connected by fibres to form the sympathetic nerve trunk/chain (recall Figure 1.1). Paravertebral ganglia are arranged segmentally and run along both sides of the vertebral column from C1-S5 segments. Although the preganglionic axons exit the spinal cord at the level of the cell body, they may innervate ganglia in the sympathetic chain either caudally or rostrally by travelling through the sympathetic nerve trunk until they reach the appropriate ganglion (Hamill et al., 2011). Sympathetic postganglionic neurons exit the ganglion in grey (unmyelinated) communicating rami and travel via spinal nerves to the target tissues (Purves, 2008). Postganglionic neurons arising from the paravertebral ganglia provide sympathetic innervation for all vaso-, sudo-, and pilomotion—or blood vessel

constriction/relaxation, sweat, and arrector pili muscle contraction/relaxation (i.e., goosebumps). Preganglionic neurons can also bypass synapsing in the paravertebral ganglia and instead travel via splanchnic nerves to synapse in prevertebral ganglia (Purves, 2008), or directly in the adrenal medulla, which releases epinephrine and norepinephrine. Prevertebral ganglia are unpaired ganglia located anterior to the vertebral column (Hamill et al., 2011)—the postganglionic neurons of these ganglia provide sympathetic innervation to and receive sensory feedback from the abdominal and pelvic viscera.

While the basic concepts of pre- and postganglionic neurons are the same between sympathetic and parasympathetic divisions, there are many important differences between them. Sympathetic preganglionic neurons are typically shorter than their postganglionic neurons as the ganglia lie close to the spinal cord (in para- and prevertebral ganglia) and further away from the target tissues. The opposite is true of parasympathetic neurons: preganglionic neurons are further from the ganglia than are the target tissues. Additionally, sympathetic ganglia regulate many targets and thus typically have a much higher ratio of postganglionic neurons to preganglionic neurons while parasympathetic ganglia typically regulate a single target. Both parasympathetic and sympathetic preganglionic neurons release acetylcholine at the ganglion; however, parasympathetic postganglionic neurons also release acetylcholine while sympathetic postganglionic neurons release norepinephrine at the target tissue. Both sympathetic and parasympathetic neurons can also release co-transmitters, such as peptides or nitric oxide. These co-transmitters, along with a variety of receptor type at the ganglia and target tissue allow for highly complex responses in these tissues.

The balance of sympathetic and parasympathetic divisions of the ANS is regulated by the central autonomic network, largely controlled by the hypothalamus. This central network consists of highly interconnected nuclei in the brain and brainstem that work together to coordinate a variety of different functions. The nucleus of the solitary tract (NST) has two key functions: integrating ANS function with the endocrine system and behaviour, and influencing regions that control and coordinate autonomic reflexes such as cardiac and gastrointestinal vagal tone. The NST receives input from several cranial nuclei and projects to regions involved in regulating blood flow in vascular beds to regulate blood pressure. Specifically, the NST projects to the parabrachial nucleus, hypothalamus, autonomic centres and preganglionic neurons in the brainstem and spinal cord (Purves, 2008). The parabrachial nucleus acts as a relay for information from NST to the

frontal cortex and insula, and projects to the hypothalamus, amygdala, and thalamus, and is responsible for coordinating behavioural responses to taste and visceral sensations (Purves, 2008). This nucleus sends information to the periaqueductal grey (PAG; Tryon & Mizumori, 2018) which produces behaviourally coordinated patterns associated with ANS function. The PAG also receives input from the hypothalamus and sends its information to the reticular formation (Purves, 2008). The amygdala, receiving input from the cortex and central autonomic network (including the NST and parabrachial nucleus; Purves, 2008) is important for regulating the parts of conditioned behavioural responses, related to the ANS, such as the autonomic responses associated with fear learning. The outputs of the amygdala include the hypothalamus and lower brainstem.

Finally, the hypothalamus, one of the most important ANS structures is responsible for maintaining homeostasis in the body and is the principal endocrine regulator of the ANS. The hypothalamus is crucial for maintaining homeostatic functions of temperature control, blood pressure, and eating/satiety mechanisms. The hypothalamus regulates the pituitary gland, responsible for the majority of endocrine function. The pituitary gland controls endocrine function both directly (via the posterior pituitary, also known as the neurohypophysis) and indirectly (via the anterior pituitary, also known as the adenohypophysis). The neurohypophysis has axons, extending from cells in the hypothalamus via the hypothalamo-hypophyseal tract that secrete hormones into the capillary bed of the posterior pituitary, including oxytocin and vasopressin (or antidiuretic hormone [ADH]). The hypothalamus indirectly influences the anterior pituitary gland by secreting regulating factors—either releasing or release-inhibiting factors—into the capillary bed (via the hypophyseal portal system) near the adenohypophysis. These hypothalamic factors thus regulate the hormones released from the anterior pituitary. The anterior pituitary hormones are important for many metabolic functions, including growth, thermogenesis, reproduction, as well as the body's stress response.

When the body is under stress, the hypothalamus releases corticotropin-releasing hormone (CRH) and ADH. The release of CRH causes adrenocorticotropic hormone (ACTH) to be released from the anterior pituitary. ACTH acts on the adrenal medulla above the kidneys to release stress hormones (cortisol, epinephrine, and norepinephrine), while ADH causes vasoconstriction, and water resorption by the kidneys to increase blood pressure. Acting in a negative-feedback loop, high levels of cortisol cause the hypothalamus to reduce the output of CRH, while low cortisol levels cause increased CRH release (Chrousos, 1998).

Around the mid-twentieth century, Hans Selye began investigating the phenomenon of the stress response and its interactions with the immune system (Chrousos, 1998; Selye, 1976). While key mediators of the immune system activate the CRH stress response pathway, the CRH pathway—specifically cortisol—suppresses immune function (Chrousos, 1998). Of note, individuals with a chronically increased hypothalamic pituitary adrenal axis response tend to exhibit physical health issues such as diabetes mellitus, gastrointestinal disease, hyperthyroidism, osteoporosis, and cardiovascular disease (Chrousos, 1998)—many of which are comorbid with mental disorders.

Based on this understanding of CNS anatomy, coupled with the heightened response to threat observed for patients with GAD, hypothesis formulation regarding neural activity differences between those with and those without chronic anxiety can begin. While we can expect that patients with GAD will have altered responses throughout the frontal lobe, associated structures, and ANS, we need a tool that will allow us to non-invasively investigate these neural differences, as well as help refine these hypotheses, based on previous research. Such a tool—magnetic resonance imaging (MRI)—has been developed and has been in use to investigate neural functioning for several decades.

1.3 Magnetic Resonance Imaging

MRI has become an increasingly important tool in medicine and research since the discovery of its underlying principles in the mid-twentieth century (Bloch, 1946; Purcell, Torrey, & Pound, 1946) and its subsequent application in image creation (Damadian, 1971; Lauterbur, 1973; Mansfield & Grannell, 1973). With the advent and widespread availability of MRI, its uses range from diagnosing disease to endeavoring to understand the human mind. MRI is a vastly complex technology and relies heavily on math and physics to measure signals and construct, rather than capture images. Below is a brief introduction of MR image construction and the underlying principles used to collect functional MRI (fMRI) data (largely from Huettel, Song, & McCarthy, 2014; Plewes & Kucharczyk, 2012).

1.3.1 MRI Physics

MRI relies on the underlying physical properties of elements in order to create images. Nuclei with odd numbers of protons and/or neutrons (most commonly Hydrogen, with a single proton) have a magnetic dipole moment and angular momentum. This is useful in MRI because, when placed in an external magnetic field (B_0, measured in Tesla [T]) they will precess (i.e., rotate and spin) about B_0 at a known frequency, called the Larmor frequency (Equation 1). The rate of precession around B_0 (ω_0) is determined by the gyromagnetic ratio (γ), which is an inherent property of the nucleus, and the magnetic field strength (B_0).

$$\omega_0 = \gamma B_0$$

Equation 1: Larmor frequency calculation.

At equilibrium, the slight majority of protons precess parallel to B_0 as this is a lower-energy state, compared to the higher-energy antiparallel state. This slight majority of parallel precessing protons results in a net magnetic vector aligned with B_0, (i.e., in a longitudinal direction). Energy added to the system via radiofrequency (RF) magnetic pulses causes protons precessing at the Larmor frequency to come into phase with one another and flip from the low-energy parallel state to the higher-energy antiparallel state. Therefore, the net magnetic vector is tipped away from the longitudinal axis toward the transverse plane, and the amount of net transverse magnetization can be measured since the MR signal is created as the net magnetic vector sweeps past a nearby receiver coil, inducing a current in the coil. However, after the RF pulse is turned off, longitudinal and transverse relaxation occur. Longitudinal relaxation is the return of net magnetization to the longitudinal vector and occurs as the slight majority of protons once again precess parallel to B_0. This longitudinal relaxation is described by the T_1 time constant, which is the time needed to reach 63% of the longitudinal magnetization observed at equilibrium. Transverse relaxation refers to the loss of net transverse magnetization, and this occurs more rapidly than longitudinal relaxation due to the additional loss of phase coherence between spins (resulting from different precession frequencies) once the RF excitation pulse is turned off. This transverse relaxation is described by the T_2 time constant, which is the time needed to reduce the transverse magnetization to 37% of its maximum value. Moreover, while T_2 is related to time-varying changes that occur at the atomic/molecular level (referred to as "true T_2"), T_2* denotes the additional effects of field inhomogeneities (e.g., susceptibility-induced field distortions produced by neighbouring tissues, etc., and is referred to as "observed T_2") and is therefore always shorter than T_2. Thus, the

relaxation rate of T_2^* is the sum of the relaxation rates of T_2 and the relaxation rate associated with field inhomogeneities ($\frac{1}{T_2^*} = \frac{1}{T_2} + \frac{1}{T_2'}$). T_2^*-weighting is commonly used for blood oxygenation level-dependent (BOLD) imaging (see section 1.3.2.1).

Now that we understand how an MR signal is created, we can discuss how to make this signal spatially meaningful. Spatial encoding is done by applying magnetic field gradients in addition to B_0, in order to predictably alter the local magnetic field (and therefore the Larmor frequency) along the x, y, and z directions. The term "pulse sequence" refers to the order, direction, and magnitude of RF pulse(s) and magnetic field gradients that are applied to spatially-encoded MRI signals. In conventional 3D MR imaging, sequences typically consist of three spatial-encoding steps: slice selection, phase encoding, and frequency encoding. During slice selection, the protons in a 'slab' of tissue (i.e., a slice) are selectively excited by using a magnetic gradient to manipulate the Larmor frequency of spins along a certain direction immediately before (or during) the RF excitation pulse. Importantly, only protons precessing at the same (resonant) frequency as the RF pulse will absorb this energy, and cause protons to flip from their low-energy (parallel to B_0) state into the high-energy (antiparallel to B_0) state. Thus, MR signal will only be produced within a specific on-resonance slice.

Although a MR signal can now be attributed to a slice of the brain, this information is not overly useful until more precise spatial encoding is applied to distinguish signals in the other two dimensions. Additional gradients, called the frequency-encoding and phase-encoding gradients, are therefore applied immediately following the RF excitation pulse and a slice-rewind gradient (to undo the effects of the initial slice select gradient). Within the selected slice, an orthogonal frequency-encoding gradient is applied to vary the magnetic field strength, which in turn varies the precession frequency of protons within the slice. In simple sequences, the MR signal is then measured during the frequency-encoding step. However, prior to this, a phase encoding gradient is applied along a different direction. This phase encoding gradient causes the protons to precess at a different rate, based on spatial location, and thus results in the protons being in different phases by the time the frequency-encoding gradient is applied. By taking measurements with different combinations of phase- and frequency-encoding, a 2D image of the slice can eventually be generated, and by then repeating this process across multiple slices, it is possible to build up a 3D image of the entire brain (i.e., a volume).

Now that MR signal can be localized, another important component of useful MR images is contrast (e.g., being able to see differences between tissues in the same image, or differences within tissues across time). Since different tissues have different magnetic properties, we can change certain parameters, such as repetition time (TR) and echo time (TE) to create different types of contrast. TR is the amount of time between successive RF excitation pulses and therefore affects the amount of steady state longitudinal magnetization, depending on the T_1 relaxation times of different tissues. TE is the time between the RF pulse and the data acquisition (i.e., when the peak signal or "echo" is detected in a receiver coil) and is related to the T_2 relaxation times of different tissues. TR and TE can be chosen depending on the desired amount of T_1 and/or T_2 contrast, respectively. For example, a long TR would minimize the amount of T_1 contrast because it would allow full recovery of the longitudinal magnetic vector. To minimize T_2 contrast, a short TE would be required to limit the signal decay as a result of dephasing.

Finally, although there are many different pulse sequences, these can mostly be divided into gradient-echo (GE) sequences and spin-echo (SE) sequences. In a simple case, the MR signal decays exponentially over time due to free induction decay (FID). GE sequences manipulate the FID to maximize signal. This is done by applying a dephasing gradient to accelerate the dephasing of protons (i.e., accelerate the loss of signal), followed by a rephasing gradient of the same strength, but opposite polarity. Since the MR signal is strongest when protons are in phase, this manipulation "recalls" the signal initially produced by returning the phase coherence to the protons, but at a later point in time. While a single RF pulse creates an FID, two successive RF pulses create a spin echo (SE). Initially, a 90° excitation pulse is produced to tip the net magnetization vector towards the transverse plane. As longitudinal and transverse relaxation begin, a 180° pulse is applied which flips the protons across the axis, resulting in a regeneration of phase information, and thus a strong signal. Although often conceptualized as a 90° excitation pulse, followed by a 180° refocussing pulse, these values can vary in practice. Importantly, the gradient reversal in GE sequences only acts upon spins that have been dephased by the gradient, meaning that magnetic field inhomogeneities and tissue susceptibilities (which are static dephasing effects) are not affected using this approach. However, in SE sequences, the second RF pulse rephrases spins that were dephased due to these static dephasing effects, which 'cancels out' field inhomogeneities and magnetic susceptibilities (Jung & Weigel, 2013). Thus, because GE sequences include both static

(T_2) and time-varying (T_2') dephasing effects, the weighting is primarily T_2*, while the weighting of SE sequences is T_2.

1.3.2 Functional MRI

1.3.2.1 BOLD Imaging

There are different ways to use MRI to obtain functional brain imaging data. The most common mechanism used for fMRI is the BOLD signal, which arises from the hemodynamic response (Kwong et al., 1992; Ogawa et al., 1992). Neurons require O_2 for their metabolic processes, which is provided in excess by the local vasculature after neurons are active (Logothetis, 2008). This is where magnetic susceptibility becomes important: oxygenated hemoglobin (HbO) and deoxygenated hemoglobin (HbR) have different magnetic properties—HbO is diamagnetic, while HbR is paramagnetic (Pauling & Coryell, 1936). This means that HbR distorts the magnetic field, resulting in a change in the field strength of the surrounding protons, and thus altering the precession frequency. This change in precession frequency translates to a quicker dephasing of the local protons, resulting in a shorter T_2^* compared to tissues with higher concentrations of HbO (Logothetis, 2008). Tissues that are active require increased HbO for their metabolic needs; however, the supply of HbO to these tissues is overabundant, meaning that the T_2^*-relaxation time increases and T_2^*-weighted MR signals in those regions (and the downstream venules and veins) are increased compared to baseline conditions (Logothetis, 2008). Finally, it is crucial to understand that functional neuroimaging is an indirect method for inferring neuronal function, because by its nature it depends upon more global hemodynamic factors than, for example, single cell recordings of electrochemical potentials within individual neurons (Figley & Stroman, 2011). In summary, the BOLD signal reflects changes in metabolic demand of neural tissues by measuring spatiotemporal changes in blood oxygenation following either intrinsic (i.e., resting-state) or task-related neural activity. Clearly, acquiring fMRI data is a complex process; however, there are additional challenges to using MRI techniques that must be understood and addressed before conducting research using fMRI technology.

1.3.2.2 Spinal Cord-Specific fMRI Challenges

In addition to these general MRI data challenges, there are several more that are specific to imaging the spinal cord, making its acquisition and analysis even more difficult. Typically, brain fMRI data is acquired using GE echo planar imaging (GE-EPI) sequence; however, these sequences present some challenges in the spinal cord, such as severe spatial distortions (Powers,

Ioachim, & Stroman, 2018). As GE-EPI sequences are more sensitive to T_2^* imaging, they are more susceptible to tissue inhomogeneities, which are more difficult to contend with than in the brain as WM, GM, CSF, bone, cartilage, and air (which all have different magnetic susceptibilities) are all in close proximity in the spinal cord (Stroman et al., 2014). These magnetic inhomogeneities result in spatial distortion as well as a loss of signal intensity (Stroman et al., 2014). One way to mitigate this issue in GE imaging is to reduce the field variation across a slice as much as possible. This can be done by acquiring data axially, especially if slices are aligned with intervertebral discs, or the centre of vertebral bodies, compared to sagittal acquisition (Stroman et al., 2014). However, one of the easiest ways to overcome this inhomogeneity problem is to use a sequence that is more sensitive to T_2 contrast, rather than T_2^* contrast. If you recall, T_2 contrast arises from time-varying changes, but not field inhomogeneity effects, unlike T_2^*. Thus, SE imaging, which is primarily T_2-weighted greatly reduces the distortions arising from tissue inhomogeneity (Stroman et al., 2014).

The SE sequences used in spinal cord fMRI are typically a variant of a partial-Fourier single-shot fast spin-echo (HASTE) sequence (Powers et al., 2018). Both GE and SE sequences can be optimized for BOLD imaging in the spinal cord by altering the TE—a TE of 25 ms is optimal using GE sequences while a TE of about 75 ms is more appropriate for SE sequences at 3 T (Powers et al., 2018). There are many pros and cons to using both GE and SE sequences in the spinal cord: GE sequences allow for faster acquisition (GE TR = 2-3 s; SE TR = 6-7 s); however axial GE acquisition results in poor image quality in the sagittal dimension, while SE imaging can be optimized to allow for better image quality with higher SNR and greater anatomical coverage (Figley, Leitch, & Stroman, 2010; Powers et al., 2018). Both methods are able to detect similar effect sizes in the spinal cord (Figley et al., 2010; Powers et al., 2018; Stroman, Kornelsen, Lawrence, & Malisza, 2005). Additionally, physiological noise is an important concern in spinal fMRI data; however, physiological noise modelling can be used to tremendously reduce this noise in SE imaging.

Another challenge of spinal fMRI is the small size of the spinal cord. Although this does reduce the impact of the multiple comparisons problem, it makes imaging itself trickier. For the best cross-sectional resolution, data should be acquired axially. However, one major disadvantage to axial acquisitions is aliasing—i.e., regions from outside the field-of-view wrapping around and potentially into the spinal cord—unless the entire width of the participant's body is included in the field-of-view (Stroman et al., 2014). Additionally, in order to view large spans of the spinal cord,

much time is needed to acquire a large enough number of slices. Alternatively, sagittal acquisition allows for large coverage of the spinal cord in a shorter amount of time, with the added bonus of likely having less aliasing, while requiring a smaller field-of-view as the anterior to posterior dimensions of a participant are typically smaller than left to right (Stroman, Kornelsen, & Lawrence, 2005; Stroman et al., 2014).

A final important concept to consider when conducting MRI research is data quality—although there are many preprocessing steps that can be used to clean up MRI data, the researcher will be limited by the initial quality of the data; preprocessing is not a solution for poor quality data. Considering the complexity of acquiring and preprocessing brain MRI data, in addition to the unique challenges associated with spinal fMRI data, it is perhaps not surprising that no spinal fMRI research has yet been conducted in a psychiatric patient population.

1.3.2.3 Previous spinal fMRI work

Until now, patient populations studied using spinal fMRI have largely been limited to those with structural deficits, most commonly including spinal cord injury or multiple sclerosis (Leitch, Figley, & Stroman, 2010; Powers et al., 2018; Wheeler-Kingshott et al., 2014); however, previous emotion research in healthy participants has paved the way for the current GAD spinal cord research. In the first study to investigate emotional responses in the spinal cord, participants completed six runs in a 3 x 2 study design: factor one was emotional valence, with negative, neutral, or positive emotion-evoking images, factor two was either passive-viewing, or a button press motoric response to the images (S. D. Smith & Kornelsen, 2011). Interestingly, in the passive viewing runs, the negative condition resulted in increased activity in the left dorsal and right ventral spinal cord, largely in regions C3-5. In the negative motoric condition, similar right ventral activity was observed, but was greater in terms of spatial extent than for the passive viewing condition. This study provides evidence for a preparatory motor response, in response to threat as activity was observed in motor regions during the passive viewing condition, i.e., *without conducting a motor action* (S. D. Smith & Kornelsen, 2011). Adding to this research, the same team furthered the investigation, showing that this emotional spinal cord response is limb-specific. In this new passive-viewing study, stimuli were separated into four groups of images depicting scenes with: 1) upper limb with neutral valence, 2) upper limbs with negative valence, 3) lower limbs with neutral valence, and 4) lower limbs with negative valence. Greater spinal cord activity was observed in regions C5-8 for negative compared to neutral images, as well as for upper compared

to lower limbs (McIver, Kornelsen, & Smith, 2013). Finally, negative emotion-evoking images of the upper limbs elicited greater activity than neutral upper limb images (McIver et al., 2013).

More recently, fMRI investigations into the thoracic spinal cord have begun, starting with proof-of-concept papers (Kornelsen et al., 2013; Kozyrev et al., 2012). In one of these, vibration stimulation was applied to the T7-11 dermatomes, resulting in significant ipsilateral activity in the corresponding dorsal (sensory) spinal cord regions (Kornelsen et al., 2013). In a follow-up study, visceral responses to emotion-evoking images were also investigated (Kornelsen, Smith, & McIver, 2015). Similar to their 2011 study, Kornelsen and colleagues (2015) had participants view neutral or negative emotion-evoking images either passively or while actively making a motoric (button press) response, this time scanning the thoracic spinal cord. The results showed that the negative motoric condition showed the greatest overall activity (in terms of spatial extent of active voxels), followed by the passive negative, then active neutral, and finally passive neutral conditions. In addition to observing increased activity in motor (ventral) regions for negative conditions, increased activity was also observed in sensory (dorsal) regions, as well as autonomic (lateral) regions, including regions that innervate the cervical and celiac ganglia, as well as the adrenal medulla. These papers indicate that the ANS can be noninvasively investigated in humans, at the level of the spinal cord (Kornelsen et al., 2015). Furthermore, this study supplies evidence that the thoracic spinal cord is also enhanced by emotion as the negative motoric condition had greater activity than the neutral motoric condition—identical motor movements were done, yet the negative emotion of the images enhanced this activity (Kornelsen et al., 2015).

1.3.2.4 fMRI Challenges

Although (f)MRI can provide a plethora of information about the brain and spinal cord, fMRI data is complex, and is likewise complex to preprocess. The noise observed in fMRI largely results from physiological origin (e.g., participant and physiological motion), and thermal noise (Kruger & Glover, 2001). Physiological noise has the highest contribution to the overall noise (Harita & Stroman, 2017; Kruger & Glover, 2001), but both types of noise can be greatly reduced following appropriate preprocessing. Finally, issues such as individual variation in physiology and the multiple comparisons problem need to be addressed in order to maximise data quality and allow for appropriate interpretation of results. While some of these issues are addressed throughout the preprocessing and analysis stages, some of these problems can be reduced prior to scanning.

Participant motion is one of the simplest ways for data to be ruined—consider that the typical voxel size in fMRI tends to be on the order of 2 x 2 x 2 mm^3; it does not take much motion for a brain or spinal cord to be in a completely different spot than when the scanning started. Motion can result from a participant twitching or shifting, relaxation of muscles as time goes on, and swallowing. As well as participant movement, the spinal cord itself can also move within the CSF (Figley & Stroman, 2007; Figley, Yau, & Stroman, 2008), in addition to movement artifacts due to CSF circulation, as well as cardiac- and lung-related movement (Powers et al., 2018; Stroman et al., 2014). For this reason, each slice collected must be aligned (also known as realignment or bulk motion correction) with each other so that a single voxel represents the same tissues throughout the entire scan. Additionally, when multiple runs are collected (e.g., anatomical and functional, or multiple functional), motion between runs also needs to be accounted for, so coregistration between images is conducted.

Although it is necessary to correct for motion after data is acquired, in order to reduce the amount of motion in the first place, some strategies can be used to limit the amount of time that a participant needs to stay still. This can be done by splitting a single long run into multiple shorter runs, as we have done in the spinal cord, or by collecting data faster, as we have done in the brain—both of which were performed and later explained in more detail in later chapters. In typical MRI experiments, data are collected one slice at a time; however, technology has improved since the early days of MRI allowing for multiple bands (slices) of data to be acquired simultaneously. This type of data acquisition can be accomplished with multi-band sequences, along with using special receiver coils (Barth, Breuer, Koopmans, Norris, & Poser, 2016). One thing to note about MRI research, however, is that almost all steps done in acquisition require a trade-off. Collecting multi-band data can result in acquiring more data for the same amount of time, at the expense of some field distortions (S. M. Smith et al., 2013). These field distortions can largely be corrected with the use of a susceptibility map created using a pair of opposite phase encoded images (e.g., left-to-right followed by right-to-left).

Another challenge in fMRI data is random, thermal noise (Kruger & Glover, 2001). Fortunately, because this noise is random, it is uncorrelated between neighbouring voxels and time. This means that averaging signal together across voxels results in an increase in signal-to-noise ratio (SNR). Spatial smoothing does this by taking a small group of voxels, and averaging their signal together. The drawbacks of this process are that it decreases spatial resolution and increases

partial volume effects—i.e., a voxel containing different types of tissues will affect the signal differently, based on tissue inhomogeneities (i.e., different chemical composition of tissues result in different magnetic susceptibilities). While an 8 mm Gaussian kernel at full-width half maximum is standard practice in many brain fMRI papers, a recent article by Chen and Calhoun (2018) suggests that a maximum range of 2-5 mm is more appropriate for current imaging methodology. Although the drawbacks of this data correction method can be tolerated in the brain, in the narrow spinal cord, which has many different tissue types within a highly concentrated area, the partial volume effects are much less tolerable.

Another challenge when analysing fMRI data is that individual brains and spinal cords are unique in terms of shape, size, and curvature (in the spinal cord) which makes comparing data within and between groups impractical, unless it can be mitigated. Spatial normalization allows each individual brain or spinal cord image to be stretched or compressed so that it fits a template. This step allows us to ascertain group-level differences, allowing for confident spatial localization. Although standardized templates have been in use for many years already (J. Mazziotta, Toga, Evans, Fox, Lancaster, Zilles, Woods, Paus, Simpson, Pike, Holmes, Collins, Thompson, MacDonald, Iacoboni, Schormann, Amunts, Palomero-Gallagher, Geyer, Parsons, Narr, Kabani, Le Goualher, Boomsma, et al., 2001; J. Mazziotta, Toga, Evans, Fox, Lancaster, Zilles, Woods, Paus, Simpson, Pike, Holmes, Collins, Thompson, MacDonald, Iacoboni, Schormann, Amunts, Palomero-Gallagher, Geyer, Parsons, Narr, Kabani, Le Goualher, Feidler, et al., 2001; J. C. Mazziotta, Toga, Evans, Fox, & Lancaster, 1995), spinal cord templates—particularly a thoracic cord template (De Leener et al., 2018; Stroman et al., 2008)—have been developed more recently, which paves the way for more research in the field in the future.

Finally, another important issue affecting fMRI data from a statistical standpoint is the multiple comparisons problem. While a brain MR image often contains around 100,000 voxels, conducting whole-brain analyses can be a complex undertaking—a *p*-value of 0.05 would result in 5%, or 5000 voxels being falsely positive, clearly an unacceptable standard (Poldrack, Mumford, & Nichols, 2011). Alternatively, Bonferroni correction for this many voxels would be incredibly restrictive. Although methods have been developed using Gaussian random field theory or Monte Carlo simulations, for example, one simple solution is to reduce the number of comparisons made by using regions-of-interest (ROIs), provided pre-existing hypotheses have been made. This greatly reduces the number of comparisons being made because each ROI,

regardless of the number of voxels, is considered as a unit that is subjected to a single statistical test. While the multiple comparisons problem still exists in the spinal cord, it is dramatically reduced as the typical spinal cord image contains approximately 5000 voxels.

1.4 Aims and Hypotheses

The following thesis addresses three aims to aid researchers' understanding of the differences in CNS activity in GAD, in response to threat. The aims include identifying how neural activation differs between patients with GAD and HC in response to threat in the 1) brain, 2) cervical spinal cord, and 3) thoracic spinal cord. In Chapter 2 (Aim 1a), I discuss previously observed brain activity, functional connectivity, and structural differences in GAD compared to HC in a systematic review and two meta-analyses. In Chapter 3 (Aim 1b), I present an fMRI study of the brain, overcoming some limitations observed in Chapter 2. Aims 2 and 3 are addressed in Chapter 4 in which the fMRI study is extended to the cervical and thoracic spinal cord. Finally, the thesis is discussed as a whole in Chapter 5. The hypotheses for which brain regions are altered in GAD come directly from the systematic review and meta-analyses of Chapter 2: reduced activity is expected for patients with GAD in the dorsolateral prefrontal cortex and culmen of the cerebellum while increased activity is expected in the amygdala. Altered activity is hypothesized in the anterior cingulate cortex and hippocampus. As a theoretical case could be made for either increased or decreased activity in the spinal cord for GAD, based on the inconsistent findings from physiological data, non-directional two-tailed tests were used for the cervical and thoracic spinal cord analyses.

1.5 Chapter 1 References

Adamaszek, M., D'Agata, F., Ferrucci, R., Habas, C., Keulen, S., Kirkby, K. C., . . . Verhoeven, J. (2017). Consensus Paper: Cerebellum and Emotion. *Cerebellum, 16*(2), 552-576. doi:10.1007/s12311-016-0815-8

Aldao, A., & Mennin, D. S. (2012). Paradoxical cardiovascular effects of implementing adaptive emotion regulation strategies in generalized anxiety disorder. *Behav Res Ther, 50*(2), 122-130. doi:10.1016/j.brat.2011.12.004

Alegria, A. A., Hasin, D. S., Nunes, E. V., Liu, S. M., Davies, C., Grant, B. F., & Blanco, C. (2010). Comorbidity of generalized anxiety disorder and substance use disorders: results from the National Epidemiologic Survey on Alcohol and Related Conditions. *J Clin Psychiatry, 71*(9), 1187-1195; quiz 1252-1183. doi:10.4088/JCP.09m05328gry

Alfano, C. A., Reynolds, K., Scott, N., Dahl, R. E., & Mellman, T. A. (2013). Polysomnographic sleep patterns of non-depressed, non-medicated children with generalized anxiety disorder. *J Affect Disord, 147*(1-3), 379-384. doi:10.1016/j.jad.2012.08.015

American Psychiatric Association. (2013). *Diagnostic and statistical manual of mental disorders* (5th ed.). Arlington, VA: American Psychiatric Association Publishing.

APA Dictionary of Psychology. (2007). Washington, DC, US: American Psychological Association.

Baldwin, D., & Rudge, S. (1995). The role of serotonin in depression and anxiety. *Int Clin Psychopharmacol, 9 Suppl 4*, 41-45. doi:10.1097/00004850-199501004-00006

Banerjee, S., & Argaez, C. (2017) *Neurofeedback and Biofeedback for Mood and Anxiety Disorders: A Review of Clinical Effectiveness and Guidelines*. Ottawa (ON).

Barger, S. D., & Sydeman, S. J. (2005). Does generalized anxiety disorder predict coronary heart disease risk factors independently of major depressive disorder? *J Affect Disord, 88*(1), 87-91. doi:10.1016/j.jad.2005.05.012

Barth, M., Breuer, F., Koopmans, P. J., Norris, D. G., & Poser, B. A. (2016). Simultaneous multislice (SMS) imaging techniques. *Magn Reson Med, 75*(1), 63-81. doi:10.1002/mrm.25897

Behar, E., DiMarco, I. D., Hekler, E. B., Mohlman, J., & Staples, A. M. (2009). Current theoretical models of generalized anxiety disorder (GAD): conceptual review and treatment implications. *J Anxiety Disord, 23*(8), 1011-1023. doi:10.1016/j.janxdis.2009.07.006

Bernstein, C. N. (2017). The Brain-Gut Axis and Stress in Inflammatory Bowel Disease. *Gastroenterol Clin North Am, 46*(4), 839-846. doi:10.1016/j.gtc.2017.08.006

Berridge, C. W. (2008). Noradrenergic modulation of arousal. *Brain Res Rev, 58*(1), 1-17. doi:10.1016/j.brainresrev.2007.10.013

Bloch, F. (1946). Nuclear induction. *Physical Review, 70*(7), 460-474.

Bonnet, L., Comte, A., Tatu, L., Millot, J. L., Moulin, T., & Medeiros de Bustos, E. (2015). The role of the amygdala in the perception of positive emotions: an "intensity detector". *Front Behav Neurosci, 9*, 178. doi:10.3389/fnbeh.2015.00178

Borkovec, T. D. (1994). The nature, functions, and origins of worry. In G. Davey & F. Tallis (Eds.), *Worrying: Perspectives on theory, assessment, and treatment* (pp. 5-33). Sussex, England: Wiley & Sons.

Borkovec, T. D., & Inz, J. (1990). The nature of worry in generalized anxiety disorder: a predominance of thought activity. *Behav Res Ther, 28*(2), 153-158. doi:10.1016/0005-7967(90)90027-g

Borkovec, T. D., Lyonfields, J. D., Wiser, S. L., & Deihl, L. (1993). The role of worrisome thinking in the suppression of cardiovascular response to phobic imagery. *Behav Res Ther, 31*(3), 321-324. doi:10.1016/0005-7967(93)90031-o

Borkovec, T. D., Robinson, E., Pruzinsky, T., & DePree, J. A. (1983). Preliminary exploration of worry: some characteristics and processes. *Behav Res Ther, 21*(1), 9-16. doi:10.1016/0005-7967(83)90121-3

Butler, G., Wells, A., & Dewick, H. (1995). Differential Effects of Worry and Imagery After Exposure to a Stressful Stimulus: A Pilot Study. *Behavioural and Cognitive Psychotherapy, 23*(1), 45-56. doi:10.1017/S1352465800017628

Butnoriene, J., Bunevicius, A., Saudargiene, A., Nemeroff, C. B., Norkus, A., Ciceniene, V., & Bunevicius, R. (2015). Metabolic syndrome, major depression, generalized anxiety disorder, and ten-year all-cause and cardiovascular mortality in middle aged and elderly patients. *Int J Cardiol, 190*, 360-366. doi:10.1016/j.ijcard.2015.04.122

Cadotte, D. W., Cadotte, A., Cohen-Adad, J., Fleet, D., Livne, M., Wilson, J. R., . . . Fehlings, M. G. (2015). Characterizing the location of spinal and vertebral levels in the human cervical spinal cord. *AJNR Am J Neuroradiol, 36*(4), 803-810. doi:10.3174/ajnr.A4192

Carpenter, J. K., Andrews, L. A., Witcraft, S. M., Powers, M. B., Smits, J. A. J., & Hofmann, S. G. (2018). Cognitive behavioral therapy for anxiety and related disorders: A meta-analysis of randomized placebo-controlled trials. *Depress Anxiety, 35*(6), 502-514. doi:10.1002/da.22728

Chandar, K., & Freeman, B. K. (2014). Spinal Cord Anatomy. In M. J. Aminoff & R. B. Daroff (Eds.), *Encyclopedia of the Neurological Sciences (Second Edition)* (pp. 254-263). Oxford: Academic Press.

Chen, Z., & Calhoun, V. (2018). Effect of Spatial Smoothing on Task fMRI ICA and Functional Connectivity. *Front Neurosci, 12*, 15. doi:10.3389/fnins.2018.00015

Chrousos, G. P. (1998). Stressors, stress, and neuroendocrine integration of the adaptive response. The 1997 Hans Selye Memorial Lecture. *Ann N Y Acad Sci, 851*, 311-335. doi:10.1111/j.1749-6632.1998.tb09006.x

Cramer, G., & Darby, S. (2014). Clinical Anatomy of the Spine, Spinal Cord, and ANS *Internal Organization of the Spinal Cord* (3rd ed. ed.): Elsevier Health Sciences.

Cuijpers, P., Sijbrandij, M., Koole, S., Huibers, M., Berking, M., & Andersson, G. (2014). Psychological treatment of generalized anxiety disorder: a meta-analysis. *Clin Psychol Rev, 34*(2), 130-140. doi:10.1016/j.cpr.2014.01.002

Culpepper, L. (2009). Generalized anxiety disorder and medical illness. *J Clin Psychiatry, 70 Suppl 2*, 20-24. doi:10.4088/jcp.s.7002.04

Cuthbert, B. N., Lang, P. J., Strauss, C., Drobes, D., Patrick, C. J., & Bradley, M. M. (2003). The psychophysiology of anxiety disorder: fear memory imagery. *Psychophysiology, 40*(3), 407-422. doi:10.1111/1469-8986.00043

Dadashi, M., Taremian, F., Momtazi, S., Khani, M., Eskandari, Z., Armani Kian, A., & Birashk, B. (2018). Comparing the Effectiveness of Metacognitive Therapy (MCT), Pharmacotherapy (SSRIs) and EEG Biofeedback in Generalized Anxiety Disorders. *Journal of Advances in Medical and Biomedical Research, 26*(117), 57-73.

Damadian, R. (1971). Tumor detection by nuclear magnetic resonance. *Science, 171*(3976), 1151-1153. doi:10.1126/science.171.3976.1151

Davis, M., & Whalen, P. J. (2001). The amygdala: vigilance and emotion. *Mol Psychiatry, 6*(1), 13-34. doi:10.1038/sj.mp.4000812

de Castro Gomes, V., Eduardo Barroso Silva, C., & Landeira-Fernandez, J. (2011). The Carioca high and low conditioned freezing lines: A new animal model of Generalized Anxiety Disorder. In V. Kalinin (Ed.), *Anxiety Disorders* (pp. 121-134). Rijeka, Croatia: InTech.

De Leener, B., Fonov, V. S., Collins, D. L., Callot, V., Stikov, N., & Cohen-Adad, J. (2018). PAM50: Unbiased multimodal template of the brainstem and spinal cord aligned with the ICBM152 space. *Neuroimage, 165*, 170-179. doi:10.1016/j.neuroimage.2017.10.041

Dell'Osso, B., Buoli, M., Baldwin, D. S., & Altamura, A. C. (2010). Serotonin norepinephrine reuptake inhibitors (SNRIs) in anxiety disorders: a comprehensive review of their clinical efficacy. *Hum Psychopharmacol, 25*(1), 17-29. doi:10.1002/hup.1074

Dugas, M. J., Gagnon, F., Ladouceur, R., & Freeston, M. H. (1998). Generalized anxiety disorder: a preliminary test of a conceptual model. *Behav Res Ther, 36*(2), 215-226. doi:10.1016/s0005-7967(97)00070-3

El-Gabalawy, R., Mackenzie, C. S., Pietrzak, R. H., & Sareen, J. (2014). A longitudinal examination of anxiety disorders and physical health conditions in a nationally representative sample of U.S. older adults. *Exp Gerontol, 60*, 46-56. doi:10.1016/j.exger.2014.09.012

Figley, C. R., Leitch, J. K., & Stroman, P. W. (2010). In contrast to BOLD: signal enhancement by extravascular water protons as an alternative mechanism of endogenous fMRI signal change. *Magn Reson Imaging, 28*(8), 1234-1243. doi:10.1016/j.mri.2010.01.005

Figley, C. R., & Stroman, P. W. (2007). Investigation of human cervical and upper thoracic spinal cord motion: implications for imaging spinal cord structure and function. *Magn Reson Med, 58*(1), 185-189. doi:10.1002/mrm.21260

Figley, C. R., & Stroman, P. W. (2011). The role(s) of astrocytes and astrocyte activity in neurometabolism, neurovascular coupling, and the production of functional neuroimaging signals. *Eur J Neurosci, 33*(4), 577-588. doi:10.1111/j.1460-9568.2010.07584.x

Figley, C. R., Yau, D., & Stroman, P. W. (2008). Attenuation of lower-thoracic, lumbar, and sacral spinal cord motion: implications for imaging human spinal cord structure and function. *AJNR Am J Neuroradiol, 29*(8), 1450-1454. doi:10.3174/ajnr.A1154

Frostell, A., Hakim, R., Thelin, E. P., Mattsson, P., & Svensson, M. (2016). A Review of the Segmental Diameter of the Healthy Human Spinal Cord. *Front Neurol, 7*, 238. doi:10.3389/fneur.2016.00238

Fuchs, P. N., Peng, Y. B., Boyette-Davis, J. A., & Uhelski, M. L. (2014). The anterior cingulate cortex and pain processing. *Front Integr Neurosci, 8*, 35. doi:10.3389/fnint.2014.00035

Gerra, G., Zaimovic, A., Zambelli, U., Timpano, M., Reali, N., Bernasconi, S., & Brambilla, F. (2000). Neuroendocrine responses to psychological stress in adolescents with anxiety disorder. *Neuropsychobiology, 42*(2), 82-92. doi:10.1159/000026677

Grant, B. F., Hasin, D. S., Stinson, F. S., Dawson, D. A., June Ruan, W., Goldstein, R. B., . . . Huang, B. (2005). Prevalence, correlates, co-morbidity, and comparative disability of DSM-IV generalized anxiety disorder in the USA: results from the National Epidemiologic Survey on Alcohol and Related Conditions. *Psychol Med, 35*(12), 1747-1759. doi:10.1017/S0033291705006069

Hamill, R. W., Shapiro, R. E., & Vizzard, M. A. (2011). Peripheral Autonomic Nervous System. In I. Biaggioni, P. A. Low, R. J. Polinsky, D. Robertson, J. F. R. Paton, & P. A. Low (Eds.), *Primer on the Autonomic Nervous System*. San Diego, USA: Elsevier Science & Technology.

Harita, S., & Stroman, P. W. (2017). Confirmation of resting-state BOLD fluctuations in the human brainstem and spinal cord after identification and removal of physiological noise. *Magn Reson Med, 78*(6), 2149-2156. doi:10.1002/mrm.26606

Harman, J. S., Rollman, B. L., Hanusa, B. H., Lenze, E. J., & Shear, M. K. (2002). Physician office visits of adults for anxiety disorders in the United States, 1985-1998. *J Gen Intern Med, 17*(3), 165-172. doi:10.1046/j.1525-1497.2002.10409.x

Hashemi, M. M., Zhang, W., Kaldewaij, R., Koch, S. B. J., Jonker, R., Figner, B., . . . Roelofs, K. (2019). Human defensive freezing is associated with acute threat coping, long term hair cortisol levels and trait anxiety. *bioRxiv*, 554840. doi:10.1101/554840

Hayes, S. C., Luoma, J. B., Bond, F. W., Masuda, A., & Lillis, J. (2006). Acceptance and commitment therapy: model, processes and outcomes. *Behav Res Ther, 44*(1), 1-25. doi:10.1016/j.brat.2005.06.006

Hazlett, R. L., McLeod, D. R., & Hoehn-Saric, R. (1994). Muscle tension in generalized anxiety disorder: elevated muscle tonus or agitated movement? *Psychophysiology, 31*(2), 189-195. doi:10.1111/j.1469-8986.1994.tb01039.x

Heim, C., Ehlert, U., & Hellhammer, D. H. (2000). The potential role of hypocortisolism in the pathophysiology of stress-related bodily disorders. *Psychoneuroendocrinology, 25*(1), 1-35. doi:10.1016/s0306-4530(99)00035-9

Hek, K., Direk, N., Newson, R. S., Hofman, A., Hoogendijk, W. J., Mulder, C. L., & Tiemeier, H. (2013). Anxiety disorders and salivary cortisol levels in older adults: a population-based study. *Psychoneuroendocrinology, 38*(2), 300-305. doi:10.1016/j.psyneuen.2012.06.006

Hettema, J. M., Prescott, C. A., Myers, J. M., Neale, M. C., & Kendler, K. S. (2005). The structure of genetic and environmental risk factors for anxiety disorders in men and women. *Arch Gen Psychiatry, 62*(2), 182-189. doi:10.1001/archpsyc.62.2.182

Hilbert, K., Lueken, U., & Beesdo-Baum, K. (2014). Neural structures, functioning and connectivity in Generalized Anxiety Disorder and interaction with neuroendocrine systems: a systematic review. *J Affect Disord, 158*, 114-126. doi:10.1016/j.jad.2014.01.022

Hilbert, K., Lueken, U., Muehlhan, M., & Beesdo-Baum, K. (2017). Separating generalized anxiety disorder from major depression using clinical, hormonal, and structural MRI data: A multimodal machine learning study. *Brain and Behavior, 7*(3). doi:10.1002/brb3.633

Hoehn-Saric, R. (1998). Psychic and somatic anxiety: worries, somatic symptoms and physiological changes. *Acta Psychiatr Scand Suppl, 393*, 32-38. doi:10.1111/j.1600-0447.1998.tb05964.x

Hoehn-Saric, R., McLeod, D. R., Funderburk, F., & Kowalski, P. (2004). Somatic symptoms and physiologic responses in generalized anxiety disorder and panic disorder: an ambulatory monitor study. *Arch Gen Psychiatry, 61*(9), 913-921. doi:10.1001/archpsyc.61.9.913

Hoehn-Saric, R., McLeod, D. R., Lee, Y. B., & Zimmerli, W. D. (1991). Cortisol levels in generalized anxiety disorder. *Psychiatry Res, 38*(3), 313-315. doi:10.1016/0165-1781(91)90021-g

Hoehn-Saric, R., McLeod, D. R., & Zimmerli, W. D. (1989). Somatic manifestations in women with generalized anxiety disorder. Psychophysiological responses to psychological stress. *Arch Gen Psychiatry, 46*(12), 1113-1119. doi:10.1001/archpsyc.1989.01810120055009

Hood, S. D., Melichar, J. K., Taylor, L. G., Kalk, N., Edwards, T. R., Hince, D. A., . . . Nutt, D. J. (2011). Noradrenergic function in generalized anxiety disorder: impact of treatment with venlafaxine on the physiological and psychological responses to clonidine challenge. *J Psychopharmacol, 25*(1), 78-86. doi:10.1177/0269881109359099

Huettel, S. A., Song, A. W., & McCarthy, G. (2014). *Functional magnetic resonance imaging* (Third edition. ed.). Sunderland, Massachusetts, U.S.A.: Sinauer Associates, Inc., Publishers.

Jung, B. A., & Weigel, M. (2013). Spin echo magnetic resonance imaging. *J Magn Reson Imaging, 37*(4), 805-817. doi:10.1002/jmri.24068

Kaczkurkin, A. N., & Foa, E. B. (2015). Cognitive-behavioral therapy for anxiety disorders: an update on the empirical evidence. *Dialogues Clin Neurosci, 17*(3), 337-346.

Kandel, E., Kandel, E. R.,], Jessell, J. H., Schwartz, J., & Jessell, T. (2000). *Principles of Neural Science, Fourth Edition*: McGraw-Hill Companies,Incorporated.

Kandel, E. R. (2013). *Principles of neural science* (5th ed.). New York: McGraw-Hill.

Katirji, B., & Devereaux, M. (2014). Spinal Roots. In M. J. Aminoff & R. B. Daroff (Eds.), *Encyclopedia of the Neurological Sciences (Second Edition)* (pp. 286-287). Oxford: Academic Press.

Kessler, R. C., Berglund, P., Demler, O., Jin, R., Merikangas, K. R., & Walters, E. E. (2005). Lifetime prevalence and age-of-onset distributions of DSM-IV disorders in the National Comorbidity Survey Replication. *Arch Gen Psychiatry, 62*(6), 593-602. doi:10.1001/archpsyc.62.6.593

Kornelsen, J., Smith, S. D., & McIver, T. A. (2015). A neural correlate of visceral emotional responses: evidence from fMRI of the thoracic spinal cord. *Soc Cogn Affect Neurosci, 10*(4), 584-588. doi:10.1093/scan/nsu092

Kornelsen, J., Smith, S. D., McIver, T. A., Sboto-Frankenstein, U., Latta, P., & Tomanek, B. (2013). Functional MRI of the thoracic spinal cord during vibration sensation. *J Magn Reson Imaging, 37*(4), 981-985. doi:10.1002/jmri.23819

Kozyrev, N., Figley, C. R., Alexander, M. S., Richards, J. S., Bosma, R. L., & Stroman, P. W. (2012). Neural correlates of sexual arousal in the spinal cords of able-bodied men: a spinal fMRI investigation. *J Sex Marital Ther, 38*(5), 418-435. doi:10.1080/0092623X.2011.606887

Kruger, G., & Glover, G. H. (2001). Physiological noise in oxygenation-sensitive magnetic resonance imaging. *Magn Reson Med, 46*(4), 631-637. doi:10.1002/mrm.1240

Kwong, K. K., Belliveau, J. W., Chesler, D. A., Goldberg, I. E., Weisskoff, R. M., Poncelet, B. P., . . . et al. (1992). Dynamic magnetic resonance imaging of human brain activity during

primary sensory stimulation. *Proc Natl Acad Sci U S A, 89*(12), 5675-5679. doi:10.1073/pnas.89.12.5675

Lang, J., & Bartram, C. T. (1982). [Fila radicularia of the ventral and dorsal radices of the human spinal cord]. *Gegenbaurs Morphol Jahrb, 128*(4), 417-462.

Lang, P. J., & McTeague, L. M. (2009). The anxiety disorder spectrum: fear imagery, physiological reactivity, and differential diagnosis. *Anxiety Stress Coping, 22*(1), 5-25. doi:10.1080/10615800802478247

Lauterbur, P. C. (1973). Image formation by induced local interactions. Examples employing nuclear magnetic resonance. *Nature, 242*, 190-191.

Leigh, E., & Hirsch, C. R. (2011). Worry in imagery and verbal form: effect on residual working memory capacity. *Behav Res Ther, 49*(2), 99-105. doi:10.1016/j.brat.2010.11.005

Leitch, J. K., Figley, C. R., & Stroman, P. W. (2010). Applying functional MRI to the spinal cord and brainstem. *Magn Reson Imaging, 28*(8), 1225-1233. doi:10.1016/j.mri.2010.03.032

Lenze, E. J., Goate, A. M., Nowotny, P., Dixon, D., Shi, P., Bies, R. R., . . . Pollock, B. G. (2010). Relation of serotonin transporter genetic variation to efficacy of escitalopram for generalized anxiety disorder in older adults. *J Clin Psychopharmacol, 30*(6), 672-677. doi:10.1097/jcp.0b013e3181fc2bef

León, L. A., Brandão, M. L., Cardenas, F. P., Parra, D., Krahe, T. E., Cruz, A. P. M., & Landeira-Fernandez, J. (2020). Distinct patterns of brain Fos expression in Carioca High- and Low-conditioned Freezing Rats. *PLoS ONE, 15*(7), e0236039. doi:10.1371/journal.pone.0236039

Llera, S. J., & Newman, M. G. (2010). Effects of worry on physiological and subjective reactivity to emotional stimuli in generalized anxiety disorder and nonanxious control participants. *Emotion, 10*(5), 640-650. doi:10.1037/a0019351

Logothetis, N. K. (2008). What we can do and what we cannot do with fMRI. *Nature, 453*(7197), 869-878. doi:10.1038/nature06976

Lohoff, F. W., Aquino, T. D., Narasimhan, S., Multani, P. K., Etemad, B., & Rickels, K. (2013). Serotonin receptor 2A (HTR2A) gene polymorphism predicts treatment response to venlafaxine XR in generalized anxiety disorder. *Pharmacogenomics J, 13*(1), 21-26. doi:10.1038/tpj.2011.47

Lyonfields, J. D., Borkovec, T. D., & Thayer, J. F. (1995). Vagal tone in generalized anxiety disorder and the effects of aversive imagery and worrisome thinking. *Behavior Therapy, 26*(3), 457-466. doi:https://doi.org/10.1016/S0005-7894(05)80094-2

Mangold, S., & Das, J. (2020, August 15, 2020). Neuroanatomy, Reticular Formation. *StatPearls*. Retrieved from https://www.ncbi.nlm.nih.gov/books/NBK556102/

Mansfield, P., & Grannell, P. K. (1973). NMR 'diffraction' in solids? *J Phys C: Solid State Phys, 6*, L422-L426.

Mantella, R. C., Butters, M. A., Amico, J. A., Mazumdar, S., Rollman, B. L., Begley, A. E., . . . Lenze, E. J. (2008). Salivary cortisol is associated with diagnosis and severity of late-life generalized anxiety disorder. *Psychoneuroendocrinology, 33*(6), 773-781. doi:10.1016/j.psyneuen.2008.03.002

Marrie, R. A., Walld, R., Bolton, J. M., Sareen, J., Walker, J. R., Patten, S. B., . . . Managing the Effects of Psychiatric Comorbidity in Chronic Immunoinflammatory, D. (2019). Rising incidence of psychiatric disorders before diagnosis of immune-mediated inflammatory disease. *Epidemiol Psychiatr Sci, 28*(3), 333-342. doi:10.1017/S2045796017000579

Mathew, R. J., Ho, B. T., Francis, D. J., Taylor, D. L., & Weinman, M. L. (1982). Catecholamines and anxiety. *Acta Psychiatr Scand, 65*(2), 142-147. doi:10.1111/j.1600-0447.1982.tb00833.x

Mathew, R. J., Ho, B. T., Kralik, P., Taylor, D. L., & Claghorn, J. L. (1981). Catecholamines and monoamine oxidase activity in anxiety. *Acta Psychiatr Scand, 63*(3), 245-252. doi:10.1111/j.1600-0447.1981.tb00671.x

Mazziotta, J., Toga, A., Evans, A., Fox, P., Lancaster, J., Zilles, K., . . . Mazoyer, B. (2001). A probabilistic atlas and reference system for the human brain: International Consortium for Brain Mapping (ICBM). *Philos Trans R Soc Lond B Biol Sci, 356*(1412), 1293-1322. doi:10.1098/rstb.2001.0915

Mazziotta, J., Toga, A., Evans, A., Fox, P., Lancaster, J., Zilles, K., . . . Mazoyer, B. (2001). A four-dimensional probabilistic atlas of the human brain. *J Am Med Inform Assoc, 8*(5), 401-430. doi:10.1136/jamia.2001.0080401

Mazziotta, J. C., Toga, A. W., Evans, A., Fox, P., & Lancaster, J. (1995). A probabilistic atlas of the human brain: theory and rationale for its development. The International Consortium for Brain Mapping (ICBM). *Neuroimage, 2*(2), 89-101. doi:10.1006/nimg.1995.1012

McIver, T. A., Kornelsen, J., & Smith, S. D. (2013). Limb-specific emotional modulation of cervical spinal cord neurons. *Cogn Affect Behav Neurosci, 13*(3), 464-472. doi:10.3758/s13415-013-0154-x

McLeod, D. R., Hoehn-Saric, R., & Stefan, R. L. (1986). Somatic symptoms of anxiety: comparison of self-report and physiological measures. *Biol Psychiatry, 21*(3), 301-310. doi:10.1016/0006-3223(86)90051-x

McLeod, D. R., Hoehn-Saric, R., Zimmerli, W. D., De Souza, E. B., & Oliver, L. K. (1990). Treatment effects of alprazolam and imipramine: physiological versus subjective changes in patients with generalized anxiety disorder. *Biol Psychiatry, 28*(10), 849-861. doi:10.1016/0006-3223(90)90567-l

Mennin, D. S., Heimberg, R. G., Turk, C. L., & Fresco, D. M. (2005). Preliminary evidence for an emotion dysregulation model of generalized anxiety disorder. *Behav Res Ther, 43*(10), 1281-1310. doi:10.1016/j.brat.2004.08.008

Minderhoud, I. M., Oldenburg, B., van Dam, P. S., & van Berge Henegouwen, G. P. (2003). High prevalence of fatigue in quiescent inflammatory bowel disease is not related to adrenocortical insufficiency. *Am J Gastroenterol, 98*(5), 1088-1093. doi:10.1111/j.1572-0241.2003.07414.x

Mochcovitch, M. D., da Rocha Freire, R. C., Garcia, R. F., & Nardi, A. E. (2014). A systematic review of fMRI studies in generalized anxiety disorder: evaluating its neural and cognitive basis. *J Affect Disord, 167*, 336-342. doi:10.1016/j.jad.2014.06.041

Moffitt, T. E., Caspi, A., Harrington, H., Milne, B. J., Melchior, M., Goldberg, D., & Poulton, R. (2007). Generalized anxiety disorder and depression: childhood risk factors in a birth cohort followed to age 32. *Psychol Med, 37*(3), 441-452. doi:10.1017/S0033291706009640

Moffitt, T. E., Harrington, H., Caspi, A., Kim-Cohen, J., Goldberg, D., Gregory, A. M., & Poulton, R. (2007). Depression and generalized anxiety disorder: cumulative and sequential comorbidity in a birth cohort followed prospectively to age 32 years. *Arch Gen Psychiatry, 64*(6), 651-660. doi:10.1001/archpsyc.64.6.651

Munjack, D. J., Baltazar, P. L., DeQuattro, V., Sobin, P., Palmer, R., Zulueta, A., . . . Leonard, M. (1990). Generalized anxiety disorder: some biochemical aspects. *Psychiatry Res, 32*(1), 35-43. doi:10.1016/0165-1781(90)90133-p

Nepon, J., Belik, S. L., Bolton, J., & Sareen, J. (2010). The relationship between anxiety disorders and suicide attempts: findings from the National Epidemiologic Survey on Alcohol and Related Conditions. *Depress Anxiety, 27*(9), 791-798. doi:10.1002/da.20674

Newman, M. G., Przeworski, A., Fisher, A. J., & Borkovec, T. D. (2010). Diagnostic comorbidity in adults with generalized anxiety disorder: impact of comorbidity on psychotherapy outcome and impact of psychotherapy on comorbid diagnoses. *Behav Ther, 41*(1), 59-72. doi:10.1016/j.beth.2008.12.005

Ogawa, S., Tank, D. W., Menon, R., Ellermann, J. M., Kim, S. G., Merkle, H., & Ugurbil, K. (1992). Intrinsic signal changes accompanying sensory stimulation: functional brain mapping with magnetic resonance imaging. *Proc Natl Acad Sci U S A, 89*(13), 5951-5955. doi:10.1073/pnas.89.13.5951

Pauling, L., & Coryell, C. D. (1936). The Magnetic Properties and Structure of Hemoglobin, Oxyhemoglobin and Carbonmonoxyhemoglobin. *Proc Natl Acad Sci U S A, 22*(4), 210-216. doi:10.1073/pnas.22.4.210

Pearson, C., Janz, T., & Ali, J. (2013). Health at a glance: Mental and substance use disorders in Canada: Statistics Canada.

Pelletier, L., O'Donnell, S., McRae, L., & Grenier, J. (2017). The burden of generalized anxiety disorder in Canada. *Health Promot Chronic Dis Prev Can, 37*(2), 54-62. doi:10.24095/hpcdp.37.2.04

Pellissier, S., Dantzer, C., Mondillon, L., Trocme, C., Gauchez, A. S., Ducros, V., . . . Bonaz, B. (2014). Relationship between vagal tone, cortisol, TNF-alpha, epinephrine and negative affects in Crohn's disease and irritable bowel syndrome. *PLoS ONE, 9*(9), e105328. doi:10.1371/journal.pone.0105328

Plewes, D. B., & Kucharczyk, W. (2012). Physics of MRI: a primer. *J Magn Reson Imaging, 35*(5), 1038-1054. doi:10.1002/jmri.23642

Poldrack, R. A., Mumford, J. A., & Nichols, T. E. (2011). Statistical Inference on Images *Handbook of Functional MRI Data Analysis* (pp. 110-129). Cambridge: Cambridge University Press.

Powers, J. M., Ioachim, G., & Stroman, P. W. (2018). Ten Key Insights into the Use of Spinal Cord fMRI. *Brain Sci, 8*(9). doi:10.3390/brainsci8090173

Purcell, E. M., Torrey, H. C., & Pound, R. V. (1946). Resonance absorption by nuclear magnetic moments in a solid. *Phys Rev, 69*, 37-38.

Purves, D. (2008). *Neuroscience* (4th ed.). Sunderland, Mass.: Sinauer.

Roelofs, K. (2017). Freeze for action: neurobiological mechanisms in animal and human freezing. *Philos Trans R Soc Lond B Biol Sci, 372*(1718). doi:10.1098/rstb.2016.0206

Roemer, L., & Orsillo, S. M. (2002). Expanding Our Conceptualization of and Treatment for Generalized Anxiety Disorder: Integrating Mindfulness/Acceptance-Based Approaches With Existing Cognitive-Behavioral Models. *Clinical Psychology: Science and Practice, 9*(1), 54-68. doi:10.1093/clipsy.9.1.54

Sareen, J., Cox, B. J., Afifi, T. O., de Graaf, R., Asmundson, G. J., ten Have, M., & Stein, M. B. (2005). Anxiety disorders and risk for suicidal ideation and suicide attempts: a population-based longitudinal study of adults. *Arch Gen Psychiatry, 62*(11), 1249-1257. doi:10.1001/archpsyc.62.11.1249

Schmidt, N. B., Richey, J. A., Zvolensky, M. J., & Maner, J. K. (2008). Exploring human freeze responses to a threat stressor. *J Behav Ther Exp Psychiatry, 39*(3), 292-304. doi:10.1016/j.jbtep.2007.08.002

Selye, H. (1976). Forty years of stress research: principal remaining problems and misconceptions. *Can Med Assoc J, 115*(1), 53-56.

Shenhav, A., Botvinick, M. M., & Cohen, J. D. (2013). The expected value of control: an integrative theory of anterior cingulate cortex function. *Neuron, 79*(2), 217-240. doi:10.1016/j.neuron.2013.07.007

Smith, S. D., & Kornelsen, J. (2011). Emotion-dependent responses in spinal cord neurons: a spinal fMRI study. *Neuroimage, 58*(1), 269-274. doi:10.1016/j.neuroimage.2011.06.004

Smith, S. M., Beckmann, C. F., Andersson, J., Auerbach, E. J., Bijsterbosch, J., Douaud, G., . . . Consortium, W. U.-M. H. (2013). Resting-state fMRI in the Human Connectome Project. *Neuroimage, 80*, 144-168. doi:10.1016/j.neuroimage.2013.05.039

Southerland, G., & Stonebridge, C. (2016). *Healthy brains at work: Estimating the impact of workplae mental health benefits and programs*. Ottawa: The Conference Board of Canada.

Stein, D. J., & Stahl, S. (2000). Serotonin and anxiety: current models. *Int Clin Psychopharmacol, 15 Suppl 2*, S1-6. doi:10.1097/00004850-200008002-00002

Stein, M. B., & Sareen, J. (2015). CLINICAL PRACTICE. Generalized Anxiety Disorder. *N Engl J Med, 373*(21), 2059-2068. doi:10.1056/NEJMcp1502514

Steudte, S., Stalder, T., Dettenborn, L., Klumbies, E., Foley, P., Beesdo-Baum, K., & Kirschbaum, C. (2011). Decreased hair cortisol concentrations in generalised anxiety disorder. *Psychiatry Res, 186*(2-3), 310-314. doi:10.1016/j.psychres.2010.09.002

Stroman, P. W. (2016). Validation of Structural Equation Modeling Methods for Functional MRI Data Acquired in the Human Brainstem and Spinal Cord. *Crit Rev Biomed Eng, 44*(4), 227-241. doi:10.1615/CritRevBiomedEng.2017020438

Stroman, P. W., Bosma, R. L., Cotoi, A. I., Leung, R. H., Kornelsen, J., Lawrence-Dewar, J. M., . . . Staud, R. (2016). Continuous Descending Modulation of the Spinal Cord Revealed by Functional MRI. *PLoS ONE, 11*(12), e0167317. doi:10.1371/journal.pone.0167317

Stroman, P. W., Figley, C. R., & Cahill, C. M. (2008). Spatial normalization, bulk motion correction and coregistration for functional magnetic resonance imaging of the human cervical spinal cord and brainstem. *Magn Reson Imaging, 26*(6), 809-814. doi:10.1016/j.mri.2008.01.038

Stroman, P. W., Ioachim, G., Powers, J. M., Staud, R., & Pukall, C. (2018). Pain processing in the human brainstem and spinal cord before, during, and after the application of noxious heat stimuli. *Pain, 159*(10), 2012-2020. doi:10.1097/j.pain.0000000000001302

Stroman, P. W., Kornelsen, J., & Lawrence, J. (2005). An improved method for spinal functional MRI with large volume coverage of the spinal cord. *J Magn Reson Imaging, 21*(5), 520-526. doi:10.1002/jmri.20315

Stroman, P. W., Kornelsen, J., Lawrence, J., & Malisza, K. L. (2005). Functional magnetic resonance imaging based on SEEP contrast: response function and anatomical specificity. *Magn Reson Imaging, 23*(8), 843-850. doi:10.1016/j.mri.2005.07.009

Stroman, P. W., Wheeler-Kingshott, C., Bacon, M., Schwab, J. M., Bosma, R., Brooks, J., . . . Tracey, I. (2014). The current state-of-the-art of spinal cord imaging: methods. *Neuroimage, 84*, 1070-1081. doi:10.1016/j.neuroimage.2013.04.124

Tafet, G. E., Idoyaga-Vargas, V. P., Abulafia, D. P., Calandria, J. M., Roffman, S. S., Chiovetta, A., & Shinitzky, M. (2001). Correlation between cortisol level and serotonin uptake in patients with chronic stress and depression. *Cogn Affect Behav Neurosci, 1*(4), 388-393. doi:10.3758/cabn.1.4.388

Tolin, D. F., Davies, C. D., Moskow, D. M., & Hofmann, S. G. (2020). Biofeedback and Neurofeedback for Anxiety Disorders: A Quantitative and Qualitative Systematic Review. *Adv Exp Med Biol, 1191*, 265-289. doi:10.1007/978-981-32-9705-0_16

Tryon, V. L., & Mizumori, S. J. Y. (2018). A Novel Role for the Periaqueductal Gray in Consummatory Behavior. *Front Behav Neurosci, 12*, 178. doi:10.3389/fnbeh.2018.00178

Tubbs, R. S., Salter, G., Grabb, P. A., & Oakes, W. J. (2001). The denticulate ligament: anatomy and functional significance. *J Neurosurg, 94*(2 Suppl), 271-275. doi:10.3171/spi.2001.94.2.0271

Vrana, S. R., Cuthbert, B. N., & Lang, P. J. (1986). Fear imagery and text processing. *Psychophysiology, 23*(3), 247-253. doi:10.1111/j.1469-8986.1986.tb00626.x

Watson, C., Paxinos, G., & Kayalioglu, G. (2009). *The Spinal Cord: A Christopher and Dana Reeve Foundation Text and Atlas* (1st ed.): Elsevier Health Sciences.

Wells, A. (1995). Meta-Cognition and Worry: A Cognitive Model of Generalized Anxiety Disorder. *Behavioural and Cognitive Psychotherapy, 23*(3), 301-320. doi:10.1017/S1352465800015897

Wheeler-Kingshott, C. A., Stroman, P. W., Schwab, J. M., Bacon, M., Bosma, R., Brooks, J., . . . Tracey, I. (2014). The current state-of-the-art of spinal cord imaging: applications. *Neuroimage, 84*, 1082-1093. doi:10.1016/j.neuroimage.2013.07.014

Wittchen, H. U., Zhao, S., Kessler, R. C., & Eaton, W. W. (1994). DSM-III-R generalized anxiety disorder in the National Comorbidity Survey. *Arch Gen Psychiatry, 51*(5), 355-364. doi:10.1001/archpsyc.1994.03950050015002

Yohn, C. N., Gergues, M. M., & Samuels, B. A. (2017). The role of 5-HT receptors in depression. *Mol Brain, 10*(1), 28. doi:10.1186/s13041-017-0306-y

Zhang, X., Norton, J., Carriere, I., Ritchie, K., Chaudieu, I., & Ancelin, M. L. (2015). Risk factors for late-onset generalized anxiety disorder: results from a 12-year prospective cohort (the ESPRIT study). *Transl Psychiatry, 5*, e536. doi:10.1038/tp.2015.31

2. Chapter 2: Systematic Review and Meta-Analyses of Neural Structural and Functional Differences in Generalized Anxiety Disorder and Healthy Controls using Magnetic Resonance Imaging

Tiffany A. Kolesar,[1] Elena Bilevicius,[2] Alyssia D. Wilson,[3] and Jennifer Kornelsen[1,4*]

[1]Department of Physiology and Pathophysiology, University of Manitoba, Winnipeg, MB, Canada

[2]Department of Psychology, University of Manitoba, Winnipeg, MB, Canada

[3]Department of Internal Medicine, University of Manitoba, Winnipeg, MB, Canada

[4]Department of Radiology, University of Manitoba, Winnipeg, MB, Canada

Corresponding author

Email: Jennifer.Kornelsen@umanitoba.ca (JK)

From: Kolesar, T. A., Bilevicius, E., Wilson, A. D., & Kornelsen, J. (2019). Systematic Review and Meta-Analyses of Neural Structural and Functional Differences in Generalized Anxiety Disorder and Healthy Controls using Magnetic Resonance Imaging. *NeuroImage: Clinical 24*(2019), 102016. https://doi.org/10.1016/j.nicl.2019.102016.

2.1 Abstract

Objective: To compare structure, functional connectivity (FC) and task-based neural differences in subjects with GAD compared to HC.

Methods: The Embase, Ovid Medline, PsycINFO, Scopus, and Web of Science databases were searched from inception until March 12, 2018. Two reviewers independently screened titles, abstracts, and full-text articles. Data were extracted from records directly contrasting GAD and HC that included structure (connectivity and local indices such as volume, etc.), FC, or task-based magnetic resonance imaging data. Meta-analyses were conducted, as applicable, using AES-SDM software.

Results: The literature search produced 4,645 total records, of which 85 met the inclusion criteria for the systematic review. Records included structural (n = 35), FC (n = 33), and task-based (n = 42) findings. Meta-analyses were conducted on voxel-based morphometry and task-based results.

Discussion: The systematic review confirms and extends findings from previous reviews. Although few whole-brain resting state studies were conducted, key nodes of resting state networks have altered physiology: the hippocampus (default network), ACC and amygdala (salience network), have reduced volume, and the dlPFC (central executive network) and ACC have reduced FC with the amygdala in GAD. Nodes in the sensorimotor network are also altered with greater pre- and postcentral volume, reduced supplementary motor area volume, and reduced FC in anterior and increased FC in posterior cerebellum.

Conclusions: Despite limitations due to sample size, the meta-analyses highly agree with the systematic review and provide evidence of widely distributed neural differences in subjects with GAD, compared to HC. Further research optimized for meta-analyses would greatly improve large-scale comparisons.

Highlights:

- PFC-amygdala FC is altered in GAD, indicating top-down processing deficits.
- GAD had reduced activity for emotion regulation and working memory in the culmen.
- Salience, default, and central executive nodes have altered structure and function.

Keywords: generalized anxiety disorder; functional magnetic resonance imaging; systematic review; meta-analysis

2.2 Introduction

Anxiety disorders are highly prevalent in the general population, and GAD is one of the most common forms (Somers, Goldner, Waraich, & Hsu, 2006). GAD is characterized by chronic, persistent worry that is present more days than not over at least the past six months (American Psychiatric Association, 2013). In addition to the psychological manifestation of this disorder, GAD also presents physically. In fact, it is often physical ailments—such as gastrointestinal upset or headaches—that cause patients to seek treatment (Stein & Sareen, 2015). According to the *Diagnostic and Statistical Manual for Mental Disorders, 5th edition* (DSM-5), an adult patient's chronic worry must be accompanied by three or more of the following symptoms—irritability, difficulty concentrating, insomnia, fatigue, restlessness, or muscle tension—again occurring more often than not in the past 6 months for a GAD diagnosis to be made (American Psychiatric Association, 2013). A comprehensive systematic review and meta-analysis of the body of work to date may elucidate the common neural correlates underlying this disorder. The purpose of the current work is to review the neural differences occurring in GAD, compared to HC, as assessed by structural and fMRI studies.

Neurophysiology can be assessed various ways, even within the field of magnetic resonance imaging (MRI). Investigations of brain structure commonly include measures of local volumetric (e.g., voxel-based morphometry), cortical thickness analysis (CTA), and surface area differences and, less common, local gyrification index (i.e., cortex within sulcal folds, compared to gyral cortex) and WM lesions (hyperintensities in a typical T2-weighted MRI). Furthermore, physical WM connections can also be assessed—diffusion tensor imaging (DTI) assesses this structural connectivity via fractional anisotropy (FA; a measure of sphericity of diffusion in neural tissue), mean diffusivity (average diffusion within a region), apparent diffusion coefficient (magnitude of diffusion in a region), tractography (a technique for modelling neural tracts), and axial (diffusivity along the principal axis) and radial diffusivity (average diffusivity along two minor axes). In addition to investigating structural neuroanatomy, much MRI research has been done elucidating neural function via task-based activation and functional connectivity (FC). Task-based fMRI identifies regions of the brain or spinal cord whose activity correlates with task performance. FC assesses how the activity of various regions correlate to each other (Friston, 2011). Various measures of FC exist: Psychophysiological interaction (PPI) examines interactions between physiological variables and experimental (e.g., task) factors (Friston, 2011), regional

homogeneity (ReHo) investigates local FC, evaluating the time-series of voxels and their nearest neighbours (Y. Zang, Jiang, Lu, He, & Tian, 2004), amplitude of low frequency fluctuations (ALFF) examines differences in the magnitude of the slow oscillating activity observed in resting state fMRI between regions, and individuals (Y. F. Zang et al., 2007) and independent component analysis (ICA) identifies signals with maximum independence from each other and can be used to separate resting state networks from each other (i.e., resting state fMRI; Calhoun, Liu, & Adali, 2009).

Several reviews have been conducted in attempts to amalgamate results from the types of neuroimaging studies described above, in order to visualise how anxious brains differ from non-anxious ones. Recent reviews indicate that anxiety and mood disorders often share a common neurological pathophysiology involving the prefrontal cortex (PFC), hippocampus, and amygdala (Duval, Javanbakht, & Liberzon, 2015), with a key feature being increased amygdala and decreased PFC activity (Quide, Witteveen, El-Hage, Veltman, & Olff, 2012). In one review, fear-based conditions (panic disorder [PD]/specific phobias) resulted in greater involvement in emotion-generating regions (e.g., dorsal anterior cingulate cortex [ACC], amygdala, insula), while anxiety-based conditions (GAD/posttraumatic stress disorder [PTSD]) had greater PFC dysregulation (Duval et al., 2015).

Looking specifically at GAD, altered function was observed in the PFC and ACC resulting from tasks investigating emotion dysregulation, conditioned fear overgeneralization, and worry induction in one systematic review (Mochcovitch, da Rocha Freire, Garcia, & Nardi, 2014). Furthermore, reduced FC between the amygdala and cortex was also reported (Mochcovitch et al., 2014). Similarly, Hilbert and colleagues (2014), reviewing many of the same papers, observed alterations in the same three areas in GAD (PFC, amygdala, ACC), with the addition of the hippocampus. The main findings from Hilbert and colleagues' systematic review were that GAD patients had abnormal activity in PFC and amygdala, increased amygdala GM, and decreased FC and structural connectivity between these regions, combined with increased reactivity of the noradrenergic system, compared to HC. More recently, Fonzo and Etkin (2017) also observed abnormal PFC and limbic activation in response to facial affect processing, affective learning and regulation, and perseverative cognition tasks and altered FC when comparing GAD and HC groups. Although these results appear vague and nondescript (i.e., "abnormal" activity rather than increased or decreased), Fonzo and Etkin (2017) discussed that this variability may actually be a

facet of GAD. These authors discuss that, because the pathological worry in GAD can be generated *without* external stimulation, this neural state may remain less impacted *by* external stimuli. All three of these systematic reviews come to the same conclusion: (f)MRI provides evidence for top-down emotion processing deficits in GAD. Since these reviews were conducted (Fonzo & Etkin, 2017; Hilbert et al., 2014; Mochcovitch et al., 2014), a large number of new studies have been published. Furthermore, no current papers have conducted meta-analyses on any aspect of GAD MRI work.

The purpose of the current systematic review and meta-analyses is to summarize all MRI studies that compare neural differences between subjects with GAD and HC, yielding structural, FC, or task-based results. We hypothesize that the results from the meta-analysis and systematic review will corroborate the findings of the previous systematic reviews conducted with fewer records, as well as identify regions previously under-recognized. The outcomes of this paper will be structural (local and connectivity measures), FC, and task-based activity from (f)MRI research in GAD and HC. The resulting synthesis will provide a more detailed understanding of the neurophysiology underlying this highly prevalent and debilitating anxiety disorder.

2.3 Methods

2.3.1 Literature Search and Selection Criteria

The GAD neuroimaging literature was systematically searched on March 12, 2018, from inception. The comprehensive search included Medical Subject Headings, text, and keywords using the Embase, Ovid Medline, PsycINFO, Scopus, and Web of Science databases. Two main themes were included in the search: 1) MRI and 2) generalized anxiety disorder (please see supplemental material for the full search terms). Note that different search terms were used for different databases, based on the requirements of each database—for example, databases that use Medical Subject Headings have specific terminology that may not be applicable to other databases. The reference lists of all included articles were reviewed to identify further relevant papers. Studies were included if they were full-text, published articles that reported on original research using MRI with human subjects and if they compared neural structure (connectivity and local indices—e.g., volume), FC, or activity in subjects with GAD to HC. Although country of origin was not restricted, language was restricted to English.

2.3.2 Study Selection

All titles and abstracts were reviewed independently by two reviewers (T.A.K. and E.B.) using EndNote X7 software. Any title or abstract selected by either reviewer was included for further examination. All full-text articles were then screened for final inclusion by the same two reviewers; any disagreements at this stage were solved by consensus. Full-text articles were included for final selection if they met the following criteria: 1) original research; 2) not solely an abstract; 3) reported human MRI findings; 4) in a GAD population where GAD was the primary or most prominent diagnosis; 5) included a contrast between GAD and HC participants. While the systematic review portion of the current work includes whole-brain, region-of-interest, and seed-based results, the meta-analyses are limited to studies that included whole-brain data.

2.3.3 Data Extraction and Synthesis

Data were extracted using a standardized form, including the publication year, sample size, populations sampled (some studies included additional diagnoses), study modality (structure, FC, task), comorbidities, disease duration, diagnostic criteria, medications, questionnaires, MRI sequence type, data analysis software, contrasts performed, and regions (including coordinates, Brodmann areas, and lateralisation, as applicable) of structural, FC, and activity differences (see supplementary data spreadsheet). Demographic data included distribution of sex, handedness, age, and location of data collection. Attempts were made to contact authors to obtain missing information; however, if authors could not be reached, information remains incomplete in some instances.

2.3.4 Meta-Analyses

Two meta-analyses were conducted: one for voxel-based morphometry (VBM), and one for task-based results (comparing neutral and negative emotion-evoking stimuli) using Anisotropic Effect Size Seed-Based D Mapping (AES-SDM) software, version 5.15 (www.sdmproject.com; Radua & Mataix-Cols, 2012; Radua et al., 2012; Radua et al., 2014). Instead of assigning voxels a conventional value, this software uses Hedge's g to assign each voxel a measure of effect size (Radua et al., 2012). This software has been used to assess a variety of structural and functional MRI findings from various populations in the past (e.g., Jiang et al., 2017; Pico-Perez, Radua, Steward, Menchon, & Soriano-Mas, 2017; X. Wang, Cheng, Luo, Qiu, & Wang, 2018). Records were included in meta-analyses only if they explored the whole brain, and used a single significance threshold throughout the brain (Radua & Mataix-Cols, 2012). Additionally, if

multiple studies were individually eligible for meta-analysis, but had confirmed or suspected participant overlap, the record with a greater sample size was included in the meta-analysis. When possible, whole brain maps were used, while peak voxels were used when maps were not available. Furthermore, our criterion for meta-analysis was a minimum of 5 studies, provided they included at least one whole-brain map. Although some records included results with a patient group in addition to GAD and were eligible for the systematic review, in some cases it was not possible to isolate results specific to only GAD and HC groups, these records were excluded from the meta-analysis (e.g., Ball, Ramsawh, Campbell-Sills, Paulus, & Stein, 2013; K. S. Blair et al., 2012; Fonzo et al., 2015). Studies were included in the meta-analysis if they reported null findings, if they met the eligibility criteria.

First, meta-analyses that included whole-brain maps were converted to a useable format for the AES-SDM software. In one task-based study (Palm, Elliott, McKie, Deakin, & Anderson, 2011), three contrasts were performed comparing negative emotion-evoking faces to a neutral baseline (fearful > neutral, angry > neutral, sad > neutral). As it would not be appropriate to add these contrasts to the meta-analysis as individual records—this would bias the results by including data from the same individuals as if they were independent—the peak coordinates from these three contrasts were combined into a single brain map so that all of the data from these negative contrasts could be used in the meta-analysis. This combined brain map was then preprocessed along with the remaining task records. For both meta-analyses, any values listed as *z*-scores were converted to *t*-scores prior to preprocessing. Data from each meta-analysis was preprocessed using 50 Monte Carlo randomizations. Next, a voxel-wise random-effects analysis was conducted in which the weighted mean differences in GM or activity between subjects with GAD and HC were computed, providing between-study heterogeneity estimates, variance (I^2), *z*, and probability maps. This mean analysis is weighted for sample size, intra-study variance, and between group heterogeneity (Radua & Mataix-Cols, 2009, 2012; Radua et al., 2014). Due to the low sample sizes of the meta-analyses, complementary meta-analyses were limited to jackknife sensitivity analyses, as such analyses looking at age-, medication-, or comorbidity-effects were not conducted. Statistical significance was set to p_{voxel} (< 0.005, uncorrected), with peak SDM-*z* score > 1, and a minimum extent of 10 contiguous voxels, for optimal balance between α and β errors (Radua & Mataix-Cols, 2012).

2.3.5 Assessment of Study Consistency

Consistency was assessed qualitatively for the systematic review. The included studies varied in a number of areas, particularly in inclusion/exclusion criteria as various age groups, comorbidities, medication use, and diagnostic criteria were either allowed or disallowed. Additionally, study design was highly varied across studies, which is not unexpected, particularly amongst task-based studies.

Upon examination of the systematic review data, many of the cerebellum results were simply labelled as 'cerebellum' and more detailed descriptions were not provided, perhaps attributable to software limitations. To develop a better understanding of cerebellar location, all cerebellum coordinates were labelled using either Talairach Client (for Talairach coordinates; http://www.talairach.org/client.html) or the aal atlas in MRIcron (for Montreal Neurological Institute [MNI] coordinates; https://www.nitrc.org/projects/mricron).

For the meta-analyses, robustness of findings was assessed using jackknife sensitivity analyses which use a leave-one-out method (Radua & Mataix-Cols, 2009). I^2 index and Egger's tests, used to assess heterogeneity of effect sizes and publication bias, respectively, were also conducted for each meta-analysis. Funnel plots were created for significant meta-analytic clusters.

2.4 Results

2.4.1 Identification of Studies

The search strategy yielded 4,645 total records, and after 1,206 duplicates were removed, 85 met the inclusion criteria (see Figure 2.1 for flow diagram). Of the included records, 35 included structural analyses (Abdallah et al., 2013; Andreescu et al., 2017; Brambilla et al., 2012; Cha, DeDora, et al., 2016; Cha, Greenberg, et al., 2014; Cha, Greenberg, et al., 2016; Chen & Etkin, 2013; De Bellis et al., 2000; De Bellis et al., 2002; Etkin, Prater, Schatzberg, Menon, & Greicius, 2009; Hettema et al., 2012; Hilbert et al., 2015; Karim et al., 2016; Liao et al., 2013; Liao et al., 2014a, 2014b; Makovac, Meeten, Watson, Garfinkel, et al., 2016; Mohlman et al., 2009; Molent et al., 2017; Moon & Jeong, 2015a, 2016, 2017a, 2017b; Moon, Kang, & Jeong, 2015; Moon, Kim, & Jeong, 2014; Moon, Yang, & Jeong, 2015; Mueller et al., 2013; Schienle, Ebner, & Schafer, 2011; Strawn et al., 2014; Strawn et al., 2013; Terlevic et al., 2013; Tromp et al., 2012; W. Wang, Qian, et al., 2016; L. Zhang et al., 2011; Y. Zhang et al., 2013), 32 included FC analyses (Andreescu et al., 2015; Andreescu, Sheu, Tudorascu, Walker, & Aizenstein, 2014; Buff et al., 2016; Cha, Carlson, et al., 2014; Cha, DeDora, et al., 2016; Chen & Etkin, 2013; Cui et al., 2016;

Etkin, Prater, Hoeft, Menon, & Schatzberg, 2010; Etkin et al., 2009; Etkin & Schatzberg, 2011; Fonzo et al., 2014; Greenberg, Carlson, Cha, Hajcak, & Mujica-Parodi, 2013; Hölzel et al., 2013; Laufer, Israeli, & Paz, 2016; C. Li, Su, Wu, & Zhu, 2018; W. Li et al., 2016; Liu et al., 2015; Makovac, Meeten, Watson, Herman, et al., 2016; Makovac et al., 2018; McClure et al., 2007; Mohlman, Eldreth, Price, Staples, & Hanson, 2017; Monk et al., 2008; Oathes, Patenaude, Schatzberg, & Etkin, 2015; Pace-Schott et al., 2017; Qiao et al., 2017; Rabany et al., 2017; Roy et al., 2013; Strawn et al., 2012; Toazza et al., 2016; Tromp et al., 2012; W. Wang, Hou, et al., 2016; Xia et al., 2017), and 42 included task-based designs (Andreescu et al., 2011; Andreescu et al., 2015; Ball et al., 2013; K. Blair et al., 2008; K. S. Blair et al., 2012; K. S. Blair et al., 2017; Buff et al., 2016; Carlson, Rubin, & Mujica-Parodi, 2017; Cha, Carlson, et al., 2014; Cha, DeDora, et al., 2016; Cha, Greenberg, et al., 2014; Cha, Greenberg, et al., 2016; Chen & Etkin, 2013; Diwadkar et al., 2017; Etkin et al., 2010; Etkin & Schatzberg, 2011; Fitzgerald et al., 2017; Fonzo et al., 2015; Fonzo et al., 2014; Greenberg et al., 2013; Guyer et al., 2012; Hölzel et al., 2013; Karim et al., 2016; Laufer et al., 2016; Makovac et al., 2018; McClure et al., 2007; Mohlman et al., 2017; Monk et al., 2006; Monk et al., 2008; Moon & Jeong, 2015b, 2017b; Moon, Sundaram, Choi, & Jeong, 2016; Moon, Yang, et al., 2015; Moon, Yang, & Jeong, 2017; Nitschke et al., 2009; Ottaviani et al., 2016; Palm et al., 2011; Paulesu et al., 2010; Price, Eldreth, & Mohlman, 2011; Strawn et al., 2012; Whalen et al., 2008; White et al., 2017; Yassa, Hazlett, Stark, & Hoehn-Saric, 2012). For reader ease, records are sorted by modality in the supplementary data spreadsheet. For information on any specific study, refer to the supplementary data spreadsheet.

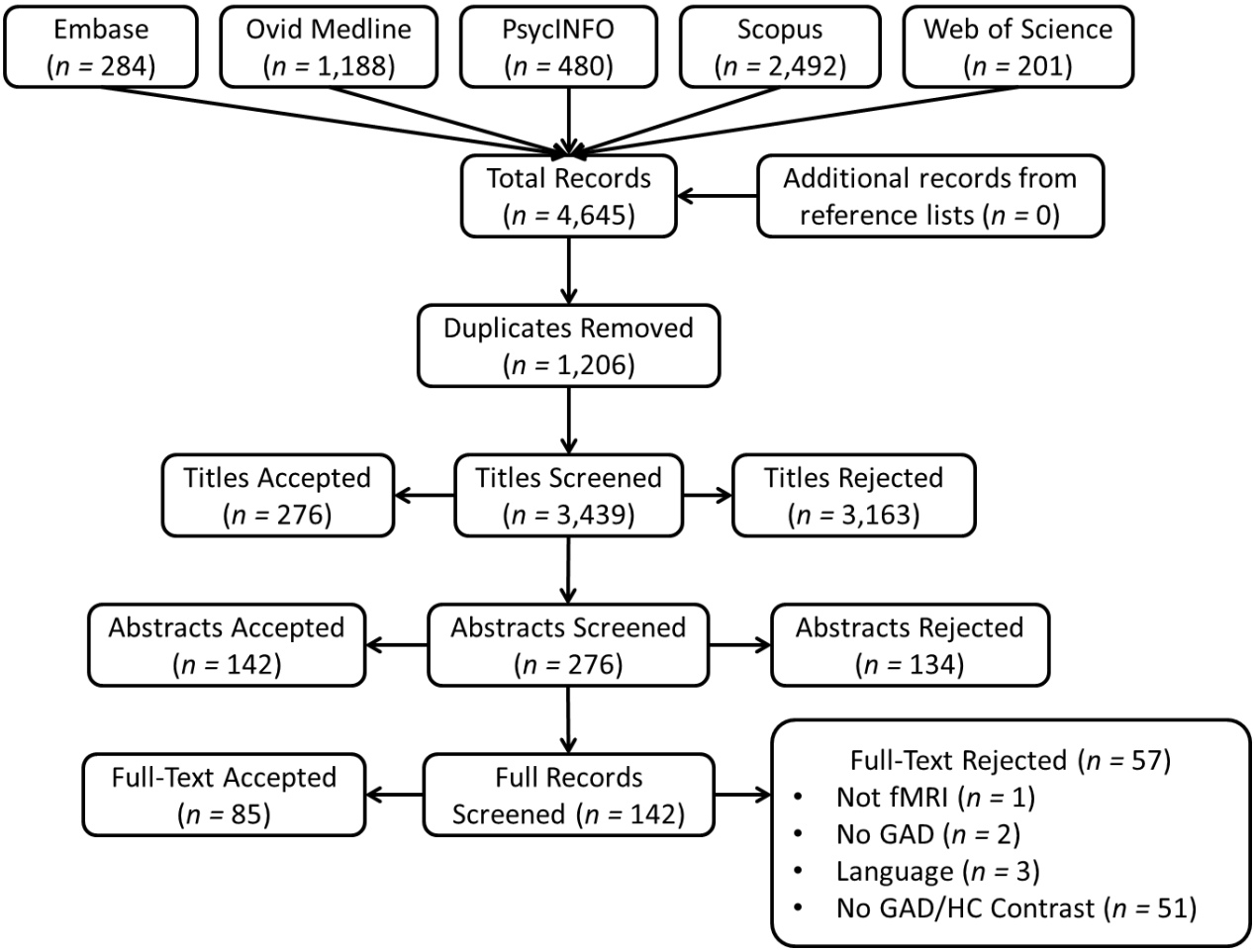

Figure 2.1: Flow diagram for inclusion of final records.

2.4.2 Details of Included Studies

Although databases were searched from inception, studies in which GAD was investigated with MRI ranged from 2008 to 2018. Out of the 85 records included, 1 was conducted in South America, 14 were conducted in Europe, 23 in Asia, and 47 in North America (see Table 2.1 for references). Handedness was recorded in 43 of the papers (see Table 2.1), of which 99% of the participants were right-handed. Across the 85 studies, there were a total of 4,160 participants (1,855 with a diagnosis of GAD) that underwent an MRI scan with approximately 63% of participants being female. However, this sample size is inflated as many papers shared participants within labs (see supplementary Table S1).

Sixteen studies included more than one patient population (i.e., in addition to a GAD group), including social anxiety disorder (SAD; also including previous iterations such as generalized social phobia and social phobia), PD, major depressive disorder (MDD), PTSD, and

primary insomnia (see Table 2.1). Additionally, of these 16 studies, five included a purposeful comorbid group in which patients had both GAD, and generalized social phobia or MDD comorbidity. These studies included these comorbidities or differential diagnoses as distinct groups, rather than simply allowing comorbidities in the inclusion criteria; i.e., many of the included studies did not exclude participants for having additional anxiety disorders or mood disorders. Two records compared anxiety disorders in general to HC, but were included as they conducted contrasts with the GAD subpopulation in their anxiety group (Mueller et al., 2013; Toazza et al., 2016). For additional information on comorbidities, see the supplementary data spreadsheet.

All records included mean, median or range of participant ages: 16 studies were done in an adolescent population, 61 were done in an adult population, 7 studies were done in an elderly population, and adult and elderly participants were compared in 1 study (see Table 2.1).

Table 2.1: Basic demographic and sample information for included records.

Sample Characteristic	***N***	**Records**
Location		
South America	1	(Toazza et al., 2016)
Europe	14	(Brambilla et al., 2012; Buff et al., 2016; Diwadkar et al., 2017; Hilbert et al., 2015; Laufer et al., 2016; Makovac, Meeten, Watson, Garfinkel, et al., 2016; Makovac, Meeten, Watson, Herman, et al., 2016; Makovac et al., 2018; Molent et al., 2017; Ottaviani et al., 2016; Palm et al., 2011; Paulesu et al., 2010; Schienle et al., 2011; Terlevic et al., 2013)
Asia	23	(Cui et al., 2016; C. Li et al., 2018; W. Li et al., 2016; Liao et al., 2013; Liao et al., 2014a, 2014b; Liu et al., 2015; Moon & Jeong, 2015a, 2015b, 2016, 2017a, 2017b; Moon, Kang, et al., 2015; Moon et al., 2014; Moon et al., 2016; Moon, Yang, et al., 2015; Moon et al., 2017; Qiao et al., 2017; W. Wang, Hou, et al., 2016; W. Wang, Qian, et al., 2016; Xia et al., 2017; L. Zhang et al., 2011; Y. Zhang et al., 2013)
North America	47	(Abdallah et al., 2013; Andreescu et al., 2011; Andreescu et al., 2015; Andreescu et al., 2014; Andreescu et al., 2017; Ball et al., 2013; K. Blair et al., 2008; K. S. Blair et al., 2012; K. S. Blair et al., 2017; Carlson et al., 2017; Cha, Carlson, et al., 2014; Cha, DeDora, et al., 2016; Cha, Greenberg, et al., 2014; Cha, Greenberg, et al., 2016; Chen & Etkin, 2013; De Bellis et al., 2000; De Bellis et al., 2002; Etkin et al., 2010; Etkin et al., 2009; Etkin & Schatzberg, 2011; Fitzgerald et al., 2017; Fonzo et al., 2015; Fonzo et al., 2014; Greenberg et al., 2013; Guyer et al., 2012; Hettema et al., 2012; Hölzel et al., 2013; Karim et al., 2016; McClure et al., 2007; Mohlman et al., 2017; Mohlman et al.,

		2009; Monk et al., 2006; Monk et al., 2008; Mueller et al., 2013; Nitschke et al., 2009; Oathes et al., 2015; Pace-Schott et al., 2017; Price et al., 2011; Rabany et al., 2017; Roy et al., 2013; Strawn et al., 2012; Strawn et al., 2014; Strawn et al., 2013; Tromp et al., 2012; Whalen et al., 2008; White et al., 2017; Yassa et al., 2012)
Handedness		
Recorded	43	(Brambilla et al., 2012; Carlson et al., 2017; Cui et al., 2016; De Bellis et al., 2002; Diwadkar et al., 2017; Etkin et al., 2010; Etkin et al., 2009; Etkin & Schatzberg, 2011; Hettema et al., 2012; Hilbert et al., 2015; Hölzel et al., 2013; C. Li et al., 2018; W. Li et al., 2016; Liao et al., 2013; Liao et al., 2014a, 2014b; Liu et al., 2015; Makovac, Meeten, Watson, Garfinkel, et al., 2016; Makovac, Meeten, Watson, Herman, et al., 2016; Makovac et al., 2018; Mohlman et al., 2017; Mohlman et al., 2009; Monk et al., 2008; Moon & Jeong, 2015b; Moon et al., 2016; Moon, Yang, et al., 2015; Nitschke et al., 2009; Ottaviani et al., 2016; Pace-Schott et al., 2017; Paulesu et al., 2010; Price et al., 2011; Qiao et al., 2017; Roy et al., 2013; Schienle et al., 2011; Terlevic et al., 2013; Toazza et al., 2016; Tromp et al., 2012; W. Wang, Hou, et al., 2016; W. Wang, Qian, et al., 2016; Whalen et al., 2008; Yassa et al., 2012; L. Zhang et al., 2011; Y. Zhang et al., 2013)
Sample Age		
Adolescent	16	(De Bellis et al., 2000; De Bellis et al., 2002; Guyer et al., 2012; Liao et al., 2013; Liao et al., 2014a, 2014b; Liu et al., 2015; McClure et al., 2007; Monk et al., 2006; Monk et al., 2008; Mueller et al., 2013; Roy et al., 2013; Strawn et al., 2012; Strawn et al., 2014; Strawn et al., 2013; Toazza et al., 2016)

Adult	61	(Abdallah et al., 2013; Ball et al., 2013; K. Blair et al., 2008; K. S. Blair et al., 2012; K. S. Blair et al., 2017; Brambilla et al., 2012; Buff et al., 2016; Carlson et al., 2017; Cha, Carlson, et al., 2014; Cha, DeDora, et al., 2016; Cha, Greenberg, et al., 2014; Cha, Greenberg, et al., 2016; Chen & Etkin, 2013; Cui et al., 2016; Diwadkar et al., 2017; Etkin et al., 2010; Etkin et al., 2009; Etkin & Schatzberg, 2011; Fitzgerald et al., 2017; Fonzo et al., 2015; Fonzo et al., 2014; Greenberg et al., 2013; Hettema et al., 2012; Hilbert et al., 2015; Hölzel et al., 2013; Laufer et al., 2016; C. Li et al., 2018; W. Li et al., 2016; Makovac, Meeten, Watson, Garfinkel, et al., 2016; Makovac, Meeten, Watson, Herman, et al., 2016; Makovac et al., 2018; Molent et al., 2017; Moon & Jeong, 2015a, 2015b, 2016, 2017a, 2017b; Moon, Kang, et al., 2015; Moon et al., 2014; Moon et al., 2016; Moon, Yang, et al., 2015; Moon et al., 2017; Nitschke et al., 2009; Oathes et al., 2015; Ottaviani et al., 2016; Pace-Schott et al., 2017; Palm et al., 2011; Paulesu et al., 2010; Qiao et al., 2017; Rabany et al., 2017; Schienle et al., 2011; Terlevic et al., 2013; Tromp et al., 2012; W. Wang, Hou, et al., 2016; W. Wang, Qian, et al., 2016; Whalen et al., 2008; White et al., 2017; Xia et al., 2017; Yassa et al., 2012; L. Zhang et al., 2011; Y. Zhang et al., 2013)
Elderly	7	(Andreescu et al., 2011; Andreescu et al., 2015; Andreescu et al., 2017; Karim et al., 2016; Mohlman et al., 2017; Mohlman et al., 2009; Price et al., 2011)
Adult + Elderly	1	(Andreescu et al., 2014)
Records with Additional Patient Groups		
GSP	1	(K. Blair et al., 2008)
GSP + GAD/GSP	1	(K. S. Blair et al., 2012)

SP	1	(Guyer et al., 2012)
SAD	2	(K. S. Blair et al., 2017; Rabany et al., 2017)
SAD + PD	2	(Buff et al., 2016; Fonzo et al., 2015)
PD	3	(Ball et al., 2013; Cui et al., 2016; Terlevic et al., 2013)
GAD/MDD	1	(Cha, Greenberg, et al., 2016)
GAD/MDD + MDD	3	(Carlson et al., 2017; Etkin & Schatzberg, 2011; Oathes et al., 2015)
PTSD	2	(Chen & Etkin, 2013; L. Zhang et al., 2011)
Primary Insomnia	1	(Pace-Schott et al., 2017)

A '+' symbol indicates multiple patient groups, while a '/' indicates comorbid groups. Adolescent = ages 11-18; Adult = ages 19-59; Elderly = ages 60+; GSP = generalized social phobia; GAD = generalized anxiety disorder; SP = social phobia; SAD = social anxiety disorder; PD = panic disorder; MDD = major depressive disorder; PTSD = posttraumatic stress disorder.

2.4.3 Study Design

Structural analyses were conducted in 35 records and spanned various methodologies, including 1) DTI (n = 10), 2) WM hyperintensity (WMH, n = 2), 3) CTA (n = 4), 4) VBM (n = 16), 5) other volumetric analyses (n = 10), 6) surface area (n = 1), and 7) local gyrification index (n = 1; see Table 2.2). FC analyses were conducted in 33 records: resting state fMRI scans were used in 12—defined here as a separate fMRI scan, acquired in the absence of a task, using basic seed-based, region-of-interest or independent components analyses (ICA). Six studies included measures of FC conducted from task-based data and 10 studies included psychophysiological interaction (PPI; 2 observed no significant results: Cha, DeDora, et al., 2016; Greenberg et al., 2013), however, between-groups contrasts were not conducted for PPI in one record (Laufer et al., 2016). A few records included FC analyses for hierarchical partner matching-ICA (n = 1), ALFF analyses (n = 1), effective connectivity (n = 2), and ReHo (n = 2, see Table 2.2). Finally, 42 records included a task, and these were separated into groups including: 1) null judgement/passive (discerning characteristics of no interest to the researchers like gender or nose width, or simply viewing emotional stimuli), 2) congruency and conflict (deciphering congruent and incongruent stimuli), 3) emotion modulation (maintaining or altering emotions during stimulation), 4) conditioned fear (generalizing fear to similar stimuli), 5) memory (e.g., memory suppression of word pairs or memory after neutral or anxiety-inducing distractors), and 6) miscellaneous tasks (see Table 2.2). For more specific task information, please see the supplementary data spreadsheet. In one record, two distinct tasks were performed (K. S. Blair et al., 2012), and these are listed separately in Table 2.2. To focus the review, neuroimaging results obtained from correlation with questionnaires or behavioural data are not reported here. For this reason, results are omitted from 2 records (Karim et al., 2016; Mohlman et al., 2009).

Table 2.2: Study design and task-based stimuli used in included records.

Modality	***N*†**	**References**	**Meta-Analyses**
Structure	*35*		
Diffusion Tensor Imaging	10	(Brambilla et al., 2012; Cha, DeDora, et al., 2016; Cha, Greenberg, et al., 2014; Cha, Greenberg, et al., 2016; Hettema et al., 2012; Liao et al., 2014b; Tromp et al., 2012; W. Wang, Qian, et al., 2016; L. Zhang et al., 2011; Y. Zhang et al., 2013)	
Fractional Anisotropy	8	(Cha, DeDora, et al., 2016; Cha, Greenberg, et al., 2014; Hettema et al., 2012; Liao et al., 2014b; Tromp et al., 2012; W. Wang, Qian, et al., 2016; L. Zhang et al., 2011; Y. Zhang et al., 2013)	
Mean Diffusivity	3	(Cha, Greenberg, et al., 2016; Tromp et al., 2012; W. Wang, Qian, et al., 2016)	
Apparent Diffusion Coefficient	1	(Brambilla et al., 2012)	
Tractography	1	(Cha, DeDora, et al., 2016)	
Axial + Radial Diffusivity	1	(W. Wang, Qian, et al., 2016)	
White Matter Hyperintensity	2	(Andreescu et al., 2017; Karim et al., 2016)	
Cortical Thickness Analysis	4	(Andreescu et al., 2017; Cha, Greenberg, et al., 2014; Molent et al., 2017; Strawn et al., 2014)	
Voxel-Based Morphometry	16	(Chen & Etkin, 2013; Etkin et al., 2009; Hilbert et al., 2015; Liao et al., 2013; Liao et al., 2014a;	(Hilbert et al., 2015; Liao et al., 2014b; Makovac, Meeten,

		Makovac, Meeten, Watson, Garfinkel, et al., 2016; Moon & Jeong, 2015a, 2016, 2017a, 2017b; Moon, Kang, et al., 2015; Moon et al., 2014; Moon, Yang, et al., 2015; Mueller et al., 2013; Schienle et al., 2011; Strawn et al., 2013)	Watson, Garfinkel, et al., 2016; Moon et al., 2014; Schienle et al., 2011; Strawn et al., 2013)
Volume	10	(Abdallah et al., 2013; Andreescu et al., 2017; Cha, Greenberg, et al., 2016; De Bellis et al., 2000; De Bellis et al., 2002; Hettema et al., 2012; Karim et al., 2016; Mohlman et al., 2009; Molent et al., 2017; Terlevic et al., 2013)	
Surface Area	1	(Molent et al., 2017)	
Local Gyrification Index	1	(Molent et al., 2017)	
Functional Connectivity	*33*		
Resting State	12	(Andreescu et al., 2014; Chen & Etkin, 2013; Cui et al., 2016; Etkin et al., 2009; W. Li et al., 2016; Liu et al., 2015; Oathes et al., 2015; Pace-Schott et al., 2017; Rabany et al., 2017; Roy et al., 2013; Toazza et al., 2016; W. Wang, Hou, et al., 2016)	
Task-Related FC	7	(Andreescu et al., 2015; Cha, Greenberg, et al., 2014; Hölzel et al., 2013; Makovac, Meeten, Watson, Herman, et al., 2016; Makovac et al., 2018; McClure et al., 2007; Strawn et al., 2012)	

Psychophysiological Interaction	10	(Buff et al., 2016; Cha, Carlson, et al., 2014; Cha, DeDora, et al., 2016; Etkin et al., 2010; Etkin & Schatzberg, 2011; Fonzo et al., 2014; Greenberg et al., 2013; Laufer et al., 2016; Monk et al., 2008; Tromp et al., 2012)	
Hierarchical partner matching-ICA	1	(Qiao et al., 2017)	
ALFF	1	(W. Wang, Hou, et al., 2016).	
Effective Connectivity	2	(Mohlman et al., 2017; Qiao et al., 2017)	
Regional Homogeneity	2	(C. Li et al., 2018; Xia et al., 2017)	
Task	*42*		
Null Judgement/ Passive	10	(K. Blair et al., 2008; Buff et al., 2016; Carlson et al., 2017; Chen & Etkin, 2013; Fitzgerald et al., 2017; Hölzel et al., 2013; McClure et al., 2007; Nitschke et al., 2009; Palm et al., 2011; Whalen et al., 2008)	(Fitzgerald et al., 2017; Hölzel et al., 2013; Palm et al., 2011)
Passively view 'Lost' episode		(Carlson et al., 2017)	
Passively view cued emotional images		(Nitschke et al., 2009)	
Passively view emotional faces		(Whalen et al., 2008)	
Passively view or appraise IAPS affect		(Fitzgerald et al., 2017)	
Appraise face affect		(Hölzel et al., 2013)	
Face hostility/nose width judgements		(McClure et al., 2007)	
Emotional faces + gender judgement		(K. Blair et al., 2008; Palm et al., 2011)	

Emotional faces+ face colour judgement		(Chen & Etkin, 2013)	
IAPS + blurry image judgement		(Buff et al., 2016)	
Congruency/ Conflict	9	(K. S. Blair et al., 2012; Etkin et al., 2010; Etkin & Schatzberg, 2011; Fonzo et al., 2015; Fonzo et al., 2014; Karim et al., 2016; Monk et al., 2006; Monk et al., 2008; Price et al., 2011)	(Monk et al., 2006; Price et al., 2011)
Top-down attention control		(K. S. Blair et al., 2012)	
Emotional conflict task		(Etkin et al., 2010; Etkin & Schatzberg, 2011)	
Emotion face assessment task		(Fonzo et al., 2014)	
Modified emotion assessment task		(Fonzo et al., 2015)	
Congruent emotional faces		(Karim et al., 2016; Monk et al., 2006; Monk et al., 2008)	
Emotional Stroop task		(Price et al., 2011)	
Emotion Modulation	6	(Andreescu et al., 2011; Andreescu et al., 2015; Ball et al., 2013; K. S. Blair et al., 2012; Mohlman et al., 2017; Paulesu et al., 2010)	
Worry induction or suppression		(Andreescu et al., 2011)	
Worry induction or neutral		(Mohlman et al., 2017; Paulesu et al., 2010)	
Worry induction		(Andreescu et al., 2015)	
Maintain or reduce reactions to images		(Ball et al., 2013)	
Explicit emotion regulation		(K. S. Blair et al., 2012)	

Conditioned Fear	6	(Cha, Carlson, et al., 2014; Cha, DeDora, et al., 2016; Cha, Greenberg, et al., 2014; Cha, Greenberg, et al., 2016; Greenberg et al., 2013; Laufer et al., 2016)
Fear generalization (shape + shock)		(Cha, Carlson, et al., 2014; Cha, DeDora, et al., 2016; Cha, Greenberg, et al., 2014; Cha, Greenberg, et al., 2016; Greenberg et al., 2013)
Fear generalization (tones + money)		(Laufer et al., 2016)
Memory	6	(Diwadkar et al., 2017; Moon & Jeong, 2015b, 2017b; Moon et al., 2016; Moon, Yang, et al., 2015; Moon et al., 2017)
Memory/suppression of word pairs		(Diwadkar et al., 2017)
Recognition of neutral/emotional words		(Moon, Yang, et al., 2015; Moon et al., 2017)
Recognition of faces after distractors		(Moon & Jeong, 2015b, 2017b; Moon et al., 2016)
Miscellaneous	6	(K. S. Blair et al., 2017; Guyer et al., 2012; Ottaviani et al., 2016; Strawn et al., 2012; White et al., 2017; Yassa et al., 2012)
Optimistic bias task		(K. S. Blair et al., 2017)
Monetary incentive anticipation task		(Guyer et al., 2012)
Visuomotor task, recall past emotion		(Ottaviani et al., 2016)
CPT-END task		(Strawn et al., 2012)
Reinforcement prediction error		(White et al., 2017)

Uncertainty + monetary loss		(Yassa et al., 2012)
Stimuli		
Emotive Faces	9	(K. Blair et al., 2008; Chen & Etkin, 2013; Fonzo et al., 2015; Fonzo et al., 2014; Karim et al., 2016; Monk et al., 2006; Monk et al., 2008; Palm et al., 2011; Whalen et al., 2008)
Emotion-evoking scenes (e.g., IAPS)	9	(Ball et al., 2013; K. S. Blair et al., 2012; Buff et al., 2016; Fitzgerald et al., 2017; Moon & Jeong, 2015b, 2017b; Moon et al., 2016; Nitschke et al., 2009; Strawn et al., 2012)
Lexical	8	(Andreescu et al., 2011; Andreescu et al., 2015; K. S. Blair et al., 2017; Diwadkar et al., 2017; Moon & Jeong, 2017b; Moon, Yang, et al., 2015; Moon et al., 2017; Price et al., 2011)
Emotive faces + lexical	5	(Etkin et al., 2010; Etkin & Schatzberg, 2011; Hölzel et al., 2013; McClure et al., 2007; Paulesu et al., 2010)
Rectangles + shock	5	(Cha, Carlson, et al., 2014; Cha, DeDora, et al., 2016; Cha, Greenberg, et al., 2014; Cha, Greenberg, et al., 2016; Greenberg et al., 2013)
Auditory stimuli	3	(Laufer et al., 2016; Makovac et al., 2018; Ottaviani et al., 2016)

Monetary Loss/Gain	3	(Guyer et al., 2012; White et al., 2017; Yassa et al., 2012)
Television episode	1	(Carlson et al., 2017)
Internal worries	1	(Mohlman et al., 2017)

[†]Numbers may not sum to the overall *N* if multiple analysis types were conducted within a record. Please refer to the supplemental data for brief task descriptions for each study. ALFF = amplitude of low frequency fluctuations; ICA = independent component analysis; IAPS = International Affective Picture System.

2.4.4 Systematic Review Results

Common MRI results for comparisons between subjects with GAD and HC can be found in supplementary Table S2. Regions were listed in Table S2 if they were found in at least two records from different laboratories, but a full list of results can be found in the supplementary data spreadsheet. The most commonly occurring regions include the same four regions consistently identified by other systematic reviews: the dlPFC, ACC, amygdala, and hippocampus.

The results from the ACC were largely mixed: results indicate both increased (n = 6; Andreescu et al., 2011; Fonzo et al., 2014; Laufer et al., 2016; McClure et al., 2007; Mohlman et al., 2017; Paulesu et al., 2010) and decreased (n = 7; K. S. Blair et al., 2012; Diwadkar et al., 2017; Etkin et al., 2010; Laufer et al., 2016; Mohlman et al., 2017; Palm et al., 2011; White et al., 2017) activity for subjects with GAD, across all different types of tasks, without any clear age-group patterns emerging (see supplementary Table S2). Although the FC results for the ACC are relatively mixed, with greater FC (n = 5; Andreescu et al., 2015; Cha, Carlson, et al., 2014; Etkin et al., 2010; Mohlman et al., 2017; W. Wang, Hou, et al., 2016) and reduced FC (n = 8; Andreescu et al., 2015; Chen & Etkin, 2013; W. Li et al., 2016; Makovac, Meeten, Watson, Herman, et al., 2016; Pace-Schott et al., 2017; Roy et al., 2013; W. Wang, Hou, et al., 2016; Xia et al., 2017), there are a few more records indicating reduced FC for GAD subjects when using an amygdala seed (Makovac, Meeten, Watson, Herman, et al., 2016; Pace-Schott et al., 2017; Roy et al., 2013), compared to greater FC with this seed (Etkin et al., 2010).

While there was some evidence to suggest greater activity in the dlPFC for subjects with GAD (for passive [Buff et al., 2016]; congruency [Fonzo et al., 2014]; and emotion modulation [Mohlman et al., 2017]), slightly more results show reduced activity for subjects with GAD across passive (Carlson et al., 2017; Palm et al., 2011), congruency (Fonzo et al., 2014; Price et al., 2011), emotion modulation (Andreescu et al., 2011; Ball et al., 2013; Mohlman et al., 2017), and memory (Moon & Jeong, 2015b, 2017b; Moon et al., 2016) tasks. Both increased and decreased activity in the dlPFC was reported for adults and adolescents, and interestingly, most of these dlPFC activation results are from whole-brain studies. Additionally, subjects with GAD tended to have reduced FC in the dlPFC (n = 9), arising from amygdala (Liu et al., 2015; Makovac, Meeten, Watson, Herman, et al., 2016; Monk et al., 2008), insula (Andreescu et al., 2015; Buff et al., 2016), precuneus/posterior cingulate cortex (PCC; W. Wang, Hou, et al., 2016), and prefrontal (Andreescu et al., 2015; Cha, Greenberg, et al., 2014; Mohlman et al., 2017; W. Wang, Hou, et al.,

2016) seeds, and in a hierarchical partner matching study (Qiao et al., 2017). However, it should be noted that a few studies (n = 3) showed increased FC in the dlPFC (Andreescu et al., 2015 [insula seed]; Toazza et al., 2016 [basolateral amygdala seed]; W. Wang, Hou, et al., 2016 [whole-brain ALFF]). Finally, results indicated that subjects with GAD had reduced dlPFC volume (n = 5; Andreescu et al., 2017; Moon & Jeong, 2015a, 2016, 2017a, 2017b).

The results for the amygdala were somewhat clearer: all structural studies consistently showed increased volume (De Bellis et al., 2000; Etkin et al., 2009; Schienle et al., 2011) and FA (Y. Zhang et al., 2013) for subjects with GAD. While one study showed reduced effective connectivity in the amygdala (Qiao et al., 2017 [frontal gyrus seeds]), and another observed reduced FC between the right and left amygdala (Liu et al., 2015), all other FC results were greater for GAD (albeit with inconsistent seed regions; Andreescu et al., 2015; Buff et al., 2016; Liu et al., 2015; Mohlman et al., 2017; Qiao et al., 2017) and spanning all age groups. Finally, the majority of task results (n = 11) indicated greater amygdala activity for subjects with GAD for passive (Fitzgerald et al., 2017; Hölzel et al., 2013; McClure et al., 2007; Nitschke et al., 2009), congruency (Etkin et al., 2010; Etkin & Schatzberg, 2011; Fonzo et al., 2015; Fonzo et al., 2014; Monk et al., 2008; Price et al., 2011), and emotion modulation (Mohlman et al., 2017) tasks, while only a few studies in adults (n = 2) showed reduced activity for subjects with GAD in passive (Carlson et al., 2017) and congruency (K. S. Blair et al., 2012) tasks. One study investigating high uncertainty observed both increased and decreased activity in the amygdala (Yassa et al., 2012). Although this included expected responses to aversive stimuli, it also included results for neutral stimuli in two cases (Hölzel et al., 2013; Nitschke et al., 2009). Additionally, a variety of studies that hypothesized amygdala volume (Hettema et al., 2012; Liao et al., 2013; Makovac, Meeten, Watson, Garfinkel, et al., 2016; Mohlman et al., 2009; Mueller et al., 2013) activity (Chen & Etkin, 2013; Whalen et al., 2008), or FC (Cha, DeDora, et al., 2016; Greenberg et al., 2013; Laufer et al., 2016; Rabany et al., 2017) differences did not observe them. Finally, the hippocampus results were left-lateralized (with exceptions in: Abdallah et al., 2013 [bilateral]; Cha, Carlson, et al., 2014; W. Wang, Hou, et al., 2016) and indicated that subjects with GAD had reduced volume (Abdallah et al., 2013; Hettema et al., 2012; Moon & Jeong, 2017a; Moon et al., 2014; Moon, Yang, et al., 2015) and increased mean diffusivity (Cha, Greenberg, et al., 2016), compared with HC. Activation results tended to be mixed: for memory tasks HC subjects had increased activity for neutral or anxiety-induced conditions (Moon, Yang, et al., 2015; Moon et al., 2017) while subjects

with GAD also had increased activity, but only for anxiety-induced conditions (Moon & Jeong, 2015b, 2017b; Moon et al., 2016). One conditioned fear task further showed increased activity for HC (Cha, Greenberg, et al., 2016), as well as for a generalized fear stimulus condition in a PPI FC study (Cha, Carlson, et al., 2014). Finally, subjects with GAD showed increased FC with the hippocampus using dlPFC (W. Wang, Hou, et al., 2016) and insula (Andreescu et al., 2015) seeds.

In addition to these four commonly accepted GAD-altered regions, a variety of other regions are also commonly altered. The insula, which has similar representation in the results as the hippocampus, appears to have reduced volume for subjects with GAD (Moon & Jeong, 2017a; Moon et al., 2014; Moon, Yang, et al., 2015), but greater FC (Buff et al., 2016; Fonzo et al., 2014; Liu et al., 2015; McClure et al., 2007; Qiao et al., 2017; Roy et al., 2013; W. Wang, Hou, et al., 2016)—particularly with amygdala seeds (Fonzo et al., 2014; Liu et al., 2015; McClure et al., 2007; Qiao et al., 2017; Roy et al., 2013). Only one result indicated reduced FC in the GAD insula (Andreescu et al., 2015). Insula activity was mixed, with greater activity in subjects with GAD for passive (Buff et al., 2016), congruency (Fonzo et al., 2014), and conditioned fear tasks (Laufer et al., 2016), mixed for emotion modulation tasks (reduced activity in Ball et al., 2013; and greater activity in Mohlman et al., 2017), and reduced in a prediction error task (White et al., 2017). The posterior cingulate cortex (PCC) is also fairly prevalent in the results, but has seldom been mentioned in previous reviews, and like the ACC tends to have mixed FC—greater in (McClure et al., 2007; Qiao et al., 2017; Strawn et al., 2012; W. Wang, Hou, et al., 2016) and reduced in (Etkin & Schatzberg, 2011; Qiao et al., 2017)—and task-based results, greater in (Buff et al., 2016; Fonzo et al., 2014; Mohlman et al., 2017) and reduced in (Carlson et al., 2017; Etkin & Schatzberg, 2011; Laufer et al., 2016; White et al., 2017), with no clear pattern emerging. Less common, but still each reported in at least 10 records, are the precuneus, precentral gyrus (largely from whole-brain analyses), superior temporal gyrus, ventrolateral PFC (vlPFC), orbitofrontal cortex (OFC) and the cerebellum (supplementary Table S2).

The precuneus appears to have reduced FC with the dlPFC (W. Li et al., 2016; W. Wang, Hou, et al., 2016), mixed FC with the amygdala—greater in (McClure et al., 2007; Toazza et al., 2016) and reduced in (Strawn et al., 2012)—and reduced activity for working memory (Diwadkar et al., 2017; Moon & Jeong, 2015b, 2017b) in subjects with GAD. The precentral gyrus results show that FC tends to be greater, using amygdala (Monk et al., 2008; Toazza et al., 2016) and dlPFC (W. Wang, Hou, et al., 2016) seeds and activity is altered for working memory—greater in

(Moon, Yang, et al., 2015) and reduced in (Moon et al., 2016; Moon et al., 2017)—reduced for a prediction error task (White et al., 2017), but increased for a conditioned fear task (Laufer et al., 2016). Reduced volume is commonly, but not always observed in the precentral gyrus (Makovac, Meeten, Watson, Garfinkel, et al., 2016; Moon & Jeong, 2016, 2017a; greater volume in Strawn et al., 2013) and superior temporal gyrus (STG; greater volume in De Bellis et al., 2002; but reduced volume in Moon & Jeong, 2017a; Moon et al., 2014; Moon, Yang, et al., 2015) for GAD patients. Emotion modulation work resulted in decreased activity (Ball et al., 2013), while activity for conditioned fear (Laufer et al., 2016) and FC (Liu et al., 2015; Monk et al., 2008; Roy et al., 2013; W. Wang, Hou, et al., 2016; Xia et al., 2017) was increased in the STG. The vlPFC showed reduced FA (Tromp et al., 2012) and increased FC (Andreescu et al., 2014; C. Li et al., 2018; W. Li et al., 2016; Monk et al., 2008; Roy et al., 2013), particularly using amygdala seeds (W. Li et al., 2016; Monk et al., 2008; Roy et al., 2013); however, decreased FC was also observed (Buff et al., 2016; Tromp et al., 2012 [amygdala seed]). Subjects with GAD had reduced activity for passive (Palm et al., 2011) and emotion modulation (Ball et al., 2013) tasks, greater activity for congruency (Monk et al., 2006) and memory tasks (Moon, Yang, et al., 2015; Moon et al., 2017), and mixed activity for conditioned fear tasks (reduced in Cha, DeDora, et al., 2016; increased in Laufer et al., 2016) in the vlPFC. The OFC has reduced mean diffusivity (Andreescu et al., 2017), cortical thickness (Andreescu et al., 2017), and surface area (Molent et al., 2017), mixed FC with prefrontal seeds, with greater FC in (Andreescu et al., 2015; Mohlman et al., 2017; Strawn et al., 2012; W. Wang, Hou, et al., 2016) and reduced FC in (Andreescu et al., 2015; Mohlman et al., 2017; W. Wang, Hou, et al., 2016). Additionally, the OFC has greater activity in subjects with GAD for emotion modulation (Mohlman et al., 2017; Paulesu et al., 2010) and passive (Fitzgerald et al., 2017) tasks, and reduced activity in conditioned fear (Laufer et al., 2016) and memory (Diwadkar et al., 2017) tasks. Finally, whole-brain results show the midbrain is consistently smaller in subjects with GAD, as compared to HC (Moon & Jeong, 2015a, 2016, 2017a, 2017b; Moon et al., 2014; Moon, Yang, et al., 2015); however, these results are all from the same laboratory, and it is likely that there is some participant overlap between these records, although the authors could not be reached to confirm this.

The cerebellum results are again fairly mixed, having both increased (Andreescu et al., 2015; Liu et al., 2015; Roy et al., 2013) and reduced (Fonzo et al., 2014; W. Li et al., 2016; Roy et al., 2013) FC in subjects with GAD. However, grouping and re-labelling the results from the

cerebellum yielded more distinct activation and FC patterns: HC > GAD contrasts were largely localized to the anterior lobe for FC (W. Li et al., 2016 [dlPFC seed]) and activity related to emotion regulation (Ball et al., 2013), congruency (Price et al., 2011), and working memory (Diwadkar et al., 2017; Moon & Jeong, 2015b, 2017b), with about half of the results localized to the culmen/vermis lobules IV and V (Ball et al., 2013; W. Li et al., 2016; Moon & Jeong, 2017b; see Table 2.3). Conversely, GAD > HC contrasts were largely observed in the posterior cerebellum with FC (Fonzo et al., 2014; Liu et al., 2015), and activity from congruency tasks (Fonzo et al., 2015; Monk et al., 2008; Price et al., 2011; see Table 2.3). Some papers in which cerebellum results were reported were excluded as specific contrasts were not done to compare subjects with GAD to HC (Benson, Guyer, Nelson, Pine, & Ernst, 2015; Brown et al., 2015; Carlisi, Hilbert, Guyer, & Ernst, 2017; Haddad, Bilderbeck, James, & Lau, 2015; Hamm et al., 2014; Lau et al., 2009; Park, Kim, Jeong, Chung, & Yang, 2016; Swartz, Phan, Angstadt, Fitzgerald, & Monk, 2014). There is also at least one case in which cerebellum FC was hypothesized, but not observed (Toazza et al., 2016). As a caution to interpretation, the spatial accuracy of the cerebellum results may be limited as MNI or Talairach normalization can result in variability in fissure localization after registration—a SPM-compatible cerebellar atlas has been created for better spatial normalization in the future (Diedrichsen, Balsters, Flavell, Cussans, & Ramnani, 2009; Diedrichsen et al., 2011).

Table 2.3: Cerebellum results across studies.

Source	Normalization (WB or Seed)	Method	Contrast	Coordinates X	Y	Z	Side	Lobe	Subregion
Healthy Control > Generalized Anxiety Disorder									
(Moon & Jeong, 2017b)	Talairach† (WB)	Task— Recognition of faces after distractors	Neutral	19	-32	-23	R	A	Culmen *(Vermis L. III)*
			Anxiety	-37	-54	-24	L	A	Culmen *(Vermis L. III)*
(Ball et al., 2013)	Talairach (WB)	Task—Maintain or reduce reactions to images	Maintain vs. Baseline	-34	-41	-20	L	A	Culmen *(Vermis L. III)*
				34	-57	-24	R	A	Culmen *(Vermis L. III)*
				-26	-69	-28	L	P	Pyramis *(Vermis L. VII)*
				18	-57	-28	R	A	N/A
(W. Li et al., 2016)	MNI (R dlPFC)	Functional Connectivity—Resting state		6	-51	0	R	A	Clivus/Folium *(Vermis L. IV, V)*
(Moon & Jeong, 2015b)	MNI (WB)	Task— Recognition of faces after distractors	Neutral	18	-34	-20	R	A	Lobule 4, 5 *(Cerebellar H.)*
			Anxiety	-36	-56	-22	L	P	Lobule 6 *(Cerebellar H.)*
(Price et al., 2011)	MNI (WB)	Task—Emotional Stroop	Negative vs. neutral	-22	-28	-24	L	A	Lobule 4, 5 *(Cerebellar H.)*
(Diwadkar et al., 2017)	MNI (WB)	Task—Memory/ suppression of word pairs	Suppression	3	-43	-26	R	A	N/A
			Retrieval	3	-43	-26	R	A	N/A

Generalized Anxiety Disorder > Healthy Control									
(Fonzo et al., 2015)	Talairach (WB)	Task—Modified emotion face assessment task	Fear vs. happy	-2	-62	-36	LR	P	Inf. Semi-Lunar Lobule *(Crus II)*
(Liu et al., 2015)	MNI (R Amygdala)	Functional Connectivity—Resting state		-45	-63	-51	L	P	Inf. Semi-Lunar Lobule *(Crus II)*
				33	-30	-36	R	P	Lobule 6 (*Cerebellar H.*)
(Monk et al., 2008)	Talairach (WB)	Task—Congruency of neutral or emotional faces	Angry vs. neutral	-46	-62	-25	L	P	Tuber (*Vermis L. VI*)
(Andreescu et al., 2015)	MNI (L dlPFC)	Functional Connectivity—Worry perseverative cognition		6	-52	-2	R	A	Clivus/Folium *(Vermis L. IV, V)*
(Fonzo et al., 2014)	Talairach (L Amygdala)	Functional Connectivity—PPI		8	-42	-21	R	A	Culmen *(Vermis L. III)*
				11	-57	-39	R	P	Cerebellar Tonsil
(Price et al., 2011)	MNI (WB)	Task—Emotional Stroop	Negative vs. neutral	-2	-74	-22	LR	P	Pyramis (*Vermis L. VII*)

MNI regions were obtained by entering coordinates into MRIcron software, and were labelled using the aal atlas overlay (https://www.nitrc.org/projects/mricron). Talairach regions were labelled by inputting coordinates into Talairach Client software (http://www.talairach.org/client.html). Although some records reported cerebellar activity within a cluster, if the peak results were outside of the cerebellum these results are not included here. †These data were analysed in Montreal Neurological Institute (MNI) space,

but results were converted to Talairach for reporting. WB = whole brain; MNI = Montreal Neurological Institute space; PPI = psychophysiological interaction; L = left; R = right; A = anterior; P = posterior; dlPFC = dorsolateral prefrontal cortex; Inf. = inferior; (Cerebellar H.) = cerebellar hemisphere; Vermis L. = Vermis Lobule.

2.4.5 Meta-Analyses

Meta-analyses were conducted for VBM and task-based research (in which negative emotion-evoking tasks were compared to a neutral or null baseline). Records were excluded if they shared participants with another study—the record with the largest sample size was used. Whole-brain spmT maps were provided for two VBM records (Hilbert et al., 2015; Makovac, Meeten, Watson, Garfinkel, et al., 2016), and one task-based record (Price et al., 2011) while peak voxels were used in the remainder.

The VBM meta-analysis included six records (Hilbert et al., 2015; Liao et al., 2014b; Makovac, Meeten, Watson, Garfinkel, et al., 2016; Moon et al., 2014; Schienle et al., 2011; Strawn et al., 2013). Global volume changes could not be assessed between groups: only two records reported controlling for intracranial volume (Makovac, Meeten, Watson, Garfinkel, et al., 2016; Moon et al., 2014), but these values were only reported in one (Moon et al., 2014). GAD patients had greater volume than HC in several areas associated with visual processing (precuneus, angular, lingual, parahippocampal, fusiform, and middle occipital gyri), the inferior parietal gyrus, the pre- and postcentral gyri (Brodmann areas 1-4), the temporal pole and middle temporal gyrus. HC had greater volume than GAD along the cingulate cortex (cingulum, anterior cingulate/paracingulate), motor/planning regions (precentral gyrus [Brodmann area 6], supplementary motor area), and language areas (superior temporal gyrus [Heschl's], inferior frontal gyrus, pars triangularis), and middle frontal gyrus (see Figure 2.2 and supplementary Table S3).

The task-based meta-analysis was conducted with five records (Fitzgerald et al., 2017; Hölzel et al., 2013; Monk et al., 2006; Palm et al., 2011; Price et al., 2011) in which authors conducted a between-subjects contrast, comparing visual, negative emotion-evoking stimuli with a neutral or null baseline. The tasks included making gender (Palm et al., 2011) or affect (Hölzel et al., 2013) judgements of emotive faces, passively viewing or appraising images from the International Affective Picture System (IAPS; Fitzgerald et al., 2017), emotional Stroop task (Price et al., 2011), and distinguishing congruency with emotional faces (Monk et al., 2006). Although coordinates were specified in one record, it was not specified whether they were peak or centre of gravity coordinates (Monk et al., 2006), and contact with the authors revealed that this information could not be recalled. However, it was decided that because of the small size of the single, significant cluster in this record, that the coordinates would be included in the meta-analysis. GAD groups had greater activity in a cluster with the peak in the left amygdala (with additional local

peaks, including in the striatum), the inferior network (uncinate fasciculus, orbital middle frontal gyrus), and the supramarginal gyrus, compared to HC groups for negative > neutral stimuli. Alternatively, the HC groups had greater activity in the orbital superior frontal gyrus (with additional local peaks throughout the middle frontal gyrus, and anterior cingulate/paracingulate gyri), and in the pars triangularis of the inferior frontal gyrus, compared to GAD groups for negative > neutral stimuli (see Figure 2.2 and supplementary Table S4). Results from the jackknife sensitivity analyses can be observed in supplementary Table S5 for both meta-analyses. Although task-based results from the leave-one-out jackknife analyses tended to yield similar results—and when they differed, tended to result in clusters losing significance—one notable exception occurred when the record by Fitzgerald and colleagues (Fitzgerald et al., 2017) was left out. For the GAD > HC contrast, a new, 104 voxel cluster in the cerebellum (hemispheric lobule 7, vermic lobules VI, VII, VIII, and crus I) was observed. These results should be regarded with caution as the Fitzgerald et al. (Fitzgerald et al., 2017) record was, in fact, included, but may point to the need for further investigation.

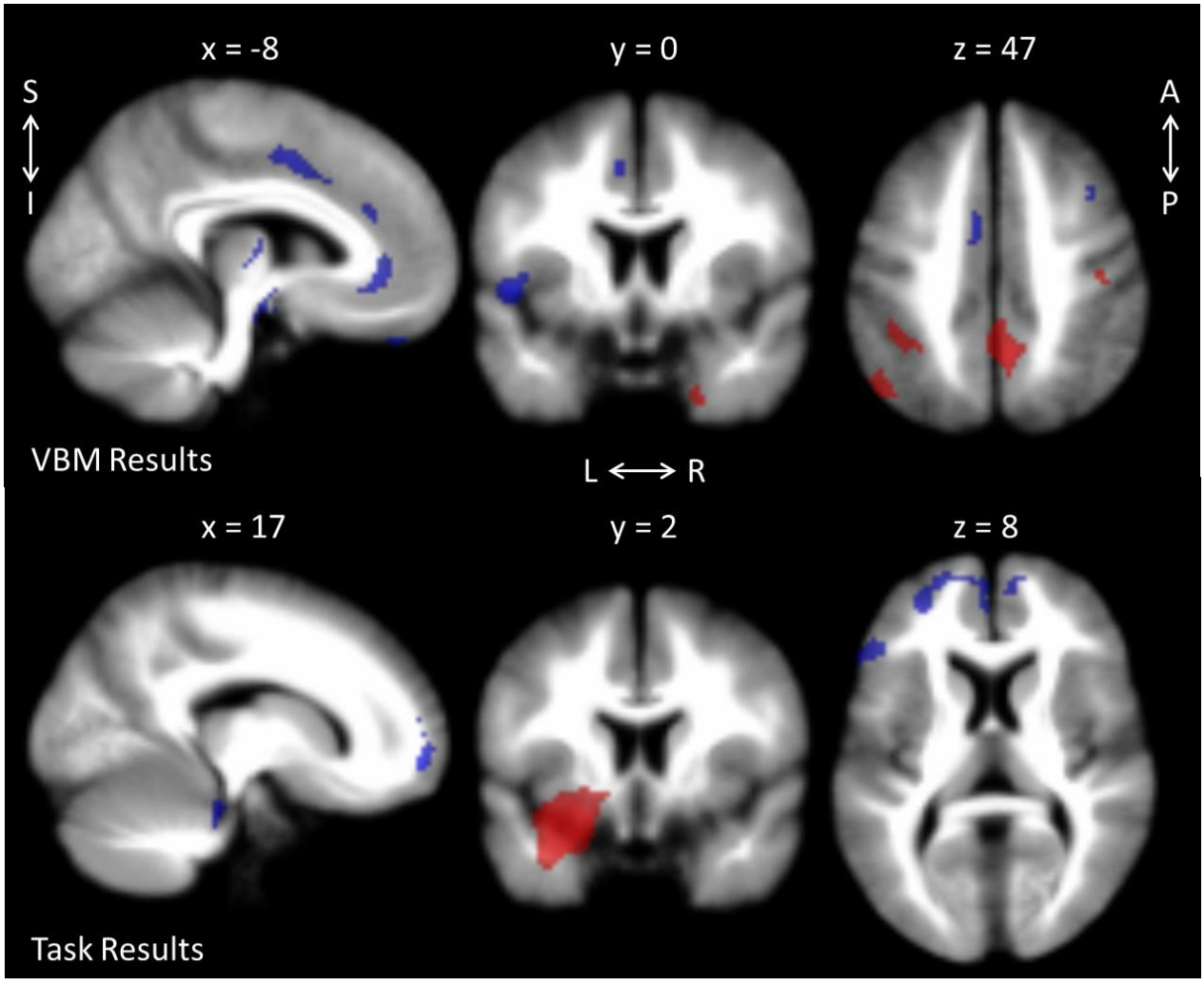

Figure 2.2: Results from the meta-analyses for GAD > HC (red) and GAD < HC (blue).Task-based results are for negative stimuli > neutral stimuli. See supplementary tables S3-4 for a full list of significant clusters. L = left; R = right; S = superior; I = inferior; A = anterior; P = posterior.

Discussion

This systematic review and meta-analyses were concerned with determining the altered neural structure, FC, and activity in GAD patients. The current work makes an important contribution to the literature by providing corroborative evidence in support of the previously identified brain regions involved in GAD, and identifying novel brain regions not previously reported in systematic reviews. To our knowledge, this is the first meta-analytic investigation of GAD, as well as the largest systematic review to-date. This systematic review includes almost twice as many records as those included in any previous reviews and therefore provides the most current and comprehensive assessment of the neural correlates underlying GAD which furthers our understanding of this disorder.

The current systematic review, by using about twice as many additional studies and conducting two meta-analyses provides evidence for altered physiology in the dlPFC, ACC, amygdala, and hippocampus—three previous systematic reviews implicate these regions as well (Fonzo & Etkin, 2017; Hilbert et al., 2014; Mochcovitch et al., 2014). Interestingly, and importantly, these results, along with the others observed in the systematic review and meta-analyses lend themselves well to the idea of network-level organization—many of the altered regions are key structures in resting state networks. Although structure and function are largely related, structural metrics do not completely explain function (Batista-Garcia-Ramo & Fernandez-Verdecia, 2018); for this reason this observation is speculative and exploratory, and it is important to note that structure, activity, and even FC alterations in these regions may not be directly related to resting state network FC or behavioural changes. Regardless, it remains interesting to consider the relationship between the implicated regions and their roles in network organization.

For example, the precuneus/PCC, medial prefrontal cortex, medial temporal lobes, and hippocampi are all nodes of the default mode network (Rosazza & Minati, 2011)—and all four of these regions had altered volume in the meta-analysis. Specifically, we found increased volume in the middle temporal gyrus (MTG) and precuneus and reduced volume in the medial PFC (mPFC) and hippocampus; reduced hippocampus volume was previously reported in one review (Hilbert et al., 2014). The default mode network is typically active during mind-wandering and self-referential thinking (Rosazza & Minati, 2011) and has often been observed as having altered FC in other psychopathologies (Broyd et al., 2009). Theoretical involvement of this resting state network in GAD makes sense as anxiety patients tend to ruminate with a self-referential focus

(Broyd et al., 2009)—a key process attributed to this network. In another GAD systematic review, Fonzo and colleagues (Fonzo & Etkin, 2017) suggest that alterations of the anterior components of this network may be responsible for the "worry cascade" of GAD and that the worries formed in GAD are resistant to change because they seem to be immune to external, contradictory evidence.

The central executive (also known as the frontoparietal) network has almost the opposite role of the default mode network, being responsible for high-order cognitive processes such as maintaining objects in working memory, attention (Bressler & Menon, 2010), and coordinating cognitive control (Dixon et al., 2018; Marek & Dosenbach, 2018). This network appears pertinent to the GAD population from a behavioural perspective, likely manifested by difficulty concentrating, a common symptom in GAD. Further lending support to this idea are the brain nodes comprising this network: the dlPFC, inferior parietal gyrus (Sylvester et al., 2012), and crus II of the cerebellum (Shirer, Ryali, Rykhlevskaia, Menon, & Greicius, 2012) have all been identified in our systematic review and the dlPFC and inferior parietal gyrus were also observed in the meta-analyses. In crus II, we observed increased FC between the right amygdala, and increased activity during the modified emotion face assessment task while our meta-analysis indicated greater volume in the inferior parietal cortex. Our results for the dlPFC were among the most prevalent: subjects with GAD had greater volume, and activity was mostly (but not entirely) reduced in response to passive, congruency, emotion modulation, and memory tasks. Additionally, FC tended to be reduced in the dlPFC, arising from amygdala, insula, and dlPFC seeds for GAD patients, although one study showed increased FC between the dlPFC and basolateral amygdala and another between the dlPFC and anterior insula. Previous GAD systematic reviews agree that PFC activity is altered (reduced in Mochcovitch et al., 2014) in subjects with GAD compared to HC (Fonzo & Etkin, 2017; Hilbert et al., 2014) for emotion regulation, and perseverative cognition. Hilbert and colleagues broke down the PFC results they observed by placing a larger emphasis on different age groups and found increased vlPFC activity for adolescents in attention/vigilance tasks, no differences in adults for an affective Stroop task, and increased dlPFC activity for neutral words, but decreased activity for negative words in an elderly GAD sample.

Because the default mode and central executive networks may have a role in GAD, it would be intuitive that the salience network may also be involved: this network is believed to act as a "switch" between the central executive and default mode networks (Shirer et al., 2012). The

salience network is responsible for orienting attention to important (i.e., salient) information, and is thus implicated in threat-based responses—another indication that this network may be implicated in GAD. Interestingly, key nodes of the salience network—the ACC, insula, and amygdala (Bressler & Menon, 2010; Menon, 2015)—have been identified in the current systematic review and meta-analyses as regions likely being altered in GAD. Again the systematic review results for the ACC were mixed among a variety of tasks, corroborating previous reviews (Fonzo & Etkin, 2017; Hilbert et al., 2014; Mochcovitch et al., 2014). Fonzo and Etkin (2017) address the variability in these results by concluding that the BOLD variability itself may be an intrinsic component of GAD, and that investigating the sources for this variability will be important for future understanding of this disorder. Although the ACC also had mixed FC results, overall, they tended to be reduced for subjects with GAD when using an amygdala seed. Furthermore, meta-analyses showed reduced ACC activity and volume. The systematic review results for the amygdala indicated increased volume and FA for subjects with GAD, although our VBM meta-analysis failed to find volume differences in the amygdala—in line with a variety of studies failing to find expected amygdala results. Most of the task-based research indicated increased activity in GAD—including the task-based meta-analysis. Additionally, all three previous reviews (Fonzo & Etkin, 2017; Hilbert et al., 2014; Mochcovitch et al., 2014) discussed altered amygdala activity in GAD—sometimes hyperactivated for emotional stimuli only, sometimes hyperactivated for emotional and neutral stimuli, other times hypoactivated for fearful faces, and finally sometimes with no activity differences despite hypotheses to the contrary. Mochcovitch and colleagues (2014) suggested interpreting these amygdala results in tandem with the PFC response—especially because the reviews all highlight altered (reduced in Hilbert et al., 2014; Mochcovitch et al., 2014) FC between the amygdala and PFC. Because FC was reduced for GAD patients in dlPFC using amygdala and insula seeds, and in ACC using an amygdala seed—it seems likely that there may be some disconnection between the central executive and salience networks, which may contribute to or result from the idea that subjects with GAD have inflexibility in top-down processing (mediated by the default mode network), as mentioned by Fonzo and Etkin (2017).

Additionally, the sensorimotor network appears to have differences in many of its key nodes in GAD. The sensorimotor network includes the pre- and postcentral gyri, SMA, and cerebellum lobules IV/V/VI (Shirer et al., 2012): the meta-analyses indicates greater volume for subjects with GAD in the pre- and postcentral gyri, reduced volume in the SMA, and reduced

activity in the cerebellum for tasks contrasting neutral and negative emotion-evoking stimuli. Although the systematic review shows mixed task-based results for the precentral gyrus for memory, fear learning, and prediction error tasks, the postcentral gyrus appears to have greater activity for subjects with GAD for fear learning, emotion modulation, and congruency tasks. As the sensorimotor network corresponds to the anatomy required for sensation and movement, and displays functionally relevant synchrony at rest (Rosazza & Minati, 2011), thus far, relation of this network to GAD remains speculative, but may be related to increased muscle tension and feelings of being "on edge" and hypervigilance in a motoric sense.

Delving deeper into the cerebellum, an often-ignored region, there is a fairly substantial representation in the systematic review for FC and activity differences in GAD. Although initially, the results looked fairly mixed, running the cerebellum coordinates through Talairach Client or MRIcron clarified the results. Compared to HC, GAD patients have *reduced* FC (largely with amygdala seeds) and activity in response to working memory, emotion modulation, and conflict tasks in the *anterior* lobe of the cerebellum (often in the culmen). Furthermore, compared to HC, GAD patients also had *greater* FC and activity for congruency and conflict, and facial affect processing tasks in the *posterior* cerebellum (Table 2.3). This anterior-posterior dichotomy becomes interesting in light of Bernard and colleagues (2012) assessment of the cerebellum FC. The authors found that the posterior cerebellar lobules correlated with prefrontal and association areas, indicating their involvement with the default mode network (Bernard et al., 2012)—it would be interesting to see if cerebellar and default mode networks had a stronger FC coupling since it appears that subjects with GAD have altered default mode and related cerebellar nodes.

Despite the relative lack of studies that report on the cerebellum, the idea of the cerebellum being altered in psychiatric disorders is not a new one: cerebellum volume or functional changes in psychiatric disorders including attention deficit hyperactivity disorder and schizophrenia has been observed (Baldacara, Borgio, Lacerda, & Jackowski, 2008; Phillips, Hewedi, Eissa, & Moustafa, 2015). Additionally, cerebellar volumes appear to be increased in OCD in the presence of childhood neglect (Brooks et al., 2016), while FC between the cerebellum and salience and executive control networks is altered in association with anxiety risk (Caulfield, Zhu, McAuley, & Servatius, 2016).

A recent consensus paper by Adamaszek and colleagues (2017) indicates that in addition to its well-known role in regulating motor control, the cerebellum also plays a role in a wide variety

of emotion processing. The culmen specifically (vermis lobules IV/V) has been shown to be hypoactive in alexithymia—a condition marked by dysfunctional emotional awareness (Adamaszek et al., 2017). Adamaszek also reported on a meta-analysis implicating vermal lobules IV and VI in explicit emotional face processing (Adamaszek et al., 2017). The inferior semi-lunar lobules (cerebellar hemisphere VIIB) have been shown to be active in response to unpleasant images when combined with noxious heat (Adamaszek et al., 2017). Although a clear picture is emerging for the localization of cerebellar alteration in GAD, the roles that each region plays remains complex as they appear to be involved in emotion-related processing, in addition to the better-known roles of motor control.

This review and meta-analysis all tend to point towards the same conclusion of the previous reviews: top-down, emotion dysregulation appears to be consistent with the neuroimaging GAD data (Fonzo & Etkin, 2017; Hilbert et al., 2014; Mochcovitch et al., 2014). However, the current review and meta-analysis adds to this framework by expanding the results outwards from the dlPFC, ACC, amygdala, and hippocampus by concluding that large scale alterations are present, likely manifesting in brain-wide networks, rather than distinct anatomical regions.

2.6 Limitations

A number of limitations exist within the present work. First, this review is limited in that only studies employing direct comparisons between GAD and HC were included. Furthermore, differences between GAD patients and additional disorders were largely ignored to maintain the focus of the systematic review. Finally, the meta-analyses performed were limited in terms of the number of records eligible for inclusion, and the availability of whole-brain maps. Although many authors were more than willing to share their data, in many cases, data loss resulting from technical limitations and maintaining ethics requirements, in addition to other hindrances, greatly limited access to whole-brain data. The resulting sample size for each of the meta-analyses further limited the complementary analyses that could be conducted, resulting in a mixture of population ages, medication use, and comorbidities. Finally, although many of the regions identified in the systematic review and meta-analyses are key nodes of resting state networks, it is important to note that many of these results are structural or activity-based in nature and may not as clearly relate to or affect the function of whole-brain resting state networks themselves—future whole-brain resting state studies of GAD can help to further investigate this.

2.7 Conclusion

This review summarizes a large body of work focusing on the neural underpinnings of GAD and has produced strong evidence for the involvement of specific brain regions. Previously accepted altered regions include the dlPFC ('[]' indicate meta-analysis results while no brackets indicate systematic review results: [reduced volume], altered FC with amygdala, altered [reduced] activity), ACC ([reduced volume], mixed FC and mixed [reduced] activity), amygdala (increased [increased] volume, increased activity), and hippocampus (greater left-lateralized volume) in the GAD literature. Additionally, previously unidentified regions including the insula (reduced volume, greater FC, mixed [greater] activity for GAD), PCC ([reduced volume], mixed FC, and mixed [increased] activity), precuneus ([increased volume], altered FC, reduced working memory activity), precentral gyrus (reduced [reduced in right, increased in left hemisphere] volume, greater FC, mixed activity), STG (reduced [reduced in left, greater right] volume, increased FC, [increased activity]), vlPFC ([reduced volume], mostly increased FC, mixed [reduced] activity), OFC (reduced mean diffusivity, cortical thickness and surface area, mixed FC and mixed [reduced] activity), and cerebellum (reduced FC and working memory activity in anterior lobe, greater FC and congruency-based activity in posterior cerebellum, [reduced activity]) are identified as regions of interest via both our systematic review and our meta-analyses. Despite the use of different modalities (i.e., structure, FC, and task-based methods) and widely varying methods of analyses within each modality (e.g., VBM vs. FA values)—a high degree of consistency was observed within the systematic review and meta-analyses. This consistency was observed despite a high degree of variability in terms of age groups, comorbidities, and medication use included in each record. Future research should be conducted to determine if and how these regions differ with severity and duration of the disorder, and between different mood and anxiety disorders. Through this process, we may begin to better understand how the alterations in neural structures and networks contribute to the development and/or maintenance of GAD, which may in turn inform treatment strategies for this patient population.

CRediT authorship contribution statement

Tiffany A. Kolesar: Conceptualization, Data curation, Formal analysis, Funding acquisition, Methodology, Writing - original draft, Writing - review & editing. **Elena Bilevicius**: Conceptualization, Data curation, Writing - review & editing. **Alyssia D. Wilson**: Data curation, Writing - review & editing. **Jennifer Kornelsen**: Resources, Software, Supervision, Writing - review & editing.

Funding

This work was supported by the Natural Sciences and Engineering Research Council of Canada (NSERC), Canada Graduate Scholarships Doctoral Program.

Declaration of Competing Interest

None.

Supplementary material

Supplementary material associated with this article can be found in the online version at doi:10.1016/j.nicl.2019.102016.

2.8 Chapter 2 References

Abdallah, C. G., Coplan, J. D., Jackowski, A., Sato, J. R., Mao, X., Shungu, D. C., & Mathew, S. J. (2013). A pilot study of hippocampal volume and n-acetylaspartate (NAA) as response biomarkers in riluzole-treated patients with GAD. *European Neuropsychopharmacology, 23*(4), 276-284. doi:10.1016/j.euroneuro.2012.05.009

Adamaszek, M., D'Agata, F., Ferrucci, R., Habas, C., Keulen, S., Kirkby, K. C., . . . Verhoeven, J. (2017). Consensus Paper: Cerebellum and Emotion. *Cerebellum, 16*(2), 552-576. doi:10.1007/s12311-016-0815-8

American Psychiatric Association. (2013). *Diagnostic and statistical manual of mental disorders* (5th ed.). Arlington, VA: American Psychiatric Association Publishing.

Andreescu, C., Gross, J. J., Lenze, E., Edelman, K. D., Snyder, S., Tanase, C., & Aizenstein, H. (2011). Altered cerebral blood flow patterns associated with pathologic worry in the elderly. *Depression and Anxiety, 28*(3), 202-209. doi:10.1002/da.20799

Andreescu, C., Sheu, L. K., Tudorascu, D., Gross, J. J., Walker, S., Banihashemi, L., & Aizenstein, H. (2015). Emotion reactivity and regulation in late-life generalized anxiety disorder: Functional connectivity at baseline and post-treatment. *American Journal of Geriatric Psychiatry, 23*(2), 200-214. doi:10.1016/j.jagp.2014.05.003

Andreescu, C., Sheu, L. K., Tudorascu, D., Walker, S., & Aizenstein, H. (2014). The ages of anxiety - Differences across the lifespan in the default mode network functional connectivity in generalized anxiety disorder. *International Journal of Geriatric Psychiatry, 29*(7), 704-712. doi:10.1002/gps.4051

Andreescu, C., Tudorascu, D., Sheu, L. K., Rangarajan, A., Butters, M. A., Walker, S., . . . Aizenstein, H. (2017). Brain structural changes in late-life generalized anxiety disorder. *Psychiatry Research - Neuroimaging, 268*, 15-21.

Baldacara, L., Borgio, J. G., Lacerda, A. L., & Jackowski, A. P. (2008). Cerebellum and psychiatric disorders. *Rev Bras Psiquiatr, 30*(3), 281-289.

Ball, T. M., Ramsawh, H. J., Campbell-Sills, L., Paulus, M. P., & Stein, M. B. (2013). Prefrontal dysfunction during emotion regulation in generalized anxiety and panic disorders. *Psychological Medicine, 43*(7), 1475-1486.

Batista-Garcia-Ramo, K., & Fernandez-Verdecia, C. I. (2018). What we know about the brain structure-function relationship. *Behav. Sci., 8*(4), 39. doi:https://doi.org/10.3390/bs8040039

Benson, B. E., Guyer, A. E., Nelson, E. E., Pine, D. S., & Ernst, M. (2015). Role of contingency in striatal response to incentive in adolescents with anxiety. *Cognitive, Affective & Behavioral Neuroscience, 15*(1), 155-168.

Bernard, J. A., Seidler, R. D., Hassevoort, K. M., Benson, B. L., Welsh, R. C., Wiggins, J. L., . . . Peltier, S. J. (2012). Resting state cortico-cerebellar functional connectivity networks: a comparison of anatomical and self-organizing map approaches. *Front Neuroanat, 6*, 31. doi:10.3389/fnana.2012.00031

Blair, K., Shaywitz, J., Smith, B. W., Rhodes, R., Geraci, M., Jones, M., . . . Pine, D. S. (2008). Response to emotional expressions in generalized social phobia and generalized anxiety disorder: Evidence for separate disorders. *American Journal of Psychiatry, 165*(9), 1193-1202. doi:10.1176/appi.ajp.2008.07071060

Blair, K. S., Geraci, M., Smith, B. W., Hollon, N., Devido, J., Otero, M., . . . Pine, D. S. (2012). Reduced dorsal anterior cingulate cortical activity during emotional regulation and top-down attentional control in generalized social phobia, generalized anxiety disorder, and comorbid generalized social phobia/generalized anxiety disorder. *Biological Psychiatry, 72*(6), 476-482. doi:10.1016/j.biopsych.2012.04.013

Blair, K. S., Otero, M., Teng, C., Geraci, M., Ernst, M., Blair, R. J. R., . . . Grillon, C. (2017). Reduced optimism and a heightened neural response to everyday worries are specific to generalized anxiety disorder, and not seen in social anxiety. *Psychological Medicine, 47*(10), 1806-1815. doi:10.1017/S0033291717000265

Brambilla, P., Como, G., Isola, M., Taboga, F., Zuliani, R., Goljevscek, S., . . . Balestrieri, M. (2012). White-matter abnormalities in the right posterior hemisphere in generalized anxiety disorder: A diffusion imaging study. *Psychological Medicine, 42*(2), 427-434. doi:10.1017/S0033291711001255

Bressler, S. L., & Menon, V. (2010). Large-scale brain networks in cognition: emerging methods and principles. *Trends Cogn Sci, 14*(6), 277-290. doi:10.1016/j.tics.2010.04.004

Brooks, S. J., Naidoo, V., Roos, A., Fouche, J. P., Lochner, C., & Stein, D. J. (2016). Early-life adversity and orbitofrontal and cerebellar volumes in adults with obsessive-compulsive

disorder: voxel-based morphometry study. *Br J Psychiatry, 208*(1), 34-41. doi:10.1192/bjp.bp.114.162610

Brown, G. G., Ostrowitzki, S., Stein, M. B., von Kienlin, M., Liu, T. T., Simmons, A., . . . Paulus, M. (2015). Temporal profile of brain response to alprazolam in patients with generalized anxiety disorder. *Psychiatry Research - Neuroimaging, 233*(3), 394-401. doi:10.1016/j.pscychresns.2015.06.016

Broyd, S. J., Demanuele, C., Debener, S., Helps, S. K., James, C. J., & Sonuga-Barke, E. J. (2009). Default-mode brain dysfunction in mental disorders: a systematic review. *Neurosci Biobehav Rev, 33*(3), 279-296. doi:10.1016/j.neubiorev.2008.09.002

Buff, C., Brinkmann, L., Neumeister, P., Feldker, K., Heitmann, C., Gathmann, B., . . . Straube, T. (2016). Specifically altered brain responses to threat in generalized anxiety disorder relative to social anxiety disorder and panic disorder. *NeuroImage: Clinical, 12*, 698-706. doi:10.1016/j.nicl.2016.09.023

Calhoun, V. D., Liu, J., & Adali, T. (2009). A review of group ICA for fMRI data and ICA for joint inference of imaging, genetic, and ERP data. *Neuroimage, 45*(1 Suppl), S163-172. doi:10.1016/j.neuroimage.2008.10.057

Carlisi, C. O., Hilbert, K., Guyer, A. E., & Ernst, M. (2017). Sleep-amount differentially affects fear-processing neural circuitry in pediatric anxiety: A preliminary fMRI investigation. *Cognitive, Affective and Behavioral Neuroscience, 17*(6), 1098-1113. doi:10.3758/s13415-017-0535-7

Carlson, J. M., Rubin, D., & Mujica-Parodi, L. R. (2017). Lost emotion: Disrupted brain-based tracking of dynamic affective episodes in anxiety and depression. *Psychiatry Research - Neuroimaging, 260*, 37-48. doi:10.1016/j.pscychresns.2016.12.002

Caulfield, M. D., Zhu, D. C., McAuley, J. D., & Servatius, R. J. (2016). Individual differences in resting-state functional connectivity with the executive network: support for a cerebellar role in anxiety vulnerability. *Brain Struct Funct, 221*(6), 3081-3093. doi:10.1007/s00429-015-1088-6

Cha, J., Carlson, J. M., DeDora, D. J., Greenberg, T., Proudfit, G. H., & Mujica-Parodi, L. R. (2014). Hyper-reactive human ventral tegmental area and aberrant mesocorticolimbic connectivity in overgeneralization of fear in generalized anxiety disorder. *Journal of Neuroscience, 34*(17), 5855-5860. doi:10.1523/JNEUROSCI.4868-13.2014

Cha, J., DeDora, D., Nedic, S., Ide, J., Greenberg, T., Hajcak, G., & Mujica-Parodi, L. R. (2016). Clinically anxious individuals show disrupted feedback between inferior frontal gyrus and prefrontal-limbic control circuit. *Journal of Neuroscience, 36*(17), 4708-4718. doi:10.1523/JNEUROSCI.1092-15.2016

Cha, J., Greenberg, T., Carlson, J. M., DeDora, D. J., Hajcak, G., & Mujica-Parodi, L. R. (2014). Circuit-wide structural and functional measures predict ventromedial prefrontal cortex fear generalization: Implications for generalized anxiety disorder. *Journal of Neuroscience, 34*(11), 4043-4053. doi:10.1523/JNEUROSCI.3372-13.2014

Cha, J., Greenberg, T., Song, I., Blair Simpson, H., Posner, J., & Mujica-Parodi, L. R. (2016). Abnormal hippocampal structure and function in clinical anxiety and comorbid depression. *Hippocampus, 26*(5), 545-553. doi:http://dx.doi.org/10.1002/hipo.22566

Chen, A. C., & Etkin, A. (2013). Hippocampal network connectivity and activation differentiates post-traumatic stress disorder from generalized anxiety disorder. *Neuropsychopharmacology, 38*(10), 1889-1898. doi:10.1038/npp.2013.122

Cui, H., Zhang, J., Liu, Y., Li, Q., Li, H., Zhang, L., . . . Northoff, G. (2016). Differential alterations of resting-state functional connectivity in generalized anxiety disorder and panic disorder. *Human Brain Mapping, 37*(4), 1459-1473. doi:http://dx.doi.org/10.1002/hbm.23113

De Bellis, M. D., Casey, B. J., Dahl, R. E., Birmaher, B., Williamson, D. E., Thomas, K. M., . . . Ryan, N. D. (2000). A pilot study of amygdala volumes in pediatric generalized anxiety disorder. *Biological Psychiatry, 48*(1), 51-57. doi:10.1016/S0006-3223(00)00835-0

De Bellis, M. D., Keshavan, M. S., Shifflett, H., Iyengar, S., Dahl, R. E., Axelson, D. A., . . . Ryan, N. D. (2002). Superior temporal gyrus volumes in pediatric generalized anxiety disorder. *Biological Psychiatry, 51*(7), 553-562. doi:10.1016/S0006-3223(01)01375-0

Diedrichsen, J., Balsters, J. H., Flavell, J., Cussans, E., & Ramnani, N. (2009). A probabilistic MR atlas of the human cerebellum. *Neuroimage, 46*(1), 39-46. doi:10.1016/j.neuroimage.2009.01.045

Diedrichsen, J., Maderwald, S., Kuper, M., Thurling, M., Rabe, K., Gizewski, E. R., . . . Timmann, D. (2011). Imaging the deep cerebellar nuclei: a probabilistic atlas and normalization procedure. *Neuroimage, 54*(3), 1786-1794. doi:10.1016/j.neuroimage.2010.10.035

Diwadkar, V. A., Re, M., Cecchetto, F., Garzitto, M., Piccin, S., Bonivento, C., . . . Brambilla, P. (2017). Attempts at memory control induce dysfunctional brain activation profiles in

Generalized Anxiety Disorder: An exploratory fMRI study. *Psychiatry Research - Neuroimaging, 266*, 42-52. doi:10.1016/j.pscychresns.2017.05.010

Dixon, M. L., De La Vega, A., Mills, C., Andrews-Hanna, J., Spreng, R. N., Cole, M. W., & Christoff, K. (2018). Heterogeneity within the frontoparietal control network and its relationship to the default and dorsal attention networks. *Proc Natl Acad Sci U S A, 115*(7), E1598-E1607. doi:10.1073/pnas.1715766115

Duval, E. R., Javanbakht, A., & Liberzon, I. (2015). Neural circuits in anxiety and stress disorders: a focused review. *Ther Clin Risk Manag, 11*, 115-126. doi:10.2147/TCRM.S48528

Etkin, A., Prater, K. E., Hoeft, F., Menon, V., & Schatzberg, A. F. (2010). Failure of anterior cingulate activation and connectivity with the amygdala during implicit regulation of emotional processing in generalized anxiety disorder. *American Journal of Psychiatry, 167*(5), 545-554. doi:10.1176/appi.ajp.2009.09070931

Etkin, A., Prater, K. E., Schatzberg, A. F., Menon, V., & Greicius, M. D. (2009). Disrupted amygdalar subregion functional connectivity and evidence of a compensatory network in generalized anxiety disorder. *Archives of General Psychiatry, 66*(12), 1361-1372. doi:10.1001/archgenpsychiatry.2009.104

Etkin, A., & Schatzberg, A. F. (2011). Common abnormalities and disorder-specific compensation during implicit regulation of emotional processing in generalized anxiety and major depressive disorders. *American Journal of Psychiatry, 168*(9), 968-978. doi:10.1176/appi.ajp.2011.10091290

Fitzgerald, J. M., Phan, K. L., Kennedy, A. E., Shankman, S. A., Langenecker, S. A., & Klumpp, H. (2017). Prefrontal and amygdala engagement during emotional reactivity and regulation in generalized anxiety disorder. *Journal of Affective Disorders, 218*, 398-406. doi:10.1016/j.jad.2017.05.013

Fonzo, G. A., & Etkin, A. (2017). Affective neuroimaging in generalized anxiety disorder: an integrated review. *Dialogues Clin Neurosci, 19*(2), 169-179.

Fonzo, G. A., Ramsawh, H. J., Flagan, T. M., Sullivan, S. G., Letamendi, A., Simmons, A. N., . . . Stein, M. B. (2015). Common and disorder-specific neural responses to emotional faces in generalised anxiety, social anxiety and panic disorders. *British Journal of Psychiatry, 206*(3), 206-215. doi:10.1192/bjp.bp.114.149880

Fonzo, G. A., Ramsawh, H. J., Flagan, T. M., Sullivan, S. G., Simmons, A. N., Paulus, M. P., & Stein, M. B. (2014). Cognitive-behavioral therapy for generalized anxiety disorder is associated with attenuation of limbic activation to threat-related facial emotions. *Journal of Affective Disorders, 169*, 76-85. doi:10.1016/j.jad.2014.07.031

Friston, K. J. (2011). Functional and effective connectivity: a review. *Brain Connect, 1*(1), 13-36. doi:10.1089/brain.2011.0008

Greenberg, T., Carlson, J. M., Cha, J., Hajcak, G., & Mujica-Parodi, L. R. (2013). Ventromedial prefrontal cortex reactivity is altered in generalized anxiety disorder during fear generalization. *Depression and Anxiety, 30*(3), 242-250. doi:10.1002/da.22016

Guyer, A. E., Choate, V. R., Detloff, A., Benson, B., Nelson, E. E., Perez-Edgar, K., . . . Ernst, M. (2012). Striatal functional alteration during incentive anticipation in pediatric anxiety disorders. *American Journal of Psychiatry, 169*(2), 205-212. doi:10.1176/appi.ajp.2011.11010006

Haddad, A. D. M., Bilderbeck, A., James, A. C., & Lau, J. Y. F. (2015). Fear responses to safety cues in anxious adolescents: Preliminary evidence for atypical age-associated trajectories of functional neural circuits. *Journal of Psychiatric Research, 68*, 301-308. doi:10.1016/j.jpsychires.2015.05.009

Hamm, L. L., Jacobs, R. H., Johnson, M. W., Fitzgerald, D. A., Fitzgerald, K. D., Langenecker, S. A., . . . Phan, K. L. (2014). Aberrant amygdala functional connectivity at rest in pediatric anxiety disorders. *Biology of Mood and Anxiety Disorders, 4*(1). doi:10.1186/s13587-014-0015-4

Hettema, J. M., Kettenmann, B., Ahluwalia, V., McCarthy, C., Kates, W. R., Schmitt, J. E., . . . Fatouros, P. (2012). Pilot multimodal twin imaging study of generalized anxiety disorder. *Depression and Anxiety, 29*(3), 202-209. doi:10.1002/da.20901

Hilbert, K., Lueken, U., & Beesdo-Baum, K. (2014). Neural structures, functioning and connectivity in Generalized Anxiety Disorder and interaction with neuroendocrine systems: a systematic review. *J Affect Disord, 158*, 114-126. doi:10.1016/j.jad.2014.01.022

Hilbert, K., Pine, D. S., Muehlhan, M., Lueken, U., Steudte-Schmiedgen, S., & Beesdo-Baum, K. (2015). Gray and white matter volume abnormalities in generalized anxiety disorder by categorical and dimensional characterization. *Psychiatry Research - Neuroimaging, 234*(3), 314-320. doi:10.1016/j.pscychresns.2015.10.009

Hölzel, B. K., Hoge, E. A., Greve, D. N., Gard, T., Creswell, J. D., Brown, K. W., . . . Lazar, S. W. (2013). Neural mechanisms of symptom improvements in generalized anxiety disorder following mindfulness training. *NeuroImage: Clinical, 2*(1), 448-458. doi:10.1016/j.nicl.2013.03.011

Jiang, J., Zhao, Y. J., Hu, X. Y., Du, M. Y., Chen, Z. Q., Wu, M., . . . Gong, Q. Y. (2017). Microstructural brain abnormalities in medication-free patients with major depressive disorder: a systematic review and meta-analysis of diffusion tensor imaging. *J Psychiatry Neurosci, 42*(3), 150-163.

Karim, H., Tudorascu, D. L., Aizenstein, H., Walker, S., Good, R., & Andreescu, C. (2016). Emotion Reactivity and Cerebrovascular Burden in Late-Life GAD: A Neuroimaging Study. *American Journal of Geriatric Psychiatry, 24*(11), 1040-1050. doi:10.1016/j.jagp.2016.07.015

Lau, J. Y. F., Goldman, D., Buzas, B., Fromm, S. J., Guyer, A. E., Hodgkinson, C., . . . Ernst, M. (2009). Amygdala Function and 5-HTT Gene Variants in Adolescent Anxiety and Major Depressive Disorder. *Biological Psychiatry, 65*(4), 349-355. doi:10.1016/j.biopsych.2008.08.037

Laufer, O., Israeli, D., & Paz, R. (2016). Behavioral and neural mechanisms of overgeneralization in anxiety. *Current Biology, 26*(6), 713-722. doi:10.1016/j.cub.2016.01.023

Li, C., Su, S., Wu, H., & Zhu, Y. (2018). Abnormal spontaneous brain activity in patients with generalized anxiety disorder revealed by resting-state functional MRI. *NeuroReport, 29*(5), 397-401. doi:10.1097/wnr.0000000000000982

Li, W., Cui, H., Zhu, Z., Kong, L., Guo, Q., Zhu, Y., . . . Li, C. (2016). Aberrant functional connectivity between the amygdala and the temporal pole in drug-free generalized anxiety disorder. *Frontiers in Human Neuroscience, 10*(NOV2016). doi:10.3389/fnhum.2016.00549

Liao, M., Yang, F., Zhang, Y., He, Z., Song, M., Jiang, T., . . . Li, L. (2013). Childhood Maltreatment Is Associated with Larger Left Thalamic Gray Matter Volume in Adolescents with Generalized Anxiety Disorder. *PLoS ONE, 8*(8). doi:10.1371/journal.pone.0071898

Liao, M., Yang, F., Zhang, Y., He, Z., Su, L., & Li, L. (2014a). Lack of gender effects on gray matter volumes in adolescent generalized anxiety disorder. *Journal of Affective Disorders, 155*(1), 278-282. doi:10.1016/j.jad.2013.10.049

Liao, M., Yang, F., Zhang, Y., He, Z., Su, L., & Li, L. (2014b). White matter abnormalities in adolescents with generalized anxiety disorder: A diffusion tensor imaging study. *BMC Psychiatry, 14*(1). doi:10.1186/1471-244X-14-41

Liu, W.-J., Yin, D.-Z., Cheng, W.-H., Fan, M.-X., You, M.-N., Men, W.-W., . . . Zhang, F. (2015). Abnormal Functional Connectivity of the Amygdala-Based Network in Resting-State fMRI in Adolescents with Generalized Anxiety Disorder. *Medical Science Monitor, 21*, 459-467.

Makovac, E., Meeten, F., Watson, D. R., Garfinkel, S. N., Critchley, H. D., & Ottaviani, C. (2016). Neurostructural abnormalities associated with axes of emotion dysregulation in generalized anxiety. *NeuroImage: Clinical, 10*, 172-181. doi:10.1016/j.nicl.2015.11.022

Makovac, E., Meeten, F., Watson, D. R., Herman, A., Garfinkel, S. N., H, D. C., & Ottaviani, C. (2016). Alterations in Amygdala-Prefrontal Functional Connectivity Account for Excessive Worry and Autonomic Dysregulation in Generalized Anxiety Disorder. *Biological Psychiatry, 80*(10), 786-795.

Makovac, E., Smallwood, J., Watson, D. R., Meeten, F., Critchley, H. D., & Ottaviani, C. (2018). The verbal nature of worry in generalized anxiety: Insights from the brain. *NeuroImage: Clinical, 17*, 882-892. doi:10.1016/j.nicl.2017.12.014

Marek, S., & Dosenbach, N. U. F. (2018). The frontoparietal network: function, electrophysiology, and importance of individual precision mapping. *Dialogues Clin Neurosci, 20*(2), 133-140.

McClure, E. B., Monk, C. S., Nelson, E. E., Parrish, J. M., Adler, A., Blair, R. J. R., . . . Pine, D. S. (2007). Abnormal attention modulation of fear circuit function in pediatric generalized anxiety disorder. *Archives of General Psychiatry, 64*(1), 97-106. doi:10.1001/archpsyc.64.1.97

Menon, V. (2015). Salience Network. In A. Toga (Ed.), *Brain Mapping: An Encyclopedic Reference* (pp. 597-611): Elsevier: Academic Press.

Mochcovitch, M. D., da Rocha Freire, R. C., Garcia, R. F., & Nardi, A. E. (2014). A systematic review of fMRI studies in generalized anxiety disorder: evaluating its neural and cognitive basis. *J Affect Disord, 167*, 336-342. doi:10.1016/j.jad.2014.06.041

Mohlman, J., Eldreth, D. A., Price, R. B., Staples, A. M., & Hanson, C. (2017). Prefrontal-limbic connectivity during worry in older adults with generalized anxiety disorder. *Aging and Mental Health, 21*(4), 426-438. doi:10.1080/13607863.2015.1109058

Mohlman, J., Price, R. B., Eldreth, D. A., Chazin, D., Glover, D. M., & Kates, W. R. (2009). The relation of worry to prefrontal cortex volume in older adults with and without generalized anxiety disorder. *Psychiatry Research - Neuroimaging, 173*(2), 121-127. doi:10.1016/j.pscychresns.2008.09.010

Molent, C., Maggioni, E., Cecchetto, F., Garzitto, M., Piccin, S., Bonivento, C., . . . Brambilla, P. (2017). Reduced cortical thickness and increased gyrification in generalized anxiety disorder: a 3 T MRI study. *Psychological Medicine*, 1-10. doi:10.1017/s003329171700352x

Monk, C. S., Nelson, E. E., McClure, E. B., Mogg, K., Bradley, B. P., Leibenluft, E., . . . Pine, D. S. (2006). Ventrolateral prefrontal cortex activation and attentional bias in response to angry faces in adolescents with generalized anxiety disorder. *American Journal of Psychiatry, 163*(6), 1091-1097. doi:10.1176/appi.ajp.163.6.1091

Monk, C. S., Telzer, E. H., Mogg, K., Bradley, B. P., Mai, X., Louro, H. M. C., . . . Pine, D. S. (2008). Amygdala and ventrolateral prefrontal cortex activation to masked angry faces in children and adolescents with generalized anxiety disorder. *Archives of General Psychiatry, 65*(5), 568-576. doi:10.1001/archpsyc.65.5.568

Moon, C. M., & Jeong, G. W. (2015a). Alterations in white matter volume and its correlation with clinical characteristics in patients with generalized anxiety disorder. *Neuroradiology, 57*(11), 1127-1134. doi:10.1007/s00234-015-1572-y

Moon, C. M., & Jeong, G. W. (2015b). Functional neuroanatomy on the working memory under emotional distraction in patients with generalized anxiety disorder. *Psychiatry and Clinical Neurosciences, 69*(10), 609-619. doi:10.1111/pcn.12295

Moon, C. M., & Jeong, G. W. (2016). Brain morphological alterations and cellular metabolic changes in patients with generalized anxiety disorder: A combined DARTEL-based VBM and 1 H-MRS study. *Magnetic Resonance Imaging, 34*(4), 429-436. doi:10.1016/j.mri.2015.12.017

Moon, C. M., & Jeong, G. W. (2017a). Abnormalities in gray and white matter volumes associated with explicit memory dysfunction in patients with generalized anxiety disorder. *Acta Radiologica, 58*(3), 353-361. doi:10.1177/0284185116649796

Moon, C. M., & Jeong, G. W. (2017b). Functional and morphological alterations associated with working memory dysfunction in patients with generalized anxiety disorder. *Acta Radiologica, 58*(3), 344-352. doi:10.1177/0284185116649794

Moon, C. M., Kang, H. K., & Jeong, G. W. (2015). Metabolic change in the right dorsolateral prefrontal cortex and its correlation with symptom severity in patients with generalized anxiety disorder: Proton magnetic resonance spectroscopy at 3 Tesla. *Psychiatry and Clinical Neurosciences, 69*(7), 422-430. doi:10.1111/pcn.12279

Moon, C. M., Kim, G. W., & Jeong, G. W. (2014). Whole-brain gray matter volume abnormalities in patients with generalized anxiety disorder: Voxel-based morphometry. *NeuroReport, 25*(3), 184-189. doi:10.1097/WNR.0000000000000100

Moon, C. M., Sundaram, T., Choi, N. G., & Jeong, G. W. (2016). Working memory dysfunction associated with brain functional deficits and cellular metabolic changes in patients with generalized anxiety disorder. *Psychiatry Research - Neuroimaging, 254*, 137-144. doi:10.1016/j.pscychresns.2016.06.013

Moon, C. M., Yang, J. C., & Jeong, G. W. (2015). Explicit verbal memory impairments associated with brain functional deficits and morphological alterations in patients with generalized anxiety disorder. *Journal of Affective Disorders, 186*, 328-336. doi:10.1016/j.jad.2015.07.038

Moon, C. M., Yang, J. C., & Jeong, G. W. (2017). Functional neuroanatomy associated with the interaction between emotion and cognition in explicit memory tasks in patients with generalized anxiety disorder. *Acta Radiologica, 58*(1), 98-106. doi:10.1177/0284185116633915

Mueller, S. C., Aouidad, A., Gorodetsky, E., Goldman, D., Pine, D. S., & Ernst, M. (2013). Gray matter volume in adolescent anxiety: An impact of the brain-derived neurotrophic factor Val66met polymorphism? *Journal of the American Academy of Child and Adolescent Psychiatry, 52*(2), 184-195. doi:10.1016/j.jaac.2012.11.016

Nitschke, J. B., Sarinopoulos, I., Oathes, D. J., Johnstone, T., Whalen, P. J., Davidson, R. J., & Kalin, N. H. (2009). Anticipatory activation in the amygdala and anterior cingulate in generalized anxiety disorder and prediction of treatment response. *American Journal of Psychiatry, 166*(3), 302-310.

Oathes, D. J., Patenaude, B., Schatzberg, A. F., & Etkin, A. (2015). Neurobiological signatures of anxiety and depression in resting-state functional magnetic resonance imaging. *Biological Psychiatry, 77*(4), 385-393. doi:10.1016/j.biopsych.2014.08.006

Ottaviani, C., Watson, D. R., Meeten, F., Makovac, E., Garfinkel, S. N., & Critchley, H. D. (2016). Neurobiological substrates of cognitive rigidity and autonomic inflexibility in generalized anxiety disorder. *Biological Psychology, 119*, 31-41. doi:10.1016/j.biopsycho.2016.06.009

Pace-Schott, E. F., Zimmerman, J. P., Bottary, R. M., Lee, E. G., Milad, M. R., & Camprodon, J. A. (2017). Resting state functional connectivity in primary insomnia, generalized anxiety disorder and controls. *Psychiatry Research - Neuroimaging, 265*, 26-34. doi:10.1016/j.pscychresns.2017.05.003

Palm, M. E., Elliott, R., McKie, S., Deakin, J. F. W., & Anderson, I. M. (2011). Attenuated responses to emotional expressions in women with generalized anxiety disorder. *Psychological Medicine, 41*(5), 1009-1018. doi:10.1017/S0033291710001455

Park, J. I., Kim, G. W., Jeong, G. W., Chung, G. H., & Yang, J. C. (2016). Brain activation patterns associated with the effects of emotional distracters during working memory maintenance in patients with generalized anxiety disorder. *Psychiatry Investigation, 13*(1), 152-156. doi:10.4306/pi.2016.13.1.152

Paulesu, E., Sambugaro, E., Torti, T., Danelli, L., Ferri, F., Scialfa, G., . . . Sassaroli, S. (2010). Neural correlates of worry in generalized anxiety disorder and in normal controls: A functional MRI study. *Psychological Medicine, 40*(1), 117-124. doi:10.1017/S0033291709005649

Phillips, J. R., Hewedi, D. H., Eissa, A. M., & Moustafa, A. A. (2015). The cerebellum and psychiatric disorders. *Front Public Health, 3*, 66. doi:10.3389/fpubh.2015.00066

Pico-Perez, M., Radua, J., Steward, T., Menchon, J. M., & Soriano-Mas, C. (2017). Emotion regulation in mood and anxiety disorders: A meta-analysis of fMRI cognitive reappraisal studies. *Prog Neuropsychopharmacol Biol Psychiatry, 79*(Pt B), 96-104. doi:10.1016/j.pnpbp.2017.06.001

Price, R. B., Eldreth, D. A., & Mohlman, J. (2011). Deficient prefrontal attentional control in late-life generalized anxiety disorder: An fMRI investigation. *Translational Psychiatry, 1*. doi:10.1038/tp.2011.46

Qiao, J., Li, A., Cao, C., Wang, Z., Sun, J., & Xu, G. (2017). Aberrant functional network connectivity as a biomarker of generalized anxiety disorder. *Frontiers in Human Neuroscience, 11*. doi:10.3389/fnhum.2017.00626

Quide, Y., Witteveen, A. B., El-Hage, W., Veltman, D. J., & Olff, M. (2012). Differences between effects of psychological versus pharmacological treatments on functional and morphological brain alterations in anxiety disorders and major depressive disorder: a systematic review. *Neurosci Biobehav Rev, 36*(1), 626-644. doi:10.1016/j.neubiorev.2011.09.004

Rabany, L., G.J, D. I., Bragdon, L. B., Pittman, B. P., Zertuche, L., Tolin, D. F., . . . Assaf, M. (2017). Resting-State Functional Connectivity in Generalized Anxiety Disorder and Social Anxiety Disorder: Evidence for a Dimensional Approach. *Brain Connectivity, 7*(5), 289-298.

Radua, J., & Mataix-Cols, D. (2009). Voxel-wise meta-analysis of grey matter changes in obsessive-compulsive disorder. *Br J Psychiatry, 195*(5), 393-402. doi:10.1192/bjp.bp.108.055046

Radua, J., & Mataix-Cols, D. (2012). Meta-analytic methods for neuroimaging data explained. *Biol Mood Anxiety Disord, 2*, 6. doi:10.1186/2045-5380-2-6

Radua, J., Mataix-Cols, D., Phillips, M. L., El-Hage, W., Kronhaus, D. M., Cardoner, N., & Surguladze, S. (2012). A new meta-analytic method for neuroimaging studies that combines reported peak coordinates and statistical parametric maps. *European Psychiatry, 27*(8), 605-611. doi:10.1016/j.eurpsy.2011.04.001

Radua, J., Rubia, K., Canales-Rodriguez, E. J., Pomarol-Clotet, E., Fusar-Poli, P., & Mataix-Cols, D. (2014). Anisotropic kernels for coordinate-based meta-analyses of neuroimaging studies. *Front Psychiatry, 5*, 13. doi:10.3389/fpsyt.2014.00013

Rosazza, C., & Minati, L. (2011). Resting-state brain networks: literature review and clinical applications. *Neurol Sci, 32*(5), 773-785. doi:10.1007/s10072-011-0636-y

Roy, A. K., Fudge, J. L., Kelly, C., Perry, J. S. A., Daniele, T., Carlisi, C., . . . Ernst, M. (2013). Intrinsic functional connectivity of amygdala-based networks in adolescent generalized anxiety disorder. *Journal of the American Academy of Child and Adolescent Psychiatry, 52*(3), 290-299.e292. doi:10.1016/j.jaac.2012.12.010

Schienle, A., Ebner, F., & Schafer, A. (2011). Localized gray matter volume abnormalities in generalized anxiety disorder. *European Archives of Psychiatry & Clinical Neuroscience, 261*(4), 303-307.

Shirer, W. R., Ryali, S., Rykhlevskaia, E., Menon, V., & Greicius, M. D. (2012). Decoding subject-driven cognitive states with whole-brain connectivity patterns. *Cereb Cortex, 22*(1), 158-165. doi:10.1093/cercor/bhr099

Somers, J. M., Goldner, E. M., Waraich, P., & Hsu, L. (2006). Prevalence and incidence studies of anxiety disorders: a systematic review of the literature. *Can J Psychiatry, 51*(2), 100-113. doi:10.1177/070674370605100206

Stein, M. B., & Sareen, J. (2015). CLINICAL PRACTICE. Generalized Anxiety Disorder. *N Engl J Med, 373*(21), 2059-2068. doi:10.1056/NEJMcp1502514

Strawn, J. R., Bitter, S. M., Weber, W. A., Chu, W. J., Whitsel, R. M., Adler, C., . . . Delbello, M. P. (2012). Neurocircuitry of generalized anxiety disorder in adolescents: A pilot functional neuroimaging and functional connectivity study. *Depression and Anxiety, 29*(11), 939-947. doi:10.1002/da.21961

Strawn, J. R., John Wegman, C., Dominick, K. C., Swartz, M. S., Wehry, A. M., Patino, L. R., . . . DelBello, M. P. (2014). Cortical surface anatomy in pediatric patients with generalized anxiety disorder. *Journal of Anxiety Disorders, 28*(7), 717-723. doi:10.1016/j.janxdis.2014.07.012

Strawn, J. R., Wehry, A. M., Chu, W. J., Adler, C. M., Eliassen, J. C., Cerullo, M. A., . . . Delbello, M. P. (2013). Neuroanatomic abnormalities in adolescents with generalized anxiety disorder: A voxel-based morphometry study. *Depression and Anxiety, 30*(9), 842-848. doi:10.1002/da.22089

Swartz, J. R., Phan, K. L., Angstadt, M., Fitzgerald, K. D., & Monk, C. S. (2014). Dynamic changes in amygdala activation and functional connectivity in children and adolescents with anxiety disorders. *Development and Psychopathology, 26*, 1305-1319. doi:10.1017/S0954579414001047

Sylvester, C. M., Corbetta, M., Raichle, M. E., Rodebaugh, T. L., Schlaggar, B. L., Sheline, Y. I., . . . Lenze, E. J. (2012). Functional network dysfunction in anxiety and anxiety disorders. *Trends Neurosci, 35*(9), 527-535. doi:10.1016/j.tins.2012.04.012

Terlevic, R., Isola, M., Ragogna, M., Meduri, M., Canalaz, F., Perini, L., . . . Brambilla, P. (2013). Decreased hypothalamus volumes in generalized anxiety disorder but not in panic disorder. *Journal of Affective Disorders, 146*(3), 390-394. doi:10.1016/j.jad.2012.09.024

Toazza, R., Franco, A. R., Buchweitz, A., Molle, R. D., Rodrigues, D. M., Reis, R. S., . . . Manfro, G. G. (2016). Amygdala-based intrinsic functional connectivity and anxiety disorders in adolescents and young adults. *Psychiatry Research - Neuroimaging, 257*, 11-16. doi:10.1016/j.pscychresns.2016.09.010

Tromp, D. P., Grupe, D. W., Oathes, D. J., McFarlin, D. R., Hernandez, P. J., Kral, T. R., . . . Nitschke, J. B. (2012). Reduced structural connectivity of a major frontolimbic pathway in generalized anxiety disorder. *Archives of General Psychiatry, 69*(9), 925-934.

Wang, W., Hou, J., Qian, S., Liu, K., Li, B., Li, M., . . . Sun, G. (2016). Aberrant regional neural fluctuations and functional connectivity in generalized anxiety disorder revealed by resting-state functional magnetic resonance imaging. *Neuroscience Letters, 624*, 78-84. doi:10.1016/j.neulet.2016.05.005

Wang, W., Qian, S., Liu, K., Li, B., Li, M., Xin, K., & Sun, G. (2016). Reduced white matter integrity and its correlation with clinical symptom in first-episode, treatment-naive generalized anxiety disorder. *Behavioural Brain Research, 314*, 159-164. doi:10.1016/j.bbr.2016.08.017

Wang, X., Cheng, B., Luo, Q., Qiu, L., & Wang, S. (2018). Gray Matter Structural Alterations in Social Anxiety Disorder: A Voxel-Based Meta-Analysis. *Front Psychiatry, 9*, 449. doi:10.3389/fpsyt.2018.00449

Whalen, P. J., Johnstone, T., Somerville, L. H., Nitschke, J. B., Polis, S., Alexander, A. L., . . . Kalin, N. H. (2008). A Functional Magnetic Resonance Imaging Predictor of Treatment Response to Venlafaxine in Generalized Anxiety Disorder. *Biological Psychiatry, 63*(9), 858-863. doi:10.1016/j.biopsych.2007.08.019

White, S. F., Geraci, M., Lewis, E., Leshin, J., Teng, C., Averbeck, B., . . . Blair, K. S. (2017). Prediction Error Representation in Individuals With Generalized Anxiety Disorder During Passive Avoidance. *Am J Psychiatry, 174*(2), 110-117. doi:10.1176/appi.ajp.2016.15111410

Xia, L., Li, S., Wang, T., Guo, Y., Meng, L., Feng, Y., . . . Jiang, G. (2017). Spontaneous alterations of regional brain activity in patients with adult generalized anxiety disorder. *Neuropsychiatric Disease and Treatment, 13*, 1957-1965. doi:10.2147/NDT.S133853

Yassa, M. A., Hazlett, R. L., Stark, C. E. L., & Hoehn-Saric, R. (2012). Functional MRI of the amygdala and bed nucleus of the stria terminalis during conditions of uncertainty in generalized anxiety disorder. *Journal of Psychiatric Research, 46*(8), 1045-1052. doi:10.1016/j.jpsychires.2012.04.013

Zang, Y., Jiang, T., Lu, Y., He, Y., & Tian, L. (2004). Regional homogeneity approach to fMRI data analysis. *Neuroimage, 22*(1), 394-400. doi:10.1016/j.neuroimage.2003.12.030

Zang, Y. F., He, Y., Zhu, C. Z., Cao, Q. J., Sui, M. Q., Liang, M., . . . Wang, Y. F. (2007). Altered baseline brain activity in children with ADHD revealed by resting-state functional MRI. *Brain Dev, 29*(2), 83-91. doi:10.1016/j.braindev.2006.07.002

Zhang, L., Zhang, Y., Li, L., Li, Z., Li, W., Ma, N., . . . Lu, G. (2011). Different white matter abnormalities between the first-episode, treatment-naive patients with posttraumatic stress disorder and generalized anxiety disorder without comorbid conditions. *Journal of Affective Disorders, 133*(1-2), 294-299. doi:10.1016/j.jad.2011.03.040

Zhang, Y., Li, L., Yu, R., Liu, J., Tang, J., Tan, L., . . . Shan, B. (2013). White matter integrity alterations in first episode, treatment-naive generalized anxiety disorder. *Journal of Affective Disorders, 148*(2-3), 196-201. doi:10.1016/j.jad.2012.11.060

3. Chapter 3: Brain activity changes in Generalized Anxiety Disorder

Although many task-based fMRI experiments have been done in GAD, implied motion has not been controlled for. In a recent study investigating the neural correlates of implied motion and negative emotion, main effects and an interaction effect were observed, specifically in regions highlighted in the GAD systematic review. I addressed and mitigated this factor in the following work. Images were obtained from image databases and internet searches and pilot-tested to ensure that neutral and negative emotions were evoked while viewing them and that they were not confounded by differing levels of implied motion (i.e., motion that is, or is about to occur) in the images. Participants viewed these stimulus images while they underwent brain fMRI scans.

3.1 Abstract

Generalized Anxiety Disorder (GAD) is characterized by chronic, excessive worry and anxiety, and results in a reduced quality of life, as well as an increased risk of other mental and physical health issues. Although many neuroimaging studies have been conducted in the past, previous task-based studies often failed to control for implied motion in their stimuli—a confounding factor associated with unique neural activity compared to emotion. A recent systematic review/meta-analysis identified a number of key regions associated with GAD—while the dlPFC, ACC, amygdala, hippocampus have been fairly widely accepted, the culmen in the cerebellum has been reported often in results tables, but seldom discussed. In the present study, a region-of-interest analysis was conducted with the culmen. Additional confirmatory ROI analyses of the dlPFC, ACC, amygdala and hippocampus were conducted, as well as an exploratory whole-brain analysis. Although no significant findings were observed in the ROI analyses, the whole-brain analysis lends support to the previous systematic review findings, and lends support to the cerebellum playing a role in GAD. A larger sample size would no doubt increase the power of this study, perhaps leading to significant results in previously identified regions, and more robust results in the whole-brain analysis.

3.2 Introduction

Generalized Anxiety Disorder (GAD) is a common anxiety disorder characterized by chronic, excessive worry and anxiety occurring for a minimum of 6 months (American Psychiatric Association, 2013). Additional psychological and physiological symptoms are required for a diagnosis to be made including at least 3 of the following occurring in adults more days than not for the past half year: restlessness, irritability, difficulty sleeping, fatigue, muscle tension, and difficulty concentrating (American Psychiatric Association, 2013). Additionally, GAD is associated with a decreased quality of life, increased risk for suicide ideation (Nepon, Belik, Bolton, & Sareen, 2010; Sareen et al., 2005) and attempts (Stein & Sareen, 2015), and an increased risk of developing various inflammatory diseases (El-Gabalawy, Mackenzie, Pietrzak, & Sareen, 2014; Stein & Sareen, 2015). Unfortunately, although treatment options such as CBT and psychotropic drugs including SSRIs and SNRIs are available, they are often only effective for one-third to half of patients (Stein & Sareen, 2015).

A recent systematic review shows that patients with GAD attend more to threat-based stimuli than HC (Goodwin, Yiend, & Hirsch, 2017); however, physiological responses in GAD do not always reflect this. Although an increased ANS response would be expected for patients with GAD, they instead appear to have an inflexible ANS response—i.e., a smaller range of ANS responses (Borkovec, 1994; Hoehn-Saric, 1998; Hoehn-Saric, McLeod, Funderburk, & Kowalski, 2004; Lyonfields, Borkovec, & Thayer, 1995). In particular, patients with GAD have been shown to have parasympathetic inflexibility as evidenced by less variance within cardiac interbeat intervals (Aldao & Mennin, 2012; Hoehn-Saric et al., 2004; Hoehn-Saric, McLeod, & Zimmerli, 1989; Llera & Newman, 2010; Lyonfields et al., 1995; Makovac et al., 2016). Additionally, reduced skin conductance—regulated by sympathetic control—in response to stress and reduced variance in skin conductance has also been observed (Hoehn-Saric et al., 2004; Hoehn-Saric et al., 1989). Early physiology research indicates that compared with HC, patients with GAD have a much less exaggerated initial physiological response to a stressor, but take longer to return to baseline levels of physiological arousal after the stressor is removed (Hoehn-Saric, 1998). Additionally, behavioural data suggest that patients with GAD struggle with perseverative cognition (i.e., uncontrollable worry and rumination), which suggests cognitive inflexibility (Ottaviani et al., 2016). Recent work suggests that this inflexibility manifests itself neurologically as well: Fonzo and Etkin (2017) reviewed neuroimaging findings and discuss that *altered* (i.e.,

sometimes increased, sometimes decreased, sometimes no difference) activity and connectivity in the PFC and ACC in GAD may reflect a neurological inflexibility. The variability observed within GAD may itself be a facet of GAD, and be a part of the systems-wide inflexibility observed (Fonzo & Etkin, 2017).

The emotion dysregulation theoretical model of GAD posits that patients with GAD have difficulty regulating emotions, arising from difficulties understanding and describing them (Behar, DiMarco, Hekler, Mohlman, & Staples, 2009; Mennin, Heimberg, Turk, & Fresco, 2005). As a result, patients with GAD experience emotions more quickly, more intensely, and in response to situations that may be viewed as neutral by those without GAD (i.e., a hyperresponsiveness to emotion; Behar et al., 2009; Mennin et al., 2005). Eventually these emotions are viewed as threatening, leading to the desire to suppress them (i.e., a hyporesponsiveness to emotion; Behar et al., 2009; Mennin et al., 2005). Several reviews of the neuroimaging literature lend support to this emotion dysregulation model of GAD (Fonzo & Etkin, 2017; Hilbert, Lueken, & Beesdo-Baum, 2014; Mochcovitch, da Rocha Freire, Garcia, & Nardi, 2014). This emotion dysregulation model builds off of the original model of GAD: the avoidance model of worry, which suggests that worry is a verbal, linguistic activity, which inhibits vivid mental imagery in order to avoid processing emotions (Borkovec, 1994). Interestingly, cardiovascular responses change minimally from baseline for verbal-linguistic stimuli, compared to imagery of the same scenario in a healthy volunteer sample (Vrana, Cuthbert, & Lang, 1986). Furthermore, healthy volunteers reported lingering anxiety following a highly aversive video when they visualized images from the video, compared to relaxing or worrying verbally about the film (Butler, Wells, & Dewick, 1995). Thus, in order to elicit an emotional response in the current study, imagery-based stimuli were used.

Much research has gone into studying GAD in the past several decades, including previous MRI studies. In fact, a recent systematic review and meta-analysis shows that at least 85 MRI articles have been published, specifically in which GAD is compared to HC (Kolesar, Bilevicius, Wilson, & Kornelsen, 2019). This review highlights several regions that appear to be altered in GAD—the dlPFC, ACC, amygdala, and hippocampus—and are commonly represented in the literature. Most commonly, as measured using fMRI, activity within the dlPFC is reduced, activity within the ACC is mixed (sometimes increased, other times decreased without any clear distinction), amygdala activity is often increased and hippocampal volume is typically increased in GAD, compared to controls (Kolesar et al., 2019). Importantly, there are also novel results that

have often been included in studies result tables, but seldom discussed, such as the cerebellum, which, although it has a long history of being implicated in emotion in physiological studies (for review, see Adamaszek et al., 2017), is often dismissed in the neuroimaging literature. Specifically, the culmen appears to have reduced activity for patients with GAD compared to HC, particularly during working memory, emotion modulation, and congruency/conflict tasks (Kolesar et al., 2019). Other regions implicated in the systematic review include the vlPFC, PCC, insula, precuneus, precentral gyrus, OFC, and STG.

Although this systematic review included 42 task-based fMRI studies, the passive viewing tasks do not control for implied motion in their stimulus sets—in fact, several task-based studies use emotion-evoking stimuli depicting a threatening scene (with much motion implied) while the neutral images often depict calm landscapes (with very little motion implied). A recent study of emotion investigated how implied motion and negative emotion are differentially represented in the brain (Kolesar, Kornelsen, & Smith, 2017). Four stimuli groups were used: 1) negative emotion-evoking images, with motion implied, 2) negative emotion-evoking images, without motion implied, 3) neutral images with motion implied, and 4) neutral images without motion implied. Main effects were observed for emotion (precentral gyrus and visual processing regions) and implied motion (insula, STG, PCC, and fusiform gyrus; Kolesar et al., 2017). Importantly, an interaction was also observed, in regions such as the precentral gyrus and culmen. Of note, there is a high degree of overlap between many of these regions and the regions commonly altered in GAD. Thus, it is important to control for implied motion across negative and neutral emotion-evoking stimuli as it is possible the results from the GAD studies arose from or were strengthened by the inadvertent inclusion of mismatched implied motion between neutral and emotion-evoking stimuli. The present fMRI study attempts to confirm findings of the recent systematic review, after controlling for implied motion. The novel finding of the culmen highlighted in the systematic review is the primary research aim as it is an important new finding, somewhat overshadowed by the possible confounding of implied motion. Next, ROI analyses are conducted for the four main regions highlighted in the past, as a confirmatory analysis. Finally, to assess the additional regions throughout the brain that appear to be implicated in GAD, as well as to identify any novel regions, a *post hoc* whole-brain analysis was conducted.

3.3 Methods

3.3.1 Participants

Stimuli, consisting of neutral and negative emotion-evoking images, were pilot-tested by 40 individuals (mean age 33.6±13.4, 29 female, 11 male) with one participant discontinuing participation over halfway through. A different group of 32 individuals participated in the fMRI experiment; data from one patient was removed due to technical difficulties and data from another was removed due to excessive motion, resulting in 16 patients with GAD (mean age 34.3 ± 12.7 years, 13 females/3 males, 14 right-handed, 2 ambidextrous) and 14 HC (mean age 35.6 ± 13.3 years, 12 females/2 males, 12 right-handed, 2 ambidextrous), recruited from the Comorbidity, Cognition and Multiple Sclerosis (C-COMS, n = 5 GAD participants) study, the University of Manitoba and its affiliated hospitals (n = 8 GAD participants), and from the community (n = 5 GAD participants) in Winnipeg, Canada. Participants were screened for eligibility and interviewed according to the structured clinical interview for the DSM-IV-TR (SCID; Brown, Di Nardo, Lehman, & Campbell, 2001). Participants were excluded for neurological disorders (e.g., Tourette's syndrome, multiple sclerosis, Alzheimer's disease, dementia, disease or injury of the brain or spinal cord, including concussion resulting in loss of consciousness), known scoliosis, pregnancy, claustrophobia, inability to undergo a one-hour MRI session without requiring sedation and other standard MRI contraindications. Participants in the HC group had no history of mood or anxiety disorder and were matched by age and sex to a participant with GAD (± 5 years; due to data collection being cut short, two participants with GAD were not matched with a HC). Participants in the GAD group were confirmed to have been on a stable course of medication, medication doses, and/or therapy for a minimum of 60 days. General exclusion criteria also included participants aged <18, unable to provide informed consent, and inadequate knowledge of the English language to complete questionnaires. Ethical approval for this study was acquired from the University of Manitoba and St. Boniface Hospital Research Ethics Boards. Participants of both the pilot testing and the MRI study received remuneration of $25 for their time.

3.3.2 Stimuli

Stimulus images were obtained from emotion-evoking image databases including the International Affective Picture System (Jayaro, de la Vega, Diaz-Marsa, Montes, & Carrasco, 2008) and the Nencki Affective Picture System (Marchewka, Zurawski, Jednorog, & Grabowska, 2014) as well as internet searches. Images included either humans or animals, with preference

given to upper body images (i.e., depicting the arms) as previous spinal fMRI work indicates that spinal cord activity is limb-specific (McIver, Kornelsen, & Smith, 2013), and these images would also be used for fMRI of the cervical spinal cord, which innervates upper limbs. Three hundred images were pilot-tested by 40 individuals (mean age 33.6±13.4, 29 female, 11 male). One participant discontinued participation part way through and only rated 172 images. Images were rated on Likert scales from 1 to 7 on valence (how neutral or negative an image made the rater feel), physiological arousal (how calm or excited an image made the rater feel, regardless of valence), and implied motion (how much motion is, or is about to occur in the image). Images for the neutral and negative emotion-evoking categories were chosen to optimize the greatest valence difference, while reducing the average rating difference for implied motion and arousal. While implied motion did not differ between the two conditions, it was not possible to eliminate differences of physiological arousal in the stimulus images and implied motion was prioritized, given the convergence of results observed between the interaction of implied motion and emotion (Kolesar et al., 2017) with the commonly altered regions in GAD (Kolesar et al., 2019). A total of 252 images were retained for the fMRI experiments; 36 images were used in the brain (18 negative, 18 neutral), while 108 images were used in each of the spinal cord regions (i.e., 3 runs each, with each run including 36 images). To investigate if images were perceived differently by participants with and participants without GAD, a subset of images were rated by the MRI participants after the completion of their scans.

3.3.3 Task

After informed consent was obtained, participants completed questionnaires, prior to entering the MRI suite. Task-based fMRI data was collected from the brain (described presently) and cervical and thoracic spinal cord (discussed in Chapter 3). During the fMRI experiment, participants passively viewed blocks of negative emotion-evoking images (herein referred to as "negative images"), alternated with blocks of neutral images. Each block was 24 seconds in duration, consisting of 6 images, randomly presented and each shown for 4 seconds (see Figure 3.1). Three negative and three neutral blocks were viewed, separated using a 7 second fixation cross. The fixation cross was used as a way to distinctly separate negative and neutral blocks to prevent habituation to continuously viewing images. The fixation cross was presented for 7 seconds to allow for acquisition of one full volume in the spinal cord (Chapter 4). The duration of the final fixation cross differed in the brain and spinal cord (6 seconds in the brain, 3 seconds in

the spinal cord runs) to use up the remaining time for each scan, while ensuring the time spent viewing stimulus pictures in each run was consistent across runs.

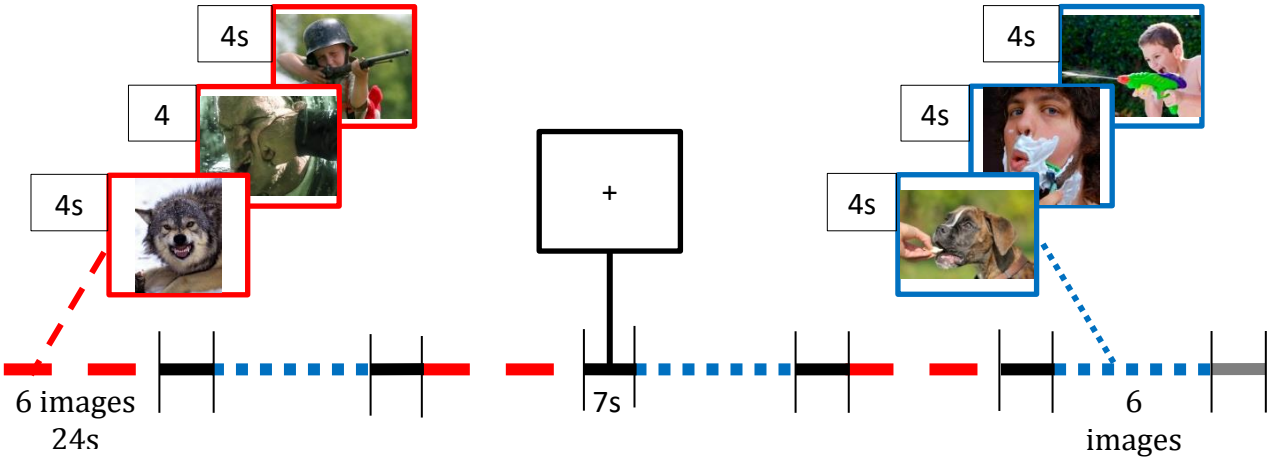

Figure 3.1: Task paradigm. Red = negative emotion-evoking stimuli; blue = neutral stimuli; black = fixation cross; s = seconds. The final fixation cross duration differed in brain and spinal cord (Chapter 4) designs: brain = 6 s, spinal cord = 3 s.

Participants were asked to rate their present moment anxiety using a visual analog scale (VAS) several times throughout the fMRI experiment—directly before entering the MRI suite (VAS1), immediately after the brain task and before the cervical task (VAS2), immediately after the cervical task and before the thoracic task (VAS3), and at the completion of the MRI experiment (VAS4).

3.3.4 Questionnaires

Several questionnaires were administered prior to MRI scanning, including sociodemographic information, the Generalized Anxiety Disorder-7 Scale (GAD-7; Cronbach α = 0.92; intraclass correlation of 0.83 for test-retest reliability; Spitzer, Kroenke, Williams, & Lowe, 2006), the Overall Anxiety Severity and Impairment Scale (OASIS; Cronbach α = 0.80, κ = 0.82; Norman, Cissell, Means-Christensen, & Stein, 2006), the Patient-Health Questionnaire-9 (PHQ-9; Cronbach α between 0.86 and 0.89; Kroenke, Spitzer, & Williams, 2001), the Alcohol Use Disorders Identification Test-Concise (AUDIT-C; Bush, Kivlahan, McDonell, Fihn, & Bradley, 1998; Cronbach α = 0.98, intraclass correlation = 0.95; Osaki et al., 2014), the Edinburgh Handedness Inventory (EHI; test-retest reliability coefficent 0.75 to 0.86; McMeekan & Lishman,

1975; Oldfield, 1971), and the Patient-Reported Outcomes Measurement Information System (PROMIS) Pain Interference Short Form 8a (PI-8a; intraclass correlation = 0.87 in general population; Broderick, Schneider, Junghaenel, Schwartz, & Stone, 2013). Scores for the GAD-7, OASIS, PHQ-9, and AUDIT-C questionnaires were summed, according to scoring instructions. The self-report symptoms measures are well validated measures with strong psychometric properties. As per the scoring instructions, scores from the PI-8a were normalised to a T-score metric; the mean score is 50 from a general US reference population, with a standard deviation of 10 points (http://www.healthmeasures.net/images/PROMIS/manuals/PROMIS_Pain_Interference_Scoring_Manual.pdf). Scores for the EHI were calculated as follows: ((R-L)/(R+L))*100, where R = the number of '+' symbols in the right-hand column, and L = the number the '+' symbols in the left-hand column (Robinson, 2013). After the VAS4 was administered (after MRI completion), participants rated a subset of the images used in the fMRI experiment to investigate whether GAD and HC groups would subjectively rate the images differently.

3.3.5 MRI Data Acquisition

MRI data were acquired using a 32-channel receive-only head coil on a Siemens MAGNETOM Trio 3 Tesla system (Erlangen, Germany). The T_1-weighted anatomical data were acquired using a magnetization prepared rapid gradient echo (MP-RAGE) sequence with TR/TE/TI = 1900/2.47/900 ms, 176 slices, and a generalized auto-calibrating partial parallel acquisition (GRAPPA) Factor = 2, flip angle = 9°, FOV = 250 mm x 250 mm, 1.00 mm x 1.00 mm x 1.00 mm resolution, for an acquisition time of 420 seconds (see Appendix A for full scanning parameters). Opposite phase encoding images were acquired to correct susceptibility artifacts arising from using an GE-EPI sequence, and exacerbated from using a multi-band sequence, collected in the right-to-left and left-to-right phase encoding directions with TR/TE = 10170/86.6 ms, 72 slices, 3 volumes, and a GRAPPA Factor = 1, flip angle = 90°, FOV = 208 mm x 180 mm, 2.00 mm x 2.00 mm x 2.00 mm resolution, for an acquisition time of 31 seconds each. T_2^*-weighted data were acquired using a multiband gradient-echo, echo planar imaging (GE-EPI) sequence with a TR/TE = 1500/38.6 ms, 123 volumes, 85 slices, FOV = 250 mm x 195 mm, 2.50 mm x 2.50 mm x 2.50 mm resolution, 0 gap between slices, flip angle = 61°, and a multiband acceleration factor = 5 (Xu et al., 2013), for an acquisition time of 185 seconds. Two "dummy" volumes were acquired to reach steady state prior to scanning.

3.3.6 fMRI Preprocessing and Analysis

MRI data were first converted from dicom to NIfTI format and were preprocessed using SPM12 (https://www.fil.ion.ucl.ac.uk/spm/). The fMRI volumes were realigned to correct for bulk motion using the estimate and reslice option. The MP-RAGE, as well as the R-L and L-R phase encoded images were then coregistered to the mean fMR image before correcting the realigned fMR images for susceptibility distortions using hyperelasticity susceptibility artifact correction (HySCO, v. 2.0; Ruthotto et al., 2012; http://www.diffusiontools.com/documentation/hysco.html). Next, the coregistered MP-RAGE image was segmented and spatially normalized to the ICBM European brain template in CAT12 (http://www.neuro.uni-jena.de/cat/), using "expert mode" to provide GM, WM, and CSF masks, as well as the forward deformation field, which was subsequently applied to warp all of the HySCO-corrected fMRI volumes to the ICBM template. The spatially normalized fMRI data were then run through ART artifact detector in the Conn Toolbox (v. 19c; https://web.conn-toolbox.org/) using intermediate (97^{th} percentile) settings. Both unsmoothed and smoothed (4 mm at full width half-maximum; Chen & Calhoun, 2018) data sets were saved for later entry in the ROI and whole-brain analyses, respectively.

3.3.7 ROI Analysis

The unsmoothed data were run through first-level analyses in SPM12 ($p < 0.001$) to compare subject-level activation differences between negative and neutral blocks. First, 'fMRI Model specification' was run, which included multiple regressors (i.e., the 6 motion parameters and the ART outlier data for each subject) in the model, followed by 'Model estimation' (see Figure 3.2). First-level contrasts were run, comparing data from negative blocks (+1) to data from neutral blocks (-1).

Next, the ROI second-level analyses were conducted on the GAD and HC first-level contrast images, using an unpaired two-sample t-test, comparing the GAD group (+1) to the HC group (-1). Given the small sample size, age and sex were not modelled; however, HC participants were matched to GAD patients by age and sex (with the exception of two participants with GAD, as data collection was cut short). As highlighted in our recent systematic review and meta-analysis of neuroimaging in GAD (Kolesar et al., 2019), the role of the culmen in the anterior cerebellum remains to be investigated. The culmen was addressed as our primary research interest as it was the most novel result from the systematic review, combined with its role in implied motion in previous work (Kolesar et al., 2019). Next, secondary ROI analyses included the four main regions

most often identified in GAD: the dlPFC, amygdala, ACC, and hippocampus as a confirmatory analysis of our systematic review findings. Lateralized ROIs were combined using the MarsBaR toolbox (version 4.4; Brett, Anton, Valabregue, & Poline, 2002) in SPM12 in order to limit the number of comparisons made at this stage. The culmen, hippocampus, and amygdala ROIs were taken from the AAL atlas while the ACC and dlPFC were obtained from a functional network atlas ('aal.nii' and 'networks.nii' contained within the conn19c software package), as these regions are poorly localized anatomically. From each of these ROIs, mean parameter estimates were extracted, with scaling from the raw data, and grand mean scaling set to 0. Results were estimated, saved, and loaded into MATLAB®, and then brought into XLSTAT in Microsoft Excel 2010 to perform t-tests. As our primary analysis included the culmen, α was set to $p < 0.05$. To correct for multiple comparisons in our confirmatory investigation of the dlPFC, ACC, amygdala, and hippocampus, a Bonferroni-corrected α was set to $p < 0.012$. One-tailed t-tests were performed for the culmen and dlPFC (GAD < HC), and amygdala (GAD > HC).

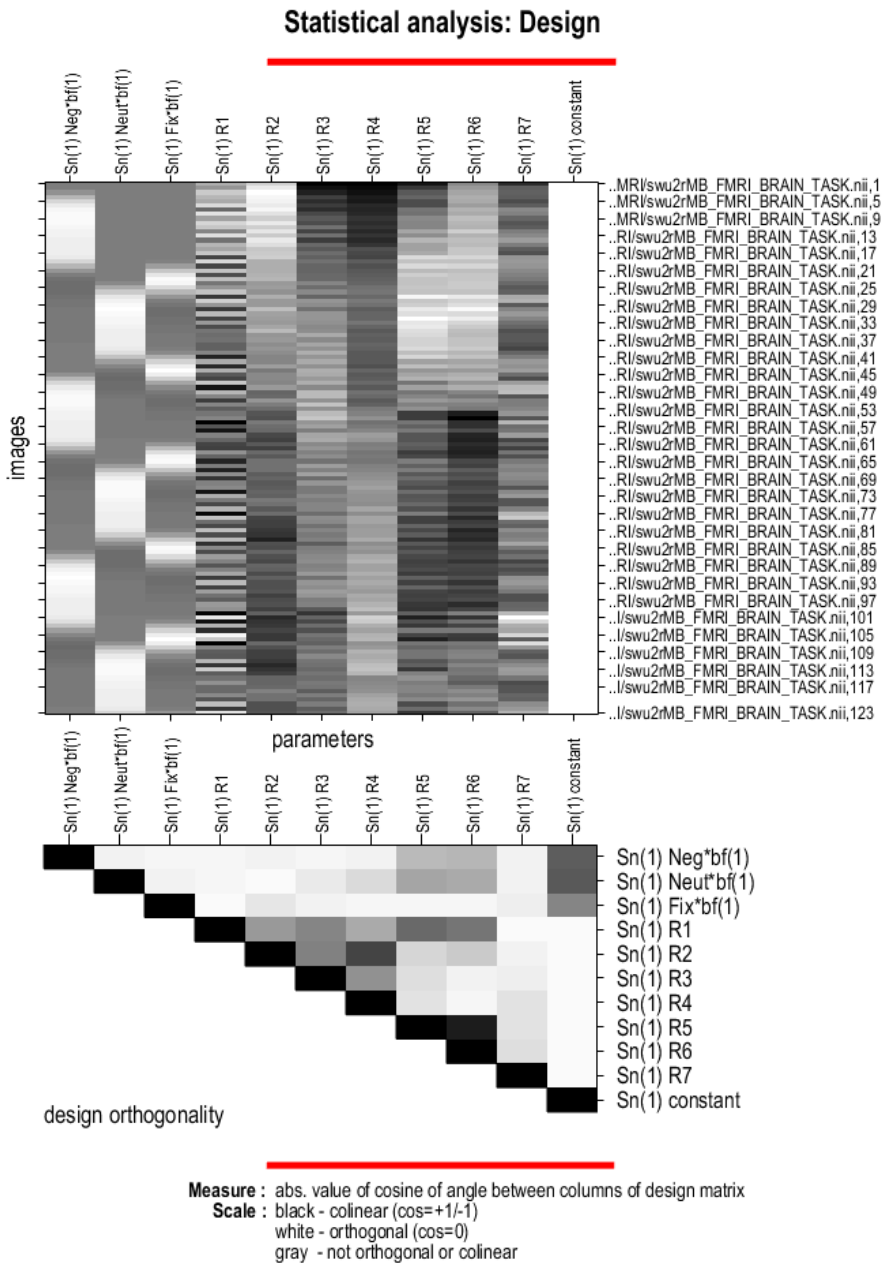

Figure 3.2: Sample first-level SPM model design. The columns represent the task paradigm, including negative (…Neg*bf(1)), neutral (…Neut*bf(1)), and fixation (…Fix*bf(1)) blocks, followed by the 6 motion parameters (3 translation parameters, 3 rotation parameters, R1 to R6), and ART outlier data measuring scan-to-scan motion differences (R7).

3.3.8 Whole-Brain Analysis

A whole-brain analysis was conducted to assess brain activation in response to threat to investigate the remaining regions identified in the systematic review (Kolesar et al., 2019), and whether they were altered after implied motion was controlled for. Whole-brain data were analysed at the first-level identically to the ROI data, with the exception that this data was smoothed using a 4 mm FWHM Gaussian kernel. For the whole-brain analysis, an analysis of variance was conducted, yielding results from main effects of group and stimuli valence, as well as the interaction between the two. Additionally, a contrast directly comparing GAD and HC groups was conducted, all corrected for multiple comparisons using FDR $p = 0.05$. The whole-brain data were masked using a grey matter mask created from the mean grey matter segments of all 30 participants—to match the data, the grey matter mask was smoothed using a 4 mm FWHM Gaussian kernel. Although additional analyses were planned—i.e., regressing the data with OASIS scores—the limited sample size precluded this investigation.

3.4 Results

3.4.1 Questionnaire Results

Demographic and questionnaire data can be found in (Table 3.1). Groups did not differ in mean age, mean education years, mean household income ($t(28) = -1.501$, $p = 0.144$), problem drinking (AUDIT-C scores), handedness (EHI scores), or current moment anxiety scores just prior to entering the MRI suite (VAS1). While both GAD and HC groups were mildly anxious before beginning the experiment (VAS1), these scores increased after the brain task (i.e., VAS2) for the GAD group, but decreased for the HC group—VAS2 scores significantly differed between GAD and HC groups (see Table 3.1). GAD and HC groups also significantly differed on GAD-7, OASIS, PHQ-9, and PI-8a questionnaires. Pilot-tested negative and neutral images had significantly different ratings for valence and physiological arousal, but values did not differ for implied motion (see Table 3.2). Furthermore, after completing the MRI experiment, ratings for valence, arousal, and implied motion on a subset of stimulus images did not differ between GAD and HC groups (Table 3.2).

Table 3.1: Demographic details of GAD and HC groups.

	GAD	**HC**	***t*-value**	***p*-value**
N	16	14		
Female/Male	13/3	12/2		
Mean age	34.3 (± 12.7)	35.6 (± 13.3)	-0.26	0.793
Mean symptom duration (years)	18.5 (± 13.0)			
Comorbidities				
MDD	4	0		
PDD, with current MDD episode	1	0		
PDD, without current MDD episode	1	0		
SAD	5	0		
PD, with agoraphobia	2	0		
PD, without agoraphobia	1	0		
OCD	2	0		
Mean education years	15.8 (± 2.8)	16.3 (± 2.0)	-0.53	0.603
Less than high school	0	0		
High school/GED	6	1		
Technical/Trade	1	4		
College	1	1		
Bachelor's degree	7	6		
Master's degree	1	2		
Employment				
Management	1	0		
Business, finance, and administration	3	0		
Health	2	7		
Education, law and social, community/government service	4	1		
Trades, Transport or Equipment operator and related occupations	1	2		
Natural resources, agriculture, and related production	0	0		

Sales and service	2	0		
Art, culture, recreation and sport	1	1		
Manufacturing and utilities	0	0		
Other—Student	1	2		
Other—Science, R&D	1	1		
Marital status				
Married/common law	8	7		
Widowed/separated/divorced	1	0		
Single, never married	7	7		
Household income				
0-$14,999	0	0		
$15,000-$29,999	3	0		
$30,000-$49,999	1	0		
$50,000-$100,000	6	8		
>$100,000	6	6		
AUDIT-C	2.8 (± 1.8)	2.9 (±1.9)	-0.066	0.948
Recreational Drug Use				
Yes (all cannabis)	4	2		
No	12	12		
Medications				
Escitalopram	2	0		
Sertraline	1	0		
Desvenlafaxine	1	0		
Bupropion	2	0		
Amitriptyline	1	0		
Zopiclone	0	1		
GAD-7	11.6 (± 4.4)	1.6 (± 2.6)	7.47	<0.001
OASIS	8.9 (± 3.2)	1.6 (± 2.3)	6.94	<0.001
PHQ-9	9.1 (± 5.4)	1.3 (± 1.9)	5.12	<0.001
PI-8a	55.5 (± 6.0)	43.1 (± 5.1)	6.08	<0.001
EHI	68.9 (± 31.0)	69.2 (± 37.7)	-0.025	0.980

VAS1	18.5 (± 20.6)	12.6 (± 19.8)	0.79	0.436
VAS2	25.3 (± 21.8)	7.7 (± 13.3)	2.62	0.014*
VAS3	31.2 (± 24.8)	8.9 (± 12.3)	3.06	0.005*
VAS4	23.9 (± 27.0)	3.8 (± 6.8)	2.70	0.012*

'*' indicates significance at $p < 0.05$. Visual Analog Scales (VAS) were administered throughout the experiment. MDD = major depressive disorder, PDD = persistent depression disorder, SAD = social anxiety disorder, PD = panic disorder, OCD = obsessive compulsive disorder. VAS1 = current moment anxiety score (0 = no anxiety, 100 = worst anxiety imaginable) just before entering the MRI suite; VAS2 = anxiety score after brain, but before cervical spinal cord task; VAS3 = anxiety score after cervical, but before thoracic spinal cord task; VAS4 = anxiety score after thoracic cord scanning. AUDIT-C = Alcohol Use Disorders Identification Test-Concise; GAD-7 = Generalized Anxiety Disorder 7-Item Scale; OASIS = Overall Anxiety Severity and Impairment Scale; PHQ-9 = Patient Health Questionnaire 9-Item Scale; PI-8a = Pain Interference Short Form 8a; EHI = Edinburgh Handedness Inventory.

Table 3.2: Average (± standard deviation) stimuli rating of implied motion, valence, and physiological arousal for neutral and negative emotion-evoking images (scales from 1 [neutral; calm; no implied motion] to 7 [negative; excited; lots of implied motion]). Data was not collected from one GAD participant due to time constraints. Pilot-testing data are from the 252 images used in the fMRI studies (each run consisted of 18 neutral and 18 negative images; brain = 1 run, cervical spinal cord = 3 runs, thoracic spinal cord = 3 runs). Post-MRI ratings were from a subset of these images (18 negative, 18 neutral images), following fMRI scanning.

	Stimuli Characteristic		
	Valence	**Arousal**	**Motion**
Pilot-testing (N = 40)			
Negative	5.0 (±0.7)	4.6 (±0.5)	3.8 (±1.0)
Neutral	1.5 (±0.3)	3.0 (±0.8)	3.7 (±1.1)
t-value	-50.6	-18.9	-0.9
p-value	<0.001*	<0.001*	0.376
Negative stimuli (post MRI ratings)			
GAD	5.3 (± 1.5)	5.1 (± 1.7)	5.4 (± 1.4)

HC	5.0 (± 2.0)	4.6 (± 2.1)	5.1 (± 2.1)
t-value	0.503	0.651	0.449
p-value	0.619	0.521	0.657
Neutral stimuli (post MRI ratings)			
GAD	2.4 (± 1.4)	3.3 (± 1.5)	5.2 (± 1.1)
HC	2.1 (± 1.1)	2.9 (± 1.7)	4.7 (± 1.3)
t-value	0.676	0.631	1.143
p-value	0.505	0.534	0.263

'*' indicates a statistically significant difference between the negative and neutral emotion-evoking stimulus sets at $p < 0.05$. Note that those pilot-testing the images rated 300 images, while the participants who underwent fMRI rated only a subset ($n = 36$) of the images presented during the fMRI runs.

3.4.2 ROI Results

Neither the primary (culmen $t(28) = 0.159$, $p = 0.562$) nor the secondary (dlPFC $t(28) = 0.500$, $p = 0.690$, ACC $t(28) = -0.434$, $p = 0.668$, amygdala $t(28) = -0.989$, $p = 0.834$, hippocampus $t(28) = -1.569$, $p = 0.128$) ROI analyses yielded significant results.

3.4.3 Whole-Brain Results

The whole-brain analysis yielded significant findings for the main effect of group. The full results for the main effect of group are included in

Table 3.3 and can be visualised in Figure 3.3. Interestingly, several clusters were observed in the culmen for the main effect of group. Additionally, the amygdala, hippocampus, and bilateral dlPFC clusters also reached significance for the main effect of group, and although less convincing, one caudate cluster included a few voxels in the ACC (x = 9, y = 19.5, z = -7.5). Several other interesting regions observed in both the systematic review and the present study include the insula, STG, precuneus, and precentral gyrus (with additional voxels in two postcentral gyrus clusters [x = -33, y = -25.5, and z = 48] and [x = -52.5, y = -9, and z = 13.5]). Finally, some regions were observed outside of those expected from the systematic review including: the uvula and nodule of the cerebellum, the thalamus, the supplementary motor area, regions of the middle temporal, middle frontal, and inferior frontal gyri, and the middle occipital gyrus.

No significant results were observed for the main effect of image valence (i.e., neutral or negative emotion-evoking images), the interaction between groups and image valence, or a direct contrast between GAD and HC groups.

Table 3.3: Main effect of group in the brain for GAD and HC groups. Results are corrected for multiple comparisons with a cluster extent threshold of 5 voxels and false discovery rate of $p < 0.05$.

			Coordinates				
Region	**Side**	**Voxels**	**X**	**Y**	**Z**	**BA**	***F***
Cerebellum							
Culmen [4,5]	L	55	-10.5	-49.5	-21		33.67
	R	5	15	-51	-19.5		27.47
	R	7	15	-34.5	-15		23.62
	R	5	27	-40.5	-25.5		18.60
Culmen [vermis 4,5]	R	34	6	-49.5	-18		40.81
Culmen [6]	L	5	-27	-58.5	-25.5		19.09
Declive [4,5]	L	8	-3	-60	-18		26.22
Uvula [vermis 8]	R	25	1.5	-66	-39		33.75
Nodule [9]	R	16	12	-49.5	-37.5		35.20
Subcortical Structures							
Amygdala	R	16	30	3	-18	34	25.73
	L	6	-22.5	-10.5	-10.5		22.14
Caudate	R	16	9	19.5	-7.5		27.18
	R	11	9	6	-10.5		25.61
	R	11	16.5	22.5	-3		22.53
	R	5	18	22.5	10.5		19.86
	R	7	15	13.5	18		17.74
Putamen	R	5	30	-16.5	6		20.53
Thalamus	R	14	6	-6	3		24.73
(VPM/VPL Nuclei)	L	6	-16.5	-22.5	6		24.35
(MD Nucleus)	R	16	10.5	-24	3		22.51
Temporal Lobe							
Hippocampus	R	6	27	-25.5	-9		27.54
Parahippocampal Gyrus	L	9	-31.5	-40.5	-3		30.27
Fusiform Gyrus	R	9	45	-51	-15	37	26.45

Insula	L	10	-39	0	-4.5	13	25.00
	R	10	42	4.5	-1.5		21.17
	R	5	37.5	15	-16.5	47	19.42
Superior Temporal Gyrus	L	37	-51	-18	1.5		30.25
	R	7	45	-15	-7.5	22	24.12
	L	27	-55.5	-30	10.5		23.70
Middle Temporal Gyrus	R	32	61.5	-48	0		46.43
	R	54	40.5	-66	12		34.36
	L	11	-45	-64.5	0		25.64
	R	5	48	-10.5	-16.5		19.84
Frontal Lobe							
Superior Frontal Gyrus, Medial	R	9	10.5	61.5	25.5		27.02
Superior Frontal Gyrus	R	22	19.5	-3	66		25.61
Middle Frontal Gyrus	L	17	-25.5	42	15		35.13
	R	10	31.5	25.5	36		27.03
	R	15	25.5	55.5	25.5	10	23.21
	R	7	33	43.5	25.5	10	21.64
(Premotor)	L	5	-25.5	-12	48	6	21.44
(dlPFC)	L	5	-40.5	45	0		19.20
(dlPFC)	R	5	42	43.5	1.5		19.13
(Orbital)	R	7	43.5	57	-3	10	21.77
Inferior Frontal Gyrus	L	6	-36	15	-18	47	18.67
(Orbital)	R	9	36	31.5	-12	47	38.21
(Triangularis)	L	19	-45	24	1.5		20.56
(Triangularis)	R	19	55.5	31.5	-1.5	47	19.66
(Triangularis)	R	5	57	31.5	4.5	45	18.41
Midcingulate Gyrus	R	12	3	-30	49.5	31	21.77
Supplementary Motor Area	L	16	-3	-12	49.5		26.71
Precentral Gyrus	L	7	-27	-28.5	63		28.53
Parietal Lobe							

Rolandic Operculum	L	6	-55.5	10.5	3		28.58
Postcentral Gyrus	L	17	-33	-25.5	48	3	30.49
	L	11	-43.5	-31.5	57		30.00
	L	8	-52.5	-9	13.5	43	26.00
Midcingulate Gyrus	L	5	-7.5	-43.5	42	31	21.43
Inferior Parietal Lobule	R	20	39	-42	49.5	40	21.74
Angular Gyrus	L	15	-39	-64.5	25.5	39	24.55
Occipital Lobe							
Middle Occipital Gyrus	L	13	-43.5	-75	-3		19.09
Precuneus	R	13	9	-42	40.5		24.90
Lingual Gyrus	R	10	16.5	-66	-6	18	31.79

Coordinates are peak coordinates; all results were significant ($p < 0.001$) at FDR $p = 0.05$. 'Voxels' refers to the number of voxels per cluster. R = right hemisphere; L = left hemisphere; BA = Brodmann Area, as applicable; '[x]' after cerebellum clusters indicates the corresponding aal cerebellar hemisphere region.

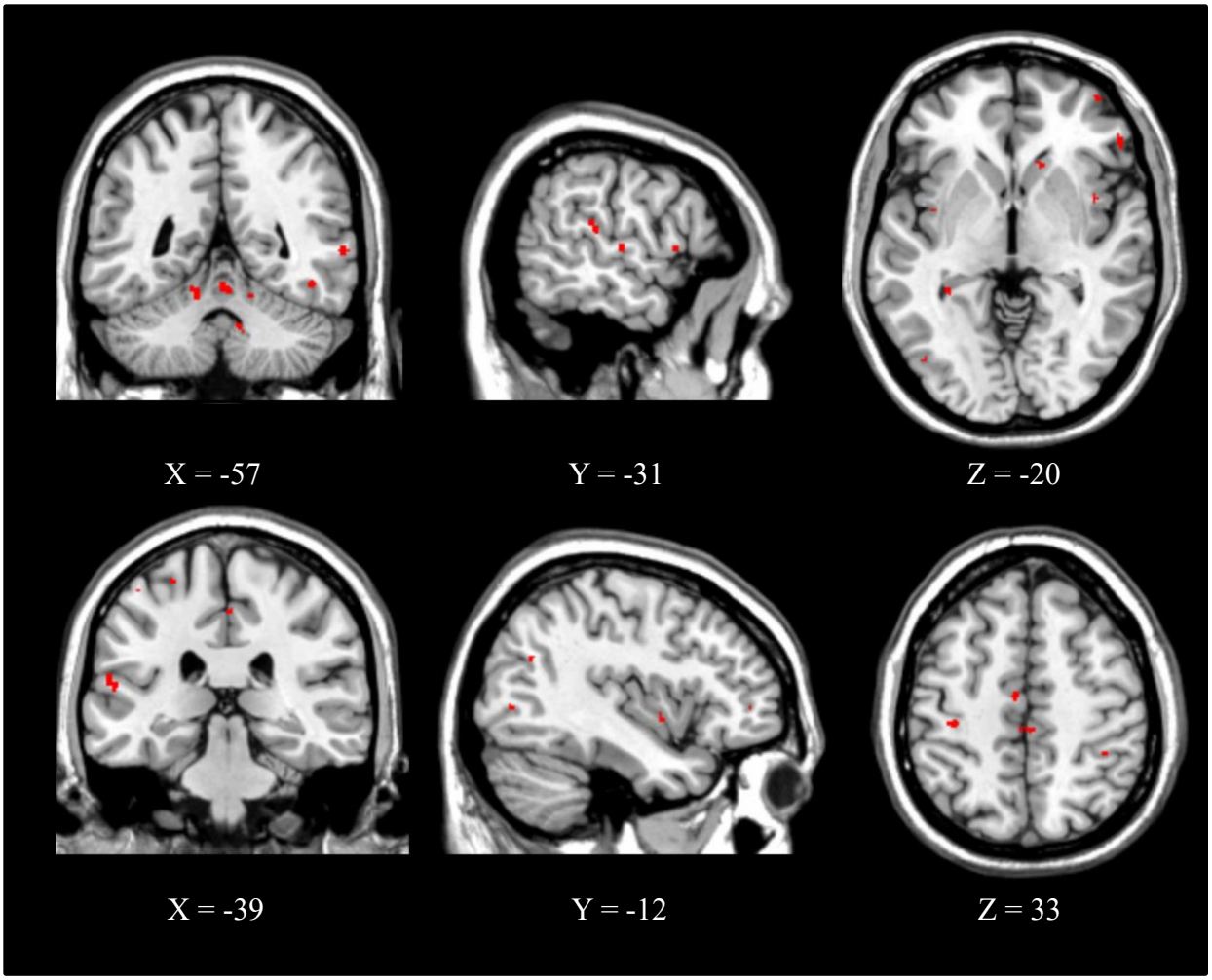

Figure 3.3: Main effect of group for GAD and HC. Correction for multiple comparisons includes a cluster extent threshold of 5 voxels and FDR $p = 0.05$.

3.5 Discussion

Although the ROI analyses did not yield significant results, the whole-brain main effect for group did. Importantly, many of the regions identified in our recent systematic review/meta-analysis (Kolesar et al., 2019) were observed in the group main effect, despite the smaller than planned sample size. Our previous work identified the dlPFC, ACC, amygdala, and hippocampus as key widely accepted regions (hence the secondary ROI analysis), while also highlighting the cerebellum (i.e., culmen), insula, precuneus, precentral gyrus, STG, vlPFC, PCC and OFC (Kolesar et al., 2019). Interestingly, clusters were observed in all of these regions except for the ACC and PCC (with the exception of a few voxels in ACC in a cluster peaking in the caudate). It is important to note that ACC activity has been shown to be mixed, sometimes showing greater

(Andreescu et al., 2011; Fonzo et al., 2014; Laufer, Israeli, & Paz, 2016; McClure et al., 2007; Mohlman, Eldreth, Price, Staples, & Hanson, 2017; Paulesu et al., 2010), and sometimes showing reduced activation (Blair et al., 2012; Diwadkar et al., 2017; Etkin, Prater, Hoeft, Menon, & Schatzberg, 2010; Laufer et al., 2016; Mohlman et al., 2017; Palm, Elliott, McKie, Deakin, & Anderson, 2011; White et al., 2017) in a GAD sample (Kolesar et al., 2019). In fact, Fonzo and Etkin (2017) discuss that this inconsistency in the ACC may itself be characteristic of GAD, and may relate to neural inflexibility, which would fall in line with theories describing physiological inflexibility, such as that observed in the ANS of patients with GAD (Aldao & Mennin, 2012; Borkovec, 1994; Hoehn-Saric, 1998; Hoehn-Saric et al., 2004; Hoehn-Saric et al., 1989; Llera & Newman, 2010; Lyonfields et al., 1995). Although these whole-brain results yielded fairly small clusters, their validity is strengthened by the fact that no significant clusters were observed for the main effect of image valence, or the interaction between group and image valence, combined with the correction for multiple comparisons. If these significant regions were simply due to noise, we would also expect similar results in these other two results maps. These regions line up incredibly well with expectations, and as discussed in our systematic review, these results may implicate the role of large-scale network dysfunction, rather than individual region dysfunction (Kolesar et al., 2019).

While ROI analyses are typically higher-powered than whole-brain analyses, it is important to keep in mind that the ROI analyses (i.e., direct contrasts) are not directly comparable to the whole-brain analyses (main effect of group), although they are conceptually similar. The small size of the significant clusters in our whole-brain analysis may provide some insight into the lack of significant findings in the ROI analysis. While the whole-brain analysis considers each voxel separately, the ROI analyses average over the entire ROI; it is likely that the findings we observed in the whole-brain analysis were simply not powerful enough to be detected in the ROI analyses because surrounding non-significant voxels washed out the signal within the much larger ROIs. It could be the case that because the stimulus images used in the current study were controlled for implied motion, the clusters observed were more localized in the tissue than in previous studies. Regardless, it would be interesting to investigate how these results differed in a fully-powered study (data collection was cut short due to the onset of the COVID-19 pandemic, see Appendix B: Letter from the VP of Research Regarding Research Activities in Response to COVID-19).

The most prominent results include the clusters in the cerebellum, mostly located within the culmen. Although the culmen may have a role in congruency and conflict (Kolesar et al., 2019; Shih et al., 2009), there is evidence to suggest that it also plays a role in emotion processing as it is hypoactive in alexithymia, a condition marked by the inability to recognize and describe emotions (Adamaszek et al., 2017). These observations become interesting and lend support when recalling the emotion dysregulation model of GAD which posits that for patients with GAD, emotions are difficult to understand and describe (Behar et al., 2009; Mennin et al., 2005), combined with the systematic review findings that culmen activity and FC is reduced in patients with GAD (Kolesar et al., 2019). These findings suggest that more attention should be given to affective identification (drawn from emotion-focused therapy; Greenberg, Goldman, & American Psychological Association, 2019; Watson, Greenberg, & American Psychological Association, 2017) in CBT. Additionally, future research should be conducted to investigate if and how culmen activity changes after affective identification training in GAD.

Furthermore, as the cerebellum does have a large role in motor function, it is interesting to note significant clusters within the premotor (x = -25.5, y = -12, z = 48, Brodmann's area 6) and supplementary motor cortex, caudate, and putamen. While motor deficits are not associated with GAD, muscle tension is (American Psychiatric Association, 2013; Hazlett, McLeod, & Hoehn-Saric, 1994; Hoehn-Saric et al., 1989; McLeod, Hoehn-Saric, & Stefan, 1986), which may partially be related to freezing in response to threat (Borkovec, 1994). The associated activity in sensory regions (ventral posterior nuclei of the thalamus, postcentral gyrus) may be related to this potential motor excitability.

Finally, several regions associated with vision or visual processing, such as the middle occipital and lingual gyri, middle temporal gyrus, and fusiform gyrus, are also significant, along with the inferior parietal lobe, concerned with locations of objects in space (Goodale & Milner, 1992), and the angular gyrus, associated with multimodal integration (Seghier, 2013). Our previous study investigating neural differences between emotion and implied motion highlighted these regions (Kolesar et al., 2017), perhaps suggesting emotion processing differences between these groups, irrespective of the stimuli present.

Although the conclusions that can be made regarding a significant main effect are limited—i.e., the main effect of group, but not the main effect of valence or interaction was significant, and further *post hoc* contrasts comparing GAD and HC groups were unable to clarify results—it is

interesting that so many of the regions previously identified in our systematic review can be observed in the current work, particularly given the relatively small sample size. Additionally, the validity of these results is increased, given the controlling for implied motion, previously lacking in earlier task-based studies (Kolesar et al., 2019).

3.6 Chapter 3 References

Adamaszek, M., D'Agata, F., Ferrucci, R., Habas, C., Keulen, S., Kirkby, K. C., . . . Verhoeven, J. (2017). Consensus Paper: Cerebellum and Emotion. *Cerebellum, 16*(2), 552-576. doi:10.1007/s12311-016-0815-8

Aldao, A., & Mennin, D. S. (2012). Paradoxical cardiovascular effects of implementing adaptive emotion regulation strategies in generalized anxiety disorder. *Behav Res Ther, 50*(2), 122-130. doi:10.1016/j.brat.2011.12.004

American Psychiatric Association. (2013). *Diagnostic and statistical manual of mental disorders* (5th ed.). Arlington, VA: American Psychiatric Association Publishing.

Andreescu, C., Gross, J. J., Lenze, E., Edelman, K. D., Snyder, S., Tanase, C., & Aizenstein, H. (2011). Altered cerebral blood flow patterns associated with pathologic worry in the elderly. *Depression and Anxiety, 28*(3), 202-209. doi:10.1002/da.20799

Behar, E., DiMarco, I. D., Hekler, E. B., Mohlman, J., & Staples, A. M. (2009). Current theoretical models of generalized anxiety disorder (GAD): conceptual review and treatment implications. *J Anxiety Disord, 23*(8), 1011-1023. doi:10.1016/j.janxdis.2009.07.006

Blair, K. S., Geraci, M., Smith, B. W., Hollon, N., Devido, J., Otero, M., . . . Pine, D. S. (2012). Reduced dorsal anterior cingulate cortical activity during emotional regulation and top-down attentional control in generalized social phobia, generalized anxiety disorder, and comorbid generalized social phobia/generalized anxiety disorder. *Biological Psychiatry, 72*(6), 476-482. doi:10.1016/j.biopsych.2012.04.013

Borkovec, T. D. (1994). The nature, functions, and origins of worry. In G. Davey & F. Tallis (Eds.), *Worrying: Perspectives on theory, assessment, and treatment* (pp. 5-33). Sussex, England: Wiley & Sons.

Brett, M., Anton, J.-L., Valabregue, R., & Poline, J.-B. (2002). *Region of interest analysis using an SPM toolbox.* Paper presented at the 8th International Conference on Functional Mapping of the Human Brain, Sendai, Japan.

Broderick, J. E., Schneider, S., Junghaenel, D. U., Schwartz, J. E., & Stone, A. A. (2013). Validity and reliability of patient-reported outcomes measurement information system instruments in osteoarthritis. *Arthritis Care Res (Hoboken), 65*(10), 1625-1633. doi:10.1002/acr.22025

Brown, T. A., Di Nardo, P. A., Lehman, C. L., & Campbell, L. A. (2001). Reliability of DSM-IV anxiety and mood disorders: implications for the classification of emotional disorders. *J Abnorm Psychol, 110*(1), 49-58. doi:10.1037//0021-843x.110.1.49

Bush, K., Kivlahan, D. R., McDonell, M. B., Fihn, S. D., & Bradley, K. A. (1998). The AUDIT alcohol consumption questions (AUDIT-C): an effective brief screening test for problem drinking. Ambulatory Care Quality Improvement Project (ACQUIP). Alcohol Use Disorders Identification Test. *Arch Intern Med, 158*(16), 1789-1795. doi:10.1001/archinte.158.16.1789

Butler, G., Wells, A., & Dewick, H. (1995). Differential Effects of Worry and Imagery After Exposure to a Stressful Stimulus: A Pilot Study. *Behavioural and Cognitive Psychotherapy, 23*(1), 45-56. doi:10.1017/S1352465800017628

Chen, Z., & Calhoun, V. (2018). Effect of Spatial Smoothing on Task fMRI ICA and Functional Connectivity. *Front Neurosci, 12*, 15. doi:10.3389/fnins.2018.00015

Diwadkar, V. A., Re, M., Cecchetto, F., Garzitto, M., Piccin, S., Bonivento, C., . . . Brambilla, P. (2017). Attempts at memory control induce dysfunctional brain activation profiles in Generalized Anxiety Disorder: An exploratory fMRI study. *Psychiatry Research - Neuroimaging, 266*, 42-52. doi:10.1016/j.pscychresns.2017.05.010

El-Gabalawy, R., Mackenzie, C. S., Pietrzak, R. H., & Sareen, J. (2014). A longitudinal examination of anxiety disorders and physical health conditions in a nationally representative sample of U.S. older adults. *Exp Gerontol, 60*, 46-56. doi:10.1016/j.exger.2014.09.012

Etkin, A., Prater, K. E., Hoeft, F., Menon, V., & Schatzberg, A. F. (2010). Failure of anterior cingulate activation and connectivity with the amygdala during implicit regulation of emotional processing in generalized anxiety disorder. *American Journal of Psychiatry, 167*(5), 545-554. doi:10.1176/appi.ajp.2009.09070931

Fonzo, G. A., & Etkin, A. (2017). Affective neuroimaging in generalized anxiety disorder: an integrated review. *Dialogues Clin Neurosci, 19*(2), 169-179.

Fonzo, G. A., Ramsawh, H. J., Flagan, T. M., Sullivan, S. G., Simmons, A. N., Paulus, M. P., & Stein, M. B. (2014). Cognitive-behavioral therapy for generalized anxiety disorder is associated with attenuation of limbic activation to threat-related facial emotions. *Journal of Affective Disorders, 169*, 76-85. doi:10.1016/j.jad.2014.07.031

Goodale, M. A., & Milner, A. D. (1992). Separate visual pathways for perception and action. *Trends Neurosci, 15*(1), 20-25. doi:10.1016/0166-2236(92)90344-8

Goodwin, H., Yiend, J., & Hirsch, C. R. (2017). Generalized Anxiety Disorder, worry and attention to threat: A systematic review. *Clin Psychol Rev, 54*, 107-122. doi:10.1016/j.cpr.2017.03.006

Greenberg, L. S., Goldman, R. N., & American Psychological Association. (2019). *Clinical handbook of emotion-focused therapy* (pp. 1 online resource).

Hazlett, R. L., McLeod, D. R., & Hoehn-Saric, R. (1994). Muscle tension in generalized anxiety disorder: elevated muscle tonus or agitated movement? *Psychophysiology, 31*(2), 189-195. doi:10.1111/j.1469-8986.1994.tb01039.x

Hilbert, K., Lueken, U., & Beesdo-Baum, K. (2014). Neural structures, functioning and connectivity in Generalized Anxiety Disorder and interaction with neuroendocrine systems: a systematic review. *J Affect Disord, 158*, 114-126. doi:10.1016/j.jad.2014.01.022

Hoehn-Saric, R. (1998). Psychic and somatic anxiety: worries, somatic symptoms and physiological changes. *Acta Psychiatr Scand Suppl, 393*, 32-38. doi:10.1111/j.1600-0447.1998.tb05964.x

Hoehn-Saric, R., McLeod, D. R., Funderburk, F., & Kowalski, P. (2004). Somatic symptoms and physiologic responses in generalized anxiety disorder and panic disorder: an ambulatory monitor study. *Arch Gen Psychiatry, 61*(9), 913-921. doi:10.1001/archpsyc.61.9.913

Hoehn-Saric, R., McLeod, D. R., & Zimmerli, W. D. (1989). Somatic manifestations in women with generalized anxiety disorder. Psychophysiological responses to psychological stress. *Arch Gen Psychiatry, 46*(12), 1113-1119. doi:10.1001/archpsyc.1989.01810120055009

Jayaro, C., de la Vega, I., Diaz-Marsa, M., Montes, A., & Carrasco, J. L. (2008). [The use of the International Affective Picture System for the study of affective dysregulation in mental disorders]. *Actas Esp Psiquiatr, 36*(3), 177-182.

Kolesar, T. A., Bilevicius, E., Wilson, A. D., & Kornelsen, J. (2019). Systematic review and meta-analyses of neural structural and functional differences in generalized anxiety disorder and healthy controls using magnetic resonance imaging. *NeuroImage: Clinical, 24*(102016), 1-14. doi:https://doi.org/10.1016/j.nicl.2019.102016

Kolesar, T. A., Kornelsen, J., & Smith, S. D. (2017). Separating neural activity associated with emotion and implied motion: An fMRI study. *Emotion, 17*(1), 131-140. doi:10.1037/emo0000209

Kroenke, K., Spitzer, R. L., & Williams, J. B. (2001). The PHQ-9: validity of a brief depression severity measure. *J Gen Intern Med, 16*(9), 606-613.

Laufer, O., Israeli, D., & Paz, R. (2016). Behavioral and neural mechanisms of overgeneralization in anxiety. *Current Biology, 26*(6), 713-722. doi:10.1016/j.cub.2016.01.023

Llera, S. J., & Newman, M. G. (2010). Effects of worry on physiological and subjective reactivity to emotional stimuli in generalized anxiety disorder and nonanxious control participants. *Emotion, 10*(5), 640-650. doi:10.1037/a0019351

Lyonfields, J. D., Borkovec, T. D., & Thayer, J. F. (1995). Vagal tone in generalized anxiety disorder and the effects of aversive imagery and worrisome thinking. *Behavior Therapy, 26*(3), 457-466. doi:https://doi.org/10.1016/S0005-7894(05)80094-2

Makovac, E., Meeten, F., Watson, D. R., Garfinkel, S. N., Critchley, H. D., & Ottaviani, C. (2016). Neurostructural abnormalities associated with axes of emotion dysregulation in generalized anxiety. *NeuroImage: Clinical, 10*, 172-181. doi:10.1016/j.nicl.2015.11.022

Marchewka, A., Zurawski, L., Jednorog, K., & Grabowska, A. (2014). The Nencki Affective Picture System (NAPS): introduction to a novel, standardized, wide-range, high-quality, realistic picture database. *Behav Res Methods, 46*(2), 596-610. doi:10.3758/s13428-013-0379-1

McClure, E. B., Monk, C. S., Nelson, E. E., Parrish, J. M., Adler, A., Blair, R. J. R., . . . Pine, D. S. (2007). Abnormal attention modulation of fear circuit function in pediatric generalized anxiety disorder. *Archives of General Psychiatry, 64*(1), 97-106. doi:10.1001/archpsyc.64.1.97

McIver, T. A., Kornelsen, J., & Smith, S. D. (2013). Limb-specific emotional modulation of cervical spinal cord neurons. *Cogn Affect Behav Neurosci, 13*(3), 464-472. doi:10.3758/s13415-013-0154-x

McLeod, D. R., Hoehn-Saric, R., & Stefan, R. L. (1986). Somatic symptoms of anxiety: comparison of self-report and physiological measures. *Biol Psychiatry, 21*(3), 301-310. doi:10.1016/0006-3223(86)90051-x

McMeekan, E. R. L., & Lishman, W. A. (1975). Retest reliabilities and interrelationship of the Annett Hand Preference Questionnaire and the Edinburgh Handedness Inventory. *British Journal of Psychology, 66*(1), 53.

Mennin, D. S., Heimberg, R. G., Turk, C. L., & Fresco, D. M. (2005). Preliminary evidence for an emotion dysregulation model of generalized anxiety disorder. *Behav Res Ther, 43*(10), 1281-1310. doi:10.1016/j.brat.2004.08.008

Mochcovitch, M. D., da Rocha Freire, R. C., Garcia, R. F., & Nardi, A. E. (2014). A systematic review of fMRI studies in generalized anxiety disorder: evaluating its neural and cognitive basis. *J Affect Disord, 167*, 336-342. doi:10.1016/j.jad.2014.06.041

Mohlman, J., Eldreth, D. A., Price, R. B., Staples, A. M., & Hanson, C. (2017). Prefrontal-limbic connectivity during worry in older adults with generalized anxiety disorder. *Aging and Mental Health, 21*(4), 426-438. doi:10.1080/13607863.2015.1109058

Nepon, J., Belik, S. L., Bolton, J., & Sareen, J. (2010). The relationship between anxiety disorders and suicide attempts: findings from the National Epidemiologic Survey on Alcohol and Related Conditions. *Depress Anxiety, 27*(9), 791-798. doi:10.1002/da.20674

Norman, S. B., Cissell, S. H., Means-Christensen, A. J., & Stein, M. B. (2006). Development and validation of an Overall Anxiety Severity And Impairment Scale (OASIS). *Depression & Anxiety, 23*(4), 245-249. doi:10.1002/da.20182

Oldfield, R. C. (1971). The assessment and analysis of handedness: the Edinburgh inventory. *Neuropsychologia, 9*(1), 97-113. doi:10.1016/0028-3932(71)90067-4

Osaki, Y., Ino, A., Matsushita, S., Higuchi, S., Kondo, Y., & Kinjo, A. (2014). Reliability and validity of the alcohol use disorders identification test - consumption in screening for adults with alcohol use disorders and risky drinking in Japan. *Asian Pac J Cancer Prev, 15*(16), 6571-6574. doi:10.7314/apjcp.2014.15.16.6571

Ottaviani, C., Watson, D. R., Meeten, F., Makovac, E., Garfinkel, S. N., & Critchley, H. D. (2016). Neurobiological substrates of cognitive rigidity and autonomic inflexibility in generalized anxiety disorder. *Biological Psychology, 119*, 31-41. doi:10.1016/j.biopsycho.2016.06.009

Palm, M. E., Elliott, R., McKie, S., Deakin, J. F. W., & Anderson, I. M. (2011). Attenuated responses to emotional expressions in women with generalized anxiety disorder. *Psychological Medicine, 41*(5), 1009-1018. doi:10.1017/S0033291710001455

Paulesu, E., Sambugaro, E., Torti, T., Danelli, L., Ferri, F., Scialfa, G., . . . Sassaroli, S. (2010). Neural correlates of worry in generalized anxiety disorder and in normal controls: A functional MRI study. *Psychological Medicine, 40*(1), 117-124. doi:10.1017/S0033291709005649

Robinson, J. (2013). Edinburgh Handedness Inventory. In F. R. Volkmar (Ed.), *Encyclopedia of Autism Spectrum Disorders* (pp. 1051-1054). New York, NY: Springer New York.

Ruthotto, L., Kugel, H., Olesch, J., Fischer, B., Modersitzki, J., Burger, M., & Wolters, C. H. (2012). Diffeomorphic susceptibility artifact correction of diffusion-weighted magnetic resonance images. *Phys Med Biol, 57*(18), 5715-5731. doi:10.1088/0031-9155/57/18/5715

Sareen, J., Cox, B. J., Afifi, T. O., de Graaf, R., Asmundson, G. J., ten Have, M., & Stein, M. B. (2005). Anxiety disorders and risk for suicidal ideation and suicide attempts: a population-based longitudinal study of adults. *Arch Gen Psychiatry, 62*(11), 1249-1257. doi:10.1001/archpsyc.62.11.1249

Seghier, M. L. (2013). The angular gyrus: multiple functions and multiple subdivisions. *Neuroscientist, 19*(1), 43-61. doi:10.1177/1073858412440596

Shih, L. Y., Chen, L. F., Kuo, W. J., Yeh, T. C., Wu, Y. T., Tzeng, O. J., & Hsieh, J. C. (2009). Sensory acquisition in the cerebellum: an FMRI study of cerebrocerebellar interaction during visual duration discrimination. *Cerebellum, 8*(2), 116-126. doi:10.1007/s12311-008-0082-4

Spitzer, R. L., Kroenke, K., Williams, J. B., & Lowe, B. (2006). A brief measure for assessing generalized anxiety disorder: the GAD-7. *Arch Intern Med, 166*(10), 1092-1097. doi:10.1001/archinte.166.10.1092

Stein, M. B., & Sareen, J. (2015). CLINICAL PRACTICE. Generalized Anxiety Disorder. *N Engl J Med, 373*(21), 2059-2068. doi:10.1056/NEJMcp1502514

Vrana, S. R., Cuthbert, B. N., & Lang, P. J. (1986). Fear imagery and text processing. *Psychophysiology, 23*(3), 247-253. doi:10.1111/j.1469-8986.1986.tb00626.x

Watson, J. C., Greenberg, L. S., & American Psychological Association. (2017). *Emotion-focused therapy for generalized anxiety*. Washington, DC: American Psychological Association.

White, S. F., Geraci, M., Lewis, E., Leshin, J., Teng, C., Averbeck, B., . . . Blair, K. S. (2017). Prediction Error Representation in Individuals With Generalized Anxiety Disorder During

Passive Avoidance. *Am J Psychiatry, 174*(2), 110-117. doi:10.1176/appi.ajp.2016.15111410

Xu, J., Moeller, S., Auerbach, E. J., Strupp, J., Smith, S. M., Feinberg, D. A., . . . Ugurbil, K. (2013). Evaluation of slice accelerations using multiband echo planar imaging at 3 T. *Neuroimage, 83*, 991-1001. doi:10.1016/j.neuroimage.2013.07.055

4. Chapter 4: Generalized Anxiety Disorder is not just "In Your Head": An fMRI experiment of the Cervical and Thoracic Spinal Cord

Now that the physiological neural underpinnings of GAD have been investigated in the brain in a systematic review/meta-analysis and an fMRI experiment, the attention can shift caudally to the spinal cord. The following section discusses how neural activity differs in the spinal cord in GAD, compared to HC. Both the cervical and thoracic spinal cord are investigated, expanding the GAD literature into this domain for the first time.

4.1 Abstract

While GAD has been investigated in previous fMRI experiments in the brain, further investigation of the CNS has not yet been conducted with neuroimaging. In this first spinal cord fMRI study of GAD, the neural activity in both the cervical and thoracic spinal cord is investigated, providing evidence that GAD is not just a disorder of the mind. Previous research has found increased muscle tension, and reduced ANS flexibility in GAD—both of which can be investigated from a neural perspective. The cervical spinal cord (which innervates the brachial plexus, supplying motor control to the neck and upper limb musculature) and the thoracic cord (which innervate autonomic ganglia) are thus key targets of the CNS in the current study. 16 patients with GAD and 14 HC participated in an emotion-based spinal fMRI study, identical (apart from the imaging methods) to that described in Chapter 3. Results indicate that generally, patients with GAD showed greater activity in response to threat than controls in the cervical and thoracic spinal cord. Specifically, patients with GAD had greater activity in left ventromedial C1/C2, left dorsal C2, right ventral C3, and left C3/C4 spanning ventral and dorsal regions, indicating a possible role of increased muscle tension and sensory feedback of this tension in the neck and shoulders. In the thoracic cord, patients with GAD showed increased ventral activity, particularly in T5-T7 and T10-T12. Importantly, these regions also included mediolateral activity, corresponding to autonomic innervation of the gut and adrenal medulla. These results align with previous behavioural and downstream ANS function measures, which helps to validate the use of this technology in patients with mental health disorders.

4.2 Introduction

GAD is a highly prevalent anxiety disorder characterized by chronic, excessive worry. GAD presents most frequently in females (Stein & Sareen, 2015), increases the risk of suicide ideation (Nepon, Belik, Bolton, & Sareen, 2010; Sareen et al., 2005), and some physical (Butnoriene et al., 2015; Culpepper, 2009; El-Gabalawy, Mackenzie, Pietrzak, & Sareen, 2014; Marrie et al., 2019), and mental health disorders (Moffitt et al., 2007).In addition to the mental anguish and reduced quality of life associated with GAD, physical symptoms are also required for a diagnosis to be made. In addition to having excessive, uncontrollable worry for a minimum of 6 months, a patient with GAD must also exhibit at least three of the following symptoms more often than not over the same time period: restlessness, fatigue, insomnia, difficulty concentrating, irritability, and/or muscle tension (American Psychiatric Association, 2013). Importantly, somatic symptoms are often what drives patients with GAD to seek medical treatment—in particular, headaches, gastrointestinal upset, or back pain (Stein & Sareen, 2015). Increased muscle tension, which can be measured objectively, has been shown in patients with GAD compared to HC using EMG recordings (Hazlett, McLeod, & Hoehn-Saric, 1994; Hoehn-Saric, McLeod, & Zimmerli, 1989; McLeod, Hoehn-Saric, & Stefan, 1986). This objective measure is an important metric as patients with GAD do not always have accurate insight into their physiological experiences (McLeod et al., 1986). Often, this muscle tension is observed in the head or neck (Malmo & Shagass, 1949a; Sainsbury & Gibson, 1954), making the cervical spinal cord an excellent candidate for study as this tissue is innervated by this region of the spinal cord.

While this disorder clearly affects the whole being, much of the physiological data for GAD are either inconsistent, or differ from expectations. Although it may seem logical that patients with GAD would have a chronically upregulated SNS response, the data are inconsistent. For example, although it may seem reasonable to hypothesize that these highly anxious individuals may have increased levels of stress hormones, this is not consistently observed in GAD. Research of stress hormones such as epinephrine and norepinephrine (Gerra et al., 2000; Mathew, Ho, Kralik, Taylor, & Claghorn, 1981; McLeod, Hoehn-Saric, Zimmerli, De Souza, & Oliver, 1990; Munjack et al., 1990) or cortisol (Alfano, Reynolds, Scott, Dahl, & Mellman, 2013; Gerra et al., 2000; Hek et al., 2013; Hilbert, Lueken, Muehlhan, & Beesdo-Baum, 2017; Hoehn-Saric, McLeod, Lee, & Zimmerli, 1991; Hood et al., 2011; Lenze et al., 2011; Mantella et al., 2008; Rosnick, Rawson, Butters, & Lenze, 2013; Steudte et al., 2011; Tafet et al., 2001) yields variable results in

GAD. However, serotonin results may be more consistent and various concentrations and receptor properties have been demonstrated to affect treatment success in GAD (Baldwin & Rudge, 1995; Hilbert, Lueken, & Beesdo-Baum, 2014; Lenze et al., 2010; Lohoff et al., 2013; Stein & Sareen, 2015; Tafet et al., 2001).

Although patients with GAD may be expected to have increased heart rate, as this is a common SNS response to stress, this too has not been consistently observed, sometimes showing no change in heart rate for chronic worriers at baseline, or after actively worrying (Borkovec, Robinson, Pruzinsky, & DePree, 1983), but sometimes showing increased heart rate measured throughout the day (Hoehn-Saric, McLeod, Funderburk, & Kowalski, 2004), or following mentally taxing activities (Gerra et al., 2000). However, heart interbeat interval (i.e., the amount of time between one beat and the next), which indicates parasympathetic tone and cardiovascular variability, has been shown to have less variance in GAD, indicating parasympathetic inflexibility (Aldao & Mennin, 2012; Hoehn-Saric et al., 2004; Hoehn-Saric et al., 1989; Llera & Newman, 2010; Lyonfields, Borkovec, & Thayer, 1995; Monk et al., 2008). Providing further evidence of autonomic inflexibility in GAD are a couple studies in which reduced variability in mean skin conductance is observed (Hoehn-Saric et al., 2004; Hoehn-Saric et al., 1989). Investigation into the role of the ANS in GAD is important, and can now be investigated using fMRI of the spinal cord.

Previous fMRI studies have been done to investigate the neural correlates of GAD (see Chapters 2 and 3), but this study has not yet extended to the spinal cord. Spinal fMRI provides another metric for investigating the muscle tension observed in GAD from a neural perspective, as well as allow a non-invasive and more direct investigation of the ANS, as compared to the downstream actions (such as circulating hormone concentrations or heart rate variability) of the ANS. In the past 20 years, spinal fMRI technology has been developed and fine-tuned to measure neural activity throughout the spinal cord (Kornelsen et al., 2013; Kornelsen & Stroman, 2004; Powers, Ioachim, & Stroman, 2018; Stroman, Krause, Malisza, Frankenstein, & Tomanek, 2002; Stroman et al., 2014; Wheeler-Kingshott et al., 2014; Yoshizawa, Nose, Moore, & Sillerud, 1996). Studies on patient populations have been limited to neurological injury or disease such as spinal cord injury, fibromyalgia, cervical spondylotic myelopathy or multiple sclerosis (Powers et al., 2018).

Although much spinal fMRI research has been conducted on sensory and motor tasks, the role of emotion has also been investigated in the cervical (McIver, Kornelsen, & Smith, 2013; Smith, Kolesar, & Kornelsen, 2018; Smith & Kornelsen, 2011; Wilson, Kolesar, Kornelsen, & Smith, 2018) and thoracic spinal cord (Kornelsen, Smith, & McIver, 2015). In the first spinal fMRI emotion study, Smith and Kornelsen (2011) used emotion-evoking or neutral images paired with both passive viewing and active motor tasks. The negative passive-viewing condition resulted in left dorsal and right ventral spinal cord between C3 and C5—interestingly, the negative-motor condition showed a similar activation pattern in the ventral cord, but had a greater spatial extent than the passive condition. The authors concluded that the emotion portrayed in the stimuli primes areas in the spinal cord related to movement (Smith & Kornelsen, 2011). Interestingly, both positive and neutral stimuli also produced significant neural activity, but in an opposite pattern to the negative stimuli. These results indicate that emotion not only primes the ventral spinal cord for movement, but it primes it differentially based on the type of emotional input (Smith & Kornelsen, 2011). In addition, further work on the topic showed that emotion-evoking images depicting upper limbs elicit greater activity in the cervical spinal cord than emotion-evoking images depicting lower limbs, which suggests that this "emo-motoric" response is limb-specific as well (McIver et al., 2013).

Stemming from this research, Kornelsen et al. (2015) imaged the thoracic spinal cord while participants viewed emotion-evoking stimuli to look indirectly at the resulting visceral activity. A negative emotion-evoking motor condition resulted in activity throughout the regions associated with autonomic innervation, while the negative emotion-evoking passive condition again showed neural thoracic activity, in the absence of a motor command, while neutral conditions were much less active (Kornelsen et al., 2015). This prior work provides evidence that passively-viewed emotion-evoking images can be used to elicit neural responses in the cervical and thoracic spinal cord, in the absence of motor responses. Additionally, the ANS itself can now feasibly be imaged in the spinal cord. Thus, we can investigate the neural correlates of muscle tension and ANS function in the cervical and thoracic spinal cord, respectively, in GAD, in response to threat. This is the first study of its kind investigating neural differences in those with a mental health disorder compared to those without in the spinal cord. As a result, this is the first paper reporting neural activation differences in GAD, occurring outside of the brain.

4.3 Methods

4.3.1 Participants

This study consisted of two participants groups: group 1 pilot-tested 300 neutral and negative emotion-evoking images to develop a stimulus set and group 2 passively viewed a subset of these images during the fMRI experiment. The pilot-testing group consisted of 40 participants (mean age 33.6±13.4, 29 female, 11 male), although one participant discontinued participation over halfway through. The fMRI group consisted of 18 participants with GAD and 14 HC—age- and sex-matching were performed (± 5 years), although scanning was cut short due to the COVID-19 pandemic, leaving two unmatched GAD participants. Data from one patient in the fMRI group were excluded from analysis due to technical difficulties during acquisition while another patient dataset was excluded due to excessive motion, resulting in 16 GAD participants (13 females, 34.3 ± 12.7 years, 14 right-handed, 2 ambidextrous) and 14 HC (12 females, 35.6 ± 13.3 years, 12 right-handed, 2 ambidextrous) for the cervical analysis. Four additional participants (two with GAD and two HC) were excluded from the thoracic analysis as all four of these thoracic spines were found to be scoliotic and spatial normalization was not possible, resulting in 14 GAD participants and 12 HC participants. Patients were recruited from the Comorbidity, Cognition and Multiple Sclerosis (C-COMS, $n = 5$) study, the University of Manitoba and its affiliated hospitals ($n = 8$), and from the community ($n = 5$) in Winnipeg, Canada. All participants were screened for eligibility: participants were excluded if they were < 18 years old, unable to provide informed consent, unable to complete the questionnaires in English, had a history of neurological disorder (e.g., Tourette's syndrome, multiple sclerosis, Alzheimer's disease, dementia, disease or injury of the brain or spinal cord, including concussion resulting in loss of consciousness, and spinal cord injury or disease), or known scoliosis, MRI contraindications including pregnancy and claustrophobia, and a history of mood or anxiety disorders in the HC group. Additionally, participants with GAD had to have maintained their treatment program, medication or medication doses for a minimum of 60 days prior to enrollment and throughout participation.

Most patients (13/16) had received prior GAD diagnoses from a health professional and had the following comorbidities: 4 MDD, 1 pervasive depressive disorder [PDD] with current MDD episode, 1 PDD without current MDD episode, 5 SAD, 2 PD with agoraphobia, 1 PD without agoraphobia, 2 OCD, and were on the following medications (Escitalopram = 2; Sertraline = 1;

Desvenlafaxine = 1; Bupropion = 2; Amitriptyline = 1; cannabis = 4). One HC was taking Zopiclone, as needed after night shift work and two HC participants used cannabis recreationally.

All participants were interviewed using the diagnostic and statistical manual, 4th edition criteria (DSM-IV-TR) structured clinical interview, which has good reliability for GAD (Brown, Di Nardo, Lehman, & Campbell, 2001) used to identify mood and anxiety disorders. Interviews were conducted by a graduate student (TAK), trained by a clinical psychologist (Dr. John Walker) with extensive experience with the SCID interview. Training included detailed review of the SCID modules, observing SCID interviews, and role-playing interviews with the instructor and other trainees. Ethical approval for this study was acquired from the University of Manitoba and St. Boniface Hospital Research Ethics Boards. Participants received $25 for their time.

4.3.2 Stimuli

As reported previously, stimuli consisting of neutral and negative emotion-evoking images taken from standardized image sets including the International Affective Picture System (Jayaro, de la Vega, Diaz-Marsa, Montes, & Carrasco, 2008) and the Nencki Affective Picture System (Marchewka, Zurawski, Jednorog, & Grabowska, 2014) as well as from internet searches were balanced for implied motion, an important consideration for emotion work (Kolesar, Kornelsen, & Smith, 2017; Lima Portugal et al., 2020). Three hundred images were rated on valence (i.e., how neutral or negative an image made the rater feel), physiological arousal (i.e., how calm or excited an image made the rater feel), and implied motion (i.e., how much motion is occurring, or is about to occur in the image) by a different participant group of forty individuals (see Chapter 3). A subset of images consisting of 252 images was used in the MRI task and were chosen to have the greatest difference in valence, while minimizing differences between implied motion and arousal; however, it was not possible to completely control for physiological arousal in the stimuli. Valence and arousal ratings significantly differed in the negative and neutral conditions (valence: negative = 5.0 ($\pm$0.7), neutral = 1.5 ($\pm$0.3), $t(250) = -50.6$, $p < 0.001$; arousal: negative = 4.6 ($\pm$0.5), neutral = 3.0 ($\pm$0.8), $t(250) = -18.9$, $p < 0.001$) while implied motion did not (negative = 3.8 ($\pm$1.0), neutral = 3.7 ($\pm$1.1), $t(250) = -0.9$, $p = 0.376$), as reported in Chapter 3. During scanning, images were displayed on a rear-projection display. Three counterbalanced cervical runs were followed by three counterbalanced thoracic runs: each run consisted of alternating negative and neutral blocks (3 x 24 s blocks for each valence, with each block including 6 images, shown for 4 s each),

interleaved by fixation intervals (7 s). Within each block, images with appropriate valence were randomized.

4.3.3 Task

After obtaining informed consent, participants completed questionnaires. After the collection of brain data (Chapter 3), task-based fMRI data was collected from the cervical, followed by the thoracic spinal cord. As in the brain task, participants passively viewed blocks of negative emotion-evoking images and alternated with blocks of neutral images. Each block lasted 24 seconds, consisting of 6 images, randomly presented and each shown for 4 seconds (see

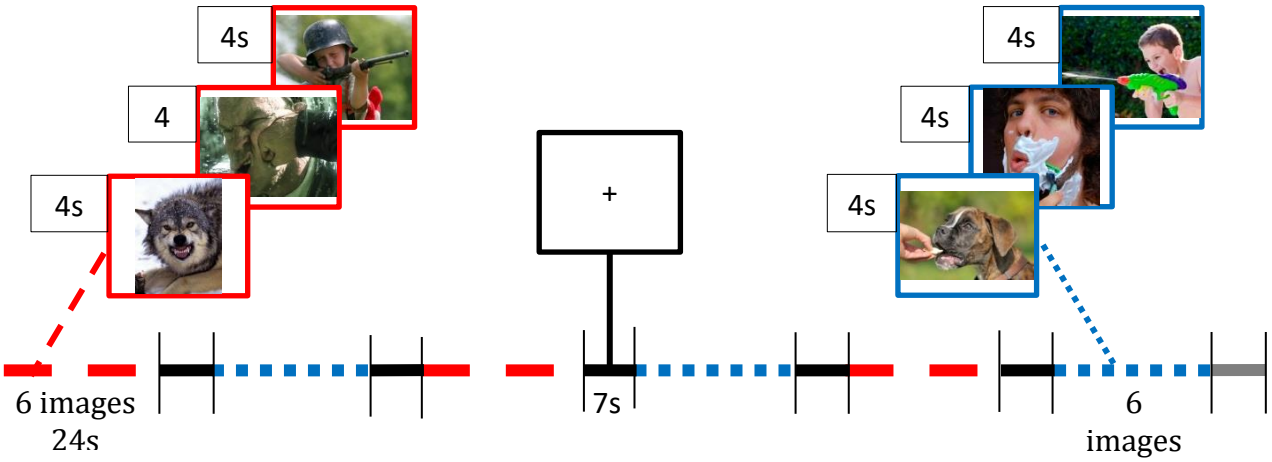

Figure 3.1: Task). Three negative and three neutral blocks were viewed, interleaved by a 7 second fixation cross (the duration of the fixation cross was chosen so that one full volume of fixation was collected between blocks). The purpose of the fixation cross was to prevent habituation to continuously viewing images, while also conceptually separating negative and neutral blocks. The final fixation cross differed in duration across the brain and spinal cord (6 s in the brain, 3 s in the spinal cord) to use up the remaining time for each scan, while ensuring the time spent viewing stimulus pictures was consistent across runs. Thirty-six images (18 negative, 18 neutral) were viewed per run for a total of 216 unique images across the 6 spinal cord runs. Runs were counterbalanced within each region so that the same stimulus images were presented (although not in the same order) while each spinal cord region was scanned.

4.3.4 Questionnaires

Prior to scanning, several questionnaires were administered including: sociodemographic information, the GAD-7 (Cronbach $\alpha = 0.92$; intraclass correlation of 0.83 for test-retest reliability; Spitzer, Kroenke, Williams, & Lowe, 2006), OASIS (Cronbach $\alpha = 0.80$, $\kappa = 0.82$; Norman,

Cissell, Means-Christensen, & Stein, 2006), PHQ-9 (Cronbach α between 0.86 and 0.89; Kroenke, Spitzer, & Williams, 2001), AUDIT-C (Bush, Kivlahan, McDonell, Fihn, & Bradley, 1998; Cronbach α = 0.98, intraclass correlation = 0.95; Osaki et al., 2014), EHI (test-retest reliability coefficient 0.75 to 0.86; McMeekan & Lishman, 1975; Oldfield, 1971), PROMIS PI-8a (intraclass correlation = 0.87 in general population; Broderick, Schneider, Junghaenel, Schwartz, & Stone, 2013), and VAS scales. The self-report symptoms measures are well validated measures with strong psychometric properties. The VAS scales asked participants how anxious they were in the current moment from 1 (no anxiety) to 100 (worst anxiety imaginable) prior to entering the MRI suite (VAS1), after the brain task, but before the cervical runs (VAS2), between cervical and thoracic runs (VAS3), and following thoracic runs (VAS4) were among them (see Table 4.1). After the VAS4 was administered (following MRI completion), participants rated a subset of the images used in the fMRI experiment to investigate whether GAD and HC groups would subjectively rate the images differently (see Table 3.2). Scores for the GAD-7, OASIS, PHQ-9, and AUDIT-C questionnaires were summed, according to scoring instructions. As per the scoring instructions, scores from the PI-8a were normalised to a T-score metric; the mean score is 50 from a general US reference population, with a standard deviation of 10 points (http://www.healthmeasures.net/images/PROMIS/manuals/PROMIS_Pain_Interference_Scoring_Manual.pdf). Scores for the EHI were calculated as follows: ((R-L)/(R+L))*100, where R = the number of '+' symbols in the right-hand column, and L = the number the '+' symbols in the left-hand column (Robinson, 2013).

4.3.5 MRI Data Acquisition

Cervical and thoracic spinal cord fMRI data were acquired using 8-channel head, neck, and spine coils on a Siemens Magnetom Trio 3T whole-body MRI system (Erlangen, Germany). A half-Fourier acquisition single-shot turbo spin-echo (HASTE) sequence was used to preserve spatial fidelity and BOLD sensitivity, with the following parameters: TR = 6.75 sec/volume, TE = 79 ms, 27 volumes per run (3 runs were acquired from the cervical cord, and 3 from the thoracic cord), 9 slices with 2 mm thickness, excitation pulse flip angle = 90°, refocussing pulse flip angle = 100°, FOV = 280 mm x 210 mm, 5/8 phase partial Fourier, resolution 1.50 mm x 1.50 mm x 2.00 mm (see Appendix A for full scanning parameters). This yielded T2-weighted images with sufficient contrast and signal to acquire anatomical and functional data simultaneously. To reduce

SAR limitations, no saturation bands were applied, and the hyperecho option provided by Siemens was turned off.

4.3.6 fMRI Preprocessing and Analyses

Cervical and thoracic fMRI data were preprocessed and analysed using custom-written MATLAB® software (spinalfmri9; Bosma & Stroman, 2014; Leitch, Figley, & Stroman, 2010; Powers et al., 2018; Stroman, 2016). First, data were converted from DICOM to NIfTI format and then co-registered to correct for bulk motion using the non-rigid 3D registration tool in the Medical Image Registration Toolbox (MIRT; Myronenko & Song, 2009, 2010). Automatic spatial normalization was then conducted: brainstem and cervical data were transformed to a brainstem/cervical template, consisting of data from 356 data sets, acquired using a HASTE sequence. Thoracic data were spatially normalized using the PAM50 spinal cord template. Importantly, cervical data were normalized first and this data was then used to guide the normalization of the thoracic cord from the same participant. After spatial normalization, data were run through a first-level general linear model (GLM) fit to a model based on the timing of the negative blocks (+1) and convolved with the canonical hemodynamic response function—neutral and fixation blocks were not modelled. Physiological noise, signal variations in WM, and bulk motion effects were also modeled in the GLM. During this stage, the three cervical runs were concatenated and the three thoracic runs were concatenated. A second-level analysis was then conducted comparing GAD and HC groups at $p < 0.001$. For correction for multiple comparisons, clusters containing fewer than 5 voxels were excluded.

4.4 Results

Demographic details can be found in Table 4.1. Ratings for VAS scores were significantly different following collection of brain data (Chapter 3) and immediately prior to the cervical runs (VAS2), between cervical and thoracic runs (VAS3), and at the completion of scanning (VAS4).

Table 4.1: Demographic details of GAD and HC groups.

	GAD	**HC**	***t*-value**	***p*-value**
N	16	14		
Female/Male	13/3	12/2		
Mean age	34.3 (± 12.7)	35.6 (± 13.3)	-0.26	0.793
Mean symptom duration (years)	18.5 (± 13.0)			

Comorbidities				
MDD	4	0		
PDD, with current MDD episode	1	0		
PDD, without current MDD episode	1	0		
SAD	5	0		
PD, with agoraphobia	2	0		
PD, without agoraphobia	1	0		
OCD	2	0		
Mean education years	15.8 (± 2.8)	16.3 (± 2.0)	-0.53	0.603
Less than high school	0	0		
High school/GED	6	1		
Technical/Trade	1	4		
College	1	1		
Bachelor's degree	7	6		
Master's degree	1	2		
Employment				
Management	1	0		
Business, finance, and administration	3	0		
Health	2	7		
Education, law and social, community/government service	4	1		
Trades, Transport or Equipment operator and related occupations	1	2		
Natural resources, agriculture, and related production	0	0		
Sales and service	2	0		
Art, culture, recreation and sport	1	1		
Manufacturing and utilities	0	0		
Other—Student	1	2		
Other—Science, R&D	1	1		
Marital status				

Married/common law	8	7		
Widowed/separated/divorced	1	0		
Single, never married	7	7		
Household income				
0-$14,999	0	0		
$15,000-$29,999	3	0		
$30,000-$49,999	1	0		
$50,000-$100,000	6	8		
>$100,000	6	6		
AUDIT-C	2.8 (± 1.8)	2.9 (±1.9)	-0.066	0.948
Recreational Drug Use				
Yes (all cannabis)	4	2		
No	12	12		
Medications				
Escitalopram	2	0		
Sertraline	1	0		
Desvenlafaxine	1	0		
Bupropion	2	0		
Amitriptyline	1	0		
Zopiclone	0	1		
GAD-7	11.6 (± 4.4)	1.6 (± 2.6)	7.47	<0.001
OASIS	8.9 (± 3.2)	1.6 (± 2.3)	6.94	<0.001
PHQ-9	9.1 (± 5.4)	1.3 (± 1.9)	5.12	<0.001
PI-8a	55.5 (± 6.0)	43.1 (± 5.1)	6.08	<0.001
EHI	68.9 (± 31.0)	69.2 (± 37.7)	-0.025	0.980
VAS1	18.5 (± 20.6)	12.6 (± 19.8)	0.79	0.436
VAS2	25.3 (± 21.8)	7.7 (± 13.3)	2.62	0.014*
VAS3	31.2 (± 24.8)	8.9 (± 12.3)	3.06	0.005*
VAS4	23.9 (± 27.0)	3.8 (± 6.8)	2.70	0.012*

'*' indicates significance at $p < 0.05$. Visual Analog Scales (VAS) were administered throughout the experiment. MDD = major depressive disorder, PDD = persistent depression disorder, SAD =

social anxiety disorder, PD = panic disorder, OCD = obsessive compulsive disorder. VAS1 = current moment anxiety score (0 = no anxiety, 100 = worst anxiety imaginable) just before entering the MRI suite; VAS2 = anxiety score after brain, but before cervical spinal cord task; VAS3 = anxiety score after cervical, but before thoracic spinal cord task; VAS4 = anxiety score after thoracic cord scanning. AUDIT-C = Alcohol Use Disorders Identification Test-Concise; GAD-7 = Generalized Anxiety Disorder 7-Item Scale; OASIS = Overall Anxiety Severity and Impairment Scale; PHQ-9 = Patient Health Questionnaire 9-Item Scale; PI-8a = Pain Interference Short Form 8a; EHI = Edinburgh Handedness Inventory.

4.4.1 Spinal Cord fMRI Results

Results from the cervical spinal cord fMRI data can be seen in Table 4.2 and Figure 4.1. Generally, patients with GAD had greater activity than HC throughout the cervical cord. Five large clusters in particular can be observed as greater for patients with GAD spanning from C2-C5: left ventromedial and left dorsal C2, right ventral, and left dorsal to ventral C3/C4, and left ventromedial C5. By far, the largest cluster with the greatest rostral-caudal spread is in left C3/C4 (consisting of 104 voxels), spanning from dorsal, to medial, to ventral regions.

Similar to the cervical cord results, patients with GAD generally had greater thoracic activity than HC, occurring largely in T5-T7 and T10-T12 (see Table 4.3 and Figure 4.2). Several large clusters of note include right dorsal to ventral T5, ventral/mediolateral T5/T6, left/medial T6/T7 spanning dorsal through ventral regions, right ventral T10/T11 and right ventral T11/T12. Importantly, several significant clusters were observed in the mediolateral horn: patients with GAD had greater mediolateral activity in T3, T5-T7, and T9-T11, while HC's had greater activity in mediolateral T4, T7, T8, and T10-T12. While both groups had similar numbers of mediolateral clusters (GAD: 9; HC: 7), two important features differed. First, the mediolateral clusters in GAD were larger in size (ranging from 7 to 77 voxels, mean cluster size [$\pm$ SD] = 25.9 $\pm$ 23.8 voxels) and spatial extent than those of the HC group (ranging from 6 to 19 voxels, mean cluster size = 9.7 $\pm$ 3.5 voxels). Second, while the GAD clusters were larger, they also included many more ventral voxels within the same cluster, compared to the more distinct HC mediolateral clusters.

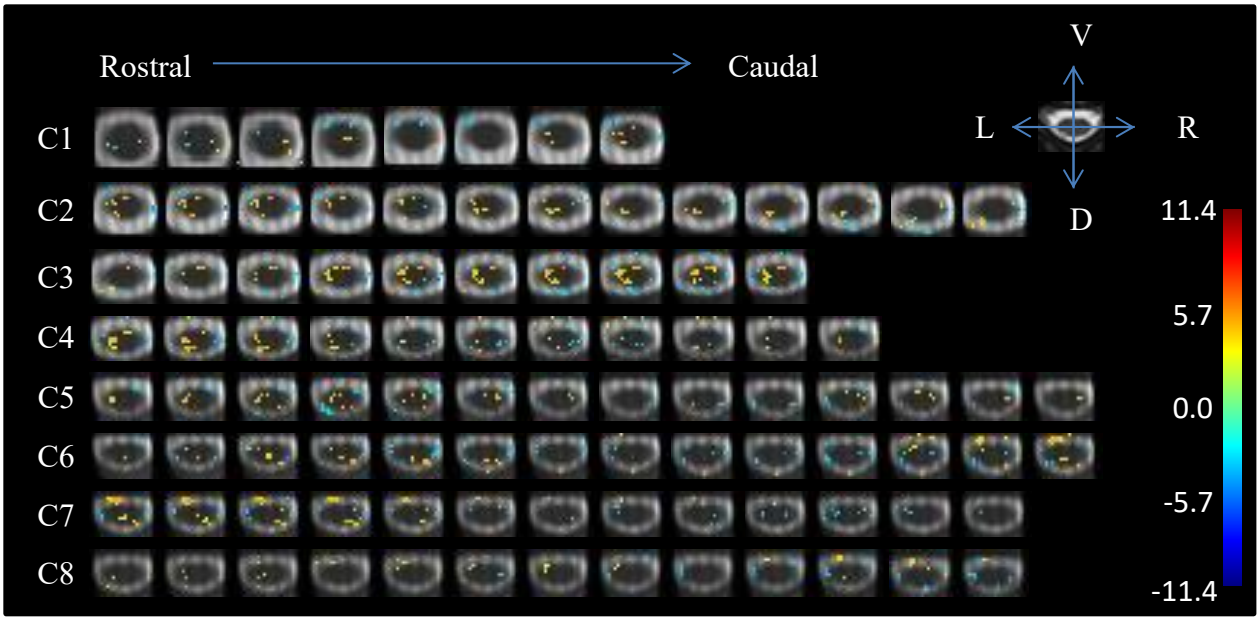

Figure 4.1: Cervical spinal cord fMRI results for the GAD > HC contrast. Results are tested at $p < 0.001$. V = ventral, D = dorsal, L = left, R = right; each slice can be viewed in neurological orientation.

Table 4.2: Cervical spinal cord activity differences between GAD and HC. Results are at $p < 0.001$, with a cluster extent threshold of 5 voxels. Where clusters span multiple segments, the voxels per segment are specified.

Segment	Side	Dorsal/Ventral	Voxels	Voxels/Region	Dermatomes (Sensory)	Myotomes (Motor)
Generalized Anxiety Disorder > Healthy Control						
C2	Left	Dorsal	8	3 C1 + 5 C2	Back of head	Neck (anterior, posterior), trapezius
	Right	Ventral	11	1 C1 + 10 C2		
	Left	Ventromedial	28	5 C1 + 23 C2		
	Left	Dorsal	27			
	Right	Ventral	7			
C3	Right	Ventral	30	26 C3 + 4 C4	Neck, trapezius	Posterior/lateral neck, trapezius, deltoids
	Left	Dorsal/Medial/ Ventral	104	68 C3 + 36 C4		
C4	Right	Ventromedial	6		Neck, trapezius, deltoids, pectorals	Neck, diaphragm, trapezius, deltoids
C5	Left	Medial/Ventral	19	3 C4 + 16 C5		Deltoid, biceps, brachioradialis, extensor carpi radialis
	Right	Ventromedial	7			
	Right	Ventromedial	8			
C6	Medial	Dorsal	12		Upper back,[1] biceps, triceps, brachioradialis, pronator teres/quadratus, thenar muscle, abductor/flexor	
	Right	Dorsal	8			

					pollicis longus, flexor digitorum profundus	
C7	Medial	Dorsal	8	3 C6 + 5 C7	Biceps, triceps, brachioradialis, pronator teres/quadratus, extensor carpi ulnaris, abductor/flexor pollicis longus, extensor digitorum, flexor digitorum profundus	
	Right	Dorsal	17	1 C6 + 16 C7		
C8	Left	Ventral	9			Pectoralis major, teres minor/ major, latissimus dorsi, triceps, flexor carpi radialis, flexor/extensor carpi ulnaris, extensor/flexor/abductor pollicis longus, thenar muscle, extensor digitorum, flexor digitorum profundus
Healthy Controls > Generalized Anxiety Disorder						
C1	Right	Ventral	6			Neck, trapezius
C4	Right	Medial	8	3 C3 + 5 C4	Neck, trapezius, deltoid, upper pectorals	
	Right	Dorsal	10			
C5	Right	Dorsomedial	5		Neck, deltoid, biceps	

C6	Right	Dorsomedial	10	Upper back,[1] biceps, triceps, brachioradialis, pronator teres/quadratus, thenar muscle, abductor/flexor pollicis longus, flexor digitorum profundus	Deltoid, biceps, pectorals, teres minor/major, latissimus dorsi, triceps, extensor carpi radialis, pronator teres/ quadratus
	Right	Ventromedial	7		
	Left	Dorsomedial	14		
C7	Left	Ventromedial	10		Deltoid, biceps, pectorals, teres minor/major, latissimus dorsi, triceps, extensor carpi radialis, pronator teres/ quadratus, flexor/extensor carpi ulnaris, extensor digitorum
C8	Left	Medial	14		

Note that the dermatomes (sensory innervations of the tissues) have been described in terms of the approximate muscles that they overlay for a simpler comparison with myotome innervation. Dermatome data is derived from (Lee, McPhee, & Stringer, 2008) and (Downs & Laporte, 2011) or (Head & Campbell, 1900) where indicated by '1', while myotome information is from (Brendler, 1968).

Table 4.3: Thoracic spinal cord activity differences between GAD and HC. Results are at $p < 0.001$, with a cluster extent threshold of 5 voxels. Where clusters span multiple segments, the voxels per segment are specified.

Segment	Side	Dorsal/Ventral	Total Voxels	Voxels per Region
Generalized Anxiety Disorder > Healthy Control				
T1	Left	Dorsal	6	
	Medial/Right	Dorsal/Medial/Ventral	6	
T2	Left	Dorsal	27	
T3	Left	Ventral/Mediolateral	12	
	Right	Dorsal	13	
T4	Left	Dorsal	8	
T5	Right/Medial	Dorsal/Medial/Ventral	86	
	Right	Ventral/Mediolateral	10	
T6	Medial/Left	Ventral/Mediolateral	51	20 T5 + 31 T6
	Right	Mediolateral	7	3 T5 + 4 T6
	Right	Mediolateral	8	
	Medial	Dorsal	8	
	Left/Medial	Ventral/Mediolateral	77	48 T6 + 29 T7
T7	Right	Dorsal	31	4 T6 + 27 T7
	Medial	Dorsal	13	
	Right/Medial	Ventromedial	19	
T8	Right/Medial	Dorsal	14	3 T7 + 11 T8
	Right/Medial/Left	Ventral	20	
	Right	Dorsomedial	9	
T9	Right/Medial	Dorsal	7	3 T8 + 4 T9
	Right/Medial	Ventral/Mediolateral	17	
T10	Right	Mediolateral/Dorsal	19	
	Left	Mediolateral	32	24 T10 + 8 T11
	Medial	Ventral	69	43 T10 + 26 T11

T12	Right/Medial/Left	Ventral	57	3 T11 + 54 T12
	Medial	Dorsal	9	
Healthy controls > Generalized Anxiety Disorder				
T1	Left	Ventral	6	
T2	Right	Dorsal/Medial	9	
T3	Medial	Medial	5	
T4	Left	Mediolateral	16	
T5	Left	Dorsal	5	1 T4 + 4 T5
T7	Right	Mediolateral	11	
	Left	Mediolateral	6	
T8	Left	Ventral	10	1 T7 + 9 T8
	Left	Mediolateral/Dorsal	8	
T9	Medial	Dorsal	5	
T10	Left	Mediolateral	6	
T11	Left	Dorsal/mediolateral	11	
T12	Right	Dorsomedial	19	
	Right	Mediolateral	10	

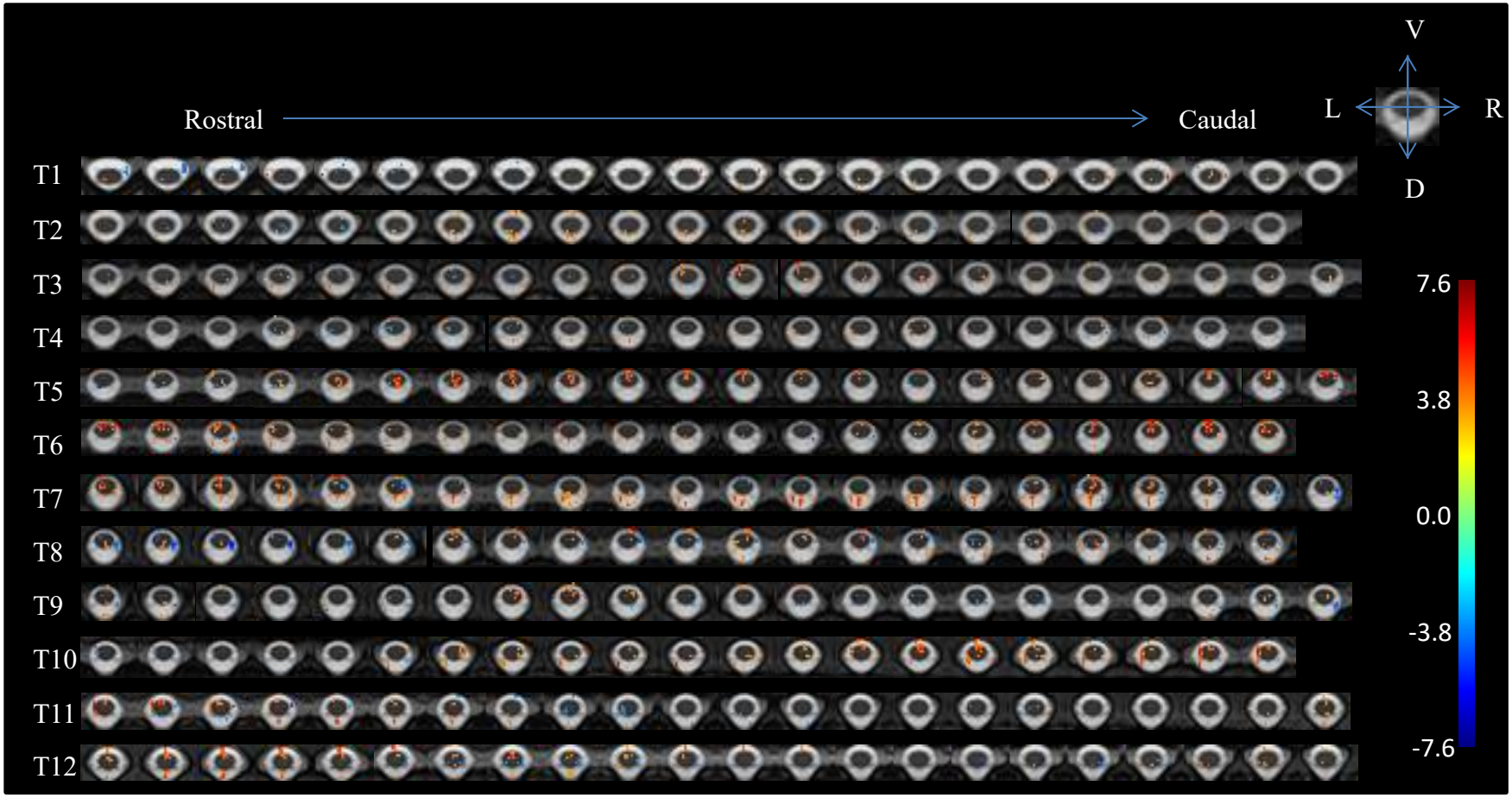

Figure 4.2: Thoracic spinal cord fMRI results for the GAD > HC contrast. Results are at $p < 0.001$. Segments go from rostral to caudal, left to right across the page. V = ventral, D = dorsal, L = left, R = right; each segment piece can be viewed in neurological orientation.

4.5 Discussion

Interestingly, for both cervical and thoracic analyses, patients with GAD had greater neural activity than HC, in general. In the cervical cord, these results included patients with GAD having greater activity throughout C2-C5, with the majority of the increased activity occurring in C3/C4. Both C2 and C3/C4 regions had dorsal and ventral activity, possibly indicating a motor response, and an associated sensory feedback response. However, this can only be speculated presently as individual spinal cord pathways cannot be determined from activation maps. In any case, ventral activity throughout C2 to C4 corresponds to myotomes in the neck, trapezius and deltoids (Brendler, 1968), and likely indicates greater muscle tension in these regions in GAD compared to HC, for negative compared to neutral stimuli. The dorsal activity likewise corresponds to the regions of the neck and trapezius areas, perhaps indicating sensory feedback to increased muscle tension.

Importantly, 9/16 patients with GAD reported muscle tension in the week leading up to their MRI visit on their GAD-7 questionnaires, compared to 1/14 HCs. These behavioural differences are likely responsible for the increased upper cervical spinal cord activity. However, this is not a shortcoming, for several reasons: first, this symptom of muscle tension provides some of the basis for investigating the spinal cord in GAD. Second, these results are from a contrast comparing the differences between GAD and HC groups, after comparing negative emotion-evoking responses to a neutral baseline at the first-level. Thus, this work provides neural evidence of increased muscle tension, to complement early studies showing increased muscle tension in GAD (Hazlett et al., 1994; Hoehn-Saric et al., 1989; McLeod et al., 1986). The location of activity is interesting as well: the ventral activity in C2-C5 corresponds to myotomes innervating the neck, trapezius muscles, and deltoids, a common place for muscle tension to be observed in anxious populations, and can be associated with headache (Malmo & Shagass, 1949a, 1949b; Sainsbury & Gibson, 1954), another common symptom in GAD (Stein & Sareen, 2015). Travelling further down the spinal cord to the thoracic region, dorsal activity in T2 and T3 corresponds to dermatomes overlying the pectorals and back between the shoulders. Several large clusters in T5-T7 and T10-T12 include mostly medial ventral activity, which correspond to the musculature of the chest (T5-T7) and abdomen (T10-T12)—because the thoracic spinal cord innervates the axial musculature, it perhaps is not surprising that this ventral activity is seen medially as the

corticospinal tract often synapses on interneurons in Rexed laminae VIII (Ralston & Ralston, 1985).

Notably, much of the activity observed for either GAD or HC groups occurred in the mediolateral horn of the thoracic cord—corresponding to the SNS. The greater splanchnic nerve, consisting of preganglionic fibres from T5-T9 (and sometimes T10) is responsible for regulating blood pressure (Bapna, Adin, Engelman, & Fudim, 2019; Loukas et al., 2010) and the enteric nervous system (Loukas et al., 2010). The GAD group had increased mediolateral activity throughout this region, particularly in T5 and T6, and T9 and T10. These results are not surprising, given the digestive and bowel complaints commonly described by patients with GAD (Stein & Sareen, 2015). Furthermore, this may prove important in the context of increased comorbidity with gastrointestinal disease (El-Gabalawy et al., 2014; El-Gabalawy, Mackenzie, Shooshtari, & Sareen, 2011).

Interestingly, the increased mediolateral activity observed in T9 and T10 (predominantly for the GAD group) corresponds to sympathetic innervation of the adrenal glands (Parker, Kesse, Mohamed, & Afework, 1993)—responsible for the release of epinephrine, norepinephrine and cortisol. Although this neural activity cannot definitively say that increased hormone release is being observed in GAD, it does lend support for this hypothesis. While there is great controversy over whether or not GAD is associated with increased concentrations of catecholamines (Gerra et al., 2000; Mathew, Ho, Francis, Taylor, & Weinman, 1982; Mathew et al., 1981; McLeod et al., 1990; Munjack et al., 1990) and cortisol (Alfano et al., 2013; Gerra et al., 2000; Hek et al., 2013; Hilbert et al., 2017; Hoehn-Saric et al., 1991; Hood et al., 2011; Mantella et al., 2008; Steudte et al., 2011; Tafet et al., 2001), some studies do suggest this for catecholamines (Gerra et al., 2000; Mathew et al., 1981) and cortisol (Hilbert et al., 2017; Hood et al., 2011; Mantella et al., 2008; Tafet et al., 2001). Additional evidence for altered catecholamine levels in GAD include that treatment with SSRIs or SNRIs can be effective in treating GAD, and these medications can sometimes lead to decreased circulating levels of these hormones (McLeod et al., 1990).

Complicating results is the greater mediolateral activity observed in the HC group in T4 and T7; however, these clusters tend to be quite a bit smaller and are observed in different regions than in GAD. This highlights that ANS activity is not an all-or-nothing phenomenon. Unfortunately, this concept is often implied in early research of GAD as non-specific increased

ANS activity is expected, and rationale for why a particular downstream effect of the ANS is expected to be different is often not given. Presently, the GAD group does not exclusively have increased ANS activity, and this group does not have increased ANS activity throughout the entire thoracic cord. The results observed follow logically from the symptomatology of GAD, and yet do not diminish early physiological findings suggesting parasympathetic inflexibility (Aldao & Mennin, 2012; Hoehn-Saric et al., 2004; Hoehn-Saric et al., 1989; Llera & Newman, 2010; Lyonfields et al., 1995). Although this inflexibility was not observed presently, it seems to indicate that the ANS response in GAD, like the brain response (see Chapter 3) is complex and likely cannot be described briefly, other than to say that variability itself may be a facet of GAD (Fonzo & Etkin, 2017; Kolesar, Bilevicius, Wilson, & Kornelsen, 2019). In other words, while there seems to be much evidence for gastrointestinal disorder and disease associated with GAD (El-Gabalawy et al., 2014; El-Gabalawy et al., 2011), and perhaps increased stress hormone release (Gerra et al., 2000; Hilbert et al., 2017; Hood et al., 2011; Mantella et al., 2008; Mathew et al., 1981; McLeod et al., 1990; Tafet et al., 2001), as well as inflexibility in cardiac interbeat intervals (Aldao & Mennin, 2012; Hoehn-Saric et al., 2004; Hoehn-Saric et al., 1989; Llera & Newman, 2010; Lyonfields et al., 1995), and perspiration (McLeod et al., 1986), all of this data needs to be considered in unison to develop an accurate understanding of GAD.

Finally, towards the treatment of GAD, the data presented in the current thesis provide support for biofeedback: GAD is experienced mentally and somatically. Biofeedback involves real-time monitoring of physiological data, along with relaxation techniques, allowing patients to observe how relaxation affects their symptoms. Unfortunately, randomized control trials are lacking that directly compare biofeedback methods with other types of psychological and pharmacological treatments. Importantly, future randomized control trials of biofeedback should investigate gender effects—women tend to experience greater somatic symptoms than men (Vesga-Lopez et al., 2008)—as well as individualized biofeedback. Evidence suggests that biofeedback is most effective when multi-modal biofeedback is used (Schoenberg & David, 2014), and one group suggests that targets of biofeedback should be congruent with symptoms (Agnihotri, Paul, & Sandhu, 2008). For example, patients experiencing increased muscle tension appear most likely to have positive outcomes if this increased muscle tension is targeted, while others showing reduced cardiac interbeat interval variability may benefit most from biofeedback targeting this

physiological measure. Unfortunately, at this time there are no evidence-based guidelines for biofeedback treatment of GAD (Banerjee & Argaez, 2017). In the very least, the current body of work provides compelling evidence for further study of biofeedback for treating GAD.

This is the first study to apply spinal fMRI technology to a psychiatric population. First, this work shows that this technology is feasible for use in such populations, and that there are likely neural activity differences between those suffering from mental health disorders, and those who are not. While the CNS includes the spinal cord, it is, for the most part, ignored in neuroimaging and is often viewed simply as an 'information highway' from the brain to the body. However, as GAD, among other disorders, affects the whole being and is not "all in one's head," neuroimaging that includes spinal cord function in addition to brain function may help to better characterize the disorder.

4.6 Limitations

Some limitations for this work include the relatively small sample size, the presence of comorbidities in the patient group, and the challenges associated with spinal cord anatomy. First, dermatome and myotome maps differ in terms of location based on individual differences (see Foerster, 1933 for an excellent example of this in various patients). Additionally, early methodology to determine dermatomes differed (e.g., rhizotomy and anaesthesia, Naloxone injection, herpes zoster infection) and degree of overlap between adjacent segments also varies; these differences are often not highlighted in medical textbooks, but remains a critical consideration (Downs & Laporte, 2011; Riew, 2019). Several maps of each dermatome and myotome are available (Bing & Haymaker, 1940; Brendler, 1968; Downs & Laporte, 2011; Foerster, 1933; Haymaker & Woodhall, 1953; Head & Campbell, 1900; Keegan & Garrett, 1948; Riew, 2019), making adoption of a single map problematic and means that specific muscle activation and overlying sensory feedback cannot be directly assessed at this time. Furthermore, as spinal cord length varies with height across individuals, spinal cord segment length is also not identical across participants. In fact, several papers report spinal cord segment lengths that vary considerably, particularly progressing towards the lower thoracic cord, which further complicates analyses (Cadotte et al., 2015; Ko, Park, Shin, & Baek, 2004; Lang & Bartram, 1982; Sass et al., 2017). Finally, the generalizability of these results is somewhat limited in terms of biological sex as only 3/16 of the GAD participants were male. Although more women are diagnosed with GAD,

the typical ratio is close to 2:1 (McLean, Asnaani, Litz, & Hofmann, 2011; Vesga-Lopez et al., 2008). Men tend to have significantly higher rates of alcohol and drug misuse disorders while women are more prone to comorbid mood and anxiety disorders and often find the disorder more disabling (Vesga-Lopez et al., 2008), although there are no gender differences for age of onset or chronicity (McLean et al., 2011). Thus, these results may be more prone to increased influence of comorbid mental health disorders than if the sample was more representative of the population. Importantly, particularly for the present study, women with GAD are more likely to experience somatic symptoms of GAD (e.g., muscle tension, elevated heart rate, and gastrointestinal symptoms) than men (Vesga-Lopez et al., 2008). Therefore, caution should be used when generalizing these results to the GAD population.

4.7 Conclusions

Despite the challenges associated with acquiring and analysing spinal fMRI data, the present study provides convincing evidence of altered spinal cord activity for a psychiatric population, compared to HC. At the very least, this work should help to dispel the harmful myth that mental health disorders are independent of physiology. In addition to the importance this study has for future psychiatric neuroimaging studies in order to develop a CNS-wide neurophysiology profile, it also has significance for the population studied: GAD. For the first time, spinal fMRI technology has been used to highlight spinal cord activity differences between GAD and non-anxious HC, highlighting the likely role of the spinal cord in some of the physical complaints of this disorder, such as muscle tension, as well as providing some evidence of autonomic function differences in regions innervating gastrointestinal organs, and the adrenal medulla. Of particular interest is that this study provides evidence supporting previous, consistent findings of muscle tension, but adds to the debate of ANS function. While previous research may have treated the ANS as an all-or-nothing response in terms of vaguely hypothesizing increased ANS activity in GAD, this is not the case. Regions associated with known symptomatology of GAD were more active than in HCs, but uniform ANS hyperactivity was not observed throughout the cord and was mostly localized to four segments. Future research is needed to fully clarify the role of the ANS in GAD, both from neuroimaging research, and simultaneous collection of downstream physiological data and mental health symptoms.

4.8 Chapter 4 References

Agnihotri, H., Paul, M., & Sandhu, S. (2008). The comparative efficacy of two biofeedback techniques in the treatment of Generalized Anxiety Disorder. *Pakistan Journal of Social and Clinical Psychology, 6*, 35-46.

Aldao, A., & Mennin, D. S. (2012). Paradoxical cardiovascular effects of implementing adaptive emotion regulation strategies in generalized anxiety disorder. *Behav Res Ther, 50*(2), 122-130. doi:10.1016/j.brat.2011.12.004

Alfano, C. A., Reynolds, K., Scott, N., Dahl, R. E., & Mellman, T. A. (2013). Polysomnographic sleep patterns of non-depressed, non-medicated children with generalized anxiety disorder. *J Affect Disord, 147*(1-3), 379-384. doi:10.1016/j.jad.2012.08.015

American Psychiatric Association. (2013). *Diagnostic and statistical manual of mental disorders* (5th ed.). Arlington, VA: American Psychiatric Association Publishing.

Baldwin, D., & Rudge, S. (1995). The role of serotonin in depression and anxiety. *Int Clin Psychopharmacol, 9 Suppl 4*, 41-45. doi:10.1097/00004850-199501004-00006

Banerjee, S., & Argaez, C. (2017) *Neurofeedback and Biofeedback for Mood and Anxiety Disorders: A Review of Clinical Effectiveness and Guidelines*. Ottawa (ON).

Bapna, A., Adin, C., Engelman, Z. J., & Fudim, M. (2019). Increasing Blood Pressure by Greater Splanchnic Nerve Stimulation: a Feasibility Study. *J Cardiovasc Transl Res*. doi:10.1007/s12265-019-09929-7

Bing, R., & Haymaker, W. (1940). *Compendium of regional diagnosis in lesions of the brain and spinal cord; a concise introduction to the principles of localization of diseases and injuries of the nervous system* (11th ed.). St. Louis,: C. V. Mosby.

Borkovec, T. D., Robinson, E., Pruzinsky, T., & DePree, J. A. (1983). Preliminary exploration of worry: some characteristics and processes. *Behav Res Ther, 21*(1), 9-16. doi:10.1016/0005-7967(83)90121-3

Bosma, R. L., & Stroman, P. W. (2014). Assessment of data acquisition parameters, and analysis techniques for noise reduction in spinal cord fMRI data. *Magn Reson Imaging, 32*(5), 473-481. doi:10.1016/j.mri.2014.01.007

Brendler, S. J. (1968). The human cervical myotomes: functional anatomy studied at operation. *J Neurosurg, 28*(2), 105-111. doi:10.3171/jns.1968.28.2.0105

Broderick, J. E., Schneider, S., Junghaenel, D. U., Schwartz, J. E., & Stone, A. A. (2013). Validity and reliability of patient-reported outcomes measurement information system instruments in osteoarthritis. *Arthritis Care Res (Hoboken), 65*(10), 1625-1633. doi:10.1002/acr.22025

Brown, T. A., Di Nardo, P. A., Lehman, C. L., & Campbell, L. A. (2001). Reliability of DSM-IV anxiety and mood disorders: implications for the classification of emotional disorders. *J Abnorm Psychol, 110*(1), 49-58. doi:10.1037//0021-843x.110.1.49

Bush, K., Kivlahan, D. R., McDonell, M. B., Fihn, S. D., & Bradley, K. A. (1998). The AUDIT alcohol consumption questions (AUDIT-C): an effective brief screening test for problem drinking. Ambulatory Care Quality Improvement Project (ACQUIP). Alcohol Use Disorders Identification Test. *Arch Intern Med, 158*(16), 1789-1795. doi:10.1001/archinte.158.16.1789

Butnoriene, J., Bunevicius, A., Saudargiene, A., Nemeroff, C. B., Norkus, A., Ciceniene, V., & Bunevicius, R. (2015). Metabolic syndrome, major depression, generalized anxiety disorder, and ten-year all-cause and cardiovascular mortality in middle aged and elderly patients. *Int J Cardiol, 190*, 360-366. doi:10.1016/j.ijcard.2015.04.122

Cadotte, D. W., Cadotte, A., Cohen-Adad, J., Fleet, D., Livne, M., Wilson, J. R., . . . Fehlings, M. G. (2015). Characterizing the location of spinal and vertebral levels in the human cervical spinal cord. *AJNR Am J Neuroradiol, 36*(4), 803-810. doi:10.3174/ajnr.A4192

Culpepper, L. (2009). Generalized anxiety disorder and medical illness. *J Clin Psychiatry, 70 Suppl 2*, 20-24. doi:10.4088/jcp.s.7002.04

Downs, M. B., & Laporte, C. (2011). Conflicting dermatome maps: educational and clinical implications. *J Orthop Sports Phys Ther, 41*(6), 427-434. doi:10.2519/jospt.2011.3506

El-Gabalawy, R., Mackenzie, C. S., Pietrzak, R. H., & Sareen, J. (2014). A longitudinal examination of anxiety disorders and physical health conditions in a nationally representative sample of U.S. older adults. *Exp Gerontol, 60*, 46-56. doi:10.1016/j.exger.2014.09.012

El-Gabalawy, R., Mackenzie, C. S., Shooshtari, S., & Sareen, J. (2011). Comorbid physical health conditions and anxiety disorders: a population-based exploration of prevalence and health outcomes among older adults. *Gen Hosp Psychiatry, 33*(6), 556-564. doi:10.1016/j.genhosppsych.2011.07.005

Foerster, O. (1933). The Dermatomes in Man. *Brain, 56*(1), 1-39. doi:https://doi.org/10.1093/brain/56.1.1

Fonzo, G. A., & Etkin, A. (2017). Affective neuroimaging in generalized anxiety disorder: an integrated review. *Dialogues Clin Neurosci, 19*(2), 169-179.

Gerra, G., Zaimovic, A., Zambelli, U., Timpano, M., Reali, N., Bernasconi, S., & Brambilla, F. (2000). Neuroendocrine responses to psychological stress in adolescents with anxiety disorder. *Neuropsychobiology, 42*(2), 82-92. doi:10.1159/000026677

Haymaker, W., & Woodhall, B. (1953). *Peripheral nerve injuries; principles of diagnosis* (2d ed.). Philadelphia,: Saunders.

Hazlett, R. L., McLeod, D. R., & Hoehn-Saric, R. (1994). Muscle tension in generalized anxiety disorder: elevated muscle tonus or agitated movement? *Psychophysiology, 31*(2), 189-195. doi:10.1111/j.1469-8986.1994.tb01039.x

Head, H., & Campbell, A. W. (1900). The pathology of Herpes Zoster and its bearing on sensory localisation. *Reviews in Medical Virology, 7*(3), 131-143. doi:10.1002/(SICI)1099-1654(199709)7:3<131::AID-RMV198>3.0.CO;2-7

Hek, K., Direk, N., Newson, R. S., Hofman, A., Hoogendijk, W. J., Mulder, C. L., & Tiemeier, H. (2013). Anxiety disorders and salivary cortisol levels in older adults: a population-based study. *Psychoneuroendocrinology, 38*(2), 300-305. doi:10.1016/j.psyneuen.2012.06.006

Hilbert, K., Lueken, U., & Beesdo-Baum, K. (2014). Neural structures, functioning and connectivity in Generalized Anxiety Disorder and interaction with neuroendocrine systems: a systematic review. *J Affect Disord, 158*, 114-126. doi:10.1016/j.jad.2014.01.022

Hilbert, K., Lueken, U., Muehlhan, M., & Beesdo-Baum, K. (2017). Separating generalized anxiety disorder from major depression using clinical, hormonal, and structural MRI data: A multimodal machine learning study. *Brain and Behavior, 7*(3). doi:10.1002/brb3.633

Hoehn-Saric, R., McLeod, D. R., Funderburk, F., & Kowalski, P. (2004). Somatic symptoms and physiologic responses in generalized anxiety disorder and panic disorder: an ambulatory monitor study. *Arch Gen Psychiatry, 61*(9), 913-921. doi:10.1001/archpsyc.61.9.913

Hoehn-Saric, R., McLeod, D. R., Lee, Y. B., & Zimmerli, W. D. (1991). Cortisol levels in generalized anxiety disorder. *Psychiatry Res, 38*(3), 313-315. doi:10.1016/0165-1781(91)90021-g

Hoehn-Saric, R., McLeod, D. R., & Zimmerli, W. D. (1989). Somatic manifestations in women with generalized anxiety disorder. Psychophysiological responses to psychological stress. *Arch Gen Psychiatry, 46*(12), 1113-1119. doi:10.1001/archpsyc.1989.01810120055009

Hood, S. D., Melichar, J. K., Taylor, L. G., Kalk, N., Edwards, T. R., Hince, D. A., . . . Nutt, D. J. (2011). Noradrenergic function in generalized anxiety disorder: impact of treatment with venlafaxine on the physiological and psychological responses to clonidine challenge. *J Psychopharmacol, 25*(1), 78-86. doi:10.1177/0269881109359099

Jayaro, C., de la Vega, I., Diaz-Marsa, M., Montes, A., & Carrasco, J. L. (2008). [The use of the International Affective Picture System for the study of affective dysregulation in mental disorders]. *Actas Esp Psiquiatr, 36*(3), 177-182.

Keegan, J. J., & Garrett, F. D. (1948). The segmental distribution of the cutaneous nerves in the limbs of man. *Anat Rec, 102*(4), 409-437. doi:10.1002/ar.1091020403

Ko, H. Y., Park, J. H., Shin, Y. B., & Baek, S. Y. (2004). Gross quantitative measurements of spinal cord segments in human. *Spinal Cord, 42*(1), 35-40. doi:10.1038/sj.sc.3101538

Kolesar, T. A., Bilevicius, E., Wilson, A. D., & Kornelsen, J. (2019). Systematic review and meta-analyses of neural structural and functional differences in generalized anxiety disorder and healthy controls using magnetic resonance imaging. *NeuroImage: Clinical, 24*(102016), 1-14. doi:https://doi.org/10.1016/j.nicl.2019.102016

Kolesar, T. A., Kornelsen, J., & Smith, S. D. (2017). Separating neural activity associated with emotion and implied motion: An fMRI study. *Emotion, 17*(1), 131-140. doi:10.1037/emo0000209

Kornelsen, J., Smith, S. D., & McIver, T. A. (2015). A neural correlate of visceral emotional responses: evidence from fMRI of the thoracic spinal cord. *Soc Cogn Affect Neurosci, 10*(4), 584-588. doi:10.1093/scan/nsu092

Kornelsen, J., Smith, S. D., McIver, T. A., Sboto-Frankenstein, U., Latta, P., & Tomanek, B. (2013). Functional MRI of the thoracic spinal cord during vibration sensation. *J Magn Reson Imaging, 37*(4), 981-985. doi:10.1002/jmri.23819

Kornelsen, J., & Stroman, P. W. (2004). fMRI of the lumbar spinal cord during a lower limb motor task. *Magn Reson Med, 52*(2), 411-414. doi:10.1002/mrm.20157

Kroenke, K., Spitzer, R. L., & Williams, J. B. (2001). The PHQ-9: validity of a brief depression severity measure. *J Gen Intern Med, 16*(9), 606-613.

Lang, J., & Bartram, C. T. (1982). [Fila radicularia of the ventral and dorsal radices of the human spinal cord]. *Gegenbaurs Morphol Jahrb, 128*(4), 417-462.

Lee, M. W., McPhee, R. W., & Stringer, M. D. (2008). An evidence-based approach to human dermatomes. *Clin Anat, 21*(5), 363-373. doi:10.1002/ca.20636

Leitch, J. K., Figley, C. R., & Stroman, P. W. (2010). Applying functional MRI to the spinal cord and brainstem. *Magn Reson Imaging, 28*(8), 1225-1233. doi:10.1016/j.mri.2010.03.032

Lenze, E. J., Goate, A. M., Nowotny, P., Dixon, D., Shi, P., Bies, R. R., . . . Pollock, B. G. (2010). Relation of serotonin transporter genetic variation to efficacy of escitalopram for generalized anxiety disorder in older adults. *J Clin Psychopharmacol, 30*(6), 672-677. doi:10.1097/jcp.0b013e3181fc2bef

Lenze, E. J., Mantella, R. C., Shi, P., Goate, A. M., Nowotny, P., Butters, M. A., . . . Rollman, B. L. (2011). Elevated cortisol in older adults with generalized anxiety disorder is reduced by treatment: a placebo-controlled evaluation of escitalopram. *Am J Geriatr Psychiatry, 19*(5), 482-490. doi:10.1097/JGP.0b013e3181ec806c

Lima Portugal, L. C., Alves, R. d. C. S., Junior, O. F., Sanchez, T. A., Mocaiber, I., Volchan, E., . . . Pereira, M. G. (2020). Interactions between emotion and action in the brain. *Neuroimage, 214*, 116728. doi:https://doi.org/10.1016/j.neuroimage.2020.116728

Llera, S. J., & Newman, M. G. (2010). Effects of worry on physiological and subjective reactivity to emotional stimuli in generalized anxiety disorder and nonanxious control participants. *Emotion, 10*(5), 640-650. doi:10.1037/a0019351

Lohoff, F. W., Aquino, T. D., Narasimhan, S., Multani, P. K., Etemad, B., & Rickels, K. (2013). Serotonin receptor 2A (HTR2A) gene polymorphism predicts treatment response to venlafaxine XR in generalized anxiety disorder. *Pharmacogenomics J, 13*(1), 21-26. doi:10.1038/tpj.2011.47

Loukas, M., Klaassen, Z., Merbs, W., Tubbs, R. S., Gielecki, J., & Zurada, A. (2010). A review of the thoracic splanchnic nerves and celiac ganglia. *Clin Anat, 23*(5), 512-522. doi:10.1002/ca.20964

Lyonfields, J. D., Borkovec, T. D., & Thayer, J. F. (1995). Vagal tone in generalized anxiety disorder and the effects of aversive imagery and worrisome thinking. *Behavior Therapy, 26*(3), 457-466. doi:https://doi.org/10.1016/S0005-7894(05)80094-2

Malmo, R. B., & Shagass, C. (1949a). Physiologic studies of reaction to stress in anxiety and early schizophrenia. *Psychosom Med, 11*(1), 9-24. doi:10.1097/00006842-194901000-00003

Malmo, R. B., & Shagass, C. (1949b). Physiologic study of symptom mechanisms in psychiatric patients under stress. *Psychosom Med, 11*(1), 25-29. doi:10.1097/00006842-194901000-00004

Mantella, R. C., Butters, M. A., Amico, J. A., Mazumdar, S., Rollman, B. L., Begley, A. E., . . . Lenze, E. J. (2008). Salivary cortisol is associated with diagnosis and severity of late-life generalized anxiety disorder. *Psychoneuroendocrinology, 33*(6), 773-781. doi:10.1016/j.psyneuen.2008.03.002

Marchewka, A., Zurawski, L., Jednorog, K., & Grabowska, A. (2014). The Nencki Affective Picture System (NAPS): introduction to a novel, standardized, wide-range, high-quality, realistic picture database. *Behav Res Methods, 46*(2), 596-610. doi:10.3758/s13428-013-0379-1

Marrie, R. A., Walld, R., Bolton, J. M., Sareen, J., Walker, J. R., Patten, S. B., . . . Managing the Effects of Psychiatric Comorbidity in Chronic Immunoinflammatory, D. (2019). Rising incidence of psychiatric disorders before diagnosis of immune-mediated inflammatory disease. *Epidemiol Psychiatr Sci, 28*(3), 333-342. doi:10.1017/S2045796017000579

Mathew, R. J., Ho, B. T., Francis, D. J., Taylor, D. L., & Weinman, M. L. (1982). Catecholamines and anxiety. *Acta Psychiatr Scand, 65*(2), 142-147. doi:10.1111/j.1600-0447.1982.tb00833.x

Mathew, R. J., Ho, B. T., Kralik, P., Taylor, D. L., & Claghorn, J. L. (1981). Catecholamines and monoamine oxidase activity in anxiety. *Acta Psychiatr Scand, 63*(3), 245-252. doi:10.1111/j.1600-0447.1981.tb00671.x

McIver, T. A., Kornelsen, J., & Smith, S. D. (2013). Limb-specific emotional modulation of cervical spinal cord neurons. *Cogn Affect Behav Neurosci, 13*(3), 464-472. doi:10.3758/s13415-013-0154-x

McLean, C. P., Asnaani, A., Litz, B. T., & Hofmann, S. G. (2011). Gender differences in anxiety disorders: prevalence, course of illness, comorbidity and burden of illness. *J Psychiatr Res, 45*(8), 1027-1035. doi:10.1016/j.jpsychires.2011.03.006

McLeod, D. R., Hoehn-Saric, R., & Stefan, R. L. (1986). Somatic symptoms of anxiety: comparison of self-report and physiological measures. *Biol Psychiatry, 21*(3), 301-310. doi:10.1016/0006-3223(86)90051-x

McLeod, D. R., Hoehn-Saric, R., Zimmerli, W. D., De Souza, E. B., & Oliver, L. K. (1990). Treatment effects of alprazolam and imipramine: physiological versus subjective changes in patients with generalized anxiety disorder. *Biol Psychiatry, 28*(10), 849-861. doi:10.1016/0006-3223(90)90567-l

McMeekan, E. R. L., & Lishman, W. A. (1975). Retest reliabilities and interrelationship of the Annett Hand Preference Questionnaire and the Edinburgh Handedness Inventory. *British Journal of Psychology, 66*(1), 53.

Moffitt, T. E., Harrington, H., Caspi, A., Kim-Cohen, J., Goldberg, D., Gregory, A. M., & Poulton, R. (2007). Depression and generalized anxiety disorder: cumulative and sequential comorbidity in a birth cohort followed prospectively to age 32 years. *Arch Gen Psychiatry, 64*(6), 651-660. doi:10.1001/archpsyc.64.6.651

Monk, C. S., Telzer, E. H., Mogg, K., Bradley, B. P., Mai, X., Louro, H. M. C., . . . Pine, D. S. (2008). Amygdala and ventrolateral prefrontal cortex activation to masked angry faces in children and adolescents with generalized anxiety disorder. *Archives of General Psychiatry, 65*(5), 568-576. doi:10.1001/archpsyc.65.5.568

Munjack, D. J., Baltazar, P. L., DeQuattro, V., Sobin, P., Palmer, R., Zulueta, A., . . . Leonard, M. (1990). Generalized anxiety disorder: some biochemical aspects. *Psychiatry Res, 32*(1), 35-43. doi:10.1016/0165-1781(90)90133-p

Myronenko, A., & Song, X. B. (2009). Image Registration by Minimization of Residual Complexity. *Cvpr: 2009 Ieee Conference on Computer Vision and Pattern Recognition, Vols 1-4*, 49-56.

Myronenko, A., & Song, X. B. (2010). Intensity-Based Image Registration by Minimizing Residual Complexity. *Ieee Transactions on Medical Imaging, 29*(11), 1882-1891. doi:10.1109/Tmi.2010.2053043

Nepon, J., Belik, S. L., Bolton, J., & Sareen, J. (2010). The relationship between anxiety disorders and suicide attempts: findings from the National Epidemiologic Survey on Alcohol and Related Conditions. *Depress Anxiety, 27*(9), 791-798. doi:10.1002/da.20674

Norman, S. B., Cissell, S. H., Means-Christensen, A. J., & Stein, M. B. (2006). Development and validation of an Overall Anxiety Severity And Impairment Scale (OASIS). *Depression & Anxiety, 23*(4), 245-249. doi:10.1002/da.20182

Oldfield, R. C. (1971). The assessment and analysis of handedness: the Edinburgh inventory. *Neuropsychologia, 9*(1), 97-113. doi:10.1016/0028-3932(71)90067-4

Osaki, Y., Ino, A., Matsushita, S., Higuchi, S., Kondo, Y., & Kinjo, A. (2014). Reliability and validity of the alcohol use disorders identification test - consumption in screening for adults with alcohol use disorders and risky drinking in Japan. *Asian Pac J Cancer Prev, 15*(16), 6571-6574. doi:10.7314/apjcp.2014.15.16.6571

Parker, T. L., Kesse, W. K., Mohamed, A. A., & Afework, M. (1993). The innervation of the mammalian adrenal gland. *J Anat, 183 (Pt 2)*, 265-276.

Powers, J. M., Ioachim, G., & Stroman, P. W. (2018). Ten Key Insights into the Use of Spinal Cord fMRI. *Brain Sci, 8*(9). doi:10.3390/brainsci8090173

Ralston, D. D., & Ralston, H. J., 3rd. (1985). The terminations of corticospinal tract axons in the macaque monkey. *J Comp Neurol, 242*(3), 325-337. doi:10.1002/cne.902420303

Riew, K. D. (2019). Variations in cervical myotomes and dermatomes. *Spine J, 19*(7), 1143-1145. doi:10.1016/j.spinee.2019.03.007

Robinson, J. (2013). Edinburgh Handedness Inventory. In F. R. Volkmar (Ed.), *Encyclopedia of Autism Spectrum Disorders* (pp. 1051-1054). New York, NY: Springer New York.

Rosnick, C. B., Rawson, K. S., Butters, M. A., & Lenze, E. J. (2013). Association of cortisol with neuropsychological assessment in older adults with generalized anxiety disorder. *Aging Ment Health, 17*(4), 432-440. doi:10.1080/13607863.2012.761673

Sainsbury, P., & Gibson, J. G. (1954). Symptoms of anxiety and tension and the accompanying physiological changes in the muscular system. *J Neurol Neurosurg Psychiatry, 17*(3), 216-224. doi:10.1136/jnnp.17.3.216

Sareen, J., Cox, B. J., Afifi, T. O., de Graaf, R., Asmundson, G. J., ten Have, M., & Stein, M. B. (2005). Anxiety disorders and risk for suicidal ideation and suicide attempts: a population-

based longitudinal study of adults. *Arch Gen Psychiatry, 62*(11), 1249-1257. doi:10.1001/archpsyc.62.11.1249

Sass, L. R., Khani, M., Natividad, G. C., Tubbs, R. S., Baledent, O., & Martin, B. A. (2017). A 3D subject-specific model of the spinal subarachnoid space with anatomically realistic ventral and dorsal spinal cord nerve rootlets. *Fluids Barriers CNS, 14*(1), 36. doi:10.1186/s12987-017-0085-y

Schoenberg, P. L., & David, A. S. (2014). Biofeedback for psychiatric disorders: a systematic review. *Appl Psychophysiol Biofeedback, 39*(2), 109-135. doi:10.1007/s10484-014-9246-9

Smith, S. D., Kolesar, T. A., & Kornelsen, J. (2018). Lateralized Brainstem and Cervical Spinal Cord Responses to Aversive Sounds: A Spinal fMRI Study. *Brain Sci, 8*(9). doi:10.3390/brainsci8090165

Smith, S. D., & Kornelsen, J. (2011). Emotion-dependent responses in spinal cord neurons: a spinal fMRI study. *Neuroimage, 58*(1), 269-274. doi:10.1016/j.neuroimage.2011.06.004

Spitzer, R. L., Kroenke, K., Williams, J. B., & Lowe, B. (2006). A brief measure for assessing generalized anxiety disorder: the GAD-7. *Arch Intern Med, 166*(10), 1092-1097. doi:10.1001/archinte.166.10.1092

Stein, M. B., & Sareen, J. (2015). CLINICAL PRACTICE. Generalized Anxiety Disorder. *N Engl J Med, 373*(21), 2059-2068. doi:10.1056/NEJMcp1502514

Steudte, S., Stalder, T., Dettenborn, L., Klumbies, E., Foley, P., Beesdo-Baum, K., & Kirschbaum, C. (2011). Decreased hair cortisol concentrations in generalised anxiety disorder. *Psychiatry Res, 186*(2-3), 310-314. doi:10.1016/j.psychres.2010.09.002

Stroman, P. W. (2016). Validation of Structural Equation Modeling Methods for Functional MRI Data Acquired in the Human Brainstem and Spinal Cord. *Crit Rev Biomed Eng, 44*(4), 227-241. doi:10.1615/CritRevBiomedEng.2017020438

Stroman, P. W., Krause, V., Malisza, K. L., Frankenstein, U. N., & Tomanek, B. (2002). Functional magnetic resonance imaging of the human cervical spinal cord with stimulation of different sensory dermatomes. *Magn Reson Imaging, 20*(1), 1-6. doi:10.1016/s0730-725x(02)00468-x

Stroman, P. W., Wheeler-Kingshott, C., Bacon, M., Schwab, J. M., Bosma, R., Brooks, J., . . . Tracey, I. (2014). The current state-of-the-art of spinal cord imaging: methods. *Neuroimage, 84*, 1070-1081. doi:10.1016/j.neuroimage.2013.04.124

Tafet, G. E., Idoyaga-Vargas, V. P., Abulafia, D. P., Calandria, J. M., Roffman, S. S., Chiovetta, A., & Shinitzky, M. (2001). Correlation between cortisol level and serotonin uptake in patients with chronic stress and depression. *Cogn Affect Behav Neurosci, 1*(4), 388-393. doi:10.3758/cabn.1.4.388

Vesga-Lopez, O., Schneier, F. R., Wang, S., Heimberg, R. G., Liu, S. M., Hasin, D. S., & Blanco, C. (2008). Gender differences in generalized anxiety disorder: results from the National Epidemiologic Survey on Alcohol and Related Conditions (NESARC). *J Clin Psychiatry, 69*(10), 1606-1616.

Wheeler-Kingshott, C. A., Stroman, P. W., Schwab, J. M., Bacon, M., Bosma, R., Brooks, J., . . . Tracey, I. (2014). The current state-of-the-art of spinal cord imaging: applications. *Neuroimage, 84*, 1082-1093. doi:10.1016/j.neuroimage.2013.07.014

Wilson, A. D., Kolesar, T. A., Kornelsen, J., & Smith, S. D. (2018). Neural Responses to Consciously and Unconsciously Perceived Emotional Faces: A Spinal fMRI Study. *Brain Sci, 8*(8). doi:10.3390/brainsci8080156

Yoshizawa, T., Nose, T., Moore, G. J., & Sillerud, L. O. (1996). Functional magnetic resonance imaging of motor activation in the human cervical spinal cord. *Neuroimage, 4*(3 Pt 1), 174-182. doi:10.1006/nimg.1996.0068

5. Chapter 5: Discussion

5.1 General Discussion

The goal of the present dissertation was to investigate how threat affects neural function in those with GAD, compared to HC. This dissertation spanned the largest expanse of the CNS to-date in GAD, using neuroimaging methods. The research conducted in this body of work addressed three specific aims: to identify neural activity differences between GAD and HC groups in response to threat in Aim 1) the brain, Aim 2) the cervical spinal cord, and Aim 3) the thoracic spinal cord. This research contributes novel information to the understanding of the neurophysiology of GAD, as well as expands the field of spinal fMRI to include, for the first time, a psychiatric population. These aims were accomplished by gathering, reviewing, and meta-analysing the current neuroimaging data in GAD, investigating if the findings from this systematic review were related to a confounding factor in previous emotion fMRI research (i.e., the emotion/implied motion relationship in stimuli), and extending this research into the cervical and thoracic spinal cord to investigate the neural origin of some of the somatic complaints in GAD. This is the most direct investigation of the ANS in GAD to date, by looking at the source of this neural activity, rather than downstream consequences.

Aim 1 was spread over Chapters 2 and 3 as much neuroimaging research has already been conducted in the brain in many different labs, using many different modalities. In the course of conducting my systematic review and meta-analysis (Kolesar, Bilevicius, Wilson, & Kornelsen, 2019), I discovered 85 eligible records, consisting of 35 structural, 33 FC, and 42 task-based MRI experiments. Despite the large number of included records, meta-analyses could only be conducted on VBM and a small subset of task-based fMRI findings. However, regardless of the small sample size for the meta-analyses, results between the systematic review and meta-analyses were highly consistent. This work identified four key regions that often differ in structure, FC, or activity in GAD. Namely, patients with GAD had reduced volume in the dlPFC and ACC, but increased volume in the amygdala and left hippocampus. Additionally, patients with GAD showed altered/reduced activity in the dlPFC and ACC, and increased activity in the amygdala. Although these regions had been highlighted in previous systematic reviews (Fonzo & Etkin, 2017; Hilbert, Lueken, & Beesdo-Baum, 2014; Mochcovitch, da Rocha Freire, Garcia, & Nardi, 2014), my work highlighted many other regions that are typically altered in GAD, but had been largely ignored.

These structures include the insula, precuneus, precentral gyrus, STG, vlPFC, OFC, PCC, and cerebellum (culmen). In particular, the culmen of the cerebellum was an interesting finding from the main effect of group, based on the frequency in which it appeared in results tables, but the infrequency with which it was discussed.

After correcting for a shortcoming of much of the previous brain task experiments—i.e., the implied motion confound—I conducted my own brain fMRI task-based experiment in Aim 1b, primarily focused on investigating the culmen of the cerebellum. After compiling a stimulus set, all 300 images were pilot-tested by 40 participants to ensure that implied motion ratings did not differ between stimuli groups while emotion ratings did. Using a subset of these images, a different group of participants were recruited—participants with, and participants without GAD. All participants viewed the stimuli while having their brain and spinal cord scanned: 1 run was conducted in the brain while 3 runs were collected from both the cervical and thoracic spinal cord (more on the spinal cord shortly). Unfortunately, scanning was cut short due to the COVID-19 pandemic, resulting in collection of fewer datasets than planned.

The primary analysis investigating the cerebellum ROI was not statistically significant, and neither was the secondary ROI analysis investigating the dlPFC, ACC, amygdala, and hippocampus. However, after conducting a whole-brain, exploratory analysis, a main effect of group identified some activity differences. Interestingly, several of the regions expected to differ between the groups were significant, including the amygdala, hippocampus, and dlPFC. Additional structures highlighted in the systematic review and meta-analysis of Chapter 2 were also significant, including the insula, precuneus, precentral gyrus, STG, vlPFC, OFC, and importantly, the culmen—in fact the only regions not represented in the main effect, but identified in the systematic review, were the ACC and PCC. Importantly, the ACC, which is often altered in activity or FC, does not have a consistent direction of change (Fonzo & Etkin, 2017; Kolesar et al., 2019). The additional brain regions identified in this study, not observed in the systematic review are associated with motor control (supplementary motor area, putamen, caudate, thalamus), perhaps related to increased muscle tension commonly observed in GAD, as well as visual processing (middle occipital gyrus, medial temporal gyrus) which are likely a direct result of the type of stimuli used. Despite not reaching our target sample size goal, this brain fMRI study was still able

to provide evidence for a whole host of regions altered in GAD, and lending further credence to the meta-analysis.

While Chapters 2 and 3 highlight regions expected based on 85 previous experiments, activity in the spinal cord (Aims 2 and 3) is an entirely novel and important contribution to this field (Chapter 3). Using the identical task as in the brain, the cervical and thoracic spinal cord yielded activity likely corresponding to increased muscle tension of the neck and shoulders, as well as autonomic activity relating to blood pressure and/or gut function, and innervation of the adrenal medulla. While this data may seem contrary to previous findings from physiological data (i.e., the inconsistent findings of downstream physiological data such as catecholamine concentrations, heart rate and skin conductance changes), it in fact highlights that the ANS is not an "all-or-none" response, a concept that seems to be overlooked in much of the early research of GAD. For example, if the fight-or-flight response was an all-inclusive response, as is somewhat implied in the expectations for the admittedly vague, often hypothesized "increased ANS activity" in GAD, there should be greater activity throughout the entire interomediolateral cell column of the GAD group, rather than in select regions. Furthermore, there should not be any regions in the thoracic spinal cord with hyperactivity in the HC group, compared to the GAD group. In fact, this is not the case in either the reported results, or in the physiological data reported throughout the decades. Furthermore, this body of work implicates regions of the ANS that are active in GAD that relate well to known symptomatology of GAD, and does not provide support for increased activity in regions that affect things like heart rate that have yielded inconclusive results in the past. These findings from the cervical and thoracic spinal cord translate well into a treatment method finding some success for treating GAD: biofeedback. Because this disorder has a great deal of somatic symptoms, targeting these symptoms directly may help to improve some of the other, more cognitive symptoms of GAD as well (Dadashi et al., 2018; Tolin, Davies, Moskow, & Hofmann, 2020).

This body of work lends support for the emotion dysregulation model of GAD. In their paper describing the emotion dysregulation model of GAD, Mennin, Heimberg, Turk, and Fresco (2005) describe how individuals with GAD experience emotions more intensely, have poorer insight into and react more negatively to emotions, and have difficulty returning to an emotionally neutral state after experiencing negative emotions. This model also discusses that as a result of this

emotional hyperresponsiveness, emotional hyporesponsiveness is then observed as worry is adopted as a strategy to reduce emotion (Mennin et al., 2005), as per the Avoidance Model of Worry (AMW) that this Emotion Dysregulation (ED) model builds off of (Borkovec, 1994). Behavioural data show that patients with GAD rated the images as no more negative or physiologically arousing than HC (); however, VAS scores showed that while both groups began the experiment equally anxious, after the experiment started, present moment anxiety was greater for those with GAD for the duration of the experiment, and immediately afterwards (see Table 3.1 or Table 4.1). These results suggest 1) heightened intensity of emotions, 2) poorer understanding of emotions, as indicated by the stimuli ratings being equal to those of HC, despite eliciting a stronger neural response to them, and 3) reduced ability to return to baseline quickly compared to the HC group, based on VAS4 scores. Interestingly, this support for the ED model of GAD lends theoretical support for affective identification in cognitive behavioural therapy treatment in GAD, drawn from emotion-focused therapy (Greenberg, Goldman, & American Psychological Association, 2019; Watson, Greenberg, & American Psychological Association, 2017).

While these results support the hyperresponsiveness to emotion described in the emotion dysregulation model, but the results from the spinal cord do not support the subsequent hyporesponsiveness that results from worrying after viewing negative emotions as threatening. However, perhaps this can be explained by a relatively new theoretical model of GAD called the contrast avoidance model of worry, which shares many features with the emotion dysregulation model, including increased emotional intensity, and difficulty regulating, processing, and describing emotions. The contrast avoidance model suggests that worry is not actually used as an emotion avoidance mechanism per se, but instead is used to maintain negative emotions in order to reduce an unexpected emotional shift (Newman & Llera, 2011). Thus, feelings of being unprepared (note the parallels here with the intolerance of uncertainty model) for a "negative emotional contrast" are considered threatening, and worry is used as a way to alleviate this contrast by increasing negative affect (Newman & Llera, 2011). The results from the present study seem to lend support to this model because of its overlap with the emotion dysregulation model, with the extension that more negative affect is observed in response to worrying—i.e., greater anxiety was observed in the chronically worrying (GAD) group after a negative emotion-evoking task. However, further research is needed to corroborate this theoretical model before such conclusions

can be made. Regardless, this work provides evidence for aspects of the emotion dysregulation model while the avoidance model of worry—which views worry as a verbal linguistic activity—was not directly tested. In fact, based on the AMW, imagery-based stimuli were chosen in an attempt to highlight the emotional aspect of GAD. While the AMW may posit that the GAD group should have showed reduced activity in emotion/autonomic-associated regions as they engage more in worrying, that does not appear to be the case in this experiment.

The similarity in results between Chapters 2 and 3, combined with the novel data presented in Chapter 3, may help to form the basis of a neurological biomarker for GAD, although much further research is needed to make this a reality (Hahn, Nierenberg, & Whitfield-Gabrieli, 2017). Future investigations should look at the specificity and sensitivity of dysfunction within these regions for qualifying GAD. Furthermore, towards the goal of personalized medicine, multimodal data consisting of neuroimaging, behavioural, and genetic data will likely be required (Hahn et al., 2017). As current pharmaceutical options are only effective in treating GAD in 30-50% of cases (Stein & Sareen, 2015), identifying candidates likely to respond to certain medications can reduce patient frustration trying different medications until an effective treatment is found, and hopefully increase treatment adherence and limit adverse side-effects (Hahn et al., 2017). For example, as there is much controversy over the state of catecholamine levels in GAD, spinal fMRI may be a useful technique for identifying patients that show increased activity in thoracic regions innervating the adrenal medulla—perhaps these patients will show an improved treatment response using SSRIs compared to patients whose activity in this region is not increased, as previous research indicates that SSRI use can decrease circulating catecholamine levels (McLeod, Hoehn-Saric, Zimmerli, De Souza, & Oliver, 1990). More practically, the hope would be that identifying neurological and physiological biomarkers in future basic science research would allow for identification of less expensive and objective measurements that can reliably predict the most effective treatment at the individual level.

5.2 Limitations

Several limitations are present in the current collection of work. The first and most obvious limitation is the small sample size, including the small number of records eligible for the meta-analyses in Chapter 2, and directly related to the onset of the COVID-19 pandemic for Chapters 3 and 3. The small sample size had a greater impact on the brain data due to the multiple comparisons

problem: the brain has 2 orders of magnitude more voxels to investigate, compared to the spinal cord. Additionally, while collecting more time points for each participant would have been ideal, we were limited to practical considerations such as participant fatigue. In order to mitigate our limited scan time per participant and in an effort to boost statistical power, we employed a multi-band acquisition in the brain to collect more data in a shorter period of time. This allowed us to collect a single run in the brain while collecting roughly the same number of volumes as in each section of the spinal cord, at about 1/3 of the time as needed in the spinal cord. In spite of the small sample size, results were obtained that provided support for my hypotheses. Following this limitation, the sex-distribution of the sample was skewed more towards women—13 female and 3 male GAD participants were included. Differences related to the increased rate of comorbid mood and anxiety disorders (except SAD) in females, as well as the greater disability experienced for females compared to males (McLean, Asnaani, Litz, & Hofmann, 2011; Vesga-Lopez et al., 2008) may have influenced the results, as well as limited the generalizability to males with GAD. Additionally, the sample consists of adults, and thus may not be generalizable to children/adolescents or elderly populations.

Additionally, the brain and spinal cord results are not directly comparable: in the brain data, the neutral stimulus condition was convolved with the hemodynamic response function and modelled in the GLM at first-level while the neutral condition was not convolved with the hemodynamic response function in the spinal cord. Because the neutral stimulus condition was not modelled in the first-level GLM in the spinal cord, an ANOVA could not be run at the second-level to address main and interaction effects in the spinal cord. Furthermore, while significant results were observed for the contrast comparing GAD and HC activity in the cervical and thoracic spinal cord, only the main effect of group was significant in the brain.

Another limitation is related to the difficulty acquiring and analysing spinal fMRI data—until now, few fMRI investigations have been done on the thoracic cord (Alexander et al., 2016; Kornelsen, Smith, & McIver, 2015; Kornelsen et al., 2013; Kozyrev et al., 2012), and as such the spatial normalization process is still being refined. One of the main challenges associated with spatial normalization of the thoracic cord is the individual differences that exist within its length, but also within each segment of the thoracic cord. Furthermore, these individual differences also carry over to innervation differences as there is variability as to which segments innervate which

nerves—for example, some individuals do not even have a least splanchnic nerve (Loukas et al., 2010). Finally, for the cervical and thoracic spinal fMRI work, acquiring the data sagittally using a HASTE sequence limits the resolution in the axial view; however, the value of the maintained data integrity in the sagittal view which allowed us to view the entire cervical and thoracic cord supersedes this limitation in this case.

5.3 Future Directions

There are several interesting directions for future research to investigate regarding the neurophysiology of GAD. First, as highlighted in Chapter 2, resting state fMRI data would make a compelling addition to the GAD literature. Although numerous studies have investigated functional connectivity in GAD, none have been presented that investigate a whole-brain independent component analysis. Several resting state networks of interest for the GAD population include the default mode, salience, sensorimotor, central executive, and cerebellar networks (for review of these networks, see Bressler & Menon, 2010; Rosazza & Minati, 2011; or Shirer, Ryali, Rykhlevskaia, Menon, & Greicius, 2012). The default mode network is active during mind wandering and daydreaming—as worrying and rumination can be parts of daydreaming, this network would be an important network to investigate (Rosazza & Minati, 2011). Additionally, the salience (i.e., threat-detecting; Menon, 2015; Shirer et al., 2012), sensorimotor (self-explanatory; Shirer et al., 2012), and central executive (i.e., problem solving and executive control; Dixon et al., 2018; Marek & Dosenbach, 2018) networks would all be interesting in view of the symptomatology of GAD, including hypervigilance to threat (Goodwin, Yiend, & Hirsch, 2017), increased muscle tension and increased prevalence of chronic pain conditions such as inflammatory bowel disease and arthritis (Bernstein, 2017; Culpepper, 2009; El-Gabalawy, Mackenzie, Shooshtari, & Sareen, 2011), and difficulty concentrating, respectively. Finally, the cerebellar network would be particularly interesting given the recent findings of the systematic review/meta-analysis of GAD (Chapter 2; Kolesar et al., 2019), and the task-based findings presented within this thesis (Chapter 3).

Furthermore, resting state fMRI investigation of the spinal cord in GAD would also be of interest, as recent studies suggest that resting state networks can also be observed in the spinal cord (Barry, Rogers, Conrad, Smith, & Gore, 2016; Barry, Smith, Dula, & Gore, 2014; Eippert et al., 2017; Harita, Ioachim, Powers, & Stroman, 2019; Kong et al., 2014; San Emeterio Nateras et al.,

2016). It would be interesting to see how the baseline CNS in GAD differs from HC groups. Further analyses of interest include DTI of the spinal cord—much work has been done in spinal cord DTI since the early 2000's (Bammer, Augustin, Prokesch, Stollberger, & Fazekas, 2002; Cohen-Adad et al., 2011; Smith et al., 2010; Thurnher & Bammer, 2006; Wheeler-Kingshott et al., 2002; Wilm et al., 2009), but so far, none have investigated this in GAD. Spinal cord DTI may provide context for the activation findings observed in the present study, and at the very least would be interesting to see if the structural connectivity correlated with the functional data, as this is not always the case in the brain (Batista-Garcia-Ramo & Fernandez-Verdecia, 2018).

Another avenue of inquiry would be large-scale comparisons of various types of mental disorders—while GAD and PD seem to be closely functionally (Cuthbert et al., 2003) and genetically related (Hettema, Prescott, Myers, Neale, & Kendler, 2005), they are quite distinct in the presenting physiology—PD patients seem to experience the ANS hyperactivity hypothesized of anxiety disorders, while this information is much more inconsistent for patients with GAD. Thus, large-scale (neuro)physiology studies investigating these disorders may help to better distinguish them from one another, with the goal of providing more objective diagnostic criteria than can currently be assessed in a clinical setting (which currently relies on subjective self-insight).

Furthermore, as the ultimate goal of mental health research should be towards preventing onset and improving treatment, another research project should investigate interpersonal differences within GAD in an attempt to discover how patients differ from each other, and if these differences can help to predict those at risk for developing GAD, or at the very least, predict an optimal treatment plan should the disorder present.

5.4 Conclusions

GAD is a complex mental health disorder, often plagued by high variability in its findings including stress hormone concentrations and neural activity. Although this variability may itself be a feature of this disorder, some more cohesive results are also found, such as increased muscle tension, and reduced variability in cardiac interbeat intervals. Additionally, enough neuroimaging studies have been conducted to begin to see reproducibility—there is consistency in which regions are often altered, even if these regions are not consistently altered in the same way. Twelve brain regions—dlPFC, ACC, amygdala, hippocampus, insula, precuneus, precentral gyrus, STG, vlPFC,

OFC, PCC and culmen—have been highlighted as key regions of interest for future investigation into developing a neurological biomarker. Furthermore, the bodily symptoms of GAD largely correspond to spinal cord activity including muscle tension and gastrointestinal issues. An important area of research for this field to progress is the role of the ANS in GAD; while I provide evidence of ANS (specifically the sympathetic division) hyperactivity in GAD, previous physiological research is less supportive. Finally, this work points to several methods of non-invasive treatment for GAD: affective identification and biofeedback. A better understanding of the complexity and variability of this disorder will likely be crucial in providing better treatment to patients with GAD.

5.5 Chapter 5 References

Alexander, M. S., Kozyrev, N., Bosma, R. L., Figley, C. R., Richards, J. S., & Stroman, P. W. (2016). fMRI Localization of Spinal Cord Processing Underlying Female Sexual Arousal. *J Sex Marital Ther, 42*(1), 36-47. doi:10.1080/0092623X.2015.1010674

Bammer, R., Augustin, M., Prokesch, R. W., Stollberger, R., & Fazekas, F. (2002). Diffusion-weighted imaging of the spinal cord: interleaved echo-planar imaging is superior to fast spin-echo. *J Magn Reson Imaging, 15*(4), 364-373. doi:10.1002/jmri.10075

Barry, R. L., Rogers, B. P., Conrad, B. N., Smith, S. A., & Gore, J. C. (2016). Reproducibility of resting state spinal cord networks in healthy volunteers at 7 Tesla. *Neuroimage, 133*, 31-40. doi:10.1016/j.neuroimage.2016.02.058

Barry, R. L., Smith, S. A., Dula, A. N., & Gore, J. C. (2014). Resting state functional connectivity in the human spinal cord. *Elife, 3*, e02812. doi:10.7554/eLife.02812

Batista-Garcia-Ramo, K., & Fernandez-Verdecia, C. I. (2018). What we know about the brain structure-function relationship. *Behav. Sci., 8*(4), 39. doi:https://doi.org/10.3390/bs8040039

Bernstein, C. N. (2017). The Brain-Gut Axis and Stress in Inflammatory Bowel Disease. *Gastroenterol Clin North Am, 46*(4), 839-846. doi:10.1016/j.gtc.2017.08.006

Borkovec, T. D. (1994). The nature, functions, and origins of worry. In G. Davey & F. Tallis (Eds.), *Worrying: Perspectives on theory, assessment, and treatment* (pp. 5-33). Sussex, England: Wiley & Sons.

Bressler, S. L., & Menon, V. (2010). Large-scale brain networks in cognition: emerging methods and principles. *Trends Cogn Sci, 14*(6), 277-290. doi:10.1016/j.tics.2010.04.004

Cohen-Adad, J., El Mendili, M. M., Lehericy, S., Pradat, P. F., Blancho, S., Rossignol, S., & Benali, H. (2011). Demyelination and degeneration in the injured human spinal cord detected with diffusion and magnetization transfer MRI. *Neuroimage, 55*(3), 1024-1033. doi:10.1016/j.neuroimage.2010.11.089

Culpepper, L. (2009). Generalized anxiety disorder and medical illness. *J Clin Psychiatry, 70 Suppl 2*, 20-24. doi:10.4088/jcp.s.7002.04

Cuthbert, B. N., Lang, P. J., Strauss, C., Drobes, D., Patrick, C. J., & Bradley, M. M. (2003). The psychophysiology of anxiety disorder: fear memory imagery. *Psychophysiology, 40*(3), 407-422. doi:10.1111/1469-8986.00043

Dadashi, M., Taremian, F., Momtazi, S., Khani, M., Eskandari, Z., Armani Kian, A., & Birashk, B. (2018). Comparing the Effectiveness of Metacognitive Therapy (MCT), Pharmacotherapy (SSRIs) and EEG Biofeedback in Generalized Anxiety Disorders. *Journal of Advances in Medical and Biomedical Research, 26*(117), 57-73.

Dixon, M. L., De La Vega, A., Mills, C., Andrews-Hanna, J., Spreng, R. N., Cole, M. W., & Christoff, K. (2018). Heterogeneity within the frontoparietal control network and its relationship to the default and dorsal attention networks. *Proc Natl Acad Sci U S A, 115*(7), E1598-E1607. doi:10.1073/pnas.1715766115

Eippert, F., Kong, Y., Winkler, A. M., Andersson, J. L., Finsterbusch, J., Buchel, C., . . . Tracey, I. (2017). Investigating resting-state functional connectivity in the cervical spinal cord at 3T. *Neuroimage, 147*, 589-601. doi:10.1016/j.neuroimage.2016.12.072

El-Gabalawy, R., Mackenzie, C. S., Shooshtari, S., & Sareen, J. (2011). Comorbid physical health conditions and anxiety disorders: a population-based exploration of prevalence and health outcomes among older adults. *Gen Hosp Psychiatry, 33*(6), 556-564. doi:10.1016/j.genhosppsych.2011.07.005

Fonzo, G. A., & Etkin, A. (2017). Affective neuroimaging in generalized anxiety disorder: an integrated review. *Dialogues Clin Neurosci, 19*(2), 169-179.

Goodwin, H., Yiend, J., & Hirsch, C. R. (2017). Generalized Anxiety Disorder, worry and attention to threat: A systematic review. *Clin Psychol Rev, 54*, 107-122. doi:10.1016/j.cpr.2017.03.006

Greenberg, L. S., Goldman, R. N., & American Psychological Association. (2019). *Clinical handbook of emotion-focused therapy* (pp. 1 online resource).

Hahn, T., Nierenberg, A. A., & Whitfield-Gabrieli, S. (2017). Predictive analytics in mental health: applications, guidelines, challenges and perspectives. *Mol Psychiatry, 22*(1), 37-43. doi:10.1038/mp.2016.201

Harita, S., Ioachim, G., Powers, J., & Stroman, P. W. (2019). Investigation of Resting-State BOLD Networks in the Human Brainstem and Spinal Cord. *Neuroscience, 404*, 71-81. doi:10.1016/j.neuroscience.2019.02.009

Hettema, J. M., Prescott, C. A., Myers, J. M., Neale, M. C., & Kendler, K. S. (2005). The structure of genetic and environmental risk factors for anxiety disorders in men and women. *Arch Gen Psychiatry, 62*(2), 182-189. doi:10.1001/archpsyc.62.2.182

Hilbert, K., Lueken, U., & Beesdo-Baum, K. (2014). Neural structures, functioning and connectivity in Generalized Anxiety Disorder and interaction with neuroendocrine systems: a systematic review. *J Affect Disord, 158*, 114-126. doi:10.1016/j.jad.2014.01.022

Kolesar, T. A., Bilevicius, E., Wilson, A. D., & Kornelsen, J. (2019). Systematic review and meta-analyses of neural structural and functional differences in generalized anxiety disorder and healthy controls using magnetic resonance imaging. *NeuroImage: Clinical, 24*(102016), 1-14. doi:https://doi.org/10.1016/j.nicl.2019.102016

Kong, Y., Eippert, F., Beckmann, C. F., Andersson, J., Finsterbusch, J., Buchel, C., . . . Brooks, J. C. (2014). Intrinsically organized resting state networks in the human spinal cord. *Proc Natl Acad Sci U S A, 111*(50), 18067-18072. doi:10.1073/pnas.1414293111

Kornelsen, J., Smith, S. D., & McIver, T. A. (2015). A neural correlate of visceral emotional responses: evidence from fMRI of the thoracic spinal cord. *Soc Cogn Affect Neurosci, 10*(4), 584-588. doi:10.1093/scan/nsu092

Kornelsen, J., Smith, S. D., McIver, T. A., Sboto-Frankenstein, U., Latta, P., & Tomanek, B. (2013). Functional MRI of the thoracic spinal cord during vibration sensation. *J Magn Reson Imaging, 37*(4), 981-985. doi:10.1002/jmri.23819

Kozyrev, N., Figley, C. R., Alexander, M. S., Richards, J. S., Bosma, R. L., & Stroman, P. W. (2012). Neural correlates of sexual arousal in the spinal cords of able-bodied men: a spinal fMRI investigation. *J Sex Marital Ther, 38*(5), 418-435. doi:10.1080/0092623X.2011.606887

Loukas, M., Klaassen, Z., Merbs, W., Tubbs, R. S., Gielecki, J., & Zurada, A. (2010). A review of the thoracic splanchnic nerves and celiac ganglia. *Clin Anat, 23*(5), 512-522. doi:10.1002/ca.20964

Marek, S., & Dosenbach, N. U. F. (2018). The frontoparietal network: function, electrophysiology, and importance of individual precision mapping. *Dialogues Clin Neurosci, 20*(2), 133-140.

McLean, C. P., Asnaani, A., Litz, B. T., & Hofmann, S. G. (2011). Gender differences in anxiety disorders: prevalence, course of illness, comorbidity and burden of illness. *J Psychiatr Res, 45*(8), 1027-1035. doi:10.1016/j.jpsychires.2011.03.006

McLeod, D. R., Hoehn-Saric, R., Zimmerli, W. D., De Souza, E. B., & Oliver, L. K. (1990). Treatment effects of alprazolam and imipramine: physiological versus subjective changes in patients with generalized anxiety disorder. *Biol Psychiatry, 28*(10), 849-861. doi:10.1016/0006-3223(90)90567-l

Mennin, D. S., Heimberg, R. G., Turk, C. L., & Fresco, D. M. (2005). Preliminary evidence for an emotion dysregulation model of generalized anxiety disorder. *Behav Res Ther, 43*(10), 1281-1310. doi:10.1016/j.brat.2004.08.008

Menon, V. (2015). Salience Network. In A. Toga (Ed.), *Brain Mapping: An Encyclopedic Reference* (pp. 597-611): Elsevier: Academic Press.

Mochcovitch, M. D., da Rocha Freire, R. C., Garcia, R. F., & Nardi, A. E. (2014). A systematic review of fMRI studies in generalized anxiety disorder: evaluating its neural and cognitive basis. *J Affect Disord, 167*, 336-342. doi:10.1016/j.jad.2014.06.041

Newman, M. G., & Llera, S. J. (2011). A novel theory of experiential avoidance in generalized anxiety disorder: a review and synthesis of research supporting a contrast avoidance model of worry. *Clin Psychol Rev, 31*(3), 371-382. doi:10.1016/j.cpr.2011.01.008

Rosazza, C., & Minati, L. (2011). Resting-state brain networks: literature review and clinical applications. *Neurol Sci, 32*(5), 773-785. doi:10.1007/s10072-011-0636-y

San Emeterio Nateras, O., Yu, F., Muir, E. R., Bazan, C., 3rd, Franklin, C. G., Li, W., . . . Duong, T. Q. (2016). Intrinsic Resting-State Functional Connectivity in the Human Spinal Cord at 3.0 T. *Radiology, 279*(1), 262-268. doi:10.1148/radiol.2015150768

Shirer, W. R., Ryali, S., Rykhlevskaia, E., Menon, V., & Greicius, M. D. (2012). Decoding subject-driven cognitive states with whole-brain connectivity patterns. *Cereb Cortex, 22*(1), 158-165. doi:10.1093/cercor/bhr099

Smith, S. A., Jones, C. K., Gifford, A., Belegu, V., Chodkowski, B., Farrell, J. A., . . . van Zijl, P. C. (2010). Reproducibility of tract-specific magnetization transfer and diffusion tensor

imaging in the cervical spinal cord at 3 tesla. *NMR Biomed, 23*(2), 207-217. doi:10.1002/nbm.1447

Stein, M. B., & Sareen, J. (2015). CLINICAL PRACTICE. Generalized Anxiety Disorder. *N Engl J Med, 373*(21), 2059-2068. doi:10.1056/NEJMcp1502514

Thurnher, M. M., & Bammer, R. (2006). Diffusion-weighted magnetic resonance imaging of the spine and spinal cord. *Semin Roentgenol, 41*(4), 294-311. doi:10.1053/j.ro.2006.07.003

Tolin, D. F., Davies, C. D., Moskow, D. M., & Hofmann, S. G. (2020). Biofeedback and Neurofeedback for Anxiety Disorders: A Quantitative and Qualitative Systematic Review. *Adv Exp Med Biol, 1191*, 265-289. doi:10.1007/978-981-32-9705-0_16

Vesga-Lopez, O., Schneier, F. R., Wang, S., Heimberg, R. G., Liu, S. M., Hasin, D. S., & Blanco, C. (2008). Gender differences in generalized anxiety disorder: results from the National Epidemiologic Survey on Alcohol and Related Conditions (NESARC). *J Clin Psychiatry, 69*(10), 1606-1616.

Watson, J. C., Greenberg, L. S., & American Psychological Association. (2017). *Emotion-focused therapy for generalized anxiety*. Washington, DC: American Psychological Association.

Wheeler-Kingshott, C. A., Hickman, S. J., Parker, G. J., Ciccarelli, O., Symms, M. R., Miller, D. H., & Barker, G. J. (2002). Investigating cervical spinal cord structure using axial diffusion tensor imaging. *Neuroimage, 16*(1), 93-102. doi:10.1006/nimg.2001.1022

Wilm, B. J., Gamper, U., Henning, A., Pruessmann, K. P., Kollias, S. S., & Boesiger, P. (2009). Diffusion-weighted imaging of the entire spinal cord. *NMR Biomed, 22*(2), 174-181. doi:10.1002/nbm.1298

SIEMENS MAGNETOM TrioTim syngo MR B17

\\USER\HSC Research\NRC\RI2016:131 GAD MB\Localizer 3 planes

TA: 0:37 PAT: Off Voxel size: 1.1×1.0×7.0 mm Rel. SNR: 1.00 SIEMENS: gre

Properties

Prio Recon	Off
Before measurement	
After measurement	
Load to viewer	On
Inline movie	Off
Auto store images	On
Load to stamp segments	On
Load images to graphic segments	On
Auto open inline display	Off
Start measurement without further preparation	Off
Wait for user to start	Off
Start measurements	single

Routine

Slice group 1	
Slices	3
Dist. factor	20 %
Position	L0.0 A40.6 H23.0
Orientation	Sagittal
Phase enc. dir.	A >> P
Rotation	0.00 deg
Slice group 2	
Slices	3
Dist. factor	20 %
Position	L0.0 A40.6 H35.1
Orientation	Transversal
Phase enc. dir.	A >> P
Rotation	0.00 deg
Slice group 3	
Slices	3
Dist. factor	20 %
Position	L0.0 A40.6 H23.0
Orientation	Coronal
Phase enc. dir.	R >> L
Rotation	0.00 deg
Phase oversampling	0 %
FoV read	250 mm
FoV phase	100.0 %
Slice thickness	7.0 mm
TR	8.6 ms
TE	4.00 ms
Averages	2
Concatenations	9
Filter	Prescan Normalize, Elliptical filter
Coil elements	HEA;HEP

Contrast

TD	0 ms
MTC	Off
Magn. preparation	None
Flip angle	20 deg
Fat suppr.	None
Water suppr.	None
Averaging mode	Short term
Reconstruction	Magnitude
Measurements	1
Multiple series	Each measurement

Resolution

Base resolution	256
Phase resolution	90 %
Phase partial Fourier	Off
Interpolation	On
PAT mode	None
Matrix Coil Mode	Auto (CP)
Image Filter	Off
Distortion Corr.	Off
Unfiltered images	Off
Prescan Normalize	On
Normalize	Off
B1 filter	Off
Raw filter	Off
Elliptical filter	On
Mode	Inplane

Geometry

Multi-slice mode	Sequential
Series	Interleaved
Saturation mode	Standard
Special sat.	None
Tim CT mode	Off

System

Body	Off
HEP	On
HEA	On
SP4	Off
SP2	Off
SP8	Off
SP6	Off
SP3	Off
SP1	Off
SP7	Off
SP5	Off
Positioning mode	REF
Table position	H
Table position	0 mm
MSMA	S - C - T
Sagittal	L >> R
Coronal	P >> A
Transversal	F >> H
Save uncombined	Off
Coil Combine Mode	Adaptive Combine
Auto Coil Select	Default
Shim mode	Tune up
Adjust with body coil	Off
Confirm freq. adjustment	Off
Assume Silicone	Off
? Ref. amplitude 1H	0.000 V
Adjustment Tolerance	Auto
Adjust volume	
Position	Isocenter
Orientation	Transversal
Rotation	0.00 deg
R >> L	350 mm
A >> P	263 mm
F >> H	350 mm

Physio

1st Signal/Mode	None
Segments	1
Tagging	None

SIEMENS MAGNETOM TrioTim syngo MR B17

Dark blood	Off
Resp. control	Off

Inline

Subtract	Off
Liver registration	Off
Std-Dev-Sag	Off
Std-Dev-Cor	Off
Std-Dev-Tra	Off
Std-Dev-Time	Off
MIP-Sag	Off
MIP-Cor	Off
MIP-Tra	Off
MIP-Time	Off
Save original images	On
Wash - In	Off
Wash - Out	Off
TTP	Off
PEI	Off
MIP - time	Off

Sequence

Introduction	On
Dimension	2D
Phase stabilisation	Off
Asymmetric echo	Allowed
Contrasts	1
Bandwidth	320 Hz/Px
Flow comp.	No
Allowed delay	0 s
RF pulse type	Normal
Gradient mode	Normal
Excitation	Slice-sel.
RF spoiling	On

SIEMENS MAGNETOM TrioTim syngo MR B17

\\USER\HSC Research\NRC\RI2016:131 GAD MB\Sag 3D MPRAGE iso

TA: 4:26 PAT: 2 Voxel size: 1.0×1.0×1.0 mm Rel. SNR: 1.00 SIEMENS: tfl

Properties

Prio Recon	Off
Before measurement	
After measurement	
Load to viewer	On
Inline movie	Off
Auto store images	On
Load to stamp segments	Off
Load images to graphic segments	Off
Auto open inline display	Off
Start measurement without further preparation	On
Wait for user to start	Off
Start measurements	single

Routine

Slab group 1	
Slabs	1
Dist. factor	50 %
Position	L2.5 A21.3 F16.0
Orientation	Sagittal
Phase enc. dir.	A >> P
Rotation	0.00 deg
Phase oversampling	0 %
Slice oversampling	18.2 %
Slices per slab	176
FoV read	250 mm
FoV phase	100.0 %
Slice thickness	0.98 mm
TR	1900 ms
TE	2.47 ms
Averages	1
Concatenations	1
Filter	Prescan Normalize
Coil elements	HEA;HEP

Contrast

Magn. preparation	Non-sel. IR
TI	900 ms
Flip angle	9 deg
Fat suppr.	None
Water suppr.	None
Averaging mode	Long term
Reconstruction	Magnitude
Measurements	1
Multiple series	Each measurement

Resolution

Base resolution	256
Phase resolution	100 %
Slice resolution	100 %
Phase partial Fourier	Off
Slice partial Fourier	Off
Interpolation	On
PAT mode	GRAPPA
Accel. factor PE	2
Ref. lines PE	24
Accel. factor 3D	1
Matrix Coil Mode	Auto (Triple)
Reference scan mode	Integrated
Image Filter	Off
Distortion Corr.	Off
Unfiltered images	Off
Prescan Normalize	On
Normalize	Off
B1 filter	Off
Raw filter	Off
Elliptical filter	Off

Geometry

Multi-slice mode	Single shot
Series	Ascending

System

Body	Off
HEP	On
HEA	On
SP4	Off
SP2	Off
SP8	Off
SP6	Off
SP3	Off
SP1	Off
SP7	Off
SP5	Off
Positioning mode	FIX
Table position	H
Table position	0 mm
MSMA	S - C - T
Sagittal	R >> L
Coronal	A >> P
Transversal	F >> H
Save uncombined	Off
Coil Combine Mode	Adaptive Combine
Auto Coil Select	Default
Shim mode	Tune up
Adjust with body coil	On
Confirm freq. adjustment	Off
Assume Silicone	Off
? Ref. amplitude 1H	0.000 V
Adjustment Tolerance	Auto
Adjust volume	
Position	Isocenter
Orientation	Transversal
Rotation	0.00 deg
R >> L	350 mm
A >> P	263 mm
F >> H	350 mm

Physio

1st Signal/Mode	None
Dark blood	Off
Resp. control	Off

Inline

Subtract	Off
Std-Dev-Sag	Off
Std-Dev-Cor	Off
Std-Dev-Tra	Off
Std-Dev-Time	Off
MIP-Sag	Off
MIP-Cor	Off
MIP-Tra	Off
MIP-Time	Off
Save original images	On

SIEMENS MAGNETOM TrioTim syngo MR B17

Sequence	
Introduction	On
Dimension	3D
Elliptical scanning	Off
Asymmetric echo	Allowed
Bandwidth	170 Hz/Px
Flow comp.	No
Echo spacing	7.3 ms
RF pulse type	Normal
Gradient mode	Fast*
Excitation	Non-sel.
RF spoiling	On

SIEMENS MAGNETOM TrioTim syngo MR B17

\\USER\HSC Research\NRC\RI2016:131 GAD MB\MB_FMRI_RL_FIELDMAP_se

TA: 0:41 PAT: Off Voxel size: 2.0×2.0×2.0 mm Rel. SNR: 1.00 USER: cmrr_mbep2d_se

Properties

Prio Recon	Off
Before measurement	
After measurement	
Load to viewer	On
Inline movie	Off
Auto store images	On
Load to stamp segments	Off
Load images to graphic segments	Off
Auto open inline display	Off
Start measurement without further preparation	On
Wait for user to start	Off
Start measurements	single

Routine

Slice group 1	
Slices	72
Dist. factor	0 %
Position	L2.5 A21.3 F16.0
Orientation	T > C4.4 > S0.3
Phase enc. dir.	R >> L
Rotation	90.00 deg
Phase oversampling	0 %
FoV read	208 mm
FoV phase	86.5 %
Slice thickness	2.00 mm
TR	10170 ms
TE	86.6 ms
Multi-band accel. factor	1
Filter	None
Coil elements	HEA;HEP

Contrast

MTC	Off
Magn. preparation	None
Flip angle	90 deg
Refocus flip angle	180 deg
Fat suppr.	Fat sat.
Grad. rev. fat suppr.	Enabled
Averaging mode	Long term
Reconstruction	Magnitude
Measurements	3
Delay in TR	0 ms
Multiple series	Off

Resolution

Base resolution	104
Phase resolution	100 %
Phase partial Fourier	Off
Interpolation	Off
PAT mode	None
Matrix Coil Mode	Auto (CP)
Distortion Corr.	Off
Prescan Normalize	Off
Raw filter	On
Elliptical filter	Off
Hamming	Off

Geometry

Multi-slice mode	Interleaved
Series	Interleaved
Special sat.	None

System

Body	Off
HEP	On
HEA	On
SP4	Off
SP2	Off
SP8	Off
SP6	Off
SP3	Off
SP1	Off
SP7	Off
SP5	Off
Positioning mode	FIX
Table position	H
Table position	0 mm
MSMA	S - C - T
Sagittal	R >> L
Coronal	A >> P
Transversal	F >> H
Coil Combine Mode	Sum of Squares
Auto Coil Select	Default
Shim mode	Standard
Adjust with body coil	Off
Confirm freq. adjustment	Off
Assume Silicone	Off
? Ref. amplitude 1H	0.000 V
Adjustment Tolerance	Auto
Adjust volume	
Position	L2.5 A21.3 F16.0
Orientation	T > C4.4 > S0.3
Rotation	90.00 deg
A >> P	208 mm
R >> L	180 mm
F >> H	144 mm

Physio

1st Signal/Mode	None

BOLD

GLM Statistics	Off
Dynamic t-maps	Off
Starting ignore meas	0
Ignore after transition	0
Model transition states	On
Temp. highpass filter	On
Threshold	4.00
Paradigm size	3
Meas[1]	Baseline
Meas[2]	Baseline
Meas[3]	Active
Motion correction	Off
Spatial filter	Off

Sequence

Introduction	Off
Contrasts	1
Bandwidth	2290 Hz/Px
Free echo spacing	Off
Echo spacing	0.69 ms
EPI factor	90
RF pulse type	Normal
Gradient mode	Fast

SIEMENS MAGNETOM TrioTim syngo MR B17

SENSE1 coil combine	Off
Invert RO/PE polarity	Off
Force equal slice timing	Off
FFT scale factor	1.00
Physio recording	Off
Triggering scheme	Standard

SIEMENS MAGNETOM TrioTim syngo MR B17

\\USER\HSC Research\NRC\RI2016:131 GAD MB\MB_FMRI_LR_FIELDMAP_se

TA: 0:41 PAT: Off Voxel size: 2.0×2.0×2.0 mm Rel. SNR: 1.00 USER: cmrr_mbep2d_se

Properties

Prio Recon	Off
Before measurement	
After measurement	
Load to viewer	On
Inline movie	Off
Auto store images	On
Load to stamp segments	Off
Load images to graphic segments	Off
Auto open inline display	Off
Start measurement without further preparation	On
Wait for user to start	Off
Start measurements	single

Routine

Slice group 1	
Slices	72
Dist. factor	0 %
Position	L2.5 A21.3 F16.0
Orientation	T > C4.4 > S0.3
Phase enc. dir.	L >> R
Rotation	-90.00 deg
Phase oversampling	0 %
FoV read	208 mm
FoV phase	86.5 %
Slice thickness	2.00 mm
TR	10170 ms
TE	86.6 ms
Multi-band accel. factor	1
Filter	None
Coil elements	HEA;HEP

Contrast

MTC	Off
Magn. preparation	None
Flip angle	90 deg
Refocus flip angle	180 deg
Fat suppr.	Fat sat.
Grad. rev. fat suppr.	Enabled
Averaging mode	Long term
Reconstruction	Magnitude
Measurements	3
Delay in TR	0 ms
Multiple series	Off

Resolution

Base resolution	104
Phase resolution	100 %
Phase partial Fourier	Off
Interpolation	Off
PAT mode	None
Matrix Coil Mode	Auto (CP)
Distortion Corr.	Off
Prescan Normalize	Off
Raw filter	On
Elliptical filter	Off
Hamming	Off

Geometry

Multi-slice mode	Interleaved
Series	Interleaved
Special sat.	None

System

Body	Off
HEP	On
HEA	On
SP4	Off
SP2	Off
SP8	Off
SP6	Off
SP3	Off
SP1	Off
SP7	Off
SP5	Off
Positioning mode	FIX
Table position	H
Table position	0 mm
MSMA	S - C - T
Sagittal	R >> L
Coronal	A >> P
Transversal	F >> H
Coil Combine Mode	Sum of Squares
Auto Coil Select	Default
Shim mode	Standard
Adjust with body coil	Off
Confirm freq. adjustment	Off
Assume Silicone	Off
? Ref. amplitude 1H	0.000 V
Adjustment Tolerance	Auto
Adjust volume	
Position	L2.5 A21.3 F16.0
Orientation	T > C4.4 > S0.3
Rotation	-90.00 deg
A >> P	208 mm
R >> L	180 mm
F >> H	144 mm

Physio

1st Signal/Mode	None

BOLD

GLM Statistics	Off
Dynamic t-maps	Off
Starting ignore meas	0
Ignore after transition	0
Model transition states	On
Temp. highpass filter	On
Threshold	4.00
Paradigm size	3
Meas[1]	Baseline
Meas[2]	Baseline
Meas[3]	Active
Motion correction	Off
Spatial filter	Off

Sequence

Introduction	Off
Contrasts	1
Bandwidth	2290 Hz/Px
Free echo spacing	Off
Echo spacing	0.69 ms
EPI factor	90
RF pulse type	Normal
Gradient mode	Fast

SIEMENS MAGNETOM TrioTim syngo MR B17

SENSE1 coil combine	Off
Invert RO/PE polarity	Off
Force equal slice timing	Off
FFT scale factor	1.00
Physio recording	Off
Triggering scheme	Standard

SIEMENS MAGNETOM TrioTim syngo MR B17

\\USER\HSC Research\NRC\RI2016:131 GAD MB\MB_FMRI_RESTING_STATE

TA: 7:12 PAT: Off Voxel size: 2.5×2.5×2.5 mm Rel. SNR: 1.00 USER: cmrr_mbep2d_bold

Properties

Prio Recon	Off
Before measurement	
After measurement	
Load to viewer	On
Inline movie	Off
Auto store images	On
Load to stamp segments	Off
Load images to graphic segments	Off
Auto open inline display	Off
Start measurement without further preparation	On
Wait for user to start	Off
Start measurements	single

Routine

Slice group 1	
Slices	85
Dist. factor	0 %
Position	L2.5 A21.3 F16.0
Orientation	T > C4.4 > S0.3
Phase enc. dir.	R >> L
Rotation	90.00 deg
Phase oversampling	0 %
FoV read	250 mm
FoV phase	78.0 %
Slice thickness	2.50 mm
TR	1500 ms
TE	38.6 ms
Multi-band accel. factor	5
Filter	None
Coil elements	HEP

Contrast

MTC	Off
Magn. preparation	None
Flip angle	61 deg
Fat suppr.	Fat sat.
Averaging mode	Long term
Reconstruction	Magnitude
Measurements	280
Delay in TR	0 ms
Multiple series	Off

Resolution

Base resolution	100
Phase resolution	100 %
Phase partial Fourier	Off
Interpolation	Off
PAT mode	None
Matrix Coil Mode	Auto (CP)
Distortion Corr.	Off
Prescan Normalize	Off
Raw filter	On
Elliptical filter	Off
Hamming	Off

Geometry

Multi-slice mode	Interleaved
Series	Interleaved
Special sat.	None

System

Body	Off
HEP	On
SP4	Off
SP2	Off
SP8	Off
SP6	Off
SP3	Off
SP1	Off
SP7	Off
SP5	Off
Positioning mode	FIX
Table position	H
Table position	0 mm
MSMA	S - C - T
Sagittal	R >> L
Coronal	A >> P
Transversal	F >> H
Coil Combine Mode	Sum of Squares
Auto Coil Select	Default
Shim mode	Standard
Adjust with body coil	Off
Confirm freq. adjustment	Off
Assume Silicone	Off
? Ref. amplitude 1H	0.000 V
Adjustment Tolerance	Auto
Adjust volume	
Position	L2.5 A21.3 F16.0
Orientation	T > C4.4 > S0.3
Rotation	90.00 deg
A >> P	250 mm
R >> L	195 mm
F >> H	213 mm

Physio

1st Signal/Mode	None

BOLD

GLM Statistics	Off
Dynamic t-maps	Off
Starting ignore meas	0
Ignore after transition	0
Model transition states	On
Temp. highpass filter	On
Threshold	4.00
Paradigm size	3
Meas[1]	Baseline
Meas[2]	Baseline
Meas[3]	Active
Motion correction	Off
Spatial filter	Off

Sequence

Introduction	Off
Contrasts	1
Bandwidth	2272 Hz/Px
Flow comp.	No
Free echo spacing	Off
Echo spacing	0.69 ms
EPI factor	78
Gradient mode	Fast*
RF spoiling	Off
Excite pulse duration	6760 us
Single-band images	Off

SIEMENS MAGNETOM TrioTim syngo MR B17

MB LeakBlock kernel	On
MB dual kernel	Off
MB RF phase scramble	Off
SENSE1 coil combine	Off
Invert RO/PE polarity	Off
Force equal slice timing	Off
Online multi-band recon.	Online
FFT scale factor	1.00
Physio recording	Off
Triggering scheme	Standard

SIEMENS MAGNETOM TrioTim syngo MR B17

\\USER\HSC Research\NRC\RI2016:131 GAD MB\MB_FMRI_BRAIN_TASK

TA: 3:17 PAT: Off Voxel size: 2.5×2.5×2.5 mm Rel. SNR: 1.00 USER: cmrr_mbep2d_bold

Properties

Prio Recon	Off
Before measurement	
After measurement	
Load to viewer	On
Inline movie	Off
Auto store images	On
Load to stamp segments	Off
Load images to graphic segments	Off
Auto open inline display	Off
Start measurement without further preparation	On
Wait for user to start	Off
Start measurements	single

Routine

Slice group 1	
Slices	85
Dist. factor	0 %
Position	L2.5 A21.3 F16.0
Orientation	T > C4.4 > S0.3
Phase enc. dir.	R >> L
Rotation	90.00 deg
Phase oversampling	0 %
FoV read	250 mm
FoV phase	78.0 %
Slice thickness	2.50 mm
TR	1500 ms
TE	38.6 ms
Multi-band accel. factor	5
Filter	None
Coil elements	HEP
Body	Off
HEP	On
SP4	Off
SP2	Off
SP8	Off
SP6	Off
SP3	Off
SP1	Off
SP7	Off
SP5	Off
Positioning mode	FIX
Table position	H
Table position	0 mm
MSMA	S - C - T
Sagittal	R >> L
Coronal	A >> P
Transversal	F >> H
Coil Combine Mode	Sum of Squares
Auto Coil Select	Default
Shim mode	Standard
Adjust with body coil	Off
Confirm freq. adjustment	Off
Assume Silicone	Off
? Ref. amplitude 1H	0.000 V
Adjustment Tolerance	Auto
Adjust volume	
Position	L2.5 A21.3 F16.0
Orientation	T > C4.4 > S0.3
Rotation	90.00 deg
A >> P	250 mm
R >> L	195 mm
F >> H	213 mm

Contrast

MTC	Off
Magn. preparation	None
Flip angle	61 deg
Fat suppr.	Fat sat.
Averaging mode	Long term
Reconstruction	Magnitude
Measurements	123
Delay in TR	0 ms
Multiple series	Off

Physio

1st Signal/Mode	None

BOLD

GLM Statistics	Off
Dynamic t-maps	Off
Starting ignore meas	0
Ignore after transition	0
Model transition states	On
Temp. highpass filter	On
Threshold	4.00
Paradigm size	3
Meas[1]	Baseline
Meas[2]	Baseline
Meas[3]	Active
Motion correction	Off
Spatial filter	Off

Resolution

Base resolution	100
Phase resolution	100 %
Phase partial Fourier	Off
Interpolation	Off
PAT mode	None
Matrix Coil Mode	Auto (CP)
Distortion Corr.	Off
Prescan Normalize	Off
Raw filter	On
Elliptical filter	Off
Hamming	Off

Sequence

Introduction	Off
Contrasts	1
Bandwidth	2272 Hz/Px
Flow comp.	No
Free echo spacing	Off
Echo spacing	0.69 ms
EPI factor	78
Gradient mode	Fast*
RF spoiling	Off
Excite pulse duration	6760 us
Single-band images	Off

Geometry

Multi-slice mode	Interleaved
Series	Interleaved
Special sat.	None

System

SIEMENS MAGNETOM TrioTim syngo MR B17

MB LeakBlock kernel	On
MB dual kernel	Off
MB RF phase scramble	Off
SENSE1 coil combine	Off
Invert RO/PE polarity	Off
Force equal slice timing	Off
Online multi-band recon.	Online
FFT scale factor	1.00
Physio recording	Off
Triggering scheme	Standard

SIEMENS MAGNETOM TrioTim syngo MR B17

\\USER\HSC Research\NRC\RI2016:131 GAD MB\Localizer brain

TA: 0:37 PAT: Off Voxel size: 1.1×1.0×7.0 mm Rel. SNR: 1.00 SIEMENS: gre

Properties

Prio Recon	Off
Before measurement	
After measurement	
Load to viewer	On
Inline movie	Off
Auto store images	On
Load to stamp segments	On
Load images to graphic segments	On
Auto open inline display	Off
Start measurement without further preparation	Off
Wait for user to start	Off
Start measurements	single

Routine

Slice group 1	
Slices	3
Dist. factor	20 %
Position	L0.0 A35.7 H98.7
Orientation	Sagittal
Phase enc. dir.	A >> P
Rotation	0.00 deg
Slice group 2	
Slices	3
Dist. factor	20 %
Position	L0.0 A35.7 H110.8
Orientation	Transversal
Phase enc. dir.	A >> P
Rotation	0.00 deg
Slice group 3	
Slices	3
Dist. factor	20 %
Position	L0.0 A35.7 H98.7
Orientation	Coronal
Phase enc. dir.	R >> L
Rotation	0.00 deg
Phase oversampling	0 %
FoV read	250 mm
FoV phase	100.0 %
Slice thickness	7.0 mm
TR	8.6 ms
TE	4.00 ms
Averages	2
Concatenations	9
Filter	Distortion Corr.(2D), Prescan Normalize, Elliptical filter
Coil elements	HEP;NE1,2

Contrast

TD	0 ms
MTC	Off
Magn. preparation	None
Flip angle	20 deg
Fat suppr.	None
Water suppr.	None
Averaging mode	Short term
Reconstruction	Magnitude
Measurements	1
Multiple series	Each measurement

Resolution

Base resolution	256
Phase resolution	90 %
Phase partial Fourier	Off
Interpolation	On
PAT mode	None
Matrix Coil Mode	Auto (CP)
Image Filter	Off
Distortion Corr.	On
Mode	2D
Unfiltered images	Off
Unfiltered images	Off
Prescan Normalize	On
Normalize	Off
B1 filter	Off
Raw filter	Off
Elliptical filter	On
Mode	Inplane

Geometry

Multi-slice mode	Sequential
Series	Interleaved
Saturation mode	Standard
Special sat.	None
Tim CT mode	Off

System

Body	Off
NE2	On
NE1	On
HEP	On
SP4	Off
SP2	Off
SP8	Off
SP6	Off
SP3	Off
SP1	Off
SP7	Off
SP5	Off
Positioning mode	ISO
Table position	H
Table position	99 mm
MSMA	S - C - T
Sagittal	L >> R
Coronal	P >> A
Transversal	F >> H
Save uncombined	Off
Coil Combine Mode	Adaptive Combine
Auto Coil Select	Default
Shim mode	Tune up
Adjust with body coil	Off
Confirm freq. adjustment	Off
Assume Silicone	Off
? Ref. amplitude 1H	0.000 V
Adjustment Tolerance	Auto
Adjust volume	
Position	Isocenter
Orientation	Transversal
Rotation	0.00 deg
R >> L	350 mm
A >> P	263 mm
F >> H	350 mm

Physio

1st Signal/Mode	None

SIEMENS MAGNETOM TrioTim syngo MR B17

Segments	1
Tagging	None
Dark blood	Off
Resp. control	Off

Inline

Subtract	Off
Liver registration	Off
Std-Dev-Sag	Off
Std-Dev-Cor	Off
Std-Dev-Tra	Off
Std-Dev-Time	Off
MIP-Sag	Off
MIP-Cor	Off
MIP-Tra	Off
MIP-Time	Off
Save original images	On
Wash - In	Off
Wash - Out	Off
TTP	Off
PEI	Off
MIP - time	Off

Sequence

Introduction	On
Dimension	2D
Phase stabilisation	Off
Asymmetric echo	Allowed
Contrasts	1
Bandwidth	320 Hz/Px
Flow comp.	No
Allowed delay	0 s
RF pulse type	Normal
Gradient mode	Normal
Excitation	Slice-sel.
RF spoiling	On

SIEMENS MAGNETOM TrioTim syngo MR B17

\\USER\HSC Research\NRC\RI2016:131 GAD MB\localizer c-spine

TA: 0:15 PAT: Off Voxel size: 1.5×1.2×6.0 mm Rel. SNR: 1.00 SIEMENS: gre

Properties

Prio Recon	Off
Before measurement	
After measurement	
Load to viewer	On
Inline movie	Off
Auto store images	On
Load to stamp segments	Off
Load images to graphic segments	Off
Auto open inline display	Off
Start measurement without further preparation	Off
Wait for user to start	Off
Start measurements	single

Routine

Slice group 1	
Slices	3
Dist. factor	50 %
Position	L2.3 A6.5 F56.0
Orientation	C > T-15.6 > S0.1
Phase enc. dir.	R >> L
Rotation	0.00 deg
Slice group 2	
Slices	3
Dist. factor	50 %
Position	L0.0 A21.8 H2.5
Orientation	Sagittal
Phase enc. dir.	A >> P
Rotation	0.00 deg
Phase oversampling	38 %
FoV read	300 mm
FoV phase	100.0 %
Slice thickness	6.0 mm
TR	7.8 ms
TE	3.69 ms
Averages	1
Concatenations	6
Filter	Distortion Corr.(2D)
Coil elements	HEP;NE1,2;SP1,2

Contrast

TD	0 ms
MTC	Off
Magn. preparation	None
Flip angle	20 deg
Fat suppr.	None
Water suppr.	None
Averaging mode	Short term
Reconstruction	Magnitude
Measurements	1
Multiple series	Each measurement

Resolution

Base resolution	256
Phase resolution	80 %
Phase partial Fourier	Off
Interpolation	On
PAT mode	None
Matrix Coil Mode	Auto (CP)
Image Filter	Off
Distortion Corr.	On
Mode	2D
Unfiltered images	Off
Prescan Normalize	Off
Normalize	Off
B1 filter	Off
Raw filter	Off
Elliptical filter	Off

Geometry

Multi-slice mode	Sequential
Series	Interleaved
Saturation mode	Standard
Special sat.	None
Tim CT mode	Off

System

Body	Off
NE2	On
NE1	On
HEP	On
HEA	Off
SP4	Off
SP2	On
SP8	Off
SP6	Off
SP3	Off
SP1	On
SP7	Off
SP5	Off
Positioning mode	ISO
Table position	F
Table position	26 mm
MSMA	S - C - T
Sagittal	L >> R
Coronal	P >> A
Transversal	H >> F
Save uncombined	Off
Coil Combine Mode	Adaptive Combine
Auto Coil Select	Default
Shim mode	Tune up
Adjust with body coil	Off
Confirm freq. adjustment	Off
Assume Silicone	Off
? Ref. amplitude 1H	0.000 V
Adjustment Tolerance	Auto
Adjust volume	
Position	Isocenter
Orientation	Transversal
Rotation	0.00 deg
R >> L	350 mm
A >> P	263 mm
F >> H	350 mm

Physio

1st Signal/Mode	None
Segments	1
Tagging	None
Dark blood	Off
Resp. control	Off

Inline

Subtract	Off

SIEMENS MAGNETOM TrioTim syngo MR B17

Liver registration	Off
Std-Dev-Sag	Off
Std-Dev-Cor	Off
Std-Dev-Tra	Off
Std-Dev-Time	Off
MIP-Sag	Off
MIP-Cor	Off
MIP-Tra	Off
MIP-Time	Off
Save original images	On
Wash - In	Off
Wash - Out	Off
TTP	Off
PEI	Off
MIP - time	Off

Sequence

Introduction	On
Dimension	2D
Phase stabilisation	Off
Asymmetric echo	Off
Contrasts	1
Bandwidth	320 Hz/Px
Flow comp.	No
Allowed delay	0 s
RF pulse type	Normal
Gradient mode	Normal
Excitation	Slice-sel.
RF spoiling	On

SIEMENS MAGNETOM TrioTim syngo MR B17

\\USER\HSC Research\NRC\RI2016:131 GAD MB\localizer t-spine

TA: 0:27 PAT: Off Voxel size: 1.7×1.4×6.0 mm Rel. SNR: 1.00 SIEMENS: gre

Properties

Prio Recon	Off
Before measurement	
After measurement	
Load to viewer	On
Inline movie	Off
Auto store images	On
Load to stamp segments	On
Load images to graphic segments	Off
Auto open inline display	Off
Start measurement without further preparation	Off
Wait for user to start	Off
Start measurements	single

Routine

Slice group 1	
Slices	10
Dist. factor	50 %
Position	L0.0 P20.1 F202.0
Orientation	C > T-5.9
Phase enc. dir.	R >> L
Rotation	0.00 deg
Slice group 2	
Slices	3
Dist. factor	50 %
Position	L6.8 P0.0 F200.0
Orientation	Sagittal
Phase enc. dir.	A >> P
Rotation	0.00 deg
Phase oversampling	25 %
FoV read	350 mm
FoV phase	100.0 %
Slice thickness	6.0 mm
TR	7.8 ms
TE	3.69 ms
Averages	1
Concatenations	13
Filter	Distortion Corr.(2D)
Coil elements	NE2;SP1-3

Contrast

TD	0 ms
MTC	Off
Magn. preparation	None
Flip angle	20 deg
Fat suppr.	None
Water suppr.	None
Averaging mode	Short term
Reconstruction	Magnitude
Measurements	1
Multiple series	Each measurement

Resolution

Base resolution	256
Phase resolution	80 %
Phase partial Fourier	Off
Interpolation	On
PAT mode	None
Matrix Coil Mode	Auto (CP)
Image Filter	Off
Distortion Corr.	On
Mode	2D
Unfiltered images	Off
Prescan Normalize	Off
Normalize	Off
B1 filter	Off
Raw filter	Off
Elliptical filter	Off

Geometry

Multi-slice mode	Sequential
Series	Interleaved
Saturation mode	Standard
Special sat.	None
Tim CT mode	Off

System

Body	Off
NE2	On
NE1	Off
HEP	Off
SP4	Off
SP2	On
SP8	Off
SP6	Off
SP3	On
SP1	On
SP7	Off
SP5	Off
Positioning mode	ISO
Table position	F
Table position	202 mm
MSMA	S - C - T
Sagittal	L >> R
Coronal	P >> A
Transversal	H >> F
Save uncombined	Off
Coil Combine Mode	Adaptive Combine
Auto Coil Select	Default
Shim mode	Tune up
Adjust with body coil	Off
Confirm freq. adjustment	Off
Assume Silicone	Off
? Ref. amplitude 1H	0.000 V
Adjustment Tolerance	Auto
Adjust volume	
Position	Isocenter
Orientation	Transversal
Rotation	0.00 deg
R >> L	350 mm
A >> P	263 mm
F >> H	350 mm

Physio

1st Signal/Mode	None
Segments	1
Tagging	None
Dark blood	Off
Resp. control	Off

Inline

Subtract	Off
Liver registration	Off

SIEMENS MAGNETOM TrioTim syngo MR B17

Std-Dev-Sag	Off
Std-Dev-Cor	Off
Std-Dev-Tra	Off
Std-Dev-Time	Off
MIP-Sag	Off
MIP-Cor	Off
MIP-Tra	Off
MIP-Time	Off
Save original images	On
Wash - In	Off
Wash - Out	Off
TTP	Off
PEI	Off
MIP - time	Off

Sequence

Introduction	On
Dimension	2D
Phase stabilisation	Off
Asymmetric echo	Off
Contrasts	1
Bandwidth	320 Hz/Px
Flow comp.	No
Allowed delay	0 s
RF pulse type	Normal
Gradient mode	Normal
Excitation	Slice-sel.
RF spoiling	On

SIEMENS MAGNETOM TrioTim syngo MR B17

\\USER\HSC Research\NRC\RI2016:131 GAD MB\localizer l-spine

TA: 0:27 PAT: Off Voxel size: 1.7×1.4×6.0 mm Rel. SNR: 1.00 SIEMENS: gre

Properties

Prio Recon	Off
Before measurement	
After measurement	
Load to viewer	On
Inline movie	Off
Auto store images	On
Load to stamp segments	On
Load images to graphic segments	On
Auto open inline display	Off
Start measurement without further preparation	Off
Wait for user to start	Off
Start measurements	single

Routine

Slice group 1	
Slices	10
Dist. factor	50 %
Position	L2.6 P3.0 F402.8
Orientation	C > T11.3
Phase enc. dir.	R >> L
Rotation	0.00 deg
Slice group 2	
Slices	3
Dist. factor	50 %
Position	L2.6 P0.0 F400.0
Orientation	Sagittal
Phase enc. dir.	A >> P
Rotation	0.00 deg
Phase oversampling	25 %
FoV read	350 mm
FoV phase	100.0 %
Slice thickness	6.0 mm
TR	7.8 ms
TE	3.69 ms
Averages	1
Concatenations	13
Filter	Distortion Corr.(2D)
Coil elements	SP2-4

Contrast

TD	0 ms
MTC	Off
Magn. preparation	None
Flip angle	20 deg
Fat suppr.	None
Water suppr.	None
Averaging mode	Short term
Reconstruction	Magnitude
Measurements	1
Multiple series	Each measurement

Resolution

Base resolution	256
Phase resolution	80 %
Phase partial Fourier	Off
Interpolation	On
PAT mode	None
Matrix Coil Mode	Auto (CP)
Image Filter	Off
Distortion Corr.	On
Mode	2D
Unfiltered images	Off
Prescan Normalize	Off
Normalize	Off
B1 filter	Off
Raw filter	Off
Elliptical filter	Off

Geometry

Multi-slice mode	Sequential
Series	Interleaved
Saturation mode	Standard
Special sat.	None
Tim CT mode	Off

System

Body	Off
NE2	Off
NE1	Off
HEP	Off
SP4	On
SP2	On
SP8	Off
SP6	Off
SP3	On
SP1	Off
SP7	Off
SP5	Off
Positioning mode	ISO
Table position	F
Table position	403 mm
MSMA	S - C - T
Sagittal	L >> R
Coronal	P >> A
Transversal	H >> F
Save uncombined	Off
Coil Combine Mode	Adaptive Combine
Auto Coil Select	Default
Shim mode	Tune up
Adjust with body coil	Off
Confirm freq. adjustment	Off
Assume Silicone	Off
? Ref. amplitude 1H	0.000 V
Adjustment Tolerance	Auto
Adjust volume	
Position	Isocenter
Orientation	Transversal
Rotation	0.00 deg
R >> L	350 mm
A >> P	263 mm
F >> H	350 mm

Physio

1st Signal/Mode	None
Segments	1
Tagging	None
Dark blood	Off
Resp. control	Off

Inline

Subtract	Off
Liver registration	Off

SIEMENS MAGNETOM TrioTim syngo MR B17

Std-Dev-Sag	Off
Std-Dev-Cor	Off
Std-Dev-Tra	Off
Std-Dev-Time	Off
MIP-Sag	Off
MIP-Cor	Off
MIP-Tra	Off
MIP-Time	Off
Save original images	On
Wash - In	Off
Wash - Out	Off
TTP	Off
PEI	Off
MIP - time	Off

Sequence

Introduction	On
Dimension	2D
Phase stabilisation	Off
Asymmetric echo	Off
Contrasts	1
Bandwidth	320 Hz/Px
Flow comp.	No
Allowed delay	0 s
RF pulse type	Normal
Gradient mode	Normal
Excitation	Slice-sel.
RF spoiling	On

SIEMENS MAGNETOM TrioTim syngo MR B17

\\USER\HSC Research\NRC\RI2016:131 GAD MB\Sag T2 HASTE fMRI 120 C-1

TA: 3:02 PAT: Off Voxel size: 1.5×1.5×2.0 mm Rel. SNR: 1.00 SIEMENS: haste

Properties

Prio Recon	Off
Before measurement	
After measurement	
Load to viewer	On
Inline movie	Off
Auto store images	On
Load to stamp segments	On
Load images to graphic segments	On
Auto open inline display	On
Start measurement without further preparation	On
Wait for user to start	On
Start measurements	single

Routine

Slice group 1	
Slices	9
Dist. factor	0 %
Position	R9.7 A6.6 F0.1
Orientation	S > T2.2 > C-0.6
Phase enc. dir.	A >> P
Rotation	0.00 deg
Phase oversampling	0 %
FoV read	280 mm
FoV phase	75.0 %
Slice thickness	2.0 mm
TR	750 ms
TE	79 ms
Averages	1
Concatenations	1
Filter	Distortion Corr.(2D), Normalize
Coil elements	HEA;HEP;NE1,2;SP1

Contrast

MTC	Off
Magn. preparation	None
Flip angle	100 deg
Fat suppr.	None
Water suppr.	None
Restore magn.	Off
Averaging mode	Long term
Reconstruction	Magnitude
Measurements	27
Pause after meas. 1	0.0 s
Pause after meas. 2	0.0 s
Pause after meas. 3	0.0 s
Pause after meas. 4	0.0 s
Pause after meas. 5	0.0 s
Pause after meas. 6	0.0 s
Pause after meas. 7	0.0 s
Pause after meas. 8	0.0 s
Pause after meas. 9	0.0 s
Pause after meas. 10	0.0 s
Pause after meas. 11	0.0 s
Pause after meas. 12	0.0 s
Pause after meas. 13	0.0 s
Pause after meas. 14	0.0 s
Pause after meas. 15	0.0 s
Pause after meas. 16	0.0 s
Pause after meas. 17	0.0 s
Pause after meas. 18	0.0 s
Pause after meas. 19	0.0 s
Pause after meas. 20	0.0 s
Pause after meas. 21	0.0 s
Pause after meas. 22	0.0 s
Pause after meas. 23	0.0 s
Pause after meas. 24	0.0 s
Pause after meas. 25	0.0 s
Pause after meas. 26	0.0 s
Multiple series	Off

Resolution

Base resolution	192
Phase resolution	100 %
Phase partial Fourier	5/8
Interpolation	Off
PAT mode	None
Matrix Coil Mode	Auto (CP)
Image Filter	Off
Distortion Corr.	On
Mode	2D
Unfiltered images	Off
Prescan Normalize	Off
Normalize	On
Intensity	Medium
Cut off	20
Width	4
Unfiltered images	Off
B1 filter	Off
Raw filter	Off
Elliptical filter	Off

Geometry

Multi-slice mode	Single shot
Series	Interleaved
Special sat.	None
Tim CT mode	Off

System

Body	Off
NE2	On
NE1	On
HEP	On
HEA	On
SP4	Off
SP2	Off
SP8	Off
SP6	Off
SP3	Off
SP1	On
SP7	Off
SP5	Off
Positioning mode	ISO
Table position	H
Table position	0 mm
MSMA	S - C - T
Sagittal	R >> L
Coronal	A >> P
Transversal	F >> H
Save uncombined	Off
Coil Combine Mode	Adaptive Combine
Auto Coil Select	Default
Shim mode	Standard

SIEMENS MAGNETOM TrioTim syngo MR B17

Adjust with body coil	Off
Confirm freq. adjustment	Off
Assume Silicone	Off
? Ref. amplitude 1H	0.000 V
Adjustment Tolerance	Auto
Adjust volume	
Position	R9.7 A6.6 F0.1
Orientation	S > T2.2 > C-0.6
Rotation	0.00 deg
F >> H	280 mm
A >> P	210 mm
R >> L	18 mm

Physio

1st Signal/Mode	None
Dark blood	Off
Resp. control	Off

Inline

Subtract	Off
Std-Dev-Sag	Off
Std-Dev-Cor	Off
Std-Dev-Tra	Off
Std-Dev-Time	Off
MIP-Sag	Off
MIP-Cor	Off
MIP-Tra	Off
MIP-Time	Off
Save original images	On

Sequence

Introduction	Off
Dimension	2D
Contrasts	1
Bandwidth	606 Hz/Px
Flow comp.	Read
Allowed delay	30 s
Echo spacing	7.22 ms
Turbo factor	144
RF pulse type	Normal
Gradient mode	Whisper

SIEMENS MAGNETOM TrioTim syngo MR B17

\\USER\HSC Research\NRC\RI2016:131 GAD MB\Sag T2 HASTE fMRI 120 T3 C-2

TA: 3:02 PAT: Off Voxel size: 1.5×1.5×2.0 mm Rel. SNR: 1.00 SIEMENS: haste

Properties

Prio Recon	Off
Before measurement	
After measurement	
Load to viewer	On
Inline movie	Off
Auto store images	On
Load to stamp segments	On
Load images to graphic segments	On
Auto open inline display	On
Start measurement without further preparation	On
Wait for user to start	On
Start measurements	single

Routine

Slice group 1	
Slices	9
Dist. factor	0 %
Position	R9.7 A6.6 F0.1
Orientation	S > T2.2 > C-0.6
Phase enc. dir.	A >> P
Rotation	0.00 deg
Phase oversampling	0 %
FoV read	280 mm
FoV phase	75.0 %
Slice thickness	2.0 mm
TR	750 ms
TE	79 ms
Averages	1
Concatenations	1
Filter	Distortion Corr.(2D), Normalize
Coil elements	HEA;HEP;NE1,2;SP1

Contrast

MTC	Off
Magn. preparation	None
Flip angle	100 deg
Fat suppr.	None
Water suppr.	None
Restore magn.	Off
Averaging mode	Long term
Reconstruction	Magnitude
Measurements	27
Pause after meas. 1	0.0 s
Pause after meas. 2	0.0 s
Pause after meas. 3	0.0 s
Pause after meas. 4	0.0 s
Pause after meas. 5	0.0 s
Pause after meas. 6	0.0 s
Pause after meas. 7	0.0 s
Pause after meas. 8	0.0 s
Pause after meas. 9	0.0 s
Pause after meas. 10	0.0 s
Pause after meas. 11	0.0 s
Pause after meas. 12	0.0 s
Pause after meas. 13	0.0 s
Pause after meas. 14	0.0 s
Pause after meas. 15	0.0 s
Pause after meas. 16	0.0 s
Pause after meas. 17	0.0 s
Pause after meas. 18	0.0 s
Pause after meas. 19	0.0 s
Pause after meas. 20	0.0 s
Pause after meas. 21	0.0 s
Pause after meas. 22	0.0 s
Pause after meas. 23	0.0 s
Pause after meas. 24	0.0 s
Pause after meas. 25	0.0 s
Pause after meas. 26	0.0 s
Multiple series	Off

Resolution

Base resolution	192
Phase resolution	100 %
Phase partial Fourier	5/8
Interpolation	Off
PAT mode	None
Matrix Coil Mode	Auto (CP)
Image Filter	Off
Distortion Corr.	On
Mode	2D
Unfiltered images	Off
Prescan Normalize	Off
Normalize	On
Intensity	Medium
Cut off	20
Width	4
Unfiltered images	Off
B1 filter	Off
Raw filter	Off
Elliptical filter	Off

Geometry

Multi-slice mode	Single shot
Series	Interleaved
Special sat.	None
Tim CT mode	Off

System

Body	Off
NE2	On
NE1	On
HEP	On
HEA	On
SP4	Off
SP2	Off
SP8	Off
SP6	Off
SP3	Off
SP1	On
SP7	Off
SP5	Off
Positioning mode	ISO
Table position	H
Table position	0 mm
MSMA	S - C - T
Sagittal	R >> L
Coronal	A >> P
Transversal	F >> H
Save uncombined	Off
Coil Combine Mode	Adaptive Combine
Auto Coil Select	Default
Shim mode	Standard

SIEMENS MAGNETOM TrioTim syngo MR B17

Adjust with body coil	Off
Confirm freq. adjustment	Off
Assume Silicone	Off
? Ref. amplitude 1H	0.000 V
Adjustment Tolerance	Auto
Adjust volume	
Position	R9.7 A6.6 F0.1
Orientation	S > T2.2 > C-0.6
Rotation	0.00 deg
F >> H	280 mm
A >> P	210 mm
R >> L	18 mm

Physio

1st Signal/Mode	None
Dark blood	Off
Resp. control	Off

Inline

Subtract	Off
Std-Dev-Sag	Off
Std-Dev-Cor	Off
Std-Dev-Tra	Off
Std-Dev-Time	Off
MIP-Sag	Off
MIP-Cor	Off
MIP-Tra	Off
MIP-Time	Off
Save original images	On

Sequence

Introduction	Off
Dimension	2D
Contrasts	1
Bandwidth	606 Hz/Px
Flow comp.	Read
Allowed delay	30 s
Echo spacing	7.22 ms
Turbo factor	144
RF pulse type	Normal
Gradient mode	Whisper

SIEMENS MAGNETOM TrioTim syngo MR B17

\\USER\HSC Research\NRC\RI2016:131 GAD MB\Sag T2 HASTE fMRI 120 T3 C-3

TA: 3:02 PAT: Off Voxel size: 1.5×1.5×2.0 mm Rel. SNR: 1.00 SIEMENS: haste

Properties

Prio Recon	Off
Before measurement	
After measurement	
Load to viewer	On
Inline movie	Off
Auto store images	On
Load to stamp segments	On
Load images to graphic segments	On
Auto open inline display	On
Start measurement without further preparation	On
Wait for user to start	On
Start measurements	single

Routine

Slice group 1	
Slices	9
Dist. factor	0 %
Position	R9.7 A6.6 F0.1
Orientation	S > T2.2 > C-0.6
Phase enc. dir.	A >> P
Rotation	0.00 deg
Phase oversampling	0 %
FoV read	280 mm
FoV phase	75.0 %
Slice thickness	2.0 mm
TR	750 ms
TE	79 ms
Averages	1
Concatenations	1
Filter	Distortion Corr.(2D), Normalize
Coil elements	HEA;HEP;NE1,2;SP1

Contrast

MTC	Off
Magn. preparation	None
Flip angle	100 deg
Fat suppr.	None
Water suppr.	None
Restore magn.	Off
Averaging mode	Long term
Reconstruction	Magnitude
Measurements	27
Pause after meas. 1	0.0 s
Pause after meas. 2	0.0 s
Pause after meas. 3	0.0 s
Pause after meas. 4	0.0 s
Pause after meas. 5	0.0 s
Pause after meas. 6	0.0 s
Pause after meas. 7	0.0 s
Pause after meas. 8	0.0 s
Pause after meas. 9	0.0 s
Pause after meas. 10	0.0 s
Pause after meas. 11	0.0 s
Pause after meas. 12	0.0 s
Pause after meas. 13	0.0 s
Pause after meas. 14	0.0 s
Pause after meas. 15	0.0 s
Pause after meas. 16	0.0 s
Pause after meas. 17	0.0 s
Pause after meas. 18	0.0 s
Pause after meas. 19	0.0 s
Pause after meas. 20	0.0 s
Pause after meas. 21	0.0 s
Pause after meas. 22	0.0 s
Pause after meas. 23	0.0 s
Pause after meas. 24	0.0 s
Pause after meas. 25	0.0 s
Pause after meas. 26	0.0 s
Multiple series	Off

Resolution

Base resolution	192
Phase resolution	100 %
Phase partial Fourier	5/8
Interpolation	Off
PAT mode	None
Matrix Coil Mode	Auto (CP)
Image Filter	Off
Distortion Corr.	On
Mode	2D
Unfiltered images	Off
Prescan Normalize	Off
Normalize	On
Intensity	Medium
Cut off	20
Width	4
Unfiltered images	Off
B1 filter	Off
Raw filter	Off
Elliptical filter	Off

Geometry

Multi-slice mode	Single shot
Series	Interleaved
Special sat.	None
Tim CT mode	Off

System

Body	Off
NE2	On
NE1	On
HEP	On
HEA	On
SP4	Off
SP2	Off
SP8	Off
SP6	Off
SP3	Off
SP1	On
SP7	Off
SP5	Off
Positioning mode	ISO
Table position	H
Table position	0 mm
MSMA	S - C - T
Sagittal	R >> L
Coronal	A >> P
Transversal	F >> H
Save uncombined	Off
Coil Combine Mode	Adaptive Combine
Auto Coil Select	Default
Shim mode	Standard

SIEMENS MAGNETOM TrioTim syngo MR B17

Adjust with body coil	Off
Confirm freq. adjustment	Off
Assume Silicone	Off
? Ref. amplitude 1H	0.000 V
Adjustment Tolerance	Auto
Adjust volume	
Position	R9.7 A6.6 F0.1
Orientation	S > T2.2 > C-0.6
Rotation	0.00 deg
F >> H	280 mm
A >> P	210 mm
R >> L	18 mm

Physio

1st Signal/Mode	None
Dark blood	Off
Resp. control	Off

Inline

Subtract	Off
Std-Dev-Sag	Off
Std-Dev-Cor	Off
Std-Dev-Tra	Off
Std-Dev-Time	Off
MIP-Sag	Off
MIP-Cor	Off
MIP-Tra	Off
MIP-Time	Off
Save original images	On

Sequence

Introduction	Off
Dimension	2D
Contrasts	1
Bandwidth	606 Hz/Px
Flow comp.	Read
Allowed delay	30 s
Echo spacing	7.22 ms
Turbo factor	144
RF pulse type	Normal
Gradient mode	Whisper

SIEMENS MAGNETOM TrioTim syngo MR B17

\\USER\HSC Research\NRC\RI2016:131 GAD MB\Sag T2 HASTE fMRI 120 T3 T-1

TA: 3:02 PAT: Off Voxel size: 1.5×1.5×2.0 mm Rel. SNR: 1.00 SIEMENS: haste

Properties

Prio Recon	Off
Before measurement	
After measurement	
Load to viewer	On
Inline movie	Off
Auto store images	On
Load to stamp segments	On
Load images to graphic segments	On
Auto open inline display	On
Start measurement without further preparation	On
Wait for user to start	On
Start measurements	single

Routine

Slice group 1	
Slices	9
Dist. factor	0 %
Position	R8.4 P44.4 F176.8
Orientation	S > T-2.9 > C-0.1
Phase enc. dir.	A >> P
Rotation	0.00 deg
Phase oversampling	0 %
FoV read	280 mm
FoV phase	75.0 %
Slice thickness	2.0 mm
TR	750 ms
TE	79 ms
Averages	1
Concatenations	1
Filter	Distortion Corr.(2D), Normalize
Coil elements	NE1,2;SP1,2

Contrast

MTC	Off
Magn. preparation	None
Flip angle	100 deg
Fat suppr.	None
Water suppr.	None
Restore magn.	Off
Averaging mode	Long term
Reconstruction	Magnitude
Measurements	27
Pause after meas. 1	0.0 s
Pause after meas. 2	0.0 s
Pause after meas. 3	0.0 s
Pause after meas. 4	0.0 s
Pause after meas. 5	0.0 s
Pause after meas. 6	0.0 s
Pause after meas. 7	0.0 s
Pause after meas. 8	0.0 s
Pause after meas. 9	0.0 s
Pause after meas. 10	0.0 s
Pause after meas. 11	0.0 s
Pause after meas. 12	0.0 s
Pause after meas. 13	0.0 s
Pause after meas. 14	0.0 s
Pause after meas. 15	0.0 s
Pause after meas. 16	0.0 s
Pause after meas. 17	0.0 s
Pause after meas. 18	0.0 s
Pause after meas. 19	0.0 s
Pause after meas. 20	0.0 s
Pause after meas. 21	0.0 s
Pause after meas. 22	0.0 s
Pause after meas. 23	0.0 s
Pause after meas. 24	0.0 s
Pause after meas. 25	0.0 s
Pause after meas. 26	0.0 s
Multiple series	Off

Resolution

Base resolution	192
Phase resolution	100 %
Phase partial Fourier	5/8
Interpolation	Off
PAT mode	None
Matrix Coil Mode	Auto (CP)
Image Filter	Off
Distortion Corr.	On
Mode	2D
Unfiltered images	Off
Prescan Normalize	Off
Normalize	On
Intensity	Medium
Cut off	20
Width	4
Unfiltered images	Off
B1 filter	Off
Raw filter	Off
Elliptical filter	Off

Geometry

Multi-slice mode	Single shot
Series	Interleaved
Special sat.	None
Tim CT mode	Off

System

Body	Off
NE2	On
NE1	On
HEP	Off
HEA	Off
SP4	Off
SP2	On
SP8	Off
SP6	Off
SP3	Off
SP1	On
SP7	Off
SP5	Off
Positioning mode	ISO
Table position	F
Table position	176 mm
MSMA	S - C - T
Sagittal	R >> L
Coronal	A >> P
Transversal	F >> H
Save uncombined	Off
Coil Combine Mode	Adaptive Combine
Auto Coil Select	Default
Shim mode	Standard

SIEMENS MAGNETOM TrioTim syngo MR B17

Adjust with body coil	Off
Confirm freq. adjustment	Off
Assume Silicone	Off
? Ref. amplitude 1H	0.000 V
Adjustment Tolerance	Auto
Adjust volume	
Position	R8.4 P44.4 F176.8
Orientation	S > T-2.9 > C-0.1
Rotation	0.00 deg
F >> H	280 mm
A >> P	210 mm
R >> L	18 mm

Physio

1st Signal/Mode	None
Dark blood	Off
Resp. control	Off

Inline

Subtract	Off
Std-Dev-Sag	Off
Std-Dev-Cor	Off
Std-Dev-Tra	Off
Std-Dev-Time	Off
MIP-Sag	Off
MIP-Cor	Off
MIP-Tra	Off
MIP-Time	Off
Save original images	On

Sequence

Introduction	Off
Dimension	2D
Contrasts	1
Bandwidth	606 Hz/Px
Flow comp.	Read
Allowed delay	30 s
Echo spacing	7.22 ms
Turbo factor	144
RF pulse type	Normal
Gradient mode	Whisper

SIEMENS MAGNETOM TrioTim syngo MR B17

\\USER\HSC Research\NRC\RI2016:131 GAD MB\Sag T2 HASTE fMRI 120 T3 T-2

TA: 3:02 PAT: Off Voxel size: 1.5×1.5×2.0 mm Rel. SNR: 1.00 SIEMENS: haste

Properties

Prio Recon	Off
Before measurement	
After measurement	
Load to viewer	On
Inline movie	Off
Auto store images	On
Load to stamp segments	On
Load images to graphic segments	On
Auto open inline display	On
Start measurement without further preparation	On
Wait for user to start	On
Start measurements	single

Routine

Slice group 1	
Slices	9
Dist. factor	0 %
Position	R8.4 P44.4 F176.8
Orientation	S > T-2.9 > C-0.1
Phase enc. dir.	A >> P
Rotation	0.00 deg
Phase oversampling	0 %
FoV read	280 mm
FoV phase	75.0 %
Slice thickness	2.0 mm
TR	750 ms
TE	79 ms
Averages	1
Concatenations	1
Filter	Distortion Corr.(2D), Normalize
Coil elements	NE1,2;SP1,2

Contrast

MTC	Off
Magn. preparation	None
Flip angle	100 deg
Fat suppr.	None
Water suppr.	None
Restore magn.	Off
Averaging mode	Long term
Reconstruction	Magnitude
Measurements	27
Pause after meas. 1	0.0 s
Pause after meas. 2	0.0 s
Pause after meas. 3	0.0 s
Pause after meas. 4	0.0 s
Pause after meas. 5	0.0 s
Pause after meas. 6	0.0 s
Pause after meas. 7	0.0 s
Pause after meas. 8	0.0 s
Pause after meas. 9	0.0 s
Pause after meas. 10	0.0 s
Pause after meas. 11	0.0 s
Pause after meas. 12	0.0 s
Pause after meas. 13	0.0 s
Pause after meas. 14	0.0 s
Pause after meas. 15	0.0 s
Pause after meas. 16	0.0 s
Pause after meas. 17	0.0 s
Pause after meas. 18	0.0 s
Pause after meas. 19	0.0 s
Pause after meas. 20	0.0 s
Pause after meas. 21	0.0 s
Pause after meas. 22	0.0 s
Pause after meas. 23	0.0 s
Pause after meas. 24	0.0 s
Pause after meas. 25	0.0 s
Pause after meas. 26	0.0 s
Multiple series	Off

Resolution

Base resolution	192
Phase resolution	100 %
Phase partial Fourier	5/8
Interpolation	Off
PAT mode	None
Matrix Coil Mode	Auto (CP)
Image Filter	Off
Distortion Corr.	On
Mode	2D
Unfiltered images	Off
Prescan Normalize	Off
Normalize	On
Intensity	Medium
Cut off	20
Width	4
Unfiltered images	Off
B1 filter	Off
Raw filter	Off
Elliptical filter	Off

Geometry

Multi-slice mode	Single shot
Series	Interleaved
Special sat.	None
Tim CT mode	Off

System

Body	Off
NE2	On
NE1	On
HEP	Off
HEA	Off
SP4	Off
SP2	On
SP8	Off
SP6	Off
SP3	Off
SP1	On
SP7	Off
SP5	Off
Positioning mode	ISO
Table position	F
Table position	176 mm
MSMA	S - C - T
Sagittal	R >> L
Coronal	A >> P
Transversal	F >> H
Save uncombined	Off
Coil Combine Mode	Adaptive Combine
Auto Coil Select	Default
Shim mode	Standard

SIEMENS MAGNETOM TrioTim syngo MR B17

Adjust with body coil	Off
Confirm freq. adjustment	Off
Assume Silicone	Off
? Ref. amplitude 1H	0.000 V
Adjustment Tolerance	Auto
Adjust volume	
Position	R8.4 P44.4 F176.8
Orientation	S > T-2.9 > C-0.1
Rotation	0.00 deg
F >> H	280 mm
A >> P	210 mm
R >> L	18 mm

Physio

1st Signal/Mode	None
Dark blood	Off
Resp. control	Off

Inline

Subtract	Off
Std-Dev-Sag	Off
Std-Dev-Cor	Off
Std-Dev-Tra	Off
Std-Dev-Time	Off
MIP-Sag	Off
MIP-Cor	Off
MIP-Tra	Off
MIP-Time	Off
Save original images	On

Sequence

Introduction	Off
Dimension	2D
Contrasts	1
Bandwidth	606 Hz/Px
Flow comp.	Read
Allowed delay	30 s
Echo spacing	7.22 ms
Turbo factor	144
RF pulse type	Normal
Gradient mode	Whisper

SIEMENS MAGNETOM TrioTim syngo MR B17

\\USER\HSC Research\NRC\RI2016:131 GAD MB\Sag T2 HASTE fMRI 120 T3 T-3

TA: 3:02 PAT: Off Voxel size: 1.5×1.5×2.0 mm Rel. SNR: 1.00 SIEMENS: haste

Properties

Prio Recon	Off
Before measurement	
After measurement	
Load to viewer	On
Inline movie	Off
Auto store images	On
Load to stamp segments	On
Load images to graphic segments	On
Auto open inline display	On
Start measurement without further preparation	On
Wait for user to start	On
Start measurements	single

Routine

Slice group 1	
Slices	9
Dist. factor	0 %
Position	R8.4 P44.4 F176.8
Orientation	S > T-2.9 > C-0.1
Phase enc. dir.	A >> P
Rotation	0.00 deg
Phase oversampling	0 %
FoV read	280 mm
FoV phase	75.0 %
Slice thickness	2.0 mm
TR	750 ms
TE	79 ms
Averages	1
Concatenations	1
Filter	Distortion Corr.(2D), Normalize
Coil elements	NE1,2;SP1,2

Contrast

MTC	Off
Magn. preparation	None
Flip angle	100 deg
Fat suppr.	None
Water suppr.	None
Restore magn.	Off
Averaging mode	Long term
Reconstruction	Magnitude
Measurements	27
Pause after meas. 1	0.0 s
Pause after meas. 2	0.0 s
Pause after meas. 3	0.0 s
Pause after meas. 4	0.0 s
Pause after meas. 5	0.0 s
Pause after meas. 6	0.0 s
Pause after meas. 7	0.0 s
Pause after meas. 8	0.0 s
Pause after meas. 9	0.0 s
Pause after meas. 10	0.0 s
Pause after meas. 11	0.0 s
Pause after meas. 12	0.0 s
Pause after meas. 13	0.0 s
Pause after meas. 14	0.0 s
Pause after meas. 15	0.0 s
Pause after meas. 16	0.0 s
Pause after meas. 17	0.0 s
Pause after meas. 18	0.0 s
Pause after meas. 19	0.0 s
Pause after meas. 20	0.0 s
Pause after meas. 21	0.0 s
Pause after meas. 22	0.0 s
Pause after meas. 23	0.0 s
Pause after meas. 24	0.0 s
Pause after meas. 25	0.0 s
Pause after meas. 26	0.0 s
Multiple series	Off

Resolution

Base resolution	192
Phase resolution	100 %
Phase partial Fourier	5/8
Interpolation	Off
PAT mode	None
Matrix Coil Mode	Auto (CP)
Image Filter	Off
Distortion Corr.	On
Mode	2D
Unfiltered images	Off
Prescan Normalize	Off
Normalize	On
Intensity	Medium
Cut off	20
Width	4
Unfiltered images	Off
B1 filter	Off
Raw filter	Off
Elliptical filter	Off

Geometry

Multi-slice mode	Single shot
Series	Interleaved
Special sat.	None
Tim CT mode	Off

System

Body	Off
NE2	On
NE1	On
HEP	Off
HEA	Off
SP4	Off
SP2	On
SP8	Off
SP6	Off
SP3	Off
SP1	On
SP7	Off
SP5	Off
Positioning mode	ISO
Table position	F
Table position	176 mm
MSMA	S - C - T
Sagittal	R >> L
Coronal	A >> P
Transversal	F >> H
Save uncombined	Off
Coil Combine Mode	Adaptive Combine
Auto Coil Select	Default
Shim mode	Standard

SIEMENS MAGNETOM TrioTim syngo MR B17

Adjust with body coil	Off
Confirm freq. adjustment	Off
Assume Silicone	Off
? Ref. amplitude 1H	0.000 V
Adjustment Tolerance	Auto
Adjust volume	
Position	R8.4 P44.4 F176.8
Orientation	S > T-2.9 > C-0.1
Rotation	0.00 deg
F >> H	280 mm
A >> P	210 mm
R >> L	18 mm

Physio

1st Signal/Mode	None
Dark blood	Off
Resp. control	Off

Inline

Subtract	Off
Std-Dev-Sag	Off
Std-Dev-Cor	Off
Std-Dev-Tra	Off
Std-Dev-Time	Off
MIP-Sag	Off
MIP-Cor	Off
MIP-Tra	Off
MIP-Time	Off
Save original images	On

Sequence

Introduction	Off
Dimension	2D
Contrasts	1
Bandwidth	606 Hz/Px
Flow comp.	Read
Allowed delay	30 s
Echo spacing	7.22 ms
Turbo factor	144
RF pulse type	Normal
Gradient mode	Whisper

SIEMENS MAGNETOM TrioTim syngo MR B17

Table of contents

7. Appendix B: Letter from the VP of Research Regarding Research Activities in Response to COVID-19

Unfortunately, due to the COVID-19 pandemic, the following letter was sent from the University of Manitoba Vice President of Research, indicating the need for on- and off-campus research to halt immediately, in order to flatten the curve of the novel coronavirus outbreak. As a result, data collection for this thesis was halted. To continue progressing with my studies, my advisory committee agreed that I should continue with the data already collected and write up the results, even though these are from a smaller-than-ideal sample size.

Dear Researchers:

On March 16th, researchers were sent the first communique regarding the impacts of COVID-19 on research. In that communique principal investigators were instructed to:

- not start new experiments until April 15 and to complete any ongoing experiments with great care with respect to the safety of all research personnel;
- develop a plan to stop all research including field research, should it become necessary to do so; and
- have their plan in place by the close of business (4:30 PM) Wednesday, March 18th.

It is necessary to operationalize the suspension of most on-campus/field sites research, scholarly works, and creative activities during this pandemic that:

- cannot be conducted remotely;
- cannot ensure health and safety requirements of research personnel; and
- might introduce coronavirus (COVID-19) into a vulnerable population.

The expectation is that researchers will continue as much research as possible remotely but only limited research will continue in university research facilities, including off-campus research sites. Researchers who feel that they have exceptional circumstances, should direct their requests to Dr. Digvir Jayas, Vice-President (Research and International).

Requests for exceptions to continue any **Research, Scholarly Works and Creative Activities** in university research facilities, including off-campus research sites and field stations must address the following.

1. Describe why continuing this research is essential. What are the consequences of suspending this work (economic, social, etc.)? Note that you must have all of your ethics protocols and biosafety program approvals in place. New protocols for new research may not be processed except for COVID-19 related research. You should have your lab supplies, etc., in place as well since the purchasing department may not be able to process orders and suppliers may not be able to fill and deliver on orders.
2. Outline in detail your plan for ensuring employee(s) safety. How will the employee get to the lab/field work/research location? What are the procedures for decontaminating the lab after use by a given employee? What is the plan if this (first) employee becomes ill and cannot continue the work? What is the plan if that (first) alternate employee becomes ill and cannot continue the work?
3. Your department head and ADR/RLO must first approve your plan to continue research. Your plan will then be reviewed by a committee designated by the VPRI and will include the two AVPs and a representative from Office of Risk Management team and/or the Environment Health and Safety Office.

The University understands the impact that this closure will have on your research programs and the granting agencies are aware of it too. The Granting agencies have provided some general updates on their response to COVID-19 and in the next few days they will be providing details of a package of measures to address upcoming grant competitions, ongoing payment of staff from grants, and the impacts of lab closures. They are currently developing mitigation strategies for all immediately scheduled grant competitions and considering approaches for awarded grants including the possibility of extensions.

Please complete the form found here and email it to Digvir.Jayas@umanitoba.ca.

Digvir S. Jayas, O.C., Ph.D., D.Sc., P.Eng., P.Ag., FRSC
Vice-President (Research and International) and Distinguished Professor
202 Administration Building, 66 Chancellors Circle
University of Manitoba
Winnipeg, MB, Canada, R3T 2N2